ZERO

ZACKENBERG ECOLOGICAL RESEARCH OPERATIONS

20th Annual Report 2014

GEM

Greenland Ecosystem Monitoring

Aarhus University
DCE – Danish Centre for Environment and Energy

ZACKENBERG ECOLOGICAL RESEARCH OPERATIONS

20th Annual Report 2014

This report is dedicated to Lillian Magelund Jensen, who passed away far too early. Lillian's dedication to the work in the Greenland Ecosystem Monitoring Programme and around Zackenberg in particular is greatly missed. All honour to her memory.

AARHUS
UNIVERSITY
DCE – DANISH CENTRE FOR ENVIRONMENT AND ENERGY

Data sheet

Title: Zackenberg Ecological Research Operations
Subtitle: 20th Annual Report 2014

Editors: Lillian Magelund Jensen(†), Elmer Topp-Jørgensen, Torben R. Christensen and Niels Martin Schmidt
Department of Bioscience, Aarhus University

Publisher: Aarhus University, DCE – Danish Centre for Environment and Energy
URL: http://dce.au.dk

Year of publication: 2016

Please cite as: Jensen, L.M., Topp-Jørgensen, E., Christensen, T.R. and Schmidt, N.M. (eds.) 2016. Zackenberg Ecological Research Operations 20th Annual Report, 2014. Aarhus University, DCE – Danish Centre for Environment and Energy. 134 pp.

Layout and drawings: Tinna Christensen and Juana Jacobsen, Department of Bioscience, Aarhus University
Front cover photo: Jørgen Skafte
Back cover photo: (top to bottom): Jakob Abermann, Louise H. Rasmussen, Bula Larsen, Thomas Juul-Pedersen and Michele Citterio

ISSN: 1904-0407
ISBN: 978-87-93129-37-5

Number of pages: 134

Internet version: The report is available in electronic format (pdf) on http://zackenberg.dk/Publications/Publications and on www.dce.au.dk

Supplementary notes: Zackenberg secretariat
Department of Bioscience
Aarhus University
P.O. Box 358
Frederiksborgvej 399
DK-4000 Roskilde, Denmark

E-mail: zackenberg@au.dk
Phone: +45 87158657

Zackenberg Ecological Research Operations (ZERO) is together with Nuuk Ecological Research Operations (NERO) operated as a centre without walls with a number of Danish and Greenlandic institutions involved. The two programmes are gathered under the umbrella organization Greenland Ecosystem Monitoring (GEM). The following institutions are involved in ZERO:
Department of Bioscience, Aarhus University: GeoBasis, BioBasis and MarineBasis programmes
Greenland Institute of Natural Resources: MarineBasis programme
Asiaq – Greenland Survey: ClimateBasis programme
University of Copenhagen: GeoBasis programme
Geological Survey of Denmark and Greenland: GlacioBasis programme

The programmes are coordinated by a secretariat at Department of Bioscience, Aarhus University and financed through contributions from:
The Danish Energy Agency
The Environmental Protection Agency
The Government of Greenland
Private foundations
The participating institutions

(†) 14 February 2016

Contents

Summary for policy makers

Elmer Topp-Jørgensen, Torben R. Christensen and Niels Martin Schmidt

The season started 2 April and ended 24 October. A total of 129 persons visited the station, 79 at Zackenberg and 50 at the research house in Daneborg. The total number of 'bed nights' was 3018 (2631 related to research and monitoring, and 387 to logistics). Aircrafts landed 49 times at the station during the field season, no larger maintenance was carried out and approximately 33 m^3 of non-burnable waste were removed from the station (Zackenberg and Daneborg combined).

The 2014 season at Zackenberg, proceeded largely as planned with the five Basis Programmes being supplemented by 27 external projects.

In 2014, more than 40 peer-reviewed papers were published by researchers from the Zackenberg Basic programme and from externally funded research projects. In addition to this Zackenberg Basic participants produced two reports, 36 presentations and 11 posters.

Infrastructure development

The bridge established in 2013 over the river Zackenberg facilitated easy access to the other side of the river in 2014. Crossings are now much safer and the bridge withstood the pressure from floods, the strongest being the glacial lake outburst flow occurring 16 August where river water discharge reached 168 $m^3 s^{-1}$ (figure 2.9).

Organisational changes

Torben R. Christensen was appointed new Scientific Leader for Greenland Ecosystem Monitoring.

Data collection and significant findings

Data collection for Zackenberg Basic was carried out according to the manuals for the individual sub-programmes http://zackenberg.dk/monitoring/.

A large snow volume and low spring temperatures in 2014 resulted in a late break up of the Zackenberg river (4 June). A diurnal cycle was observed with four periods with increased river discharge in late June and the first half of July, due to sunny weather and hence increased melt. On 16 august, however, the discharge peaked as a result of a lake outburst from the glacier dammed lake at A.P. Olsen glacier. The peak discharge rate during this event was 168 $m^3 s^{-1}$, resulting in increased sediment transport and changes to the shape of the river bed. In late August discharge peaked again due to heavy rainfall. The total runoff from the Zackenberg river catchment was estimated to be 219×10^6 m^3 and total suspended sediment transport amounted to 45575 tons.

Melting of permafrost and subsequent increase greenhouse gas emissions is a well known climate feedback mechanism. The active layer depth was slightly deeper than normal and it was the second year on record where the heath acted as a source rather than a sink for CO_2. The CH_4 flux dynamics had an unusual seasonal curve with maximum emission around 1 August and a little autumn peak around 14 October.

The late snowmelt also resulted in late onset of flowering and nesting, and fewer flowers, lowest number of flying insects recorded and low breeding success for many species. Large amounts of snow in the winter most likely resulted in the many dead muskoxen observed in the valley. The carcasses, however, meant that Arctic fox survival was good, but their breeding success was still low probably due to late snowmelt and low breeding success of prey species.

The melting glacier ice and snow contributes to a freshwater discharge that also affects the marine ecosystem. Data obtained during 2014 demonstrated that even in the absence of sea ice, the biomass and productivity of key species are much lower than in the Godthåbsfjord and Disko Bay which are related to the large

influence of freshwater in Young Sound which limits both light availability and nutrient replenishment. This underlines that the coastal marine ecosystem around Greenland is influenced not only by changes in sea ice but perhaps even more by the increased melting of the Greenland Ice Sheet.

Also, the seasonal data from Young Sound allow comparison with the monitoring program in the Godthåbsfjord which indicate that land and marine terminating glaciers may influence the marine ecosystem very differently where sub-glacial discharge from marine terminating glaciers may stimulate productivity and meltwater from land terminating glaciers may depress productivity.

International cooperation

Zackenberg Basic plays a central role in Arctic Council's monitoring programmes; Circumpolar Biodiversity Monitoring Programme (CBMP) and Arctic Monitoring and Assessment Programme (AMAP), influencing the design of the programmes and being at the forefront of implementing protocols. CBMP has strong international linkages to global biodiversity initiatives (e.g. CBD, IPBES, GEOBON) and is the biodiversity component of the Sustaining Arctic Observing Networks (SAON). AMAP has strong international linkages to climate, ecosystem and health related initiatives, including WMO and the International Panel on Climate Change (IPCC).

Zackenberg Basic is engaged in numerous scientific networks to influence and implement international standards. Data is often shared in the networks to enable larger assessments and more precise predictions. All data of the 2014 season has been added to the GEM open access database, www.data.g-e-m.dk.

Zackenberg Basic is also at the core of several larger international research projects:

- **Defrost** (Nordic Centre of Excellence, led by Torben R. Christensen, Lund University),
- **CENPERM** (Centre for Permafrost Dynamics in Greenland led by Bo Elberling, Copenhagen University).

Zackenberg Research Station is also involved in INTERACT (International Network for Terrestrial Research and Monitoring in the Arctic), an infrastructure network funded by the EU, that provides a platform for coordinated research and monitoring across terrestrial field stations in the Arctic.

Researchers from Zackenberg Basic are also involved in/associated with the Arctic Research Centre at Aarhus University and Arctic Science Partnership (Aarhus University, Greenland Institute of Natural Resources and the University of Manitoba (Canada)).

Economy

In 2014, the monitoring programme Zackenberg Basic received almost 10.74 million DKK from the Danish Energy Agency and the Environmental Protection Agency for the five programmes – ClimateBasis, GeoBasis, GlacioBasis, BioBasis and MarineBasis. The funding includes means for long-term monitoring as well as analytical and strategic initiatives. On top of this, the five Zackenberg Basic monitoring programmes co-funded the monitoring with approximately 1.5 million DKK.

Zackenberg Research Station received 3.2 million DKK from the Danish Agency for Science, Technology and Innovation for running and maintaining the station, salaries and logistics support, and the Zackenberg secretariat.

During the period April to October 2014, 28 projects visited the station. Among these were ClimateBasis, GeoBasis, GlacioBasis, BioBasis and MarineBasis programmes, as well as 23 external research projects. The five Zackenberg Basic monitoring programmes spent about 25% of the logistics handled by the station, (travel, accommodation, cargo and subsistence); while the external funded research projects spent approximately 75%. The overall economy of the external research projects is not known, and therefore only funding related to travels and accommodation could be estimated – not salaries and laboratory analyses.

Seven externally research projects (15 researchers) were supported by the INTERACT Transnational Access (which included 285 'bed nights').

Executive summary

Kirstine Skov, Magnus Lund, Jakob Abermann, Michele Citterio, Niels Martin Schmidt, Mikael K. Sejr and Lillian Magelund Jensen

GeoBasis and ClimateBasis

In 2014 the winter snow pack in the Zackenberg valley was slightly above average compared to the monitoring period (1997-2013). The maximum snow depth at the climate station was 0.85 m. Snow depletion started in mid-May, but the valley was not snow free before the beginning of July, due to unstable weather in June. At the beginning of October 2014, the valley was covered by 0.1 m of snow.

The mean annual air temperature in 2014 was 0.4 °C above the long-term average (1996-2013). Spring and early summer were slightly colder than average, whereas the late summer and autumn were warmer. The first positive temperatures occurred on 26 January. The maximum temperature of 16.5 °C was measured on 20 July. Night frost occurred in all summer months, and the first negative mean daily temperature was measured on 5 September.

The river Zackenberg broke up on 4 June and a pronounced diurnal cycle was recorded throughout the season. Four periods with increased river discharge occurred in late June and the first half of July, due to sunny weather and hence increased melt. The maximum runoff occurred on 16 August, due to a lake outburst from the glacier dammed lake at A.P. Olsen glacier. The peak discharge rate during this event was 168 $m^3 s^{-1}$, resulting in increased sediment transport and changes to the shape of the river bed. In late August discharge peaked again due to heavy rainfall. The total runoff from the Zackenberg river catchment was estimated to be 219×10^6 m^3 and total suspended sediment transport amounted to 45575 tons.

The active layer depth monitoring in 2014 in the two CALM plots (ZEROCALM-1 and ZEROCALM-2) began on 26 and 8 June, respectively. Maximum thaw depths were reached in early September and were slightly deeper than the long-term average.

Methane (CH_4) fluxes were measured from 20 June until 20 October. In general, the CH_4 emission in 2014 was similar to the wet year of 2012, but lower than the highest recorded emissions in 2007. The maximum emissions were measured at the end of July and beginning of August. In the autumn, a few occasions with high emissions were recorded, possibly due to freezing of the soil column.

Fluxes of carbon dioxide (CO_2) were monitored both at a heath site and at a fen site. At the heath, measurements began on 20 April and lasted until 18 October. In April and May when the heath was covered by a thick snowpack, CO_2 fluxes were low. The daily net uptake period did not start until 16 July, which is the latest start of net uptake on record. The period with net uptake lasted until 19 August, which is also among the latest dates on record. The late onset of the growing season is mainly attributed to the late snowmelt. The net CO_2 budget of 2014 amounted to 4.8 g C m^{-2}. Year 2014 is the second year on record when the heath acts as a source rather than a sink for CO_2.

In 2014, data from the eddy covariance system in the fen were retrieved from 1 January to 19 October. During the entire period about 14 % of the data are missing, mainly due to periods with insufficient power supply during winter months and also maintenance during summer. The net CO_2 uptake period in the fen lasted from16 July to 30 August, with the relatively late onset caused by late snowmelt. The entire CO_2 budget from 1 January to 19 October was –74.8 g C m^{-2}.

GlacioBasis

The GlacioBasis monitoring programme at the A.P. Olsen Ice Cap in the Zackenberg river catchment (NE Greenland) started in March 2008, with subsequent field visits taking place every year in springtime.

GlacioBasis is operated by GEUS on funding administered by the Danish Energy Agency.

In 2014 the monitoring, processing and data management tasks included: maintenance of three automatic weather stations (AWS), two with satellite telemetry to Denmark;

- measurement and re-drilling of the network of ablation and displacement stakes;
- survey of surface velocity and elevation by dual frequency differential GPS;
- recording and post-processing of dual frequency GPS data, providing high accuracy positions of master and rover GPS receivers;
- collaboration with the ZAMG (Vienna) and ETH (Zurich) colleagues monitoring the ice-dammed lake;
- setup of two new field experiments: 1. the acquisition of very high resolution digital photographs of the glacier surface using a calibrated camera and subsequent photogrammetric processing to map the microtopography, useful in refining the modelling of turbulent energy and moisture fluxes at the surface and in studying the effect of surface roughness on albedo observed *in situ* and from satellite; 2. the evaluation of a new instrument capable of recording rain and hail at the AWS1, useful to calibrate the partitioning of solid and liquid precipitation when temporally upscaling using the weather mast close to Zackenberg station
- joint late-summer field campaign with ZAMG to survey the ablation stakes at the end of the ablation season;
- the collection of a comprehensive set of optical remote sensing datasets in the visible and infrared bands, including the complete Landsat archive and the MODIS MOD10A1 snow and surface albedo product was continued and analysis started to upscale ground observations using satellite imagery;
- standardized data validation and archival, including reformatting and delivery of the GlacioBasis 2008-2014 monitoring data and metadata (primarily AWS, snow radar, ablation stakes and GPS positions) to the upcoming GEM database;
- joined the Steering Group of WMO Global Cryosphere Watch (GCW) and supported the establishment of the WMO CryoNet in-situ observation network within the World Meteorological Organization (WMO), promoting GEM and PROMICE as WMO CryoNet sites in Greenland.

Fieldwork and data management in 2014 were completed as planned. Data analysis related to the GEM Strategic Initiatives was developed to extend the record of glacier lake level fluctuations from optical satellite imagery and to use the expanded radiometer network to relate remotely sensed surface albedo with in-situ observations at the GlacioBasis AWS on A.P. Olsen.

BioBasis

In the BioBasis programme, the relatively late snowmelt in 2014 resulted in relatively late onset of plant flowering phenology, and most plants had later than average dates for 50 % flowering and 50 % senescence. Also, most plant plots had lower than the average peak number of flowers or catkins hitherto recorded. The late snowmelt was also reflected in the dates of plant peak growth (NDVI), which were later than average in most plots. Peak values, however, were comparable to those of previous years.

Trapping of arthropods revealed the lowest number of total catches in the flight intercept traps since the start of the monitoring. Especially, very low numbers of midges, Chironomids, and house flies, Muscidae, were caught in 2014. Chironomids, however, were still the most abundant taxa caught in the flight intercept traps. Total catches in the pitfall traps were comparable to previous years, and here Chironomids were caught in high numbers, while Muscids were similar to the average of previous years. In 2014, a fly from the family Ephydridae (shore flies) and a member of the Lepidopteran family Gracillariidae were trapped by BioBasis. While the first is known from the area, the latter has not been observed before. Also, although BioBasis did not capture any adult ladybirds this year, coccinellidae larvae were caught for the first time.

The late snowmelt resulted in later than average of date of nest initiation in all breeding bird species in the area. Their nest success was low, and less than one fifth of the nests hatched. The

abundance of breeding birds was below average for the wader species in the area. No long-tailed skuas were breeding in the area in 2014, which reflects the low abundance of lemmings. Also, none of the lemming nests encountered was depredated by stoats. Arctic fox, on the other hand, were breeding in three dens. The extremely high abundance of musk ox carcasses found after the snow-rich winter of 2013/14 may have ensured sufficient food for the Arctic foxes in winter, though Arctic fox cub production was fairly low. The abundance of musk oxen observed in summer on the weekly censuses was low.

The monitoring of the two lakes showed that spring ice break up was late, and this combined with the relatively cold summer, resulted in lower than average water temperatures. Water chemistry parameters, however, were low but still within the range of previous years. Abundance of phytoplankton was low, but the composition comparable to previous years. The abundance and composition of zooplankton were similar to previous years.

MarineBasis

The 2014 season was the 12th of the marine monitoring programme. As a GEM strategic initiative, the usual sampling in late July and early August was complemented by three additional campaigns in July, September and early October. In addition to providing improved seasonal resolution of our monitored parameters, an additional aim was to improve our understanding of the marine carbon cycling by additional measurement not usually included in the monitoring. This included for example measurements of bacterial and phytoplankton production, zooplankton grazing and measurements of methane concentration in the water column. In total 497 visitor days were spent at Daneborg, with participants from 10 different research institutions in Denmark, Norway and Spain. Previous studies in Young Sound have usually related the very low biological productivity to the short duration of the ice-free season. However, the data obtained during 2014 demonstrated that even in the absence of sea ice, the biomass and productivity of key species are much lower than in the Godthåbsfjord and Disko Bay which are related to the large influence of freshwater in Young Sound which limits both light availability and nutrient replenishment. This underlines that the coastal marine ecosystem around Greenland is influenced not only by changes in sea ice but perhaps even more by the increased melting of the Greenland Ice Sheet. Also, the seasonal data from Young Sound allow comparison with the monitoring program in the Godthåbsfjord which indicate that land and marine terminating glaciers may influence the marine ecosystem very differently where sub-glacial discharge from marine terminating glaciers may stimulate productivity and meltwater from land terminating glaciers may depress productivity.

Research projects

28 research projects were carried out at Zackenberg Research Station in 2014. Of these, five projects were part of the Zackenberg monitoring programmes, 21 projects used Zackenberg Research Station as a base for their activities, and six projects used Daneborg. One projects used both Zackenberg and Daneborg as a base for their activities.

1 Introduction

Niels Martin Schmidt

The 2014 season was very busy season at Zackenberg, and a total of 129 scientists from a total of 27 different research projects visited the station, resulting in a total number of 3018 bed nights this season. The field season started 2 April and ended 24 October.

In 2014, the Greenland Ecosystem Monitoring program and strategy was evaluated by an international evaluation panel. As part of the evaluation the panel, consisting of Stephen Albon, Jörn Thiede and Kim Holmén, visited Zackenberg in mid July 2014. Earlier in the season, the newly established bridge over the Zackenberg river was inspected and approved. Minor adjustments will however be implemented.

During the season almost the entire Zackenberg valley was mapped using drones, thus fulfilling an old wish for better background maps and data. The new high resolution digital terrain model and RGB and NIR orthophotos can be accessed via the GEM database.

A large campaign lead by Arctic Research Centre, Aarhus University, resulted in high activity, not only at Zackenberg and Daneborg, but in the area in general. The campaign included both marine and terrestrial components.

International cooperation

In 2014, Zackenberg Basic continued to feed into international networks. Hence, Zackenberg plays a central role in the development of protocols within the circumarctic monitoring of biodiversity within the Circumpolar Biodiversity Monitoring Program (CBMP). CBMP is an international network of scientists, government agencies, Indigenous organizations and conservation groups working together to harmonize and integrate efforts to monitor the Arctic's living resources. The CBMP coordinates marine, freshwater, terrestrial and coastal ecosystem monitoring activities and develops best practice protocols for monitoring. CBMP has strong international linkages to global biodiversity initiatives. CBMP is the biodiversity component of the Sustaining Arctic Observing Networks (SAON).

As part of the Greenland Ecosystem Monitoring (GEM), Zackenberg also plays a central role in the EU project "International Network for Terrestrial Research and Monitoring in the Arctic" (INTERACT), and GEM is co-leading the project and coordinating two work packages within the project. In 2014, the transnational access component of INTERACT enabled 15 researchers from seven projects to visit Zackenberg free of charge, spending a total of 285 bed nights.

Outreach

Results from the Zackenberg Basic monitoring programme and the research projects working under the auspices of Zackenberg are continuously published in scientific papers and popular science articles. Data collected as part Zackenberg Basic programme is freely available. In 2014, more than 39 scientific papers were publish by researchers from the Zackenberg Basic programme and from externally funded research projects. Amongst these papers, several papers appeared in high-impact journals, such as Nature Climate Change. Additionally, scientists working at Zackenberg presented their work in Danish and international newspapers and radio several times in 2014.

Throughout the field season, visiting scientists are encouraged to post diaries describing the daily life at Zackenberg at the Zackenberg web site (www.zackenberg.dk).

Further information

For further information about Zackenberg Research Station and the work at Zackenberg are collected in previous annual reports available at www.zackenberg.dk. On the web site, one can also access the ZERO Site Manual, manuals for each of the monitoring sub-programmes, as well as an updated Zackenberg bibliography. Data from the monitoring programmes are available at http://data.g-e-m.dk.

Photo: Lars Holts Hansen.

2 Zackenberg Basic

The ClimateBasis and GeoBasis programme

Kirstine Skov, Jakob Abermann, Maria Rask Mylius, Torben R. Christensen, Per Hangaard, Birger Ulf Hansen, Dorthe Petersen, Mikkel P. Tamstorf, Mikhail Mastepanov, Majbritt Westring Sørensen, Lau Gede Petersen, Laura Helene Rasmussen, Line Vinter Hansen, Charlotte Sigsgaard, Stefan Wacker and Magnus Lund

GeoBasis and ClimateBasis provide long-term data of climatic, hydrological and physical landscape variables describing the environment at Zackenberg. This includes climatic measurements, seasonal and spatial variations in snow cover and local microclimate in the Zackenberg area, the water balance of the Zackenberg River drainage basin, the sediment and solute transport of the Zackenberg River, carbon dioxide (CO_2) and methane (CH_4) fluxes from a well-drained heath and a fen area, seasonal development of the active layer, temperature conditions and soil water chemistry of the active layer, and dynamics of selected coastal and periglacial landscape elements. For a map of the main study sites, see figure 2.1.

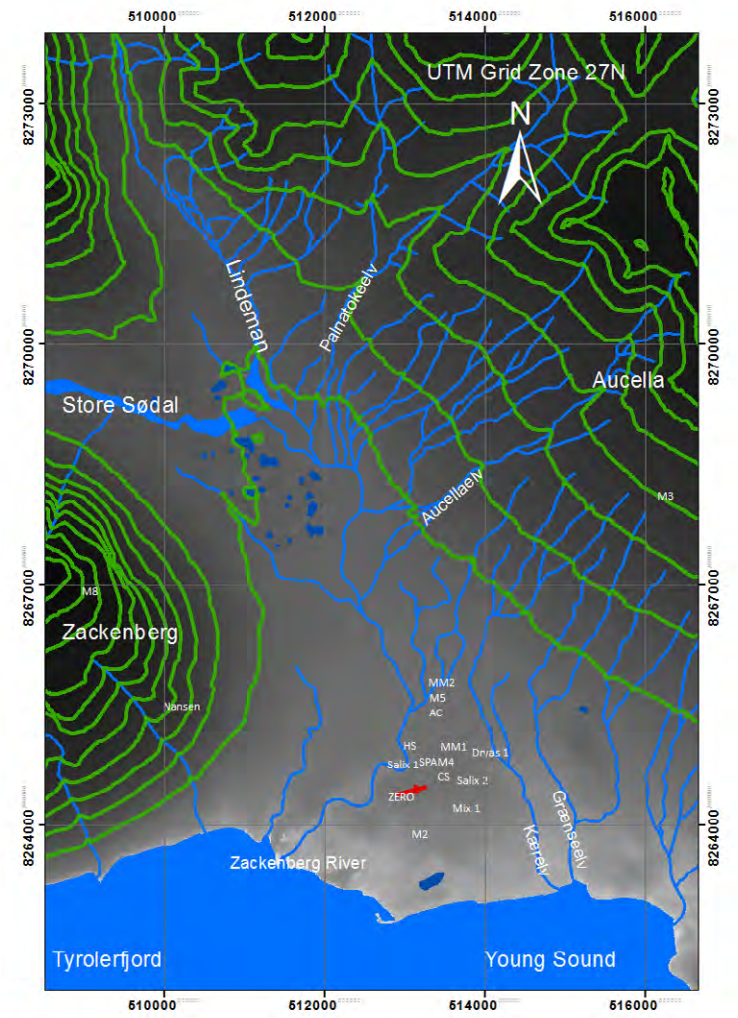

Figure 2.1 Map of GeoBasis and ClimateBasis plots. Nansenblokken (automatic photo monitoring site), the meteorological stations M2, M3, M4, M5 and M8, the soil water and moisture plots Salix 1, Salix 2, Dryas 1 and Mix 1, the automatic chamber site (AC), the micro meteorological stations MM1 and MM2, the snow pack analyser (SPA), the climate station (CS) and the hydrometric station (HS). The red cross indicates the location of the landing strip and the Zackenberg Research Station (ZERO).

GeoBasis is operated by Department of Bioscience, Aarhus University, in collaboration with Department of Geosciences and Natural Resource Management, University of Copenhagen. In 2014, GeoBasis was funded by the Danish Ministry of Climate and Energy (now Danish Ministry of Energy, Utilities and Climate) as part of the environmental support programme DANCEA – Danish Cooperation for Environment in the Arctic. ClimateBasis is run by ASIAQ, Greenland Survey who operates and maintains the climate station and the hydrometric station. ClimateBasis is funded by the Government of Greenland.

More details about sampling procedures, instrumentation, locations and installations are given in the GeoBasis Manual and the ClimateBasis Manual. Both can be downloaded from http://zackenberg.dk/monitoring. Validated data from the monitoring programmes are accessible from the Greenland Ecosystem Monitoring programme database at data.g-e-m.dk. For more information concerning GeoBasis data – please contact Kirstine Skov (ksk@ign.ku.dk) or programme manager Magnus Lund (ml@bios.au.dk). For matters concerning the ClimateBasis programme and data please contact Jakob Abermann (jab@asiaq.gl).

2.1 Meteorological data

The climate station at Zackenberg was installed during summer 1995. Technical specifications of the station are described

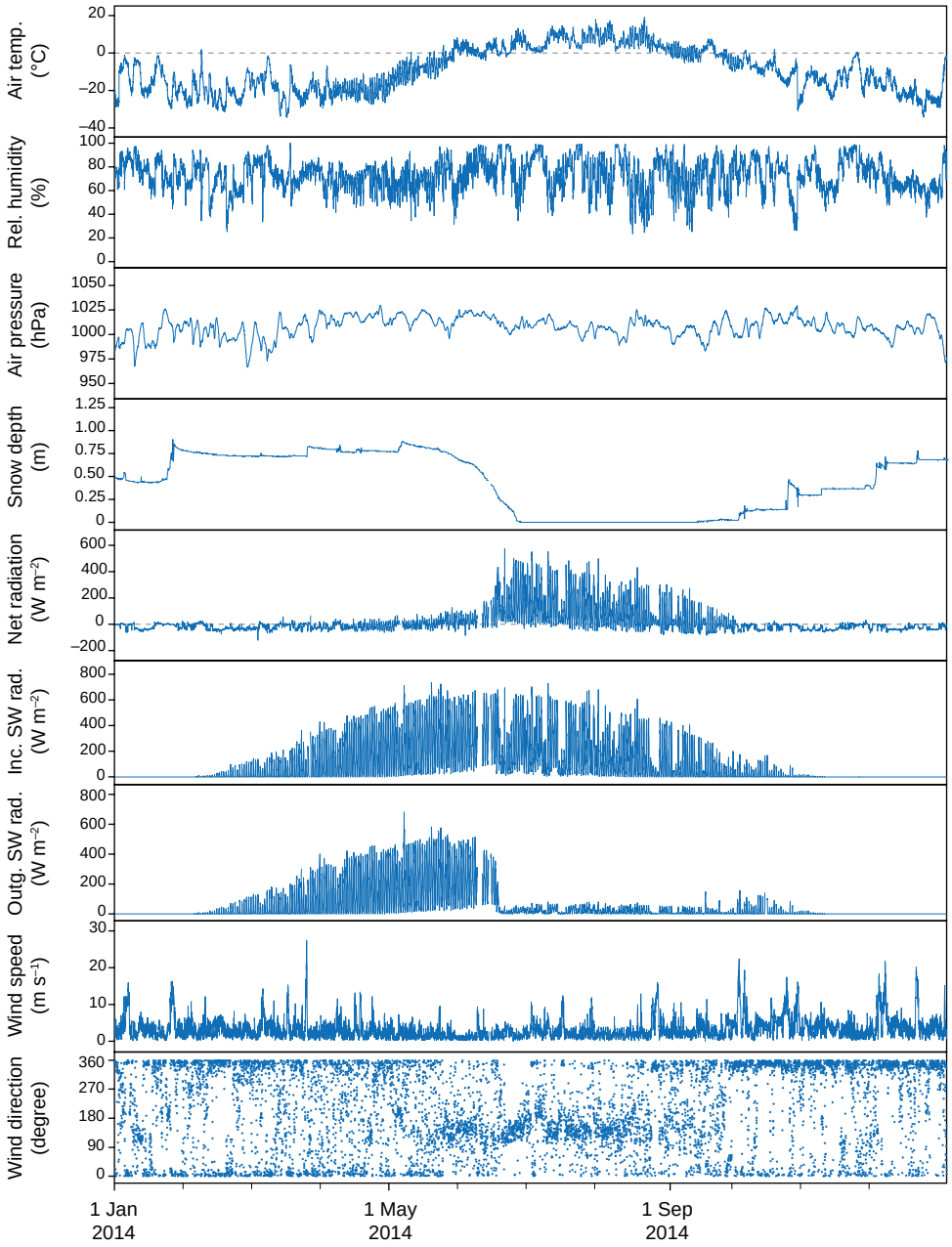

Figure 2.2 Variation of selected climate parameters during 2014. Wind speed and direction are measured 7.5 m above terrain; the remaining parameters are measured 2 m above terrain.

Table 2.1 Monthly mean values of climate parameters 2014.

Month	Air temperature (°C)		Rel. humidity (%)	Air press. (hPa)	Net rad.[1] (W m⁻²)	Shortwave rad.[1] (W m⁻²)		Wind velocity (m s⁻¹)		Dominant wind dir.
	2.0 m[1]	7.5 m				In	Out	2.0 m	7.5 m	7.5 m
Jan	–13.8	–12.8	77	1008.9	–15	0	0	3.1	3.9	N
Feb	–19.4	–17.8	68	1005.4	–26	7	7	2.7	3.2	N
Mar	–18.0	–17.1	70	1003.4	–19	51	49	2.9	3.5	N
Apr	–15.9	–15.1	65	1010.7	–19	166	143	2.4	3.0	N
May	–5.6	–5.1	76	1014.6	4	270	223	1.5	2.0	N
Jun	1.5	1.5	85	1012.6	106	272	128	1.5	1.9	SE
Jul	6.8	6.6	79	1009.2	127	210	24	2.5	3.0	SE
Aug	5.6	5.6	76	1009.8	64	130	17	2.5	3.0	SE
Sept	–0.6	–0.4	70	1003.2	5	62	12	2.7	3.3	NNW
Oct	–7.7	–6.9	78	1008.3	–22	13	12	4.4	5.4	NNW
Nov	–15.2	–14.0	72	1007.8	–26	0	0	2.6	3.2	NNW
Dec	–21.7	–20.3	70	1003.0	–27	0	0	3.9	4.8	NNW

Table 2.2 Annual mean, maximum and minimum values of climate parameters 1996 to 2013.

Year	1996	1997	1998	1999	2000	2001	2002	2003	2004	2005	2006	2007	2008	2009	2010	2011	2012	2013	2014
Annual mean values																			
Air temp., 2 m above terrain (°C)	–9.0	–10.1	–9.7	–9.5	–10.0	–9.7	–8.6	–9.2	–8.5	–7.7	–8.1	–8.7	–8.1	–9.4	–9.7	–8.5	–8.9	–9.0	–8.6
Air temp., 7.5 m above terrain (°C)	–8.4	–9.3	–9.1	–8.9	–9.4	–9.2	–	–8.7	–7.9	–6.9	–7.6	–8.2	–7.9	–8.6	–8.6	–7.4	–7.9	–8.6	–7.9
Rel. air hum., 2 m above terrain (%)	67	68	73	70	70	71	72	71	72	71	72	69	72	71	73	74	72	71	74
Air pressure (hPa)	1009	1007	1010	1006	1008	1009	1009	1008	1007	1008	1007	1006	1008	1010	1012	1005	1009	1009	1008
Incoming short-wave radiation (W m^{-2})	113	104	101	100	107	112	105	104	99	101	107	107	107	104	104	104	108	99	97
Outgoing short-wave radiation (W m^{-2})	52	56	55	56	52	56	54	49	42	43	54	45	52	38	45	45	57	40	51
Net radiation** (W m^{-2})	16	9	6	4	14	13	–	8	–	–	10	13	8	13	9	13	5	16	13
Wind velocity, 2 m above terrain (m s^{-1})	2.7	3.0	2.6	3.0	2.9	3.0	2.8	2.6	3.0	2.9	2.8	2.6	2.9	2.6	2.4	2.6	2.4*	2.8	2.7
Wind velocity, 7.5 m above terrain (m s^{-1})	3.1	3.4	3.2	3.7	3.3	3.4	3.3	3.1	3.6	3.5	3.4	3.2	3.5	3.2	3.1	3.5	3.1	3.7	3.4
Precipitation (mm w.eq.), total	223	307	255	161	176	236	174	263	253	254	171	178	202	169	–	238	93	229	–
Annual maximum values																			
Air temp., 2 m above terrain (°C)	16.6	21.3	13.8	15.2	19.1	12.6	14.9	16.7	19.1	21.8	22.9	16.4	18.4	18.1	16.1	19.7	19.4	17.6	16.5
Air temp., 7.5 m above terrain (°C)	15.9	21.1	13.6	14.6	18.8	12.4	–	16.7	18.5	21.6	22.1	15.6	18.2	17.7	15.7	19.2	17.8	17.1	15.8
Air pressure (hPa)	1042	1035	1036	1035	1036	1043	1038	1038	1033	1038	1038	1037	1043	1034	1046	1031	1030	1052	1035
Incoming short-wave radiation (W m^{-2})	857	864	833	889	810	818	920	802	795	778	833	769	747	822	804	791	837	793	734
Outgoing short-wave radiation (W m^{-2})	683	566	632	603	581	620	741	549	698	629	684	547	563	488	607	578	564	561	681
Net radiation** (W m^{-2})	609	634	556	471	627	602	–	580	–	–	538	469	565	548	539	496	537	575	572
Wind velocity, 2 m above terrain (m s^{-1})	20.2	22.6	25.6	19.3	25.6	20.6	21.6	20.6	22.2	19.9	20.8	27.6	24.5	20.5	17.0	26.6	18.6	21.5	23.0
Wind velocity, 7.5 m above terrain (m s^{-1})	23.1	26.2	29.5	22.0	23.5	25.0	25.4	23.3	25.6	22.0	22.8	29.6	28.9	24.4	23.2	30.1	23.0	25.7	27.3
Annual minimum values																			
Air temp., 2 m above terrain (°C)	–33.7	–36.2	–38.9	–36.3	–36.7	–35.1	–37.7	–34.0	–34.0	–29.4	–38.7	–33.9	–35.3	–33.9	–32.5	–32	–34.7	–33.9	–34.3
Air temp., 7.5 m above terrain (°C)	–31.9	–34.6	–37.1	–34.4	–34.1	–33.0	–	–32.4	–32.1	–27.9	–37.2	–32.5	–33.9	–33.0	–29.3	–29.2	–31.4	–32.7	–32.3
Rel. air hum., 2 m above terrain (%)	20	18	31	30	19	22	23	21	17	22	21	18	24	25	22	18	21	23	25
Air pressure (hPa)	956	953	975	961	969	972	955	967	955	967	968	969	963	967	976	961	967	957	971
Incoming short-wave radiation (W m^{-2})	0	0	0	0	0	0	0	0	0	0	0	0	0	0	0	0	0	0	0
Outgoing short-wave radiation (W m^{-2})	0	0	0	0	0	0	0	0	0	0	0	0	0	0	0	0	0	0	0
Net radiation** (W m^{-2})	–86	–165	–199	–100	–129	–124	–	–98	–	–	–99	–99	–104	–146	–119	–127	–87	–127	–121
Wind velocity, 2 m above terrain (m s^{-1})	0	0	0	0	0	0	0	0	0	0	0	0	0	0	0	0	0	0	0
Wind velocity, 7.5 m above terrain (m s^{-1})	0	0	0	0	0	0	0	0	0	0	0	0	0	0	0	0	0	0	0

* – only 15 % of data for March exists. ** until 2013: NRlite. from 2014: CNR1

Table 2.3 Mean wind statistics based on wind velocity and direction measured at 7.5 m above the surface in 1997, 1998, 2000 and 2002-2014. Calm is defined as wind speed lower than 0.5 m s^{-1}. Maximum speed is maximum of 10 minute mean values. Mean of maxima is the mean of the yearly maxima. The frequency for each direction is given as percent of the time for which data exist. Missing data amounts to less than 1% of data for the entire year.

Year	Mean[1)]				2014		
Direction	Frequency	Velocity (m s^{-1})			Frequency	Velocity (m s^{-1})	
	%	mean	mean of max	max	%	mean	max
N	15.7	5.4	24.7	29.7	20.4	4.7	27.3
NNE	3.6	2.8	18.8	28.9	4.5	3.1	21.1
NE	2.4	2.4	14.9	23.2	2.4	2.0	9.2
ENE	2.7	2.4	12.8	17.4	2.4	1.8	9.0
E	3.7	2.1	8.5	10.7	3.1	1.8	7.8
ESE	6.5	2.5	8.3	10.3	5.7	2.4	8.9
SE	8.8	2.8	9.5	18.1	7.7	2.3	12.6
SSE	5.8	2.7	9.3	16.2	6.0	2.2	11.4
S	4.1	2.6	7.9	9.9	4.5	2.3	6.9
SSW	3.0	2.3	8.2	13.4	3.6	2.1	7.2
SW	2.6	2.1	7.8	12.2	2.6	1.9	11.3
WSW	3.0	2.3	9.3	15.9	2.7	2.1	10.9
W	2.9	2.4	14.8	23.5	2.8	2.1	11.8
WNW	3.4	2.6	15.4	20.6	3.2	2.1	10.1
NW	6.6	3.6	18.3	25.1	5.2	2.9	14.0
NNW	22.2	5.9	23.2	30.1	19.2	5.1	25.2
Calm	3.0				3.8		

[1)]Data from 1997, 1998, 2000, 2002, 2003, 2004, 2005, 2006, 2007, 2008, 2009, 2010, 2011, 2012, 2013 and 2014

in Meltofte and Thing (1996). Once a year the sensors are calibrated and checked by Asiaq – Greenland Survey.

Data for 2014 are shown in figure 2.2 and monthly mean values of climate parameters are listed in table 2.1. Annual values for selected parameters for 1996 to 2014 and mean wind statistics are summarized in tables 2.2 and 2.3, respectively.

Mean annual temperature was 0.4 °C above the long-term mean (1996-2013) with spring and early summer below average and a warm late summer and autumn (figure 2.3).

The first positive air temperatures in 2014 occurred on 26 January, the next time was on 23 April. The maximum temperature measured in 2014 was 16.5 °C on 20 July. During summer, there were six days, when the mean daily temperature exceeded 10 °C, while mean daily temperatures fell below –30 °C only on four days

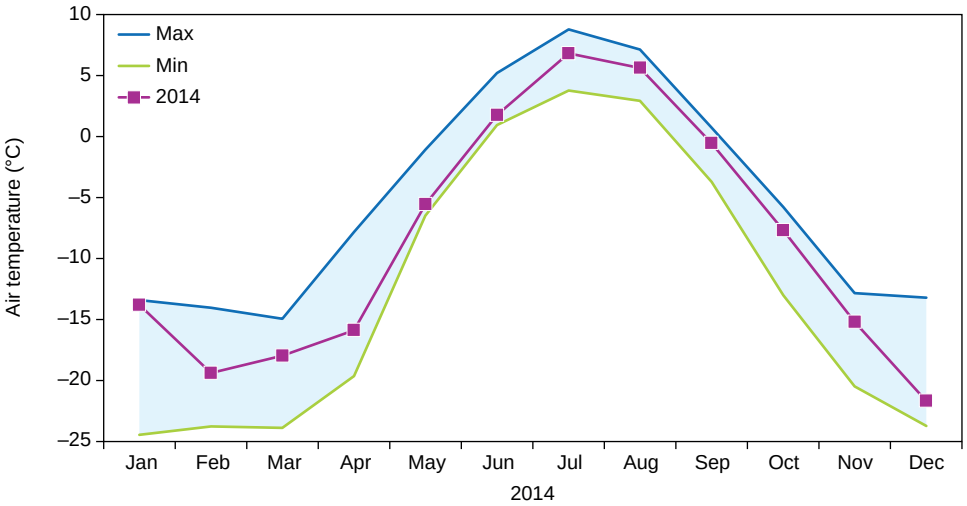

Figure 2.3 Mean monthly air temperatures at Zackenberg as measured at the main climate station during the period 1995-2014.

Table 2.4 Climate parameters for June, July and August, 2003 to 2014. 1 Wind velocity, max is the maximum of 10 minute mean values. From July 2009, the monthly mean values are calculated on the basis of the 30 minute time series where available.

Year	Month	Shortwave rad. (W m^{-2})		Net rad. (W m^{-2})	PAR (µmol m^{-2} s^{-1})	Air temperature (°C)			Precip. (mm)	Wind velocity (m s^{-1})		Dominant wind dir.
		mean in	mean out	mean	mean	mean 2 m	min. 2 m	max. 2 m	total	mean 7.5 m	max[1)] 7.5 m	7.5 m
	Jun	294	108	106	612	2.2	–4.8	14.7	7	1.6	5.4	SE
2003	Jul	210	26	96	431	7.7	1.8	16.7	6	2.8	14.2	SE
	Aug	151	20	56	313	6.6	–0.5	15.4	3	2.5	10.1	SE
	Jun	279	73	111	571	2.5	–3.4	19.1	3	2.3	13.6	SE
2004	Jul	225	30	95	464	7.2	–0.7	19.0	10	2.8	10.5	SE
	Aug	150	20	62	302	5.6	–1.4	17.2	4	2.4	12.6	SE
	Jun	261	53	–	519	2.7	–3.5	13.4	6	2.4	11.8	SE
2005	Jul	215	29	–	428	6.9	–0.6	21.8	28	2.9	13.3	SE
	Aug	154	21	51	321	4.6	–2.7	14.0	4	3.2	10.9	SE
	Jun	312	208	54	675	1.0	–4.4	9.5	0	1.7	6.9	SE
2006	Jul	256	28	131	550	6.6	–1.2	22.8	12	2.5	11.3	SE
	Aug	158	21	61	336	5.5	–4.5	16.3	2	2.6	12.0	SE
	Jun	287	86	116	609	3.3	–2.4	15.8	9	2.2	14.8	SE
2007	Jul	251	32	118	531	5.9	–1.8	16.4	8	2.2	6.5	SE
	Aug	149	20	56	320	6.6	–2.6	13.6	6	2.7	12.3	SE
	Jun	284	145	74	612	5.2	–1.5	12.8	3	1.9	11.7	ESE
2008	Jul	260	32	126	551	8.8	0.0	18.4	8	2.8	14.2	SE
	Aug	141	19	51	296	8.0	0.3	17.1	49	3.3	16.9	SE
	Jun	257	32	134	532	1.9	–2.4	9.3	3	2.6	11.0	SE
2009	Jul	233	30	103	487	7.9	0.4	18.1	26	3.3	15.4	SE
	Aug	145	18	48	292	4.4	–1.8	11.6	31	2.8	24.4	SE
	Jun	272	95	98	548	1.9	–8.1	12.8	13	2.0	10.2	SE
2010	Jul	264	40	123	529	5.3	–1.7	15.1	1	2.6	15.7	SE
	Aug	164	27	58	325	5.3	–2.6	16.1	2	2.6	15.0	SE
	Jun	301	84	122	590	2.3	–5.9	13.8	1	2.1	12.3	SE
2011	Jul	255	41	118	503	5.8	–0.8	16.1	6	2.4	15.0	SE
	Aug	149	23	61	–	5.6	–2.4	19.7	33	2.7	12.6	SE
	Jun	295	182	60	–	3.1	–3.7	13.5	2	1.6	9.9	SE
2012	Jul	239	31	117	–	7.4	0.5	18.3	4	2.3	6.6	SE
	Aug	154	24	56	–	7.1	–2.1	19.4	7	2.9	11.8	SE
	Jun	290	39	176	614	3.0	–2.8	12.6	2	3.0	17.2	SE
2013	Jul	231	34	134	496	7.2	–0.8	17.6	7	3.3	12.2	SE
	Aug	127	20	–	276	5.4	–1.3	16.1	76	3.8	17.8	SE
	Jun	272	128	106	599	1.5	–7.8	14.8	–	1.9	13.0	SE
2014	Jul	210	24	127	454	6.8	–0.7	16.7	40	3.0	12.9	SE
	Aug	130	17	64	282	5.6	–0.2	13.8	28	3.0	16.1	SE

in late December. The continuous period of mean daily temperatures above 0 °C was seven days longer than the 1996-2013 average, caused by an onset (8 June) that was earlier than average.

Monthly mean values of selected climate parameters for June, July and August from 2003-2014 are shown in table 2.4. In each summer month of 2014 night frost occurred and the predominant wind direction was from the southeast (SE). Growing degree days (sum of daily mean air temperature above 0 °C) were slightly below the 1996-2014 average (table 2.5). The first negative mean daily temperature was measured on 5 September.

Table 2.5 Positive degree-days calculated on a monthly basis as the sum of daily mean air temperature above 0 °C.

Degree days	1996	1997	1998	1999	2000	2001	2002	2003	2004	2005	2006	2007	2008	2009	2010	2011	2012	2013	2014
Jan										1.5		3.6							
Feb																			
Mar																			
Apr								0.2	1.1		2.9								
May	1.1	1.3	0.1	3.6	0.5	0.5	18.2	3.3	4.1	5.4	3.1		10.0	12.3	0.4	0.6	12.7	3.4	0.5
Jun	63.7	74.6	32.5	52.9	71.8	68.2	81.8	74.2	73.9	84.6	37.2	99.7	155.0	64.6	73.3	78.1	95.9	87.5	72.6
Jul	181.0	115.4	147.36	192.7	164.4	152.0	175.6	237.2	222.2	214.7	205.3	182.2	270.8	265.6	165.6	180.1	229.4	222.1	209.6
Aug	140.5	154.2	143.6	89.2	127.3	181.2	152.5	203.2	169.4	141.5	171.5	204.5	213.7	141.3	164.3	172.5	219.4	167.4	172.8
Sep	15.3	4.5	11.3	19.7	5.7	31.1	41.2	42.5	41.4	17.7	15.7	10.1	63.1	8.9	29.6	18.7	32.7	48.7	27.6
Oct		1.5				0.3	1.8										0.0		0.6
Nov																			
Dec																			
Sum	401.7	351.5	334.8	358.0	369.7	433.2	471.1	560.6	514.8	466.4	435.7	500.1	712.6	492.7	433.2	450.1	590.0	529.1	483.6

2.2 Climate gradients, snow, ice and permafrost

In order to increase the spatial resolution of meteorological data and to describe the gradients (both altitudinal and coast/inland), several smaller automatic weather stations have been installed in the area. In 2003, the station M2 was installed in the valley and the station M3 was installed half-way up on the Aucella mountain (Rasch and Caning 2004). M7 was installed in 2008 in the area just west of Store Sø in Store Sødal (Jensen and Rasch 2009). In 2013 an automatic weather station was also installed near the top of the Zackenberg mountain (1150 m above sea level), in order to record standard meteorological parameters, with the objective to optimize meteorological modelling for the entire valley. However, due to technical problems, data from this station are not yet available for the public. Furthermore, there are three automatic weather stations operating on the A.P. Olsen Glacier and data from these are reported in the GlacioBasis section.

Monthly mean temperatures from the four weather stations are shown in figure 2.4. The three lower altitude stations (M2, climate station and M7) experienced lower temperatures on average than M3 from March to June. This is mainly due to the effect of cold air sinking down during calm weather and creating frequent inversions. Data from M3 in December, January and February are not reported as measurements were sporadic due to insufficient power supply. Furthermore, the M3 average for July is based on data from 1-24 July, as data from the last week of July were lost due to problems with data retrieval. At M2 data are missing from 22-26 July. No data are missing from M7 and the climate station.

Winter hot spells (where the temperature suddenly rises above the freezing point) were only registered at the low altitude weather stations. On 26 January 21:00 the temperature at M2 became positive and stayed above zero until 27 January 7:00, reaching a maximum of 0.6 °C. At M7 the temperature reached 0.1 °C in the hours between 4:30 and 7 on 27 January and at the climate station a maximum of 0.9 °C was registered during the period from 26 January 22:00 to 27 January 10:00. Whether the hot spell also occurred on the Aucella slope at 400 meters altitude, cannot be determined due to the lack of data from the M3 station.

Figure 2.4 Mean monthly temperatures September 2013 to September 2014 from automatic weather station M2 (17 m a.s.l.), M3 (420 m a.s.l.), the climate station on the heath (38 m a.s.l.) and M7 (145 m a.s.l.).

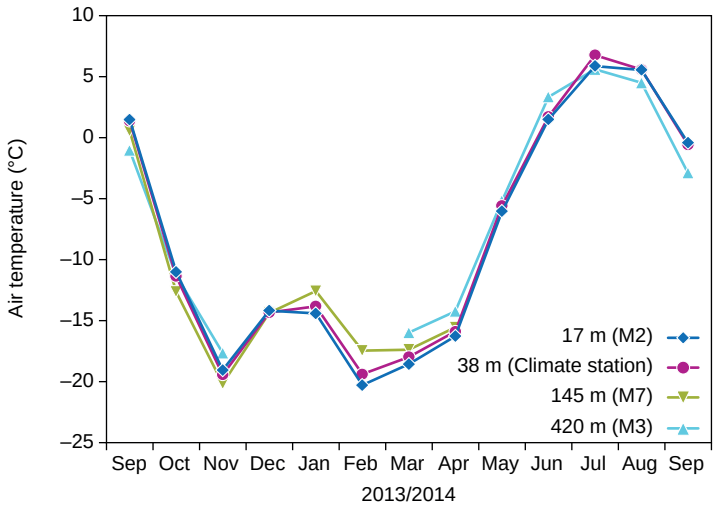

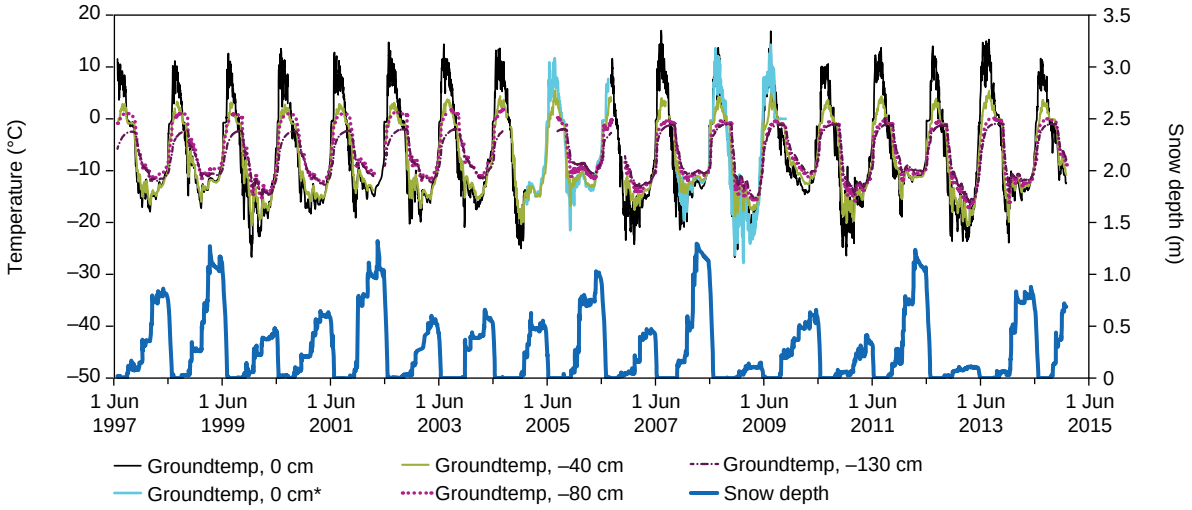

*Figure 2.5 Daily mean soil temperatures and snow depth from the climate station. In August 2006 soil temperature sensors were replaced. *Data from sensor at the climate station.*

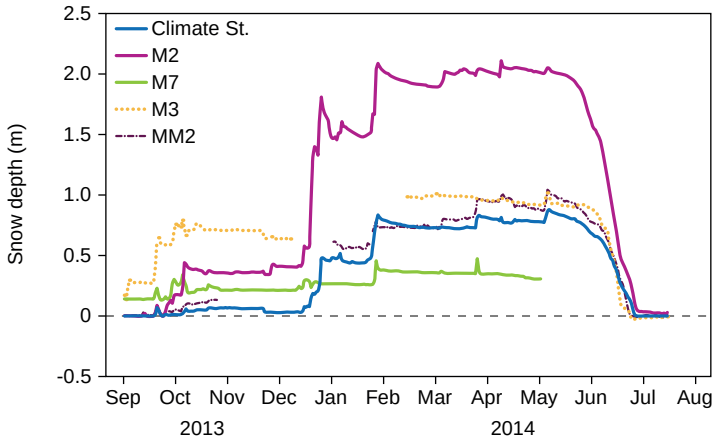

Figure 2.6 Snow depths at the automatic weather stations, M2 (17 m a.s.l.), M3 (420 m a.s.l.), M7 (145 m a.s.l.), the climate station (38 m a.s.l.) and MM2 (40 m a.s.l.).

Snow depth

The snow depth measured at the climate station was slightly above average for the 1997-2013 period, corresponding to the end of winter snow depths of the winters 1998 and 2006. Snow started to build up at the beginning of December and reached its maximum of about 85 cm at the beginning of May (figure 2.5 and figure 2.6). The snowmelt started shortly after, in the middle of May and the ground was free of snow on 26 June (table 2.6 and figure 2.6).

Snow depth is also measured at the automatic weather stations M2, M3, M7 and MM2 (figure 2.6). However, gaps in data during winter (especially at M3 and MM2) exist, due to insufficient power supply. The build-up of the snow pack started earlier on the slope of Aucella (M3), in late September, compared to the stations in the valley, where the build-up started in December. Contrary, the size of the snow pack in Store Sødal (M7) is much more stable over the winter period, due to the exposed location of the mast. The snow

Table 2.6 Key figures describing the amount of snow at the climate station during the last 17 winters.

Winter	1997/1998	1998/1999	1999/2000	2000/2001	2001/2002	2002/2003	2003/2004	2004/2005	2005/2006
Max. snow depth (m)	0.9	1.3	0.5	0.7	1.3	0.6	0.7	0.7	1.1
Max. snow depth reached	29 Apr	11 Mar	19 May	25 Mar	15 Apr	13 Apr	13 Apr	12 Feb	26 Apr
Snow depth exceeds 0.1 m from	19 Nov	27 Oct	1 Jan	16 Nov	19 Nov	6 Dec	24 Nov	27 Dec	19 Dec
Snow depth is below 0.1 m from	25 Jun	3 Jul	14 Jun	24 Jun	20 Jun	14 Jun	13 Jun	7 Jun	1 Jul

Winter	2006/2007	2007/2008	2008/2009	2009/2010	2010/2011	2011/2012	2012/2013	2013/2014
Max. snow depth (m)	0.6	1.3	0.2	0.7	0.4	1.3	0.1	0.9
Max. snow depth reached	4 May	6 Mar	17 Feb	19 May	25 Apr	17 Mar	30 Mar	7 May
Snow depth exceeds 0.1 m from	12 Jan	26 Oct	29 Jan	25 Sep	26 Jan	14 Oct	5 Mar	19 Dec
Snow depth is below 0.1 m from	8 Jun	24 Jun	16 May	16 Jun	10 Jun	26 Jun	–*	25 Jun

*Winter 2012/2013 had exceptionally low snow height; 0.1 m were reached various times during the winter.

pack at M2 is generally double the snow pack on the heath (Snow mast) and the fen (MM2), due to the south facing slope at this site, which is leeward of the dominating wind direction during winter storms.

In order to achieve a better spatial resolution of snow depths for modelling, snow depths are also being measured along two main transects: one transect (called SNM) running from Lomsø into the valley and another (called SNZ) running along the ZERO-line from the old delta up to 420 m a.s.l. These snow depths are used as input for the Snow Model covering the central valley.

At the beginning of October 2014, the valley was more or less completely covered by 10 cm of new snow with a bulk density of 0.23 g cm^{-3}. As for most occasions with snow fall in the valley, it occurred during periods characterized by high wind speeds packing the snow.

Snow cover

The thickness and extent of the snow cover at the end of the 2013/2014 winter was approximately the same as the average for the 1998-2013 period. Snow depletion started in late May and was accelerated by a ten day period at the beginning of June with almost no cloud cover and relatively high temperatures. This rapid melt slowed down in the second part of June, due to cloudy and unstable weather. The date with 50 % snow cover was 25 June, which is a little later than the average for the whole period (figure 2.7).

The snow cover of 10 June is used to compare early season conditions in different biological sub-sections. In 2014 the snow cover on this date was higher in all regions (except region 6 and 7 on Palnatoke mountain), compared to the long-term mean (table 2.7).

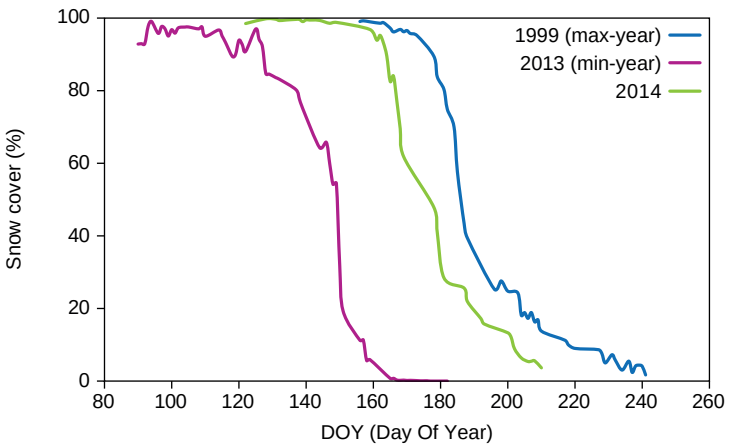

Figure 2.7 Snow depletion curves for the central part of the Zackenberg valley and the lower slopes of the mountain Aucella. The three years shown in the figure are 2013 with very early melt off, 1999 with late melt off and the depletion curve for 2014. Curves exist from 1998-2014.

*Table 2.7 Area size and snow cover 10 June in 13 bird and mammal study sections in the Zackenberg valley and on the slopes of the mountain Aucella 1995-2014 and mean for the period 1995-2013 (see figure 4.1 in Caning and Rasch 2003 for map of sections). Photos were taken from a fixed point 480 m a.s.l. on the east facing slope of the mountain Zackenberg within +/- three days of 10 June and extrapolated according to the methods described by Pedersen and Hinkler 2000. Furthermore, the proportions of the areas not visible from the photo point are given. *Based on satellite photos (9 June 1995 and 11 June 1996). Grey values are based on only part of the given section due to missing photo coverage.*

Section	Area (km^2)	Area hidden (%)	1995*	1996*	1997	1998	1999	2000	2001	2002	2003	2004	2005	2006	2007	2008	2009	2010	2011	2012	2013	2014	Mean (1995-2013)
1 (0-50 m)	3.52	3.5	78	74	65	77	91	60	73	77	68	48	31	74	38	62	13	53	51	77	2	75	59
2 (0-50 m)	7.97	7.1	89	88	90	85	91	57	87	87	92	49	25	81	43	77	5	61	47	81	2	78	65
3 (50-150 m)	3.52	0.0	88	81	83	83	94	51	89	82	83	51	35	77	40	74	11	48	32	86	1	87	62
4 (150-300 m)	2.62	0.0	73	74	68	66	86	33	79	56	73	39	28	65	36	54	19	32	23	85	0	85	52
5 (300-600 m)	2.17	0.0	16	54	73	43	85	31	56	36	49	16	25	62	25	46	17	12	15	80	0	78	39
6 (50-150 m)	2.15	67.8	86	86	84	87	98	55	84	78	74	56	50	80	50	59	18	49	11	29	0	29	60
7 (150-300 m)	3.36	64.2	90	81	76	90	97	54	84	74	90	56	46	82	58	69	34	44	15	34	1	34	62
8 (300-600 m)	4.56	26.1	49	55	66	64	84	37	45	52	66	30	29	67	26	45	16	25	9	60	1	61	43
9 (0-50 m)	5.01	8.2	92	87	96	91	97	54	96	96	100	58	23	73	49	80	18	56	66	77	3	84	69
10 (50-150 m)	3.84	2.9	94	85	95	97	98	60	97	93	100	56	47	92	57	85	43	55	80	92	4	96	75
11 (150-300 m)	3.18	0.2	91	72	86	92	96	69	97	88	100	66	61	88	54	73	77	51	79	90	9	100	76
12 (300-600 m)	3.82	0.0	40	66	89	68	89	65	73	65	98	53	70	85	38	53	64	43	50	71	11	94	63
13 (Lemmings)	2.05	11.4	89	80	76	80	87	58	83	83	89	46	25	79	41	73	4	64	49	72	0	70	62
Total area	45.70	13.8	76	77	81	80	92	54	82	77	83	49	37	77	43	65	28	44	41	72	4	77	61

Active layer depth

Development of the active layer (the layer above the permafrost that thaws during the summer) starts when the air temperature becomes positive and snow has disappeared from the ground. The depth of soil thaw was measured throughout the field season at two grid-plots: ZERO-CALM-1 (ZC-1) covering a 100×100 meter area with 121 grid nodes and ZERO-CALM-2 (ZC-2) covering a 120×150 meter area with 208 grid nodes.

In ZC-1, the first grid node was free of snow on 17 June and on 26 June the first active layer measurements were carried out when only a few spots of snow were left in this relatively homogenous grid site. The maximum thaw depth was reached by 1 September and was approx. 1 cm less than previous maximum thaw depths measured in these grids (figure 2.8 and table 2.8).

In ZC-2, one grid node was free of snow on 3 June and the first 23 grid nodes were measured on 8 June. The snow patch in ZC-2 was melted away on 27 July and all grid nodes were by then free of snow. The maximum thaw depth was reached early September. The average depth of the active layer was a little higher than the average for the entire monitoring period.

Data from the two ZEROCALM-sites are reported to the circumpolar monitoring programme CALM III (Circumpolar Active Layer Monitoring-Network (2009-2014)) maintained by the University of Delaware, Centre for International Studies (http://www.gwu.edu/~calm).

Figure 2.9 Glacier dammed lake at A.P. Olsen. The lake was empty in the fall of 2014 and there was no build-up during winter 2014/2015.

Lake drainage

Photos from the digital camera at the A.P. Olsen glacial dammed lake were collected on 30 April 2015. The camera was installed in April 2008 to cover fluctuations of the glacier dammed lake (figure 2.9). Daily photos have been obtained since 10 May 2008 except from a gap between October 2009 and May 2010 because of a full memory card. The camera only worked until 23 September 2014, thus photos from

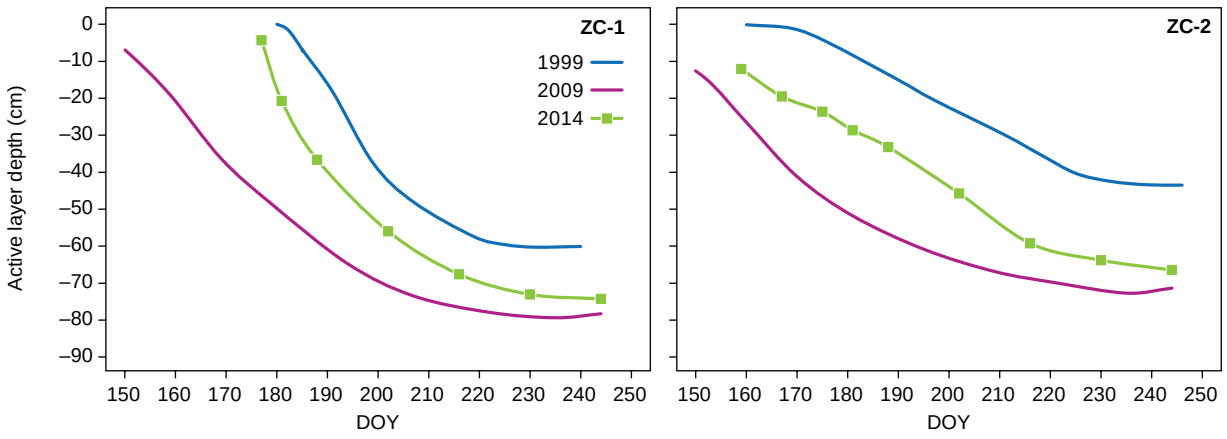

Figure 2.8 Thaw depth progression in ZEROCALM-1 and ZERO-CALM-2 during summer 2014 (green line). Minimum and maximum thaw years (1999 and 2009, respectively) are shown in blue and red respectively.

Table 2.8 Average maximum thaw depth (in cm) for grid points in ZEROCALM-1 and ZEROCALM-2 measured late August, 1997-2014.

	1997	1998	1999	2000	2001	2002	2003	2004	2005	2006	2007	2008	2009	2010	2011	2012	2013	2014
ZEROCALM-1	61.7	65.6	60.3	63.4	63.3	70.5	72.5	76.3	79.4	76.0	74.8	79.4	79.4	78.2	82.0	82.4	74.7	74.3
ZEROCALM-2	57.4	59.5	43.6	59.8	59.7	59.6	63.4	65.0	68.6	67.6	67.1	67.5	72.9	69.5	75.3	72.1	69.6	66.6

the winter 14/15 are missing. The lake was emptied between the 15 and 16 August 2014 and had not built up, when visited in late April 2015.

2.3 River water discharge and sediment transport

The river Zackenberg

The drainage basin of Zackenbergelven includes Zackenbergdalen, Store Sødal, Lindemansdalen and Slettedalen. The basin covers an area of 514 km^2, of which 10^6 km^2 are covered by glaciers. The first hydrometric station was established in 1995 on the western river bank near the river mouth (Meltofte and Thing 1996). In 1998 the hydrometric station was moved to the eastern bank of the river, due to problems with the station being buried under thick snowdrifts each winter. The station stayed at the river near the barracks, however, in the course of the years, it has been destroyed several times by major floods from the ice-dammed lake at the A.P. Olsen Land.

In 2014, an entirely new hydrometric station has been built at the new bridge, ca 600 m further up the river from the old station. The time series can be considered consistent with previous years as there are no additional riverets between the two locations feeding into Zackenbergelven. Being mounted on the bridge directly, we are optimistic that it suffers less from the outburst flood from the ice-dammed lake.

Water level, water temperature, air temperature, conductivity and turbidity are logged every 15 minutes. Since 2014 also surface flow velocity is logged permanently. The water level is measured with a sonic range sensor and different pressure transducers. For 2014, both the old and the new station have been running in order to have a backup dataset. The new station's data have been used for the data analyses.

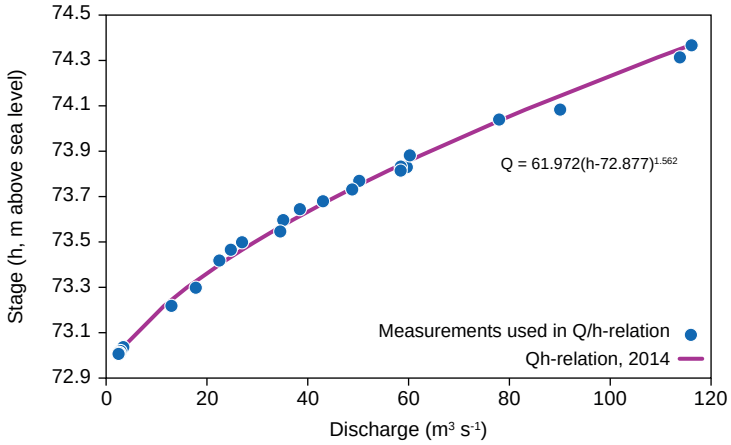

Figure 2.10 Stage-discharge relation (Q/h-relation) for the river Zackenberg at the new hydrometric station for 2014.The coefficient of correlation (R2) is 0.998.

Q/h-relation

With the relocation of the station to the bridge it was necessary to establish a new Q/h-relation. Discharge measurements have been carried out both with propellers and with an Acoustic Doppler Current Profiler (ADCP, type: Q-liner). The operation of the Q-liner has greatly improved due to the better setup at the bridge.

In 2014, 44 discharge measurements were carried out of which 24 fed into the valid Q/h-relation (figure 2.10).

The ones that have not been used in the Q/h-relation have been performed when the river was still influenced by ice (Larsen *et al.* 2011).

River water discharge

In 2014, water started to flow on 4 June and after a steep increase of discharge during the first half of June, the first maximum, mainly triggered by snowmelt, was reached on 17 June (75 m^3 s^{-1}) (figure 2.11). Only exceeded by the flood

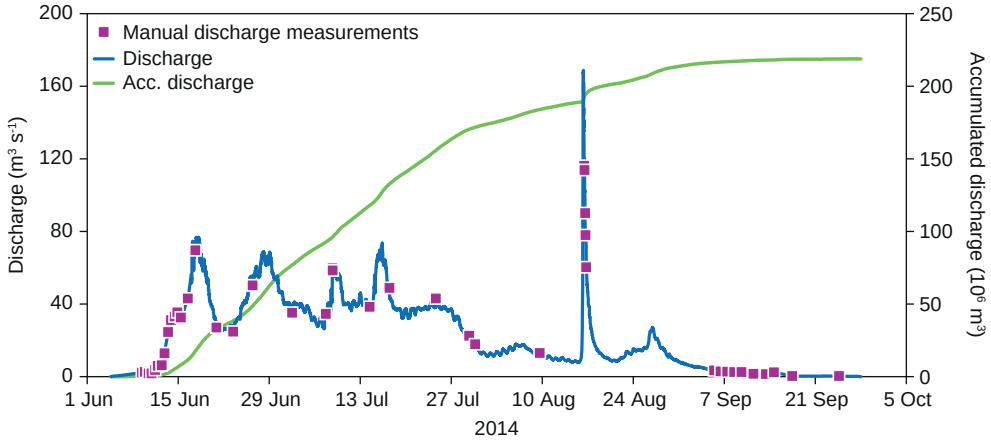

Figure 2.11 River water discharge in the river Zackenberg in 2014.

*Table 2.9 Total discharge in river Zackenberg in the years 1996-2014, corresponding water loss for the drainage area (514 km²) and precipitation measured at the meteorological station. [1)]The hydrological year is set to 1 October previous year to 30 September present year. *For 2005 no data is available during the flood from 25 July 05:00 until 28 July 00:00. After this date and until the new hydrometric station was set up 5 August the discharge are estimated from manual readings of the water level from the gauge. **Too many missing values in order to provide a total annual precipitation value.*

Hydrological year[1)]	1996	1997	1998	1999	2000	2001	2002	2003	2004	2005	2006	2007	2008	2009	2010	2011	2012	2013	2014
Total discharge (10^6 m^3)	132	188	232	181	150	137	338	189	212	>185*	172	183	201	146	173	197	231	147	219
Water loss (mm)	257	366	451	352	292	267	658	368	412	>360	335	356	391	284	337	383	449	286	426
Precipitation (mm)	239	263	255	227	171	240	156	184	279	266	206	133	219	157	>125**	189	166	249	>287**
Total annual transport																			
Suspended sediment (ton)		29.4	130.1	18.7	16.1	16.9	60.1	18.2	21.9	71.3	27.2	51.1	39.0	44.7	23.5	38.3	31.1	35.3	30.3
River break-up	late May	4 Jun	10 Jun	9 Jun	8 Jun	8 Jun	4 Jun	30 May	1 Jun	3 Jun	12 Jun	2 Jun	7 Jun	22 May	30 May	23 May	6 Jun	15 May	4 Jun

later in the season, this was the strongest discharge observed at Zackenbergelven in 2014, occurring less than two weeks after the onset of the river flow. During June and July about three quarters of the total annual runoff occurred with fluctuations both caused by snowmelt and temperature variations. Discharge dropped below 20 m^3 s^{-1} in late July and values remained quite low until the flood on 16 August 2014. Several manual discharge measurements were performed during the flood, which allows an estimate of the maximum discharge of around 168 m^3 s^{-1}. After the flood only one last major discharge peak occurred around 27 August, associated with a heavy precipitation event and up to 26 m^3 s^{-1} runoff. The river started to build up ice gradually and froze entirely on 27 September. Total annual runoff was 219x10^6 m^3 (table 2.9).

Suspended sediment and river water chemistry

Three times a week water samples were collected in the morning (8:00) and in the evening (20:00) in order to determine suspended sediment concentrations (SSC). As shown in figure 2.12b, SSC shows highest concentrations at the end of June/beginning of July. Sediment concentrations are generally higher in the evening, except on special occasions, like the 16 July, where the concentration was much higher in the morning, due to heavy rainfall in the previous days. This diurnal pattern followed the diurnal variation in discharge (figure 2.12a) and was the most pronounced in the first half of the season, when diurnal discharge variations were greater. The relatively low sediment concentration in August and September is directly linked to the falling water table, resulting in less bank erosion along the Zackenberg River.

Early in the morning on the 16 August there was a summer river burst. The highest suspended sediment concentration measured during this event was 5245 mg l^{-1} at 8:00 on the 16 August (figure 2.12b). The SSC did not stabilize until the night on the 18 August. During the runoff period until 27 September, the total suspended sediment transport amounted to 30348 ton (table 2.9). In order to compare values between years, the total amount of sediment given is based solely on the SSC measured in the morning, but includes any measurements carried out during flood events. If evening values were included, the total transport in 2014 would amount to 45575 ton. This indicates that all the calculated sediment yields given in the table are underestimated.

Water samples for dissolved organic carbon were collected once a week during the season. As shown in figure 2.12c, the content was high at the beginning of the season and then very stable over the rest of the season. Unfortunately, no samples for DOC were taken during the surge on 16 August.

Daily variations of conductivity and water temperature are shown in figure 2.12d and 2.12e, respectively. The very first meltwater early in the season shows high conductivity; a well-known phenomenon ascribed to solutes being washed

out of the snow (Rasch *et al.* 2000). During summer the conductivity was relatively stable. The conductivity in the river peaks during rainy periods due to increased surface and subsurface drainage from land, transporting solutes from the terrestrial environment to the fjord system.

Three to four times during the season, soil water was collected from various depths in the active layer at four different sites; *Cassiope* heath, *Salix arctica* heath, mixed heath vegetation and a fen site. Water collected from these sites has been analysed for chemical composition.

2.4 Soil water

Soil moisture and soil water

Variation in soil moisture content is measured at several sites. In the field season, soil moisture was measured once a week at all the soil water sites and in two transects in ZC-2 (the active layer grid site). Besides the manual measurements, soil moisture is monitored continuously at three automatic stations; M2, M3 and M4 (figure 2.13). M2 is located on a slope and affected by large snow accumulation but dries out quickly due to the primarily sandy material. M3 is located on a gentle slope at 420 m a.s.l. and in the early summer this site is affected by flow of meltwater from snow patches further up the mountain. Finally, M4 is located in the *Cassiope* heath just north of the meteorological station.

The early season peak in soil moisture, following snowmelt, was a couple of days delayed at M2 compared to M3 (no data exist for the snowmelt period from M4 due to unstable power supply). The thickness of the snow pack at M2 was about double the size of the snow pack at M3. Following the snowmelt period there was a relatively steady drying at M2, only interrupted by rain events on 18 July and 28 August. At M3 the soil moisture at 10 and 30 cm depth was more or less constant over the growing season, before the soil started freezing in September. This was probably due to the relatively wet summer of 2014, with several periods with unstable weather in both July and August, resulting in relatively continuous runoff from snow fans. The rain events around 18 July and 28 August are also depicted in the soil moisture measurements at M4, where there was a delay of 6 days between 5 cm and 50 cm depth during the first event and almost no delay during the second event. Soil moisture decreased rapidly at all three sites in the first part of September and by mid-October most of the active layer was frozen at these sites.

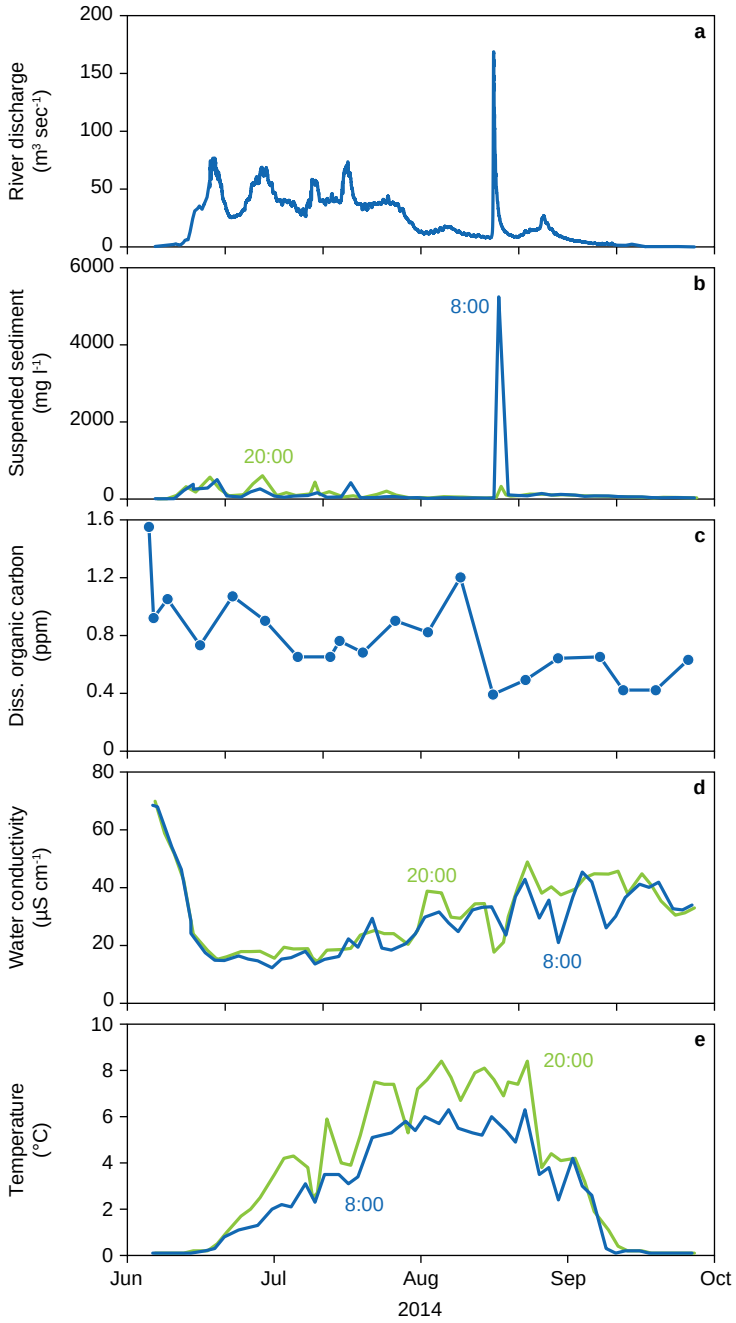

Figure 2.12 Seasonal variations of selected parameters in the river Zackenberg: River discharge (a), suspended sediment concentrations at 08:00 (blue line) and 20:00 (green line) (b), dissolved organic matter (c), conductivity at 08:00 (blue line) and 20:00 (green line) (d), Water temperature at 08:00 (blue line) and 20:00 (green line) (e).

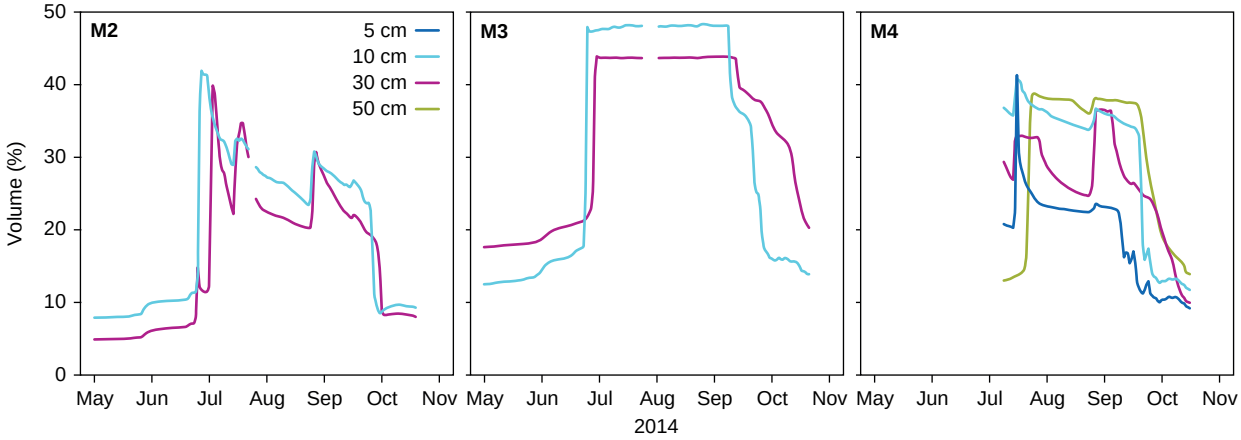

Figure 2.13 Soil moisture content throughout the field season 2014 at the three automatic weather stations M2, M3 and M4.

2.5 Carbon gas fluxes

Carbon gas fluxes are monitored on plot and landscape level in the Zackenberg valley using two measurement techniques:

- Automatic chamber measurements of CH_4 and CO_2 exchange on plot scale in a fen site
- Eddy covariance measurements of CO_2 and H_2O exchange on landscape scale in heath and fen sites

Automatic chamber measurements

The CH_4 exchange has been monitored in six automatic chambers in a wet fen area (AC) since 2006 (Klitgaard *et al.* 2007). During 2011-2012, the automatic chamber system has been expanded to include four new chambers, giving a total of ten chambers. The temporal variation in CH_4 production is mainly associated with temperature, water table depth and substrate quality and availability. It has also been found from this site that autumn time frost action resulting in accumulated CH_4 gas being squeezed out from the soil matrix can be of high importance for the annual CH_4 exchange (Mastepanov *et al.* 2008).

In 2014, CH_4 flux measurements began 22 June and lasted until 20 October (figure 2.14). In general, the measurement system performed well throughout the period with only minor gaps in data due to maintenance and interruptions during periods with anticipated high wind speeds. When measurements began shortly after snowmelt and until early July, CH_4 fluxes were generally below 0.1 mg CH_4 m^{-2} h^{-1}. During the end of July/early August, CH_4 peaked around 2.5 mg CH_4 m^{-2} h^{-1}. The peak was followed by a steady decrease. During the end of the measurement period, there were a few occasions of high emissions (figure 2.14), possibly associated with frost action releasing CH_4 stored in the soil profile.

The growing season fluxes were similar to those observed in 2012 but lower than in 2007, which was the year with the highest emissions on record. However, it should be noted that since the number of chambers have been increased, the averages are not fully comparable between years.

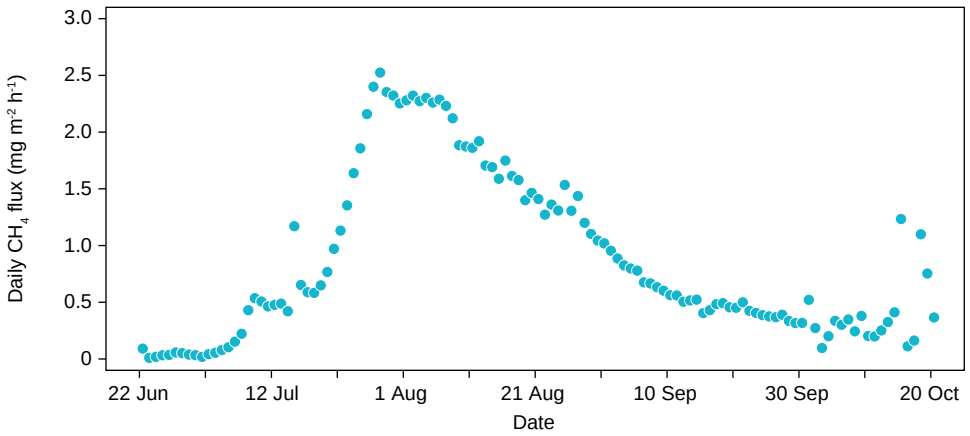

Figure 2.14 Daily average methane fluxes measured at the fen site (AC) in 2014.

Eddy covariance measurements

The land-atmosphere exchange of CO_2 is measured using the eddy covariance technique in two sites in Zackenberg: one located in a *Cassiope* heath site (MM1) where measurements have been conducted since 2000, and one located in a wet fen area (MM2) where measurements have been conducted since 2007. The heath site instrumentation consists of a 3D sonic anemometer (Gill R3) and a closed-path CO_2 and H_2O gas analyser (Licor-7000). See Klitgaard *et al.* (2008) and Rasch and Caning (2003) for further details on the heath site instrumentation. The fen site instrumentation was upgraded in 2011 to include a 3D sonic anemometer (Gill HS) and an enclosed-path CO_2 and H_2O gas analyser (Licor-7200); see Jensen (2012) for more details.

The temporal variation in the mean daily net ecosystem exchange of CO_2 (NEE) and air temperature during 2014 for the heath and fen sites are shown in figures 2.15 and 2.16 and tables 2.10 and 2.11. NEE refers to the sum of all CO_2 exchange processes; including photosynthetic CO_2 uptake by plants, and plant and microbial respiration. The CO_2 exchange is controlled by climatic conditions, mainly temperature and photosynthetic active radiation (PAR), along with amount of biomass and soil moisture content. The sign convention used in figures and tables is the standard for micrometeorological measurements: fluxes directed from the surface to the atmosphere are positive, whereas fluxes directed from the atmosphere to the surface are negative.

Heath site

Eddy covariance CO_2 flux measurements at the heath site (MM1) in 2014 were initiated 20 April and lasted until 18 October (figure 2.15). When measurements began, the heath was covered by a thick layer of snow, amounting to approx. 0.8 m. During the cold, snow-covered period in late April and May, CO_2 fluxes were small, generally below 0.1 g C m^{-2} d^{-1}. As the snow began to melt in June, fluxes increased and a maximum spring-time daily NEE was recorded on 27 June, amounting to 0.55 g C m^{-2} d^{-1}. As the vegetation developed during July, the photosynthetic uptake of CO_2 started, and on 16 July the heath ecosystem switched from being a source to a sink for atmospheric CO_2 on a daily basis. This is the latest start of a net uptake period on record, related to the late timing of snowmelt.

The period with net CO_2 uptake ended 19 August, which is among the latest end of a net uptake period on record. The onset of the uptake period varies from year to year due to timing of snowmelt. The end of the uptake period is more stable as it is governed by fading solar radiation. The accumulated CO_2 uptake during the net uptake period in 2014, –17.7 g C m^{-2}, is among the least on record (in 2001 and 2002 the accumulated uptake during net uptake period was –17.5 and –16.6 g C m^{-2}, respectively). The maximum diurnal CO_2 uptake (–1.01 g C m^{-2} d^{-1}, measured 26 July) is less than the mean of all years (–1.14 g C m^{-2} d^{-1}).

By 19 August, ecosystem respiration exceeded gross primary production and the heath ecosystem returned to being a net source for atmospheric CO_2. At the beginning of this period, soil temperatures remain comparably high, allowing decomposition processes to continue at a decent rate. Highest autumn daily emission was measured on 25 August (0.40 g C m^{-2} d^{-1}).

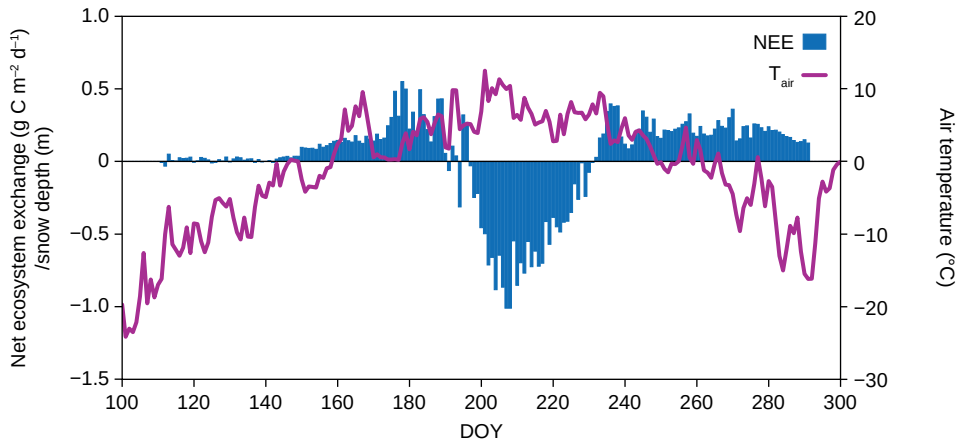

Figure 2.15 Daily net ecosystem exchange (NEE) and air temperature (Tair) measured at the heath site (MM1) in 2014.

Table 2.10 Summary of the CO_2 exchanges 2005-2014 at the heath site. Note that the measuring period varies from year to year.

Year	2005	2006	2007	2008	2009	2010	2011	2012	2013	2014
Measurements start	21 May	28 May	27 May	30 Mar	16 May	5 May	3 May	26 Apr	1 May	20 Apr
Measurements end	25 Aug	27 Aug	28 Oct	28 Oct	22 Oct	31 Oct	16 Aug	29 Oct	26 Oct	18 Oct
Start of net uptake period	8 Jun	8 Jul	16 Jun	6 Jul	13 Jun	1 Jul	26 Jun	11 Jul	14 June	16 Jul
End of net uptake period	16 Aug	23 Aug	19 Aug	20 Aug	15 Aug	14 Aug	15 Aug	22 Aug	6 Aug	19 Aug
NEE for measuring period (g C m^{-2})	–37.9	–24.9	–28.2	–11.2	–11.1	5.0	–23.0	–4.6	–0.7	4.8
NEE for net uptake period (g C m^{-2})	–38.1	–28.9	–37.8	–32.0	–23.1	–26.8	–31.5	–28.9	–26.8	–17.7
Max. daily accumulation (g C m^{-2} d^{-1})	–1.40	–1.11	–1.32	–1.30	–0.97	–1.14	–0.97	–1.11	–1.14	–1.01

When air temperature fell below 0 °C in late September daily NEE decreased. During the entire measuring period (181 days), the net CO_2 budget amounted to 4.8 g C m^{-2} (table 2.10). This is the second year on record during which the heath ecosystem has functioned as a source for atmospheric CO_2 during the measurement period.

Fen site

Since autumn 2012, the eddy covariance equipment in the fen (MM2) is allowed to run year round, powered by solar panels and a wind mill connected to a battery pack when power is not supplied from the Zackenberg research station. Still, power outages occur during the dark winter months when the sun does not rise above the horizon, especially during periods with low wind speeds. There were 14 % gaps in the period 1 January – 19 October 2014, mainly due to lack of power but also due to system calibration and maintenance.

During the snow-covered period before snowmelt started in June, CO_2 fluxes were generally low (figure 2.16). Periods with negative NEE, i.e. net CO_2 uptake, occurred on several occasions. As air temperature was below freezing and snow covered the ground, plant photosynthetic uptake cannot be considered as a reasonable explanation for CO_2 uptake. However, it can be noted that three occasions with daily net CO_2 uptake (4-8 January, 25-27 January and 5-6 March) were associated with rapid increases in air temperature (figure 2.16). Although speculative, such warming events may have triggered changes to the snow pack causing a small net CO_2 uptake. A recent study from a high Arctic location on Svalbard (Lüers *et al.* 2014) did also record negative NEE events during winter, associated with high wind speed and changes of air masses and atmospheric air pressure. Continuous flux measurements during winter in the high Arctic are very rare, and as such the knowledge on the CO_2 exchange between atmosphere and snow pack is limited and requires further scientific studies.

As air temperatures became positive and snow began to melt, NEE increased. Maximum NEE values around 2 mg C m^{-2} d^{-1} occurred in mid-July. On 16 July, the fen ecosystem switched from being a source for atmospheric CO_2 to a sink. This switch occurred one month later compared with 2013, associated with the different timing of snowmelt. The period with net

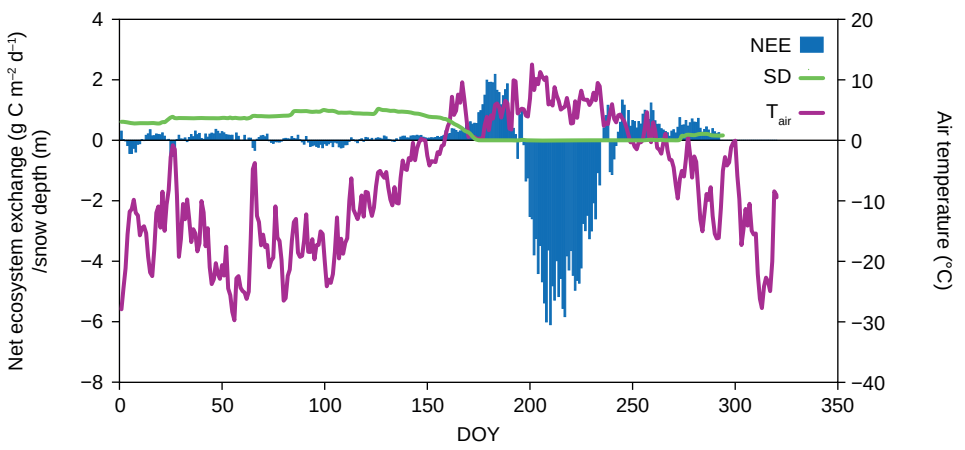

Figure 2.16 Daily net ecosystem exchange (NEE), snow depth (SD) and air temperature (Tair) measured at the fen site (MM2) in 2014.

Table 2.11. Summary of the CO_2 exchanges 2007-2014 at the fen site. Note that the measuring period varies from year to year.

Year	2007	2008	2009	2010	2011	2012*	2013*	2014
Measurements start	20 Sep	10 Apr	31 Jul	9 May	7 May	29 Aug	1 Apr	1 Jan
Measurements end	19 Oct	30 Aug	13 Oct	1 Nov	25 Oct	26 Oct	25 Oct	19 Oct
Start of net uptake period	–	10 Jul	–	–	26 Jun	–	17 Jun	16 Jul
End of net uptake period	–	22 Aug	16 Aug	16 Aug	15 Aug	–	9 Aug	30 Aug
NEE for measuring period (g C m^{-2})	9.8	–65.8	3.5	–73.5	–80.5	40.3	–81.6	–74.8
NEE for net uptake period (g C m^{-2})	–	–94.6	–	–	–129.9	–	–156.3	–140.7
Max. daily accumulation (g C m^{-2} d^{-1})	–	–4.03	–	–5.15	–4.49	–	–6.27	–6.09

* = Values re-calculated compared with earlier annual reports

diurnal CO_2 uptake lasted until 30 August; and during this period the fen absorbed approx. 141 g C m^{-2}. Maximum daily CO_2 uptake amounted to –6.1 g C m^{-2} d^{-1}.

After the net uptake period had terminated, CO_2 fluxes remained relatively high (around 1 g C m^{-2} d^{-1}) until air temperatures fell below 0 °C in late September. Maximum daily emission during autumn (1.3 g C m^{-2}) was detected on 2 September. During the entire period for which data are presented in this report (1 January – 19 October), the preliminary CO_2 budget of the fen ecosystem amounts to –74.8 g C m^{-2} (table 2.11).

The growing season daily uptake rates as well as shoulder seasons daily emissions are generally higher in the fen site compared with the heath site. This is because of denser vegetation with higher leaf area index in the fen site, allowing for higher CO_2 uptake per area unit.

2.6 Geomorphology

Coastal geomorphology

In 2008, the cliff top along the northern site of the active delta lobe was measured, while the shoreline has been measured the past five years (figure 2.17).

The shoreline at the river delta showed a rapid decrease from 2008 towards 2010. Most of the protruding glacial cliff was eroded and a small island remained on the delta plain. The small island eroded away during the summer of 2012. The lines measured in 2010 and 2012 are almost similar. The line from 2011 was recorded after the first snow and it was not possible to see the high-water mark on the beach. From 2011 to 2012, the shoreline at the delta mouth has eroded up to several metres. The coast line measured in 2012, 2013 and 2014 (see figure 2.17) is almost identical to each other and no major erosion has happened since the big river burst in 2012 (Jensen *et al.* 2013).

Figure 2.17 Delta- and coastal cliff line measured by DGPS in 2008 (green line), 17 October 2010 (blue line), 12 October 2011 (purple line), 28 September 2012 (red line), 10 September 2013 (dark blue line) and 8 September 2014 (dotted yellow line) on an aerial photo from 8 August 2000.

3 Zackenberg Basic

The GlacioBasis programme

Michele Citterio, Charalampos Charalampidis, Signe Hillerup Larsen, Erik Vest Sørensen and Andreas P. Ahlstrøm

Since 2008, the GlacioBasis monitoring programme at Zackenberg has carried out detailed glaciological observations to monitor the mass balance, near-surface weather, surface energy balance, and surface ice velocities of A.P. Olsen Ice Cap and its outlet glacier in the Zackenberg river basin (figure 3.1). The A.P. Olsen Ice Cap is located at 74° 39′ N, 21° 42′ W. The summit of the ice cap reaches an elevation of 1425 m and the terminus of the outlet glacier contributing to the Zackenberg river basin is at 525 m. Zackenberg Research Station is located SE of the site, approximately 35 km downriver from the glacier terminus. The most direct access to the glacier terminus is through Store Sødal.

The severe scarceness of glacier mass balance measurements from the local glaciers and ice caps surrounding the Greenland Ice Sheet, the strong impact that such ice masses are expected to exert on sea level rise in the present century (Machguth *et al.* 2013), and the particularly marked warming expected to take place in the Arctic (Stocker *et al.* 2013) highlight the scientific relevance of GlacioBasis monitoring tasks. The monitoring data are being used for modelling the surface energy balance and the glacier mass budget, and for assessing the sensitivity to future climate change scenarios of local glaciers and ice caps in this region.

In order to measure winter accumulation, fieldwork must be carried out during springtime, immediately before the onset of snowmelt. This timing is also required for snowmobile use, which is the only practical means to reach the glacier and transport the required equipment and instrumentation. Fieldwork must be carried out every year in order to maintain the stakes network operational, to service the automatic weather stations (AWS) on the glacier, and to carry out the DGPS and snow radar surveys. The GlacioBasis 2008-2014 datasets and accompanying metadata have been reformatted and delivered to the upcoming GEM database.

Figure 3.1 Map of the Zackenberg area, with A.P. Olsen Ice Cap in the north-western corner of the map. The main investigation area is marked by the circle.

The A.P. Olsen ice cap monitoring and the other cryosphere-related activities within ZERO have now been included in the pre-operational WMO (World Meteorological Organization) GCW (Global Cryosphere Watch) CryoNet network of *in situ* monitoring sites. In May 2015 it is expected that the 17th WMO Congress will vote a resolution to establish GCW as a core WMO initiative. GlacioBasis together with PROMICE are supporting the work of M.C. in the GCW Steering Group and in the GCW CryoNet Team to assist in their design and implementation.

3.1 Overview of fieldwork in 2014

In 2014 the complete GlacioBasis programme was carried out successfully, and a second visit to A.P. Olsen was carried out at the end of August. This was necessary because the stakes installed in April were of the flexible type, which are very practical but unsuitable to survive the winter without being buried and therefore were unusable by the following visit in spring 2015. The summer visit also provided an opportunity to remove and clean up some of the old stakes on the glacier.

All existing ablation stakes were revisited and measured in April, while only the stakes in the ablation area were reachable safely in August due to a layer of fresh snow which hid crevasses and made the terrain unsafe at higher elevations. Snow pits were dug in April to measure snow density and the snow pack water equivalent at locations over the altitudinal range of the ice cap.

During the April-May campaign two new field experiments were initiated. The first included the acquisition, at several sites along the central flow-line of the A.P. Olsen outlet glacier, of very high resolution digital photographs of the glacier surface using a calibrated camera, from a distance of about 2 metres above the surface. Later the images have been processed at the GEUS aerophotogrammetry lab to map the microtopography of the glacier surface (Sørensen *et al.* submitted). Processing was continued in 2015 and preliminary results indicate that sub-millimetre details can be resolved. Knowledge of surface roughness, in particular at the AWS sites, will assist in refining the modelling of turbulent energy and moisture fluxes at the surface and in studying the effect of surface roughness on albedo observed *in situ* and from satellite.

The second experiment is a field evaluation of a new instrument, the Vaisala WXT520. A unit was installed at the lower AWS (AWS1) to evaluate its performance and suitability for wider adoption with the GEUS AWS within GlacioBasis, PROMICE and other projects. The characteristic of this sensor is the ability to measure rain and hail, as well as atmospheric pressure, air temperature and humidity, and wind speed and direction. Rain events are not expected to play a major role on A.P. Olsen, but this sensor will provide urgently needed calibration for the parameterization we are currently using to partition precipitations between rain and snow in upscaling from the ClimateBasis weather mast close to Zackenberg Station. In the April-May campaign the three AWS were serviced, data retrieved and the sensor recalibration plan implemented. All stations were found in good conditions and left in full working order. At all elevations the depth of the snow cover was significantly higher than in 2013, and the summit AWS was buried almost completely. This is unusual because in most years wind redistribution tends to remove almost all of the snow from the summit part of the ice cap and transport it toward intermediate elevations. Later in the year, AWS2 experienced power supply problems which resulted in a data gap from November 2014 to late March 2015. The cause appears to be incomplete charge of the battery during summer 2014 due to bad orientation of the solar panel, aggravated by burial of the solar panel by snow.

Dual frequency GPS surveys were carried out in static mode at the sites of the ablation stakes in order to track surface elevation and velocity by comparison with the measurements taken in 2013 and those that will be acquired in 2015. The master reference station was set up at the forefront of the glacier, occupying a temporary, unsurveyed position. The precise coordinates of this reference station were later determined to centimetric accuracy by precise post-processing (PPP). The positions of the stakes were obtained by carrier phase static differential post-processing.

Michele Citterio (GEUS, GlacioBasis) and Charalampos Charalampidis (GEUS, GlacioBasis) took part in the April-May fieldwork; Charalampos Charalampidis

together with Daniel Binder (ZAMG, Vienna) took part in the August-September fieldwork.

3.2 Automatic Weather Stations

The GlacioBasis programme operates one larger automatic weather station (AWS) and two smaller stations deployed on the glacier to obtain *in situ* time series of physical parameters describing the weather at the glacier surface. The main GlacioBasis AWS was deployed in March-April 2008 on A.P. Olsen ice cap (AWS1 in this report). AWS1 is the prototype unit of all the current GEUS glaciological weather stations in Greenland and it continues to prove very reliable, having now completed the seventh year of uninterrupted operation without repairs except for routine sensor swaps for recalibration. Technical and design details are provided in Citterio *et al.* (2015). In 2014, planned sensor replacement for recalibration was carried out and a Vaisala WXT520 weather monitor was installed as part of the ongoing instrument tests based at AWS1. The passive vs. active radiation shield intercomparison experiment started in 2012 is also being continued.

AWS2 required some maintenance to the tripod to ensure the supporting guy wires were correctly tensioned, in addition to planned sensor replacement. Snow cover lasts relatively long in the season at the site of AWS2, and the variability of surface albedo is an important element controlling the surface energy balance. Radiative fluxes have been monitored since 2012 with radiometers and tilt sensors installed as part of a GEM Strategic Initiative. The total width of the glacier tongue is near to its maximum at this elevation, which simplifies comparison of surface albedo measured by the AWS and by satellite remote sensing. After the thick 2012 snow cover and very thin 2013 one, the intermediate snow depth in 2014 will provide a good range of conditions to assess inter-annual variability.

AWS3 was found in good conditions and scheduled replacement of sensors with freshly calibrated units was carried out. GlacioBasis uses the same recalibration plan developed for PROMICE (Ahlstrøm *et al.* 2009). The tripod, however, was almost completely buried by snow and the horizontal sensor boom at the top was therefore raised to prevent burial and damage to sensors (figure 3.2).

Following the April-May field visit, satellite data transmissions indicate that all stations are working properly. No action was required during the August-September campaign. AWS1, which is still using its original batteries from 2008, is now configured near maximum allowable power consumption with the Vaisala WXT520 weather monitor and higher GPS and transmission rates compared to a standard GEUS AWS.

During AWS data validation and calibration, data were calibrated based on the manufacturer's calibration report and visually inspected for signs of instrument malfunction. The calibration factors are traced to the corresponding devices through the device serial number using the same Glaciobase database used at GEUS to handle the sensors inventory for PROMICE. Details on Glaciobase are provided by Ahlstrøm *et al.* (2009) and are not repeated here. Validation of the data was carried out using the same procedures established for PROMICE; again, details on this are provided by Ahlstrøm *et al.* (2009) and are not repeated here.

Detailed information on each AWS and a selection of the observed data is shown below, where plots show the entire availability of data starting from the establishment of the first two AWS's in late March 2008.

Figure 3.2 Snow cover at the summit station AWS3 had almost buried the sensors (left image) and required the boom to be raised (right image), taking advantage of the flexibility of the GEUS AWS tripod design that can accommodate an extended-length mast for sites where thick snow cover can be expected. Photos by Michele Citterio (Copyright GEUS).

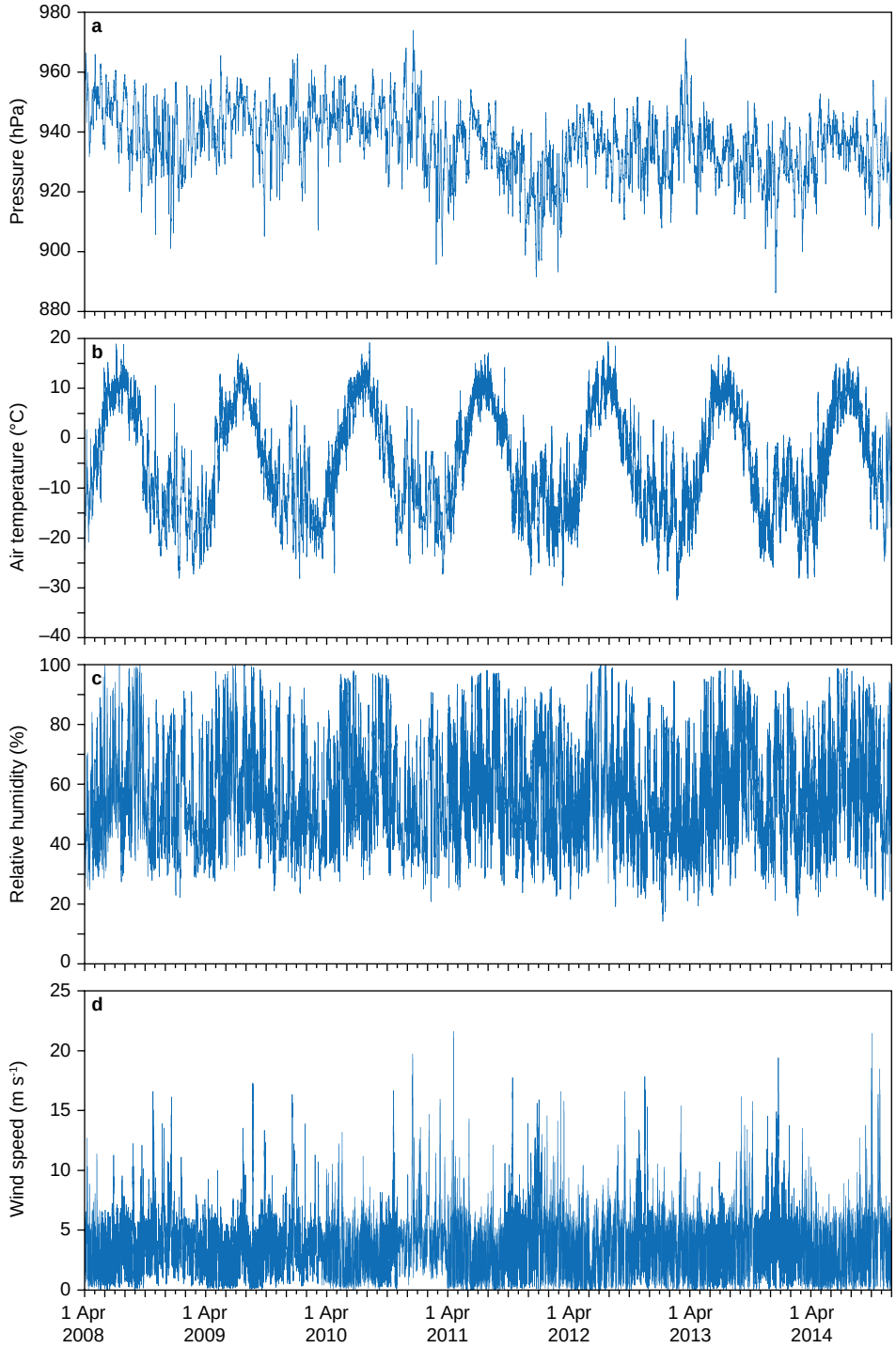

Figure 3.3 The complete available time series of selected parameters at AWS1: barometric pressure (a), air temperature (b), relative humidity (c) and wind speed (d).

The AWS1

Description: AWS1 – A.P. Olsen main AWS (centreline, lower tongue).
Coordinates: 74° 37.5′ N, 21° 22.55′ W, elevation (WGS84): 660 m.
Measured parameters: barometric pressure, aspirated T_{air}, aspirated RH_{air}, wind speed, wind direction, downwelling SW, upwelling SW, downwelling LW, upwelling LW radiation, T of LW radiometer, ice ablation, ice level, snow level, eight-levels thermistor string, two axes station tilt, GPS position, diagnostics, experimental sensors (variable from year to year, currently a passive radiation shield with a second Rotronics temperature and humidity probe identical to the one in the aspirated radiation shield).
Time series: uninterrupted from 29 March 2008 to today for all sensors except the sonic rangers, whose support stake often fails toward the end of the ablation season.
Current availability: all transmitted data (hourly summer/3-hourly winter); 10 minutes from flash card between 29 March 2008 and 20 April 2015.

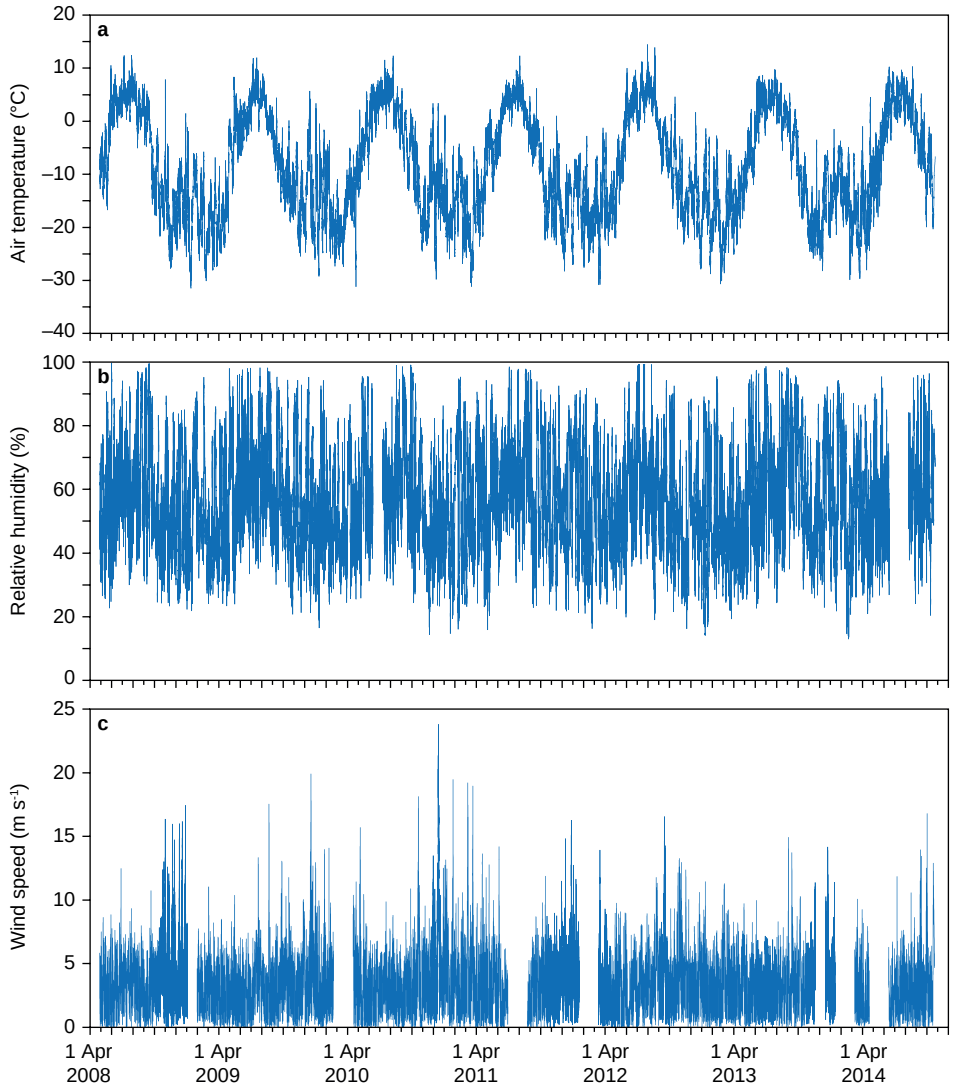

Figure 3.4 The complete available time series of selected parameters at AWS2: air temperature (a), relative humidity (b) and wind speed (c).

AWS1 has been working without interruption since the day it was set up on 29 March 2008, and satellite telemetry delivers near real-time data. As a site and station especially well-suited to technical experiments and testing of new devices, the ongoing experiment comparing a passive Campbell Scientific radiation shield against the aspirated Rotronic radiation shield that is used in all other GEUS glacier AWS is being continued. Complete time series of barometric pressure, air temperature, relative humidity and wind speed are shown in figure 3.3.

The AWS2

Description: AWS2 – A.P. Olsen small AWS (centreline, middle tongue, just upflow of lake and lateral glacier confluence).
Coordinates: 74° 38.6′ N, 21° 28.2′ W, elevation (WGS84): 880 m.
Measured parameters: aspirated T_{air}, aspirated RH_{air}, wind speed, wind direction, ice level, snow level, GPS position, downwelling SW, upwelling SW, downwelling LW, upwelling LW radiation, T of LW radiometers, and two axes station tilt diagnostics.
Time series: uninterrupted from 31 March 2008 to today for all sensors except the sonic rangers, whose support stake often fails toward the end of the ablation season.
Current availability: 10 minutes from flash card from 31 March 2008 to 23 April 2015, with a gap between November 2014 and March 2015. There is no satellite data telemetry; therefore data are only retrieved once a year in the field.

This AWS2 is a smaller version of AWS1 not equipped with satellite transmission, and data retrieval in the field is required for this station. Air temperature, relative humidity and wind speed are shown in figure 3.4.

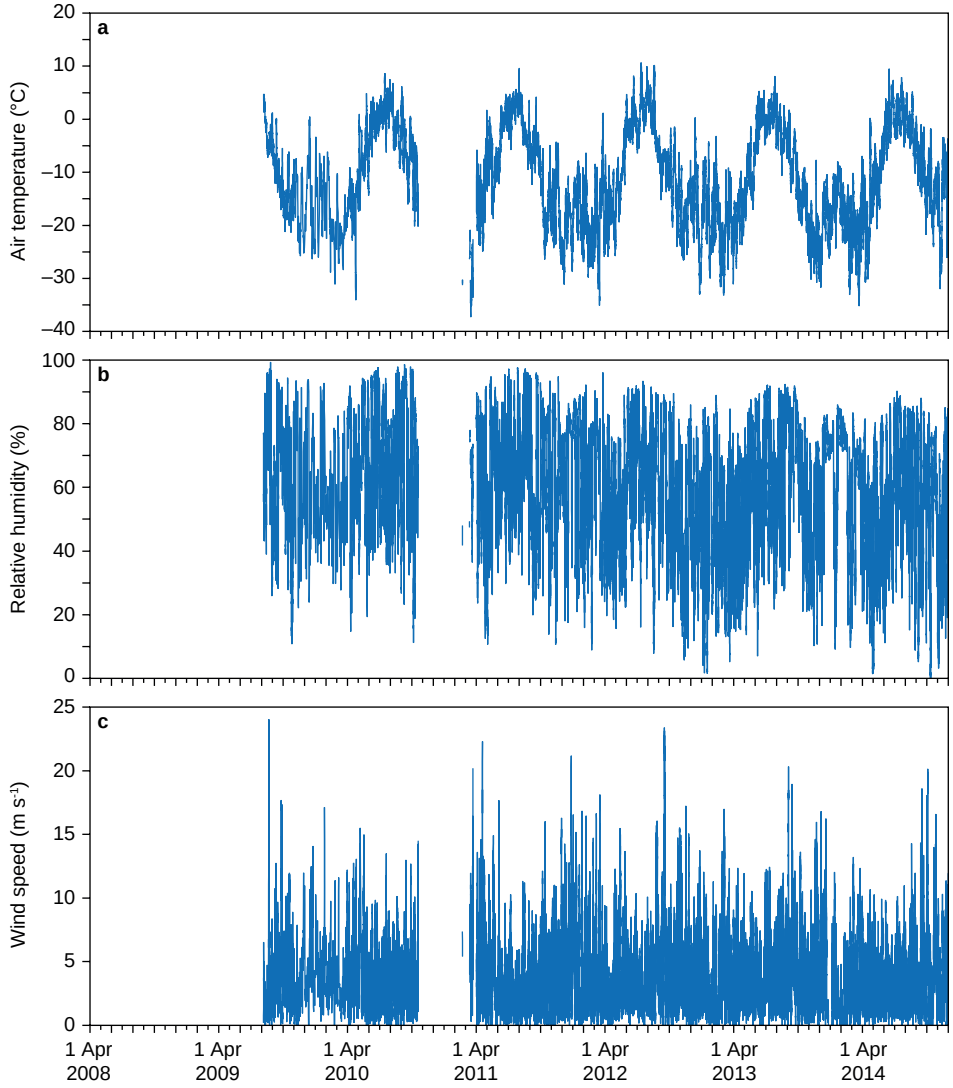

Figure 3.5 The complete available time series of selected parameters at AWS3: air temperature (a), relative humidity (b) and wind speed (c).

The AWS3

Description: AWS3 – A.P. Olsen summit (at the wide open flat just SSW of A.P. Olsen summit).
Coordinates: 74° 38.9′ N, 21° 39.1′ W, elevation (WGS84): 1475 m.
Measured parameters: aspirated T_{air}, aspirated RH_{air}, wind speed, wind direction, downwelling SWi, upwelling SW, downwelling LW, upwelling LW, sensor T of the LW radiometer, ice and snow level, eight-levels thermistor string, two axes station tilt, GPS fix, diagnostics.
Time series: From 6 August 2009 to 19 October 2010, for all sensors except the sonic rangers, which had intermittent problems, with a four-day gap for unknown reasons just before the revisit on 11 May 2010. In winter 2010 and 2013 the station entered low power operation suspending satellite data transmissions, but without data gaps as the data were stored locally on the memory card and retrieved during the field visits.
Current availability: 10 minutes from flash card from 6 August 2009 to 25 April 2015, then 1- or 3-hourly transmitted data until next revisit.
Notes: fitted for extension with one additional thermistor string.

This AWS3 was set up by helicopter in August 2009. It was initially equipped with a subset of the sensors on AWS1 and since 2012 with a full sensor suite. The GPS receiver in this station is faulty and it will be replaced during the next field visit. Being close to the summit of the ice cap, this station is not moving significantly. Figure 3.5 shows air temperature, relative humidity and wind speed from AWS3.

3.3 Ablation stakes network

A network of ablation and surface velocity stakes distributed along the central flow line was established in spring 2008 on the outlet glacier of the A.P. Olsen ice cap and along three transects at elevations of approximately 675, 900 and 1300 m. Since May 2010 one more stake is maintained very close to the terminus in order to better include a site with the highest ablation in the area. Accurate location of the stakes is provided in the 2012 ZERO report (Jensen *et al.* 2013).

Surveying the network of ablation stakes is a core task of GlacioBasis, because it provides a direct measurement of the glacier mass balance, which is central to the entire programme. Standard GlacioBasis ablation stakes are 6 m long metal rods drilled into the ice and measured periodically to quantify the amount of water lost to ablation. Stakes are distributed over the glacier surface with the primary aim to cover the entire elevation range of the glacier, because glacier mass balance shows the strongest gradient with elevation. Stakes are also arranged in transects at roughly the same elevation in order to capture the lateral variability moving out from the centreline of the glacier, due e.g. to shading and long wave radiation from the surrounding rock walls. In 2014, it was not possible to re-drill the stakes in the ablation areas with similar aluminium ones because the stock of poles left at the glacier terminus was buried by snow and could not be found. Plastic stakes borrowed from ZAMG, Vienna and of the same type as used on Freya Glacier were used instead. These are very convenient but are too flexible to remain vertical during the following winter season, which required the August-September campaign to be organised, again in collaboration with ZAMG.

3.4 Differential GPS surveys

Surface ice velocities are being monitored by repeated precision survey of ablation stake positions. The GPS phase recordings are post-processed as individual baselines from the master station located at the glacier terminus and the rover station positioned at the site of each ablation stake. In 2014, accurate GPS profiles have been recorded along all snow radar lines to provide an extensive record of surface elevation. The coordinates of the master station were determined for each survey day by the PPP (Precise Post-Processing) method, the measurement baselines for the static solutions of the stake positions follow the layout illustrated in the 2012 ZERO report (Jensen *et al.* 2013). To minimize kinematic processing difficulties, the coincident GPS-snow radar lines recorded on a sled pulled by snow-scooter were recorded at a comparatively high rate of 10 Hz.

3.5 Enabling upscaling: integration of satellite remote sensing and *in situ* observations

Surface albedo and its seasonal evolution have a large impact on the surface energy balance. In the past years the systematic archival of past and current imagery was carried out as an ongoing joint GlacioBasis – PROMICE activity at GEUS to enable geographic upscaling and also to drive or validate the models used for simulating the surface energy and mass balance of the A.P. Olsen Ice Cap. During 2014 satellite products from moderate resolution imagery like the MODIS MOD10A1 snow albedo product have been added to the archive. These publicly available products are fully documented and are distributed by the NSIDC (National Snow and Ice Data Centre). However, these existing datasets have significant limitations when used over relatively small targets like the A.P. Olsen Ice Cap (approx. 300 km^2) due to their relatively coarse resolution of 500 × 500 m and due to the much coarser surface elevation model used to correct for terrain effects. Figure 3.6 shows albedo for 9 August, 2014: the MOD10A1 product shown in the top-left panel is coarsely pixelated and the incompletely corrected effect of slopes facing toward and away from the sun is manifested as brighter and darker areas, respectively. Progress has been made to improve these third party datasets with the GlacioBasis using higher resolution imagery in combination with GlacioBasis *in situ* observations. The top-right panel in figure 3.6 shows a preliminary product derived from a Landsat 8 scene on the same date, after atmospheric correction and conversion

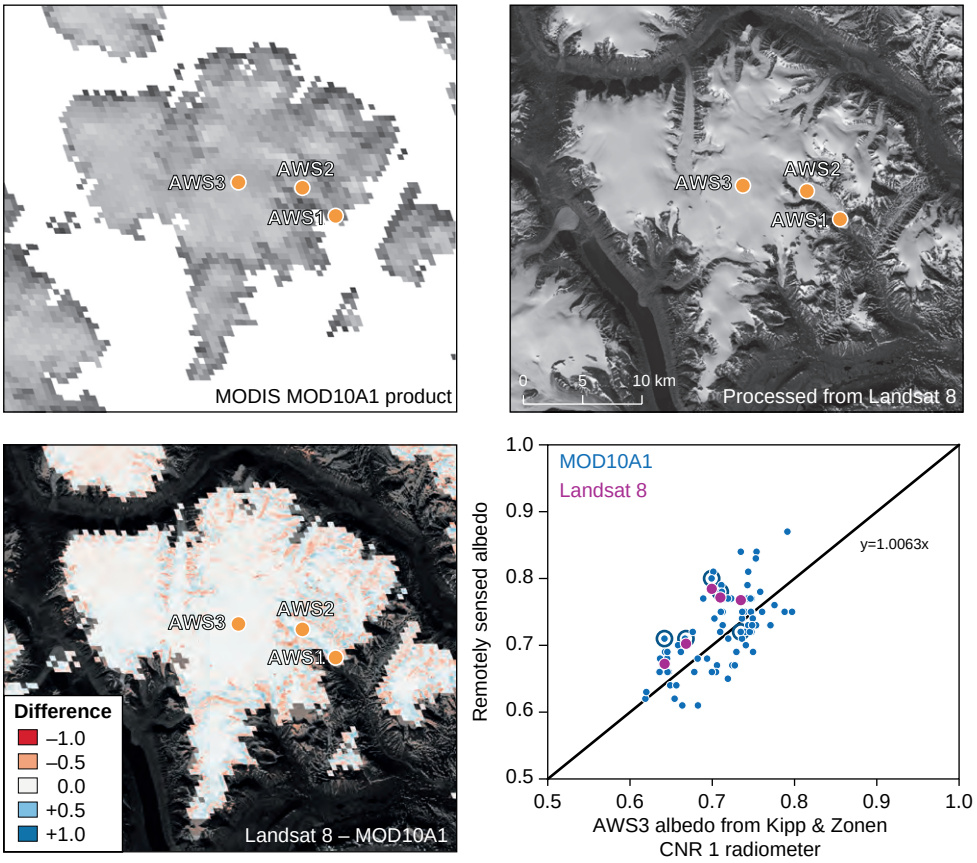

Figure 3.6 Comparison of surface albedo on 9 August 2014 from the MODIS MOD10A1 product distributed by NSIDC (top-left) and from our processing of Landsat 8 imagery (top-right). The difference between the two satellite products is shown in the bottom-left panel and a validation against in situ measurements at the GlacioBasis AWS3 station (bottom-right).

from spectral reflectance to broadband albedo using the equations of Liang (2001) but before terrain correction, so that the same illumination effects on the slopes are still visible as in the MOD10A1 product. The resulting resolution is much finer (30 × 30 m) and smaller features like the outlet glacier tongues are clearly resolved.

The bottom-left panel shows the difference between our Landsat 8 albedo product and the MOD10A1 product, clearly evidencing the larger errors on steep slopes. The bottom-right panel finally shows a comparison of MOD10A1 (blue dots) and our Landsat 8 product (red dots) vs. the *in situ* GlacioBasis measurements at AWS3. The Landsat 8 points have a small positive bias likely due to terrain and directional reflectance effects not yet being completely modelled, however, their scatter is tighter and the bias smaller than the corresponding points in the MOD10A1 dataset (circled blue dots). These preliminary results are encouraging especially considering the large solar zenith angles occurring at such high latitudes. Further work is ongoing to refine the surface reflectance model in our code, to characterize the performance of the algorithm against *in situ* AWS observations, to upscale to the entire A.P. Olsen ice cap and the surrounding glaciers and ice caps, and to create a time series of surface albedo exploiting all available Landsat 8 imagery.

4 Zackenberg Basic

The BioBasis programme

Lars Holst Hansen, Jannik Hansen, Palle Smedegaard Nielsen, Kirsten S. Christoffersen, Jesper Bruun Mosbacher and Niels Martin Schmidt

This chapter reports the 2014 field season of BioBasis. The BioBasis programme at Zackenberg is carried out by Department of Bioscience, Aarhus University, Denmark, and is funded by the Environmental Protection Agency as part of the environmental support programme Danish Cooperation for Environment in the Arctic (DANCEA). The authors are solely responsible for all results and conclusions presented in the report, which do not necessarily reflect the position of the Environmental Protection Agency.

Please refer to previous Zackenberg Annual Reports for presentation of data covering the earliest years of monitoring. Detailed information on the BioBasis methods and updated sampling protocols are available at the Zackenberg home page (http://zackenberg.dk/).

The 2014 BioBasis field team consisted of Lars Holst Hansen (day 144-203 and day 231-281), Jannik Hansen (day 155-231), Jannie Linnebjerg (day 163-189), Palle Smedegaard Nielsen (day 189-245), and Niels Martin Schmidt (day 217-231).

Table 4.1 Inter- and extrapolated date of 50 % snow cover 2004-2014 for white arctic bell-heather Cassiope tetragona*, mountain avens* Dryas integrifolia/octopetala*, arctic poppy* Papaver radicatum*, arctic willow* Salix arctica*, purple saxifrage* Saxifraga oppositifolia *and moss campion* Silene acaulis. **Denote extrapolated dates.*

Plot	2004	2005	2006	2007	2008	2009	2010	2011	2012	2013	2014
Cassiope 1	<155	143	164	155	164	138	150	147	168	<129	162
Cassiope 2	168	158	183	167	174	145	164	153	182	145	162
Cassiope 3	159	148	179	158	172	140	164	159	176	135	166
Cassiope 4	159	158	174	164	174	148	167	161	178	141	169
Dryas 1	<154	<140	150*	<145	147	<135	<142	<135	153	132	144
Dryas 2/*Salix* 7	173	168	192	170	182	157	174	168	187	151	182
Dryas 3	<155	<140	151	<145	147	136	<142	<136	153	<129	162
Dryas 4	<153	<140	164	152	162	135	<142	150	168	126*	160
Dryas 5	<153	<140	177	<145	152	<135	142	<136	161	130	159
Dryas 6/*Papaver* 4	173	165	191	164	184	149	170	169	184	144	181
Papaver 1	166	152	179	162	169	139	162	146	181	136	162
Papaver 2/*Salix* 5	163	158	183	161	178	149	166	160	178	148	176
Papaver 3	160	158	174	163	174	148	167	161	177	142	170
Salix 1	<155	<140	145*	<145	137	<135	<142	<135	148	<129	143
Salix 2	161	156	178	160	169	148	162	159	176	146	169
Salix 3	<155	138*	160	151	163	<135	146	145	167	<129	160
Salix 4	157	150	165	154	161	147	158	157	162	130	161
Salix 6	173	166	186	165	182	149	169	166	185	148	180
Saxifraga/*Silene* 1	<154	<140	<146	<145	<131	<135	<142	<135	147	<129	145
Saxifraga/*Silene* 2	<154	<140	<146	<145	<131	<135	<142	<135	152	<129	147
Saxifraga/*Silene* 3	<154	128*	158	152	145	<135	<142	<136	158	128*	150
Silene 4	170	163	186	164	176	150	167	165	181	146	175

4.1 Vegetation

The weekly records of snow cover, plant flowering and reproduction were conducted by Lars Holst Hansen, Jannik Hansen and Palle Smedegaard Nielsen. No gas flux measurements were conducted for the Biobasis Programme and no pinpoint analyses and fluorescence measurements were carried out in 2014.

Reproductive phenology and amounts of flowering

The 2014 BioBasis field season began on 24 May (day 144). Snowmelt was rather late, and 17 of 22 plant phenology plots had a later date of 50 % snow cover than the median day of previous seasons. None of the 22 had a date of 50 % snow cover later than the latest hitherto recorded (table 4.1). The late snowmelt resulted in relatively late 50 % flowering in all of the 28 plots with dates between the median and the 3rd quartile of previous recordings (table 4.2). All plant plots had late dates of 50 % open seed capsules, with all later than the median and 12 of 14 even later than the 3rd quartile of the previous years (table 4.3). Two *Papaver*, five *Salix* plots and one *Saxifraga* plot had new record late dates and one *Salix* plot had a date equalling the hitherto latest. In the 2014 season, 37 of 44 categories of flowers or catkins had lower than the average peak number of flowers or catkins hitherto recorded (table 4.4). There were five new minima (in *Papaver*, *Salix*, *Silene* and *Eriophorum*) and five new maxima (in *Salix*).

Table 4.2 Inter- and extrapolated date of 50 % open flowers (50/50 ratio of buds/open flowers) 2004-2014 for white arctic bell-heather Cassiope tetragona*, mountain avens* Dryas integrifolia/octopetala*, arctic poppy* Papaver radicatum*, arctic willow* Salix arctica*, purple saxifrage* Saxifraga oppositifolia *and moss campion* Silene acaulis*. *Denote interpolated dates based on less than 50 buds + flowers. # Denote a DOY between 154 and 161.*

Plot	2004	2005	2006	2007	2008	2009	2010	2011	2012	2013	2014
Cassiope 1	175	167	185	178	186	173	176	172	187	167	187
Cassiope 2	187	173	201	186	193	180	186	176	198	173	192
Cassiope 3	182	173	200	185	194	178	184	183	195	173	194
Cassiope 4	185	183	200	186	195	183	190	185	195	176	199
Dryas 1	173	164	177	173	172	170	170	170	173	171	177
Dryas 2	200	198	215	192	204	188	200	193	207	183	213
Dryas 3	175	164	180	177	174	175*	174	171	176	177*	194
Dryas 4	174	164	187	178	186	173	172	172	190	171	188
Dryas 5	172	164	172	171	175	172*	172	167	182	171	187
Dryas 6	199	194	214	191	206	185	200	194	207	180	213
Papaver 1	193	185	206	188*	195	184	190*	179*	203*	184*	199*
Papaver 2	190	190	208	188	204	185	194	187	203	185	206
Papaver 3	187	187	201	187*	199	186	193	187	200	185	200
Papaver 4	194	194	214	192*	204	186*	197*	194	207*	182	211*
Salix 1	156	155	165	161	161	155	162	156	167	157	165
Salix 2	173	165	196	177	187	167	177	174	192	164	188
Salix 3	159	157	174	165	174	152*	161	159	180	<161#	179
Salix 4	173	164	180	170	174	167	174	171	<184	<161#	188
Salix 5	175	164	194	174	193	168	179	174	193	164	193
Salix 6	197	184	200	179	194	171	184	180	197	164	200
Salix 7	187	187	202	182	195	179	186	185	194	170	201
Saxifraga 1	157	144	151	160*	159*	149*	153	144	158*	159	159
Saxifraga 2	157	152	157	158	158	150	157	151*	<155	159	162
Saxifraga 3	<154	146	172	165	159*	146*	161	151	166	159	164
Silene 1	173	165	170	173	172	174	174	172	176	173	182
Silene 2	181	166	182	179	173	184	179	175	175	175	191
Silene 3	172	166	194	179*	173	180	178	172	190	177	193
Silene 4	201	197	194	193	207	187	199	198	208	182	210

Table 4.3 Inter- and extrapolated date of 50% open seed capsules 2004-2014 for arctic poppy Papaver radicatum, *arctic willow* Salix arctica *and purple saxifrage* Saxifraga oppositifolia. **Denote interpolated dates based on less than 50 flowers + open capsules.*

Plot	2004	2005	2006	2007	2008	2009	2010	2011	2012	2013	2014
Papaver 1	219	212	232	223	211*	203	223*	207	229*	217*	229*
Papaver 2	219	215	234	221	226	206	221	214	225	214	240
Papaver 3	216	212	223	220	215	212	225	216	226	217	231
Papaver 4	227	220	239*	222*	222*	214*	222*	220	229	213	243*
Salix 1	208	201	219	218	211*	220	223	218	211	214	217
Salix 2	218	215	231	220	227	218	222	222	233	213	242
Salix 3	209	206	223	215	225	213*	218	212	228	210	234
Salix 4	219	210	223	219	225	220	222	221	226	212	242
Salix 5	220	219	>240	221	229	215	227	222	234	218	243
Salix 6	223	226	>240	222	234	217	228	229	239	217	244
Salix 7	223	226	>240	224	234	221	229	232	241	218	246
Saxifraga 1	205	203	217*	218	195	209*	212	218*	189	>231	223
Saxifraga 2	209	212	217	216	205	213	214	193	189	214	229
Saxifraga 3	205	212	225	221	188	215*	218	207	188	215	241

Photo: Mikke P. Tamsdorf

Table 4.4 Area size (m²) and peak pooled numbers of flower buds, flowers (or catkins) and senescent flowers (or catkins) 2004-2014 of white arctic bell-heather Cassiope tetragona*, mountain avens* Dryas integrifolia/octopetala*, arctic poppy* Papaver radicatum*, arctic willow* Salix arctica*, purple saxifrage* Saxifraga oppositifolia*, moss campion* Silene acaulis*, arctic cottongrass* Eriophorum scheuzerii *and 'dark cottongrass'* Eriophorum triste. *Saxifraga *1 had a second flowering peak with a number of 77 buds/flowers.*

Plot	Area	2004	2005	2006	2007	2008	2009	2010	2011	2012	2013	2014
Cassiope 1	2	2080	1392	973	435	1183	233	431	890	799	148	152
Cassiope 2	3	1745	1204	593	300	958	555	340	1045	1459	689	229
Cassiope 3	2	791	864	432	86	704	256	227	489	490	193	226
Cassiope 4	3	1274	1856	520	223	1340	437	304	659	615	497	268
Dryas 1	4	444	392	321	147	190	254	334	530	533	288	179
Dryas 2	60	1174	520	521	561	806	395	410	483	401	628	140
Dryas 3	2	273	200	134	90	94	32	129	281	403	43	49
Dryas 4	6	218	144	168	181	141	90	192	279	215	91	106
Dryas 5	6	351	232	123	115	103	51	318	560	571	342	240
Dryas 6	91	1854	880	1324	1144	1606	593	889	1185	1351	955	241
Papaver 1	105	286	207	153	95	80	68	53	84	31	28	12
Papaver 2	150	402	682	418	234	500	341	419	251	365	234	164
Papaver 3	90	221	316	234	233	190	188	150	259	92	123	53
Papaver 4	91	37	68	71	31	71	26	83	96	92	128	23
Salix 1 mm.	60	1127	375	183	184	2	243	857	207	790	782	180
Salix 1 ff.	60	1606	386	303	241	3	234	1172	425	1075	961	334
Salix 2 mm.	300	1276	737	654	317	758	304	521	578	697	379	560
Salix 2 ff.	300	1862	1089	1076	386	506	570	1512	877	1069	397	893
Salix 3 mm.	36	693	285	204	169	492	40	294	194	562	265	57
Salix 3 ff.	36	476	188	129	154	332	51	261	183	328	151	33
Salix 4 mm.	150	1984	1317	1509	1108	1894	1414	1085	2310	1109	1259	998
Salix 4 ff.	150	1755	1038	906	827	1768	1529	821	1443	875	1090	725
Salix 5 mm.	150	844	945	1052	417	831	513	287	972	954	326	1076
Salix 5 ff.	150	1314	1333	1365	525	1209	681	526	1082	1170	434	1594
Salix 6 mm.	150	2162	2445	591	525	1565	137	447	2264	2016	1365	2253
Salix 6 ff.	150	2736	2010	947	1085	2401	404	1875	3599	1715	1570	3910
Salix 7 mm.	60	621	746	287	351	515	274	172	405	918	–	202
Salix 7 ff.	60	512	705	180	266	570	318	207	548	1002	–	477
Saxifraga 1	7	463	159	43	190	124	23*	293	108	55	270	133
Saxifraga 2	6	584	522	167	311	98	123	171	234	89	484	161
Saxifraga 3	10	609	241	150	394	90	134	506	540	653	436	249
Silene 1	7	1187	312	430	84	171	159	1085	691	603	980	214
Silene 2	6	1406	740	540	268	267	260	288	489	408	354	152
Silene 3	10	719	503	739	378	176	168	493	485	406	181	60
Silene 4	1	509	483	312	420	373	499	424	611	435	-	431
E. scheuz. 1	10	780	201	302	533	310	98	194	308	225	124	55
E. scheuz. 2	6	956	597	540	142	193	61	57	19	56	16	8
E. scheuz. 3	10	359	67	44	31	37	17	21	65	116	30	7
E. scheuz. 4	8	342	57	23	55	74	14	153	54	121	145	183
E. triste 1	10	12	0	0	1	1	0	1	0	0	0	0
E. triste 2	6	117	44	49	13	14	25	27	9	2	1	0
E. triste 3	10	0	0	0	0	0	0	0	0	0	0	0
E. triste 4	8	0	0	0	0	0	0	0	0	0	0	0

Table 4.5 Peak NDVI recorded in 16 plant plots 2004-2014 together with date of maximum values as day of year (DOY). NDVI values from 2003-2006 are based on data from hand held Ratio Vegetation Index (RVI) measurements, and have been recalculated to account for varying incoming radiation that otherwise affects the measurements. Note that the greening measured accounts for the entire plant community, in which the taxon denoted may only make up a smaller part. Data from 2004 are not included due to instrumental error that season.

	2005		2006		2007		2008		2009	
Plot	**NDVI**	**DOY**	**NDVI**	**DOY**	**NDVI**	**DOY**	**NDVI**	**DOY**	**NDVI**	**DOY**
Cassiope 1	0.37	217	0.36	220	0.35	218	0.36	239	0.33	238
Cassiope 2	0.40	217	0.38	220	0.37	218	0.39	239	0.36	205
Cassiope 3	0.38	210	0.35	224	0.41	218	0.34	239	0.31	213
Cassiope 4	0.44	210	0.41	220	0.39	218	0.45	239	0.39	238
Eriophorum 1	0.60	196	0.60	220	0.51	190	0.57	219	0.54	205
Eriophorum 2	0.52	196	0.52	220	0.47	218	0.51	206	0.49	213
Eriophorum 3	0.47	196	0.47	220	0.43	218	0.50	206	0.53	213
Eriophorum 4	0.72	210	0.72	220	0.68	197	0.64	206	0.67	196
Papaver 1	0.42	217	0.41	220	0.41	218	0.42	239	0.40	213
Papaver 2/*Salix* 5	0.46	210	0.44	220	0.45	218	0.44	239	0.42	213
Papaver 3	0.45	210	0.41	212	0.40	218	0.46	239	0.38	238
Salix 1	0.52	196	0.51	220	0.51	197	0.53	206	0.50	213
Salix 2	0.52	196	0.53	220	0.48	197	0.50	211	0.47	205
Salix 3	0.41	210	0.41	220	0.38	197	0.41	206	0.37	213
Salix 4	0.49	196	0.49	220	0.47	218	0.48	206	0.44	213
Salix 6	0.48	210	0.46	220	0.47	218	0.44	239	0.42	213

	2010		2011		2012		2013		2014	
Plot	**NDVI**	**DOY**	**NDVI**	**DOY**	**NDVI**	**DOY**	**NDVI**	**DOY**	**NDVI**	**DOY**
Cassiope 1	0.32	224	0.31	189	0.33	204	0.28	180	0.25	211
Cassiope 2	0.39	216	0.37	208	0.41	225	0.33	180	0.36	211
Cassiope 3	0.33	217	0.3	217	0.30	204	0.29	188	0.30	218
Cassiope 4	0.38	211	0.35	217	0.39	204	0.37	195	0.39	218
Eriophorum 1	0.55	203	0.49	196	0.55	211	0.44	180	0.57	218
Eriophorum 2	0.51	203	0.52	196	0.54	218	0.46	195	0.51	211
Eriophorum 3	0.51	203	0.47	182	0.48	204	0.37	195		
Eriophorum 4	0.69	203	0.63	210	0.72	218	0.62	195	0.69	225
Papaver 1	0.42	203	0.39	189	0.41	218	0.36	180	0.38	218
Papaver 2/*Salix* 5	0.43	217	0.41	217	0.44	225	0.41	202	0.41	218
Papaver 3	0.39	211	0.36	196	0.39	204	0.37	195	0.39	205
Salix 1	0.56	183	0.5	196	0.58	197	0.53	195	0.55	218
Salix 2	0.53	203	0.48	196	0.52	221	0.44	188	0.52	211
Salix 3	0.39	189	0.38	182	0.40	204	0.34	180	0.36	218
Salix 4	0.47	196	0.44	196	0.45	204	0.40	195	0.45	211
Salix 6	0.46	211	0.42	210	0.44	211	0.40	188	0.45	218

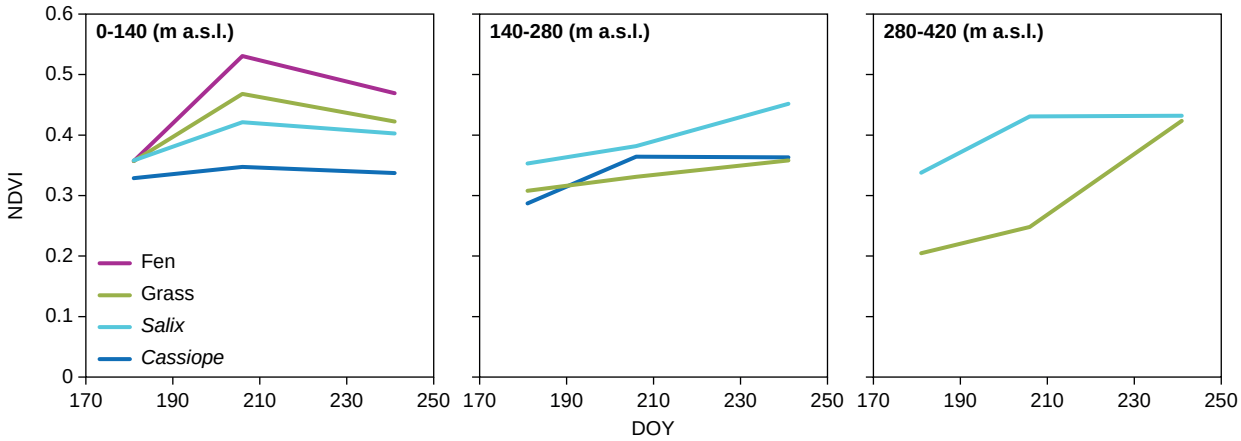

Figure 4.1 Mean NDVI from the four main vegetation types (fen, grassland, Salix heath, Cassiope heath) along an altitudinal gradient in Zackenberg during the 2014 season, averaged for three altitude intervals: 0-140, 140-280 and 280-420 m above sea level.

Table 4.6 Day of year (DOY)) of 50 % snow cover in the arthropod stations (ice-cover on pond at station 1) in 2004-2014. a) 0 % snow, b) <1 % snow, c) 7 % ice cover, d) 3 % snow, e) 31 % snow, f) 2 % snow, g) 6 % snow, h) 11 % snow.

Station	2004	2005	2006	2007	2008	2009	2010	2011	2012	2013	2014
Arthropod 1	<153[c]	<140	156	148	154	144	151	141	155	136	158
Arthropod 2	<153[a]	<140[a]	<147	<146[a]	147	135	<142[a]	<136[a]	158	137	143
Arthropod 3	156	154	174	158	172	147	162	156	175	140	165
Arthropod 4	158	156	179	161	174	138	163	153	178	134	165
Arthropod 5	<153[a]	<140	154	<176[b]	150	138	145	<136[e]	154	<129[g]	161
Arthropod 7	<153[a]	<140	<147	<176[b]	144	134	<142[d]	<136[f]	151	<129[h]	146

Vegetation greening

Table 4.5 lists the dates (as day of year – DOY) of the peak NDVI of 16 of the permanent plots. In 13 of the 16 tabulated plant plots, peak NDVI was later than the average of previous years. One plot could not be measured due to flooding. Also, peak NDVI values from 2014 were about average for all the previous seasons.

Transect NDVI was measured from snowmelt and into the autumn until the ground was covered with snow. Figure 4.1 summarises the NDVI transect data across the 2014 season in three altitude categories. The different vegetation types had very similar developments in NDVI in the two lower altitude categories. As usual, the magnitude of the NDVI values for the vegetation types changed with altitude. Due to technical problems, the mid-summer NDVI values cannot be reported this year.

4.2 Arthropods

All five pitfall trap stations (with four pitfall traps each) and the one window trap station (four trap chambers) were open during the 2014 season. Sampling procedures were concurrent with previous years. Fieldwork was carried out by Lars Holst Hansen, Jannik Hansen and Palle Smedegaard Nielsen. Samples were sorted by personnel from Department of Bioscience, Aarhus University, Denmark. The material was stored in 96 % ethanol (before 2008 in 70 % ethanol) at the Museum of Natural History, Aarhus. Please contact the BioBasis manager, Niels Martin Schmidt (nms@bios.au.dk) regarding access to the collection. The total number of arthropods collected in 2014 was 20151, which is a very low total.

Dates of 50 % snow or ice cover for the six arthropod plots were around average for two, earlier than median for two and later than median for two plots in comparison with previous years (table 4.6).

Window traps

In 2014, the window traps were opened on 17 June (day 168). The traps worked continuously until 22 September (day 265).

In the summer period, June through August, the window traps were open for 312 trap days, the second most since the start of the BioBasis programme. Nonetheless, the total number of specimens caught in the window traps in June, July and August 2014 was 4221 (table 4.7). This is the lowest number caught during the BioBasis programme, with almost 2000 less specimens caught than the second lowest year in 1998.

Especially very low numbers of midges, Chironomids, and house flies, Muscidae, were caught in 2014, with both groups having their lowest number of specimens caught during the BioBasis programme (table 4.7). These groups have traditionally been the most abundant. In 2014, the Chironomids was still the most abundant group during the summer, accounting for 77 % of all arthropods caught in the window traps, while Muscidae accounted for 5 %. Also, Ichneumonid wasps, Ichneumonidae, were caught with the lowest numbers since the start of the BioBasis programme. However, the dung flies, Scathophagidae, were caught in large numbers this year, together with root-maggot flies, Anthomyiidae, and mosquitoes, Culicidae.

Wolf spiders, Lycosidae, were caught below average numbers during June-August in 2014, while the dwarf spiders, Linyphiidae, were caught in numbers higher than average compared to earlier years. Both groups' numbers vary markedly between years. Mites and ticks, Acarina, were caught in low numbers in the summer period of 2014.

Table 4.11 summarises the 2014 window trap captures in the extended fall season until day 265 with totals for 2009-2013 for comparison.

Table 4.7 Weekly totals of arthropods caught in the window trap stations during summer 2014. The station holds two window traps situated perpendicular to each other. Each window measures 20 × 20 cm. Values from each date represents catches from the previous week. Totals from previous years are given for comparison. Asterisks mark groups not separated from related group(s) that particular year.

DOY / Year	**168**	**175**	**183**	**190**	**196**	**203**	**210**	**217**	**224**	**231**	**239**
No. of trap days	**28**	**28**	**32**	**28**	**24**	**28**	**28**	**28**	**28**	**28**	**32**
COLLEMBOLA						14	4	5			5
COLEOPTERA											
Latridius minutus											
Coccinella transversoguttata											
Coccinella transversoguttata, larvae											
Coccinellidae larvae											
HEMIPTERA											
Nysius groenlandicus											
Aphidoidea											
Coccoidea											
Psylloidea											
PSOCOPTERA											
THYSANOPTERA				1		1	1	1			
LEPIDOPTERA											
Lepidoptera larvae											
Tortricidae											
Colias hecla											
Clossiana sp.											
Lycaenidae											
Geometridae											
Gracilariidae											
Noctuidae											
DIPTERA											
Nematocera larvae											
Nematocera undet.											
Tipulidae											
Trichoceridae							1				
Culicidae			4	14	18	35	24	37	32	14	5
Chironomidae	418	244	780	435	258	124	71	97	222	430	168
Ceratopogonidae			2		2		1				
Mycetophiliidae						2	2	3	3		1
Sciaridae	9	1	1	1	6	9	3				
Cecidomyiidae											
Empididae						1					
Cyclorrhapha larvae											
Phoridae											
Syrphidae				1	1	1	1	2	1		
Heleomyzidae	1										
Piophilidae							1			1	2
Agromyzidae	2										
Tachinidae								1	1		
Calliphoridae						3	2			2	
Scatophagidae	200	10	6	1	2			1	3	2	
Anthomyiidae	147	8	17	3	2	2			1		1
Muscidae	1		7	19	57	47	26	16	15	13	9
Ephydridae				1							
HYMENOPTERA											
Bombus sp.											
Ichneumonidae				2	1	2			1		
Braconidae											
Chalcidoidea											
Latridiidae											
Ceraphronoidea											
ARANEA											
Lycosidae			1				2	1		1	1
Linyphiidae	18	2				2	3	2			2
Unidentified Aranea											
ACARINA	2			7		21					
NOTOSTRACA											
Lepidurus arcticus											
Total	**798**	**265**	**818**	**485**	**347**	**264**	**142**	**166**	**279**	**463**	**194**

2014	2013	2012	2011	2009	2008	2007	2006	2005	2004	2003	2002	2001	2000	1999	1998	1997	1996
312	**340**	**156**	**194**	**196**	**176**	**184**	**178**	**195**	**172**	**168**	**168**	**168**	**166**	**153**	**174**	**184**	**182**
28	11	24	13	70	71	33	58	112	175	31	191	119	102	61	5	15	65
0	0	0	0	0	0	0	0	0	0	0	0	0	0	2	0	0	0
0	0	1	0	0	0	0	0	0	0	0	0	0	0	0	0	0	0
0	0	1	0	0	0	0	0	0	0	0	0	0	0	0	0	0	0
0	0	0	0	0	0	0	0	0	0	0	0	0	0	0	0	0	0
0	9	0	3	0	3	1	1	6	10	0	1	0	0	0	0	0	4
0	0	0	2	0	1	0	0	8	3	1	0	2	0	0	0	0	0
0	1	0	0	0	0	0	0	0	0	0	0	0	3	0	0	0	14
0	0	0	1	0	0	0	0	0	0	0	0	0	0	0	0	0	0
0	0	0	0	4	0	0	0	0	0	0	0	0	0	0	0	0	0
4	54	10	12	2	13	5	7	7	11	0	3	1	0	0	0	0	8
0	0	1	0	1	0	0	0	0	0	0	0	0	0	0	0	0	0
0	3	1	0	0	0	0	0	0	0	0	0	0	0	0	0	0	0
0	23	0	0	0	0	0	0	1	9	2	6	0	2	0	0	0	1
0	3	0	3	6	3	9	3	1	5	4	1	1	2	1	1	1	6
0	0	0	10	1	1	13	3	0	0	0	0	0	0	0	0	0	0
0	0	0	1	0	0	0	0	0	0	0	2	3	0	0	0	1	3
0	0	0	0	0	0	0	0	0	0	0	0	0	0	0	0	0	0
0	9	0	5	8	6	1	4	7	1	1	0	0	0	0	0	2	2
0	0	0	0	0	0	0	0	0	0	0	2	0	0	1	0	0	0
0	0	0	0	0	0	0	0	0	0	0	0	1418	0	0	0	0	0
0	0	0	2	0	0	0	0	0	0	1	0	0	0	1	0	0	0
1	0	0	1	0	0	0	0	0	2	0	0	0	0	0	1	1	0
183	23	133	63	71	88	53	68	128	104	96	232	209	111	322	138	142	98
3247	5430	17993	7344	9402	14207	12788	9290	6470	5203	7792	6378	3876	8522	5787	3743	7725	6477
5	86	16	26	60	17	83	32	9	21	66	1598	168	*	1799	*	*	*
11	10	31	42	36	21	7	17	18	21	2	6	23	11	16	624	240	64
30	242	90	121	67	613	179	125	749	53	12	56	33	13	171	*	*	*
0	0	1	1	0	1	0	0	0	0	0	3	4	32	6	0	0	1
1	40	2	16	3	1	8	9	7	7	8	1	8	10	9	9	1	77
0	0	0	0	0	1	0	0	0	0	0	0	0	0	0	0	0	0
0	4	1	2	0	0	1	3	0	0	0	1	1	2	3	0	0	0
7	4	1	8	5	11	9	8	10	12	6	10	4	5	1	8	16	4
1	3	0	3	1	0	0	0	0	0	0	1	2	0	1	0	0	0
4	4	0	0	0	0	0	0	0	3	0	0	0	0	0	0	0	0
2	9	3	5	0	1	3	17	99	34	2	3	0	0	0	0	4	0
2	23	1	4	9	2	1	3	7	10	7	0	2	6	1	0	0	0
7	19	0	4	12	3	5	1	9	4	1	1	1	4	5	7	6	2
225	13	42	15	81	6	15	0	31	11	3	7	0	2	10	0	30	11
181	41	602	87	83	88	65	43	28	12	10	8	2	*	3	26	11	*
210	732	579	1350	374	522	514	394	935	1423	866	554	1312	1455	754	745	809	1355
1	0	0	0	0	0	0	0	0	0	0	0	0	0	0	0	0	0
0	6	1	3	0	2	3	0	7	5	3	1	0	0	1	2	6	5
6	63	15	95	78	29	29	33	68	47	70	24	34	48	24	18	44	43
0	1	0	0	0	1	1	0	0	1	0	0	0	0	0	1	1	0
0	2	0	0	0	3	3	1	1	1	1	2	14	0	0	0	2	0
0	0	0	0	1	0	0	0	0	0	0	0	0	0	0	0	0	0
0	5	1	0	3	1	0	0	0	0	2	0	0	0	0	0	0	0
0																	
6	22	51	6	6	17	18	31	10	1	1	1	0	2	0	0	1	0
29	5	66	24	3	15	2	8	12	4	8	8	15	10	6	1	1	8
0	1	0	0	0	0	0	0	0	0	0	0	0	0	0	0	0	0
30	39	59	16	25	7	27	120	704	524	54	347	358	246	191	826	189	299
0																	
0	0	1	0	0	0	0	0	0	0	0	0	0	0	0	0	0	0
4221	**6947**	**19745**	**9288**	**10412**	**15755**	**13876**	**10279**	**9444**	**7717**	**9050**	**9448**	**7610**	**10588**	**9177**	**6155**	**9248**	**8547**

Table 4.8 Weekly totals of arthropods caught at the five pitfall trap stations during summer 2014. Each station holds eight yellow pitfall traps measuring 10 cm in diameter. Values from each date represent catches from the previous period. Totals from previous years are given for comparison. Since 2007, the number of pitfall traps has been reduced compared to 1996-2006. Asterisks mark groups that were not separated from closely related groups in that year.w

DOY / Year	154	161	168	175	183	190	196	203	210	217	224	231	239
No. of active stations	2	2	2	5	5	5	5	5	5	5	5	5	5
No. of trap days	32	56	56	94	148	140	120	140	140	140	140	140	160
COLLEMBOLA	2	51	237	705	463	654	372	978	236	191	63	67	93
HEMIPTERA													
Nysius groenlandicus								1					
Aphidoidea		2				1	2	5	3	9	7	28	4
Coccoidea				1	4	5	3		11	4		2	
THYSANOPTERA	1	1	4		5	4	6	5		1	1	1	6
LEPIDOPTERA													
Lepidoptera larvae			1	1	6	5	4	2	2	3		3	1
Tortricidae							1						
Colias hecla										2	4		
Clossiana sp.							1	1		16	8	6	2
Lycaenidae													
Plebeius franklinii													
Geometridae													
Gracilariidae											1		
Noctuidae									1	1	3	8	6
Unidentified *Lepidoptera*													
DIPTERA													
Unidentified Diptera larvae	2									2			
Nematocera larvae									1				1
Tipulidae larvae													
Tipulidae									1		2		
Trichoceridae													
Culicidae							3	11	11	9	3	4	
Chironomidae			457	556	907	371	158	118	36	51	85	28	16
Ceratopogonidae					1		2			1			
Mycetophiliidae					1	19	15	11	5	4	4	3	5
Sciaridae		6	35	11	20	22	46	103	25	16	4	4	5
Cecidomyiidae						1							1
Brachycera larvae													
Empididae									1		1		1
Cyclorrhapha larvae											2	4	6
Phoridae								5	3	40	61	198	74
Syrphidae					1	1	2	1	3	13	20	13	7
Heleomyzidae													
Agromyzidae	1						1	1			1	3	2
Tachinidae											2	1	1
Calliphoridae		1			1	2	1	1			6	2	5
Scatophagidae		1		6	4	6	2		2		1	1	1
Fannidae													
Anthomyiidae	10	8	37	41	85	12	2	1		3	15	7	8
Muscidae			8	27	115	141	279	501	395	622	269	250	106
Ephydridae													
SIPHONAPTERA													
HYMENOPTERA													
Tenthredinidae													
Hymenoptera larvae													
Bombus sp.													
Ichneumonidae					1	5	13	8	7	10	11	15	14
Braconidae					7	2	5	8	6	3	3	4	3
Chalcidoidea							1	1	2	2	1	5	13
Scelionidae													
Ceraphronoidea								3					
Cynipoidae													
COLEOPTERA													
Coccinella transversoguttata													
Coccinellidae larvae													
ARANEA													
Thomisidae	1	1	2	2	12	4	11	9	10	13	3	8	2
Lycosidae	1	1	6	6	92	89	181	140	48	123	37	174	67
Lycosidae egg sac								10	4	9	2	7	
Dictynidae					2	1			1				
Linyphiidae	6	10	34	29	60	26	29	52	39	14	19	20	17
Unidentified Aranea													
ACARINA	4	7	254	203	166	162	180	246	212	190	96	167	159
Total	**28**	**89**	**1075**	**1588**	**1953**	**1533**	**1320**	**2222**	**1065**	**1352**	**735**	**1033**	**626**

2014	2013	2012	2011	2009	2008	2007	2006	2005	2004	2003	2002	2001	2000	1999	1998	1997	1996
57	70	56	5	5	5	5	5	5	5	5	5	5	5	5	5	5	5
1506	1997	1422	1785	1936	1578	1709	2979	3686	3437	3101	3059	2954	3155	2706	2702	2797	(1512)
4112	1486	2747	3193	3781	1633	1292	7100	9586	13277	17510	20312	17970	21726	23443	8957	10830	4636
1	46	36	11	5	10	4	13	471	96	3	0	2	0	1	0	5	40
61	71	11	22	12	48	33	61	524	277	1624	157	359	3	11	185	10	6
30	256	296	231	152	1228	431	617	1092	1288	42	634	9	781	431	3	548	254
35	97	67	28	27	22	6	2	19	4	0	5	0	0	2	0	0	2
28	144	17	51	33	43	32	116	82	280	37	63	16	18	21	106	168	354
1	4	5	1	0	0	0	1	0	0	1	0	1	0	0	0	0	0
6	130	45	0	0	0	0	0	15	38	156	29	0	77	42	12	19	88
34	267	37	77	93	178	140	210	174	240	468	381	49	329	82	56	180	1052
0	1	0	37	15	14	16	45	0	0	0	0	0	4	1	0	0	0
0	0	0	0	0	0	0	0	1	1	0	7	19	0	0	1	1	2
0	0	1	0	0	0	0	0	2	2	0	6	0	0	0	0	0	0
1	0	0	0	0	0	0	0	0	0	0	0	0	0	0	0	0	0
19	26	30	5	13	38	19	19	183	14	110	1	15	4	6	2	45	68
0	0	0	0	0	2	0	0	0	0	0	0	0	0	0	0	0	0
4	0	4	0	0	0	0	0	0	0	0	0	0	0	0	0	0	0
2	0	0	0	3	2	0	21	10	18	29	46	15	279	105	58	39	52
0	0	0	2	0	3	1	2	1	6	3	3	3	4	1	0	0	0
3	3	3	2	2	5	3	4	5	1	7	4	14	2	4	1	4	14
0	0	0	0	0	0	0	1	0	1	1	1	7	0	3	0	1	0
41	1	22	19	6	5	0	33	13	19	23	86	34	61	83	22	16	2
2783	293	1209	1225	1316	2415	3559	4365	1492	1596	4768	5982	1958	3666	8542	2402	3337	3292
4	2	4	11	76	7	97	92	6	16	107	102	7	0	68	*	*	*
67	5	40	13	30	104	1	74	104	63	70	48	181	37	205	1764	1194	526
297	821	325	1060	426	548	533	1256	819	912	1101	762	573	787	796	*	*	*
2	34	2	0	0	1	0	2	8	13	8	6	8	24	0	1	0	0
0	0	0	0	0	0	0	0	0	0	3	0	0	4	3	0	0	0
3	2	1	2	7	0	2	2	3	5	8	24	28	14	21	10	6	8
12	2	4	0	39	3	1	1	77	60	23	22	0	7	7	19	75	16
381	1338	1403	2964	1610	775	620	461	386	461	665	489	445	1316	435	344	214	118
61	11	29	6	37	35	28	9	93	45	35	30	18	43	50	28	81	72
0	0	0	0	0	0	0	1	0	1	1	5	6	1	7	0	0	0
9	49	19	20	4	11	3	29	151	60	10	6	4	2	0	0	1	0
4	75	38	49	64	27	19	16	39	42	60	23	29	37	37	0	19	0
19	93	2	65	237	6	20	6	96	31	17	44	5	218	26	49	48	48
24	1	1	6	41	18	22	1	106	7	42	24	0	1	41	0	385	26
0	0	0	0	0	0	0	0	0	0	0	0	0	0	0	0	1	0
229	119	184	200	299	213	210	183	535	124	108	238	57	*	88	416	573	*
2713	1977	3231	3897	2919	1647	1525	2313	5464	5623	8385	7499	6766	12805	10005	5463	6217	8114
0	0	0	0	0	0	0	0	0	0	0	0	0	0	0	0	0	0
0	0	0	0	0	0	0	0	0	0	0	0	0	0	3	0	0	0
0	0	0	0	0	0	0	0	1									
0	6	2	0	0	0	0	0	3	4	8	0	0	4	0	2	0	0
0	16	24	11	9	8	14	6	18	40	15	7	3	10	2	6	12	2
84	299	198	406	250	98	115	269	717	720	974	436	442	710	386	297	567	954
41	22	32	16	36	35	20	42	80	61	52	11	11	15	10	105	59	44
25	202	105	175	345	625	437	287	747	746	120	190	106	21	9	2	123	48
0	0	1	0	0	0	0	4	0	0	310	5	3	0	101	0	0	0
3	7	15	5	7	9	5	8	17	13	3	8	3	15	5	0	0	0
0	0	1	0	0	1	0	0	24	3	0	0	1	0	0	0	1	0
0																	
0	0	5	0	1	0	0	0	0	0	0	0	0	0	0	0	0	0
0	0	0	0	0	0	0	0	0	0	0	0	0	0	0	0	0	0
78	171	116	130	93	101	121	164	98	90	164	219	177	134	144	89	245	198
965	2088	1531	2523	1040	2162	2450	2869	3316	3428	3438	1760	2618	3254	2118	2123	3806	4548
32	24	18	27	23	91	18	56	45	69	85	12	85	101	160	160	138	82
4	39	6	18	11	12	11	10	84	40	18	107	0	0	79	0	53	0
355	838	837	445	360	229	261	834	1411	1483	2526	1438	1833	3523	2243	1108	1644	1436
0	0	3															
2046	2309	3203	3899	1748	2835	1141	3837	10096	17616	18602	21282	9929	15256	8263	6304	19781	8182
14619	**13375**	**17388**	**20852**	**15171**	**15247**	**13210**	**25916**	**38217**	**48935**	**61756**	**62523**	**43811**	**65344**	**58174**	**30095**	**50446**	**34404**

Table 4.9 Weekly totals of arthropods caught at the five pitfall stations and the window trap station during autumn 2014. Values from each date represent catches from the previous period. Totals from previous years are given for comparison.

	Window traps										Pitfall traps									
DOY/Year	**246**	**252**	**259**	**265**	**2014**	**2013**	**2012**	**2011**	**2010**	**2009**	**246**	**252**	**259**	**265**	**273**	**2014**	**2013**	**2012**	**2011**	**2010**	**2009**
No. of active stations	1	1	1	1	4	1	1	1	1	1	5	5	5	5	5	25	20	25	5	5	5
No. of trap days	28	24	28	24	104	104	68	56	48	56	140	120	140	120	160	680	520	696	720	700	600
COLLEMBOLA	1	1			2	0	3	0	35	2	59	59	25	31	9	183	1063	229	190	416	56
HEMIPTERA																					
Nysius groenlandicus					0	0	0	0	0	0						0	37	28	51	1	3
Aphidoidea					0	0	0	0	0	0	6	1		2		9	34	4	15	8	0
Coccoidea					0	0	0	0	1	0	1					1	0	1	0	2	0
THYSANOPTERA					0	6	0	0	0	0	4	2	4			10	2	2	1	1	1
LEPIDOPTERA																0					
Lepidoptera larvae					0	0	0	0	0	0	2	1				3	0	5	1	0	2
Noctuidae					0	0	0	0	0	0	3					3					
Clossiana sp.					0	0	0	0	0	0	1					1	0	0	0	0	2
DIPTERA																0					
Culicidae					0	0	0	0	0	0						0					
Chironomidae					0	26	8	147	20	6	5	1				6	13	2	7	1	7
Ceratopogonidae					0	0	0	0	1	0						0	0	0	0	0	0
Mycetophiliidae		2	5	3	10	0	4	1	0	2	2	1	1	1	2	7	7	2	3	4	5
Sciaridae					0	0	0	0	0	0	10					10	3	1	1	1	2
Syrphidae	1				1	0	0	0	1	0	6					6	1	1	0	1	2
Cyclorrhapha larvae					0	0	0	0	0	0	10	11	8			29	1	6	0	0	0
Phoridae		1			1	0	0	1	21	0	98	4				102	1	124	18	316	0
Agromyzidae	2	1	1	2	6	2	2	6	1	0	3		5	6		14	32	10	10	9	2
Tachinidae					0	0	0	0	0	0	6					6	0	0	1	1	0
Calliphoridae	1			1	2	1	0	2	0	3	34	11	7	3		55	3	0	1	0	12
Scatophagidae	1	1			2	0	0	10	16	4	1	3		1		5	0	1	5	7	12
Anthomyiidae	4				4	11	10	22	13	6	35	2	6	3		46	23	25	47	10	31
Muscidae	4	1	1		6	0	7	9	5	0	41	1	1			43	0	11	6	9	2
Ephydridae					0	0	0	0	0	0						0	0	0	0	0	0
Tipulidae larvae					0	0	0	0	0	0		3				3					
HYMENOPTERA																					
Ichneumonidae	1				1	2	1	3	4	1	21	2	1	1	1	26	25	42	36	61	9
Braconidae					0	0	0	0	0	0	2	1	1			4	25	4	2	0	5
Chalcidoidea					0	0	0	0	18	0	8	3	1	1		13	1	12	6	12	11
Ceraphronoidea					0	0	1	0	0	0	2		1			3	3	6	1	1	0
COLEOPTERA																					
Coccinella transversoguttata					0	0	1	0	0	0						0	0	0	0	0	0
Coccinellidae larvae					0	0	0	0	0	0	2					2	0	0	0	0	0
ARANEA																					
Thomisidae					0	0	0	0	0	0	3	5	2	2		12	12	11	11	11	11
Lycosidae	1				1	1	4	0	19	1	62	13	12	11		98	53	99	89	30	30
Lycosidae egg sac					0	0	0	0	0	0	3					3	0	1	4	1	5
Dictynidae					0	0	0	0	2	1	2	2	2		1	7	4	8	13	3	3
Linyphiidae	4	2	3	4	13	3	5	2	17	2	56	40	40	49	31	216	244	462	176	212	48
Unidentified Aranea					0	0	0	0	0	0						0	0	1	0	0	0
ACARINA	2	1			3	1	3	0	31	2	188	37	68	20	20	333	313	30	228	303	34
Total	**22**	**10**	**10**	**10**	**52**	**53**	**49**	**195**	**205**	**30**	**676**	**203**	**185**	**131**	**64**	**1259**	**1901**	**1128**	**923**	**1421**	**295**

Pitfall traps

The first pitfall traps were established on 3 June (day 154), and all traps were in use from 24 June (day 175) and until 30 September (day 273). Since 2007, only half of the pitfall traps have been established. During the summer period, June through August, the number of trap days was 1506, which is a little below average since 2007. The total number of specimens caught was 14619, which is comparable to the previous years in catch per trap day. Weekly totals were pooled for all five stations and are presented in table 4.8 with totals from

previous years for comparison. In the following, this year will be compared to years since 2007.

Collembola, spring tails, were caught in very high numbers this year, almost double as many as the average. Hence, it was the most abundant arthropod group in 2014, and accounted for 28 % of the total number of caught specimens. Midges, Chironomids, and house flies, Muscidae, were the second and third most abundant groups (table 4.8). Chironomids were caught in large numbers, while Muscids were similar to the average since 2007. Thus, Chironomids is back among the most abundant groups, after 2013 where they experienced record low numbers. The emergence of house flies, Muscidae showed a late and low peak (figure 4.2). Scuttle flies, Phoridae, which former were among the most caught Dipterans, were caught in very low numbers this year. Likewise, dark-winged fungus gnats, Sciaridae, usually an abundant Dipteran family, were caught in low numbers this year. Nematocera larvae were earlier caught in high numbers, but no individuals have been caught since 2009 until the captures this year. Two individuals were caught. Mosquitoes, Culicidae, were caught in record high numbers in 2014 (since 2007) after several years with low numbers.

In the Lepidopteran families and species, both the hecla sulphur, *Colias hecla*, and the Fritillaries, *Clossiana* sp., were caught in low numbers. Lepidopteran larvae numbers were back to average numbers after a year with high abundance in 2013. Hymenopteran families were also caught in low numbers in 2014. Ichneumon wasps, Ichneumonidae, remain the most abundant hymenopteran family. Likewise, the Chalcidoidea also had a record low year since 2007. Thysanoptera were caught in numbers a little below average in 2014, after it had a record high year last year.

Among the Aranea, the wolf spiders, Lycosidae, are still the most dominant family, even though they were caught in very low numbers this year. The dwarf spiders, Linypiidae, were also caught in low numbers compared to previous years since 2007.
Mites and ticks, Acarina, were caught in numbers a little below the average from previous years.

Table 4.9 summarises the 2014 pitfall trap captures in the extended fall season until day 273 with totals from 2009 to 2012 for comparison.

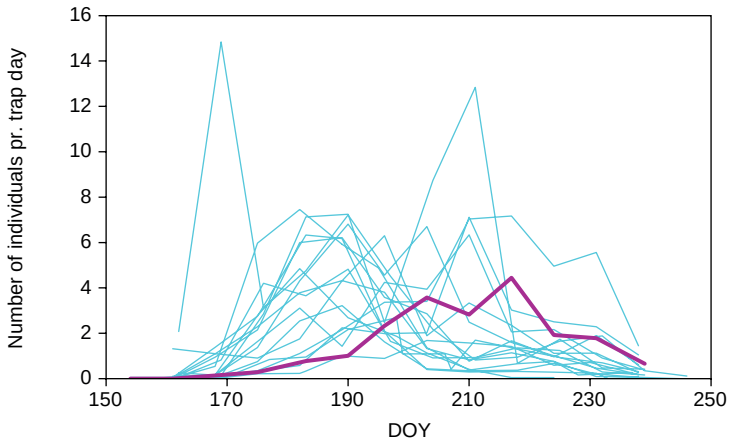

Figure 4.2 Numbers of house flies, Muscidae, caught per trap day every week in the pitfall traps in 2014 (thick red line) compared with 1996-2009 and 2011-2013 (thin blue lines). Only part of the samples from the 2010 season is available, and 2010 is hence not included in the figure.

Table 4.10 Peak ratio (percent) of mountain avens Dryas integrifolia/octopetala *flowers depredated by larvae of* Sympistis nigrita *ssp. zetterstedtii in mountain avens plots in 1996-2014.*

Plots	*Dryas* 1	*Dryas* 2	*Dryas* 3	*Dryas* 4	*Dryas* 5	*Dryas* 6
1996	2	0	11	17	2	0
1997	6	5	18	1	8	0
1998	3	0	3	7	2	0
1999	0	0	0	0	0	0
2000	0	0	0	0	0	0
2001	0	0	0	0	0	0
2002	15	1	7	11	9	0
2003	2	0	1	5	2	0
2004	15	4	33	39	3	1
2005	1	1	10	3	0	0
2006	27	3	6	18	2	6
2007	0	2	8	4	0	5
2008	34	25	67	32	2	8
2009	8	5	27	14	33	5
2010	7	7	16	11	6	47
2011	3	3	6	2	2	4
2012	7	1	12	1	0	0
2013	8	4	42	29	10	5
2014	50	2	25	4	1	2

New observations in 2014

In 2014, for the first time in the BioBasis programme, a fly from the family Ephydridae (shore flies) was caught in the window traps. Eight species from this family has recorded in Greenland (Zatwarnicki and Mathis 2015), and it has been recorded from Zackenberg before by independent research studies (Tomas Roslin, pers. comm.). Likewise, for the first time at Zackenberg during the Biobasis programme, a member of the Lepidopteran family Gracillariidae was caught in

the pitfalls (table 4.8). This family is the principal family of leaf miners. So far, only one species of Gracillariidae has been found in Greenland, namely *Phyllonorycter ledella*, whose larvae mines the leaves of *Ledum groenlandicum* (J. Böcher, pers.com). *L. groenlandicum*, however, does not occur at Zackenberg.

The ladybird *Coccinella transversoguttata* was first caught in pitfall traps in 2009 (cf. Böcher 2009), but was not caught this year (table 4.7). However, Coccinellidae larvae were caught for the first time at Zackenberg this year (table 4.9). Both moths from the family Noctuidae and larvae from the dipteran family Tipulidae were for first time observed in the autumn since collections began in 2009 (table 4.9).

Insect predation on Dryas flowers

Predation on *Dryas* flowers by *Sympistis nigrita* ssp. *zetterstedtii* was recorded in six of six plots. The peak percentages of flowers marked by predation were about average for three plots and above average for three plots when compared to previous years (table 4.10).

4.3 Birds

Bird observations were carried out by Palle Smedegaard Nielsen, Jannik Hansen, Lars Holst Hansen and Jannie Fries Linnebjerg. Other researchers and staff – not least Jeroen Reneerkens and colleagues – provided much valued information throughout the season. Local site names can be found in Schmidt *et al.* (2014).

Breeding populations

During five days – between 25 June (day 176) and 6 July (day 197) – a complete, initial census was carried out. Late snowmelt and unstable weather conditions meant that the survey had to be undertaken over a longer period than usual, and longer than desirable. The completion of the survey took 42 'man-hours', which is above average. In addition, large parts of the census area were surveyed regularly during June, July and most of August, exceptions being the closed goose moulting area along the coast and the slopes of Aucellabjerg above 350 m a.s.l. The latter were surveyed on seven occasions only, in addition to the many visits by Reneerkens and colleagues. The total effort in June and July 2014 was near average (142 hours in June and 101 hours in July) compared to previous years. The results of the initial census supplemented with records from the rest of the season (Schmidt *et al.* 2014) are presented in tables 4.11 and 4.12, and compared with the estimates of previous years.

The first two red-throated divers *Gavia stellata* were seen on 5 June (day 156), while the first settled pair was recorded the following day. At least four pairs attempted to breed within the census area and four nests were found. All nests fell victim to predation.

Table 4.11 Estimated numbers of pairs/territories in four sectors of the 15.8 km² census area in the Zackenberg valley 2014.

Species	<50 m a.s.l. 7.77 km²	50-150 m a.s.l. 3.33 km²	150-300 m a.s.l. 2.51 km²	300-600 m a.s.l. 2.24 km²	Total
Red-throated diver	3	0	0	0	3
King eider	0	0	0	0	0
Long-tailed duck	2	0	0	0	0
Rock ptarmigan	0	0	0	0	0
Common ringed plover	6-10	4-5	10-11	4-7	24-33
Red knot	1-2	11-13	2-3	0	14-18
Sanderling	21-25	4-5	8	5	38-43
Dunlin	57-68	17-19	0-1	1	75-89
Ruddy turnstone	4	13-16	0	1	18-21
Red-necked phalarope	1	0	0	0	1
Arctic skua	1	0	0	0	1
Long-tailed skua	18-19	5-7	0	0	23-26
Arctic skua	1	0	0	0	1
Glaucous gull	0	0	0	0	0
Arctic redpoll	2	1	0	0	3
Snow bunting	12-14	22	8	7	49-51

Table 4.12 Estimated numbers of pairs/territories in the 15.8 km² census area in the Zackenberg valley 2014 compared with the 1996-2013 averages.

Regular breeders				
Species	**No. of territories**	**Average min. and max no. territories 1996-2013**	**No. of nests found[1]**	**Comments**
Red-throated diver	4	2.7	4	
Common eider	0	0.3	0	
King eider	0	1.5	0	
Long-tailed duck	5	5.8	2	
Rock ptarmigan	0	2.3-3.1	0	
Common ringed plover	24-33	27.8-33.1	3	
Red knot	14-18	29.9-31.1	0	
Sanderling	38-43	51.8-58.8	16	
Dunlin	78-89	81.7	17	
Ruddy turnstone	18-21	38.6-43.7	5	
Red-necked phalarope	1	0.8-1.6	0	
Long-tailed skua	23-26	17.5-21.5	0	A non-breeading year, few pairs stayed for long
Glaucous gull	1	0.6	0	
Common raven	2	0	0	Nests outside the census area.
Snow bunting	49-51	47.7-51.8	1	Nests of passerines are only found opportunistically
Irregular breeders				
Species	**No. of territories**	**Average min. and max. no. territories 1996-2011**	**No. of nests found[1]**	**Comments**
Pink-footed goose	0	0.11	0	Min. 3921 immatures migrated northwards from the area
Eurasian golden plover	0	0.06	0	Few observations of a single bird
Red phalarope	2-3	0.5-0.7	0	
Arctic skua	1	0	0	
Snowy owl	0	0.06	0	
Northern wheatear	1	0.09	0	Nests of passerines are only found opportunistically
Arctic redpoll	3	0.8-1.3	0	Nests of passerines are only found opportunistically
Lapland longspur	1	0.14-0.17	0	Nests of passerines are only found opportunistically. See table 4.25

[1]Within the census area

Table 4.13 Median first egg dates for waders at Zackenberg 2014 as estimated from incomplete clutches, egg floating and hatching dates, as well as weights and observed sizes of pulli.

Species	**Median date**	**Range**	**N**	**Average 1996-2013**
Common ringed plover	173	164-178	8	165.9
Red knot	N/A	N/A	0	166.9
Sanderling	177	154-185	26	168.6
Dunlin	182	176-200	12	167.1
Ruddy turnstone	170	167-175	8	164.1

The number of common ringed plover *Charadrius hiaticula*, red knot *Calidris canutus* and sanderling *Calidris alba* territories was below average (table 4.12). Dunlin *Calidris alpina* territories were found in numbers near average. Please note, that dunlin territory numbers in early years are likely to have been underestimated (Meltofte 2006). Ruddy turnstone *Arenaria interpres* territories were found in low numbers (tables 4.11 and 4.12). The last three years have had record low numbers of turnstone territories.

No phalarope nests (red-necked phalarope *Phalaropus lobatus* and red phalarope *P. fulicarius*) were found in 2014. On 7

Table 4.14 Snow cover 10 June together with median first egg dates for waders at Zackenberg 1995-2014. Data based on less than 10 nests/ broods are marked with asterisk, less than five are omitted. The snow cover is pooled (weighted means) from section 1, 2, 3 and 4, where the vast majority of the egg laying phenology data originates.

Species	1995	1996	1997	1998	1999	2000	2001	2002	2003	2004
Snow cover 10 June	84	82	76	80	91	53	84	79	83	48
Sanderling		168*	169	169	174.5	168	173.5	168	164	160
Dunlin	169*	163.5	164	167.5	173	163.5	176	159	163	164
Ruddy turnstone	163*	170.5	164	163.5	175	163	174	160	159	160
Species	**2005**	**2006**	**2007**	**2008**	**2009**	**2010**	**2011**	**2012**	**2013**	**2014**
Snow cover 10 June	28	85	48	71	4	72	78	83	0.2	80
Sanderling	166*	181	166	169	167	163	166	175	167	177
Dunlin	163	178	166	169	162	165.5	173	174	166	174
Ruddy turnstone	162	172*	158	170	154	165	162	161	160.5	168

Table 4.15 Mean nest success (%) 1996-2014 according to the modified Mayfield method (Johnson 1979). Poor data (below 125 nest days or five predations) are marked with asterisk. Data from species with below 50 nest days have been omitted. If no nest was found, it is indicated by "–". Nests with at least one pipped egg or one hatched young are considered successful. Also given are total numbers of adult foxes observed by the bird observer in the bird census area during June and July (away from the research station proper), along with the number of fox dens holding pups.

Species	1996	1997	1998	1999	2000	2001	2002	2003	2004	2005
Common ringed plover				60*		38*				–
Red knot	–	–			–		–			–
Sanderling	72*	33–100*	88*	40	46*	19	33*	45	71–85	
Dunlin			28–47	65	68	75*		63	93	43*
Ruddy turnstone	21–68	67–100	16	23–28	29	60*	52	21–27	83	
Red-necked phalarope	–	–	–		–	–	–	–	–	
Red phalarope	–	–	–	–	–	–	–	–	–	–
All waders	**33–63**	**52–100**	**32–37**	**42–44**	**44**	**43**	**43**	**42–44**	**87–90**	**22**
N nests	17	31	44	44	47	32	21	51	55	15
N nest days	163	228	334	520.8	375	328.4	178.9	552	700	104
Fox encounters	14	5	7	13	11	14	21	11	16	18
Fox dens with pups	2	0	1	0	2	2	0–1	2	3	0
Species	**2006**	**2007**	**2008**	**2009**	**2010**	**2011**	**2012**	**2013**	**2014**	**1996–2013**
Common ringed plover	0*	–	2*	–		–			4.3*	37.6–40
Red knot	–	100*				3*		8.6	–	12.1
Sanderling	7*	3	5	7.5	3	17	14.3	29.5	15.0	16.3–17.2
Dunlin	47	48	17	80*	62*	21.1*	33.7	18.6*	23.7	49.6–52.6
Ruddy turnstone		36	22*	27*	34*	2.9*	9.9*	2.7*	2.4*	28.8–32.4
Red-necked phalarope	–	–	–		–	–	–	–	–	
Red phalarope		–	–	–		–	–	–	–	
All waders	**37**	**18**	**16**	**14**	**9**	**14.4**	**15.3**	**19.7**	**17.3**	**27.3–29.2**
N nests	28	60	58	66	46	47	56	47	45	730
N nest days	332.2	532.7	423.5	508.5	306.5	349	552.2	483.6	472.6	6972.5
Fox encounters	22	23	20	11	9	20	34	13	15	
Fox dens with pups	2	3	5	3	3	3	5	3	3	

Table 4.16 Mean clutch sizes in waders at Zackenberg 1995-2014 compared to the weighted mean of all years (Weighted mean). Samples of fewer than five clutches are marked with asterisk.

Species	1995	1996	1997	1998	1999	2000	2001	2002	2003	2004	2005
Common ringed plover	4.00*	4.00*	3.50*	4.00*	3.50*	4.00*	3.50*	4.00*	4.00*	4.00*	
Red knot				4.00*	4.00*		4.00*		4.00*	4.00*	
Sanderling	4.00*	4.00	3.86	4.00	3.67	4.00	3.43	3.83	4.00	4.00	3.75
Dunlin		4.00*	3.75*	3.90	3.70	3.93	3.63	4.00*	4.00	3.92	4.00
Ruddy turnstone		3.71	3.79	3.82	3.58	3.80	3.75	4.00	3.77	3.92	3.86
Weighted mean	4.00	4.00	3.76	3.90	3.65	3.89	3.63	3.95	3.94	3.94	3.89

Species	2006	2007	2008	2009	2010	2011	2012	2013	2014	W. mean
Common ringed plover	3.75*		3.75*		4.00*		3.75*	3.00*	3.76*	3.71
Red knot		4.00*	4.00*	4.00*	4.00*	4.00*	4.00*	4.00*		3.59
Sanderling	3.63	3.73	3.77	3.91	3.92	3.85	3.93	3.75	3.04	3.79
Dunlin	3.13	3.79	3.67	4.00	4.00	3.70	3.75	4.00	3.93	3.81
Ruddy turnstone	3.00*	4.00*	3.71	3.78	3.92	3.90	4.00	4.00	3.50	3.81
Weighted mean	3.33	3.76	3.74	3.91	3.80	3.84	3.90	3.81	3.46	3.87

Table 4.17 Egg-laying phenology, breeding effort and success in long-tailed skuas Stercorarius longicaudus *at Zackenberg 1996-2014. Median egg laying date is the date when half the supposed first clutches were laid. Number of clutches found includes replacement clutches. Mean hatching success according to the modified Mayfield method (Johnson 1979). Poor data (below 125 nest days or five predations) are marked with asterisk. Nests with at least one pipped egg or one hatched young are considered successful.*

Long-tailed skua breeding	1996	1997	1998	1999	2000	2001	2002	2003	2004	2005	2006	2007	2008	2009	2010	2011	2012	2013	2014
Median 1st egg date		158	163	168	170	166	160	166	160	159	170	163	164	168	172	165	161	159	N/A
No. of clutches found	8	17	23	8	5	21	14	7	21	8	2	15	9	2	1	6	14	6	0
No. of young hatched	1	25	16	2	2	18	14	5	36	6	1	11	3	1	0	0	3	0	0
Nest success % (Mayfield)		80.6*	26.7	18.1*	17.5*	39.5	44.1	76.2*	94*	51.8*	100*	23	33	25.9	0	44	80	0*	0
Estimated no. of young fledged	0	5	6	1	0	5	4	2	22	1	0	1	2	1	0	0	1	0	0

June (day 158), two female red phalaropes *P. fulicarius* were seen in a pond near the research station. Following this observation, a pair and later a single male were seen within the same week at this pond. On 12 June (day 163), a copulating pair of red-necked phalaropes was recorded at a small pond. The following day another copulation attempt was seen in the same area. A pair or the male or female was observed at this site until 24 June (day 175).

Long-tailed skua *Stercorarius longicaudus* territories were found in numbers near average (table 4.12). No nests were found, and many territories were only defended for a short period. However, several birds that had defended territories were present in the area long into the season. Since some of these birds were individually marked, we could determine which birds stayed.

No glaucous gull *Larus hyperboreus* nests were found this season, yet a pair defended the same stretch of the river Zackenberg, that has had nests since at least 2004. Glaucous gulls were seen daily throughout the season. Only one minor flock is reported: 17 July (day 198; 8 individuals).

No rock ptarmigan *Lagopus muta* territories were recorded in 2014.

The number of snow bunting *Plectrophenax nivalis* territories was average, compared to previous seasons (table 4.12). The first female was recorded as early as 12 June (day 163). Early August,

a small flock of adults and juveniles were recorded, 9 August (day 221).

Three arctic redpoll *Carduelis hornemanni* territories were recorded this year (table 4.12).

In 2014, only a single male Lapland bunting *Calcarius lapponicus* was seen on several occasions from 17 June (day 168) to 9 July (day 190), but no females were recorded.

Reproductive phenology in waders, Charadriiformes

Only 1.6 % (one nest) of all wader nests were initiated before 10 June (day 161) and 25.8 % before 20 June (day 171, table 4.13).

The snow cover on 10 June (day 161) was 80 % and nest initiation was late for all wader species (table 4.14).

Reproductive success in waders, Charadriiformes

The overall wader nest success was low in 2014. Using the modified Mayfield method (Johnson 1979), 17.3 % of the wader nests were successful.

Dunlin nests suffered predation harder than usual, although similar to 2011, and better than 2013. Sanderling nests had a year similar to 2012 with just under the average level of nest success. Ruddy turnstones had a very low success rate, and nested in low numbers (table 4.15). No red knot nests were found in the census area in 2014.

The number of arctic fox encounters was below average, while numbers of active fox dens were near average (table 4.15). The number of lemming winter nests was 59 (table 4.21).

The mean wader clutch size was 3.46 in 2014, which is near the weighted mean for previous years (table 4.16). Nests containing other than four eggs were: Common ringed plover: one nest held five eggs – sanderling: three nests of one egg, one with only two eggs and eleven nests with three eggs – dunlin: one nest containing 3 eggs – ruddy turnstone: one nest containing 2 eggs, one containing 3 eggs.

In late July and early August, alarming parents – and later juveniles – were found in the fens and marshes (dunlins and sanderlings), and on the slopes of Aucellabjerg and in the dry lowlands (common ringed plovers, sanderlings, dunlins and turnstones).

Data on chick survival are almost negligible, but survival is considered low. This is partly due to the fact that from 24 June (day 175) to early August, flocks of long-tailed skua roamed the lower slopes of Aucellabjerg and the lowlands' fens and heaths. The largest flocks held 13 individuals.

Reproductive phenology and success in long-tailed skuas *Stercorarius longicaudus*

This was a non-breeding year at Zackenberg (table 4.17), and colleagues from other parts of Northeast Greenland report on a similar situation at Hochstetter Forland (O. Gilg, pers. comm.) and Traill Ø (J. Lang and B. Sittler, pers. com.). No collared lemmings *Dicrostonyx groenlandicus* were observed by the bird observer, reflecting a season with very low numbers of lemming winter nests found (table 4.21). Roaming flocks of long-tailed skuas were observed in the second half of June, which is very early.

Four observations of a third calendar year bird were reported this season, on 30 June and 18, 19 and 26 July (day of year 181 and 199, 200 and 207, respectively), all considered to be the same individual. A second calendar year bird was observed on 19 July (day 200) in a flock of adults.

Barnacle geese *Branta leucopsis*

During an early June visit to the ice covered bay below the barnacle goose colony on the southern face of the mountain Zackenberg, a few individuals were seen in the colony. Also, adults flying to and from the cliffs during the breeding season suggest that the colony was in use to some degree. For further details on the colony, see Hansen *et al.* (2009).

The first barnacle goslings in the Zackenberg valley were seen 10 July (day 191). Thirteen broods were seen this season, which is near average for the period 2000-2013 (table 4.18). A maximum number of five goslings were seen at any one time.

Southward migrating barnacle geese were seen from 8 August (day 220). In the following three days 131 other barnacle geese migrated south. The last barnacle geese left late August.

The percentage of young in wintering flocks on Isle of Islay, Western Scotland, was not available at the deadline for this report (table 4.18). Immature barnacle geese moulted in numbers above average at Zackenberg (1995-2013 average: 208; table 4.19).

Table 4.18 Average brood sizes of barnacle geese Branta leucopsis *in the Zackenberg valley during July and early August 1995-2014, together with the total number of broods brought to the valley. Samples of fewer than ten broods are marked with asterisk. Average brood size data from autumn on the Isle of Islay in Scotland are given for comparison, including the percentage of juveniles in the population (M. Ogilvie pers. comm.).*

Year	1995	1996	1997	1998	1999	2000	2001	2002	2003	2004	2005	2006	2007	2008	2009	2010	2011	2012	2013	2014
Primo July		3.0*	3.1	2.9*	1.9	3.2*	1.8*	2.4	1.8*	2.6	1.7*	2.0*	1.3	4*	1*	1.5*	0	0	1.0*	1.0*
Medio July		2.3*	2.7	2.3	1.8	3.1*	1.7*	2.4	1.2*	2.3	2.7	1.5*	1.5	1.6	1.33*	1.8*	1*	1.5	1.6	1.6
Ultimo July	2.0*	3.0*	2.6	2.2	1.7	3.1		2.3	1.1*	2.3	2.2*	1.1*	3.3*	1.5*	1*	1.4*	0	1.1	1.7*	1.7*
Primo August	2.3*	2.3*	2.4		1.8		2.0*	2.2	1.2*	1.9*		1.5*	–	1*	1.5*	1.6*	0	1.3	1.3*	1.3*
No. of broods	≥7	6-7	19-21	≥18	29	11	4	32	8	26	14	9	28	15	9	18	3	11	11	13
Scotland	2.00	2.30	1.95	2.28	1.92	2.20	1.94	2.23	1.59	2.35	1.67	1.15	2.14	1.9	1.9	2.26	2.1	1.8	NA	NA
Percent juv.	7.2	10.3	6.1	10.5	8.1	10.8	7.1	12.5	6.4	15.9	6.3	3.23	9.8	8.2	3.8	11.2	11.2	7.0	NA	NA

Table 4.19 Number of immature pink-footed geese Anser brachyrhynchus *and barnacle geese* Branta leucopsis *moulting in the study area at Zackenberg 1995-2014.The closed area is Zone 1c (see www.zackenberg.dk/maps).*

	1995	1996	1997	1998	1999	2000	2001	2002	2003	2004
Pink-footed goose										
Closed moulting area and further east	310	246	247	5	127	35	0	30	41	11
Coast west of closed area	230	40	60?	0	29	0	0	0	0	10
Upper zackenbergdalen	0	0	15	0	0	0	0	0	0	0
Pink-footed goose total	540	286	322	5	156	35	0	30	41	21
Barnacle goose										
Closed area at Lomsø and Kystkærene	21	0	29	21	60	84	137	86	120	81
Coast east of closed area	>120	150?	96	55	66	0	109	80	45	0
Coast west of closed area	0	0	0	0	0	30	0	0	0	0
Upper zackenbergdalen	41	85	2	75	<57	27	60	0	14	0
Barnacle goose total	>182	235?	127	151	<183	141	306	166	179	81
	2005	**2006**	**2007**	**2008**	**2009**	**2010**	**2011**	**2012**	**2013**	**2014**
Pink-footed goose										
Closed moulting area and further east	17	27	0	0	1	10	17	37	42	34
Coast west of closed area	0	3	2	0	0	0	0	0	0	4
Upper zackenbergdalen	0	1	0	2	1	0	6	32	44	3
Pink-footed goose total	17	31	2	2	2	10	23	69	86	41
Barnacle goose										
Closed area at Lomsø and Kystkærene	87	148	66	106	70	80	48	77	62	200
Coast east of closed area	2	218	46	125	77	13	0	25	120	0
Coast west of closed area	29	29	106	65	34	0	66	35	77	38
Upper zackenbergdalen	25	30	6	41	51	0	0	69	0	0
Barnacle goose total	143	425	224	337	232	93	114	206	259	238

Common birds, not breeding in the census area

Migration of immature pinkfooted geese *Anser brachyrhynchus* was recorded during the summer. First, four immatures were flying over the research station on 8 June (day 159). Between 14 June and 8 July (day 165-172), the northbound migration main bouts came. A total of 3555 pink-footed geese were recorded migrating north. Southbound migration never reached high numbers, and most geese must have migrated further east than Zackenberg. Only two records of flocks (18 July and 16 August, respectively) comprised the southbound migration numbers of only16 pink-footed geese. We are cautious to make any comparisons due to the unsystematic nature of the data.

The 41 immature pink-footed geese found moulting in the Zackenberg area in 2014 are higher than the 2000-2013 average of 207.6 birds (table 4.19).

Table 4.20 Numbers of individuals and observations of avian visitors and vagrants at Zackenberg 2014, compared with the numbers of individuals observed in previous seasons, 1995-2013. Multiple observations reasonably believed to have been of the same individual have been reported as one individual.

	Visitors and vagrants																				
	Previous records																			2014	
Species	1995	1996	1997	1998	1999	2000	2001	2002	2003	2004	2005	2006	2007	2008	2009	2010	2011	2012	2013	No. of individuals	No. of observations
Great northern diver	0	0	0	0	0	0	1	0	0	0	0	0	2	2	0	1	0	0	0	0	0
Wooper swan	0	0	0	0	0	4	0	0	0	0	0	0	0	0	0	0	0	0	0	0	0
Greylag goose	0	0	0	0	0	0	0	0	0	0	0	0	0	0	0	1	0	0	0	0	0
Snow goose	0	0	0	0	0	2	11	0	23	0	0	0	1	0	0	0[a]	0	4	0	0	0
Canada goose	0	0	0	0	0	0	0	0	0	0	0	4	3	0	1	0	2	0	5	8	4
Merlin	0	0	0	0	0	1	0	0	0	0	0	0	0	0	0	0	0	0	0	0	0
Gyr falcon	1	1	1	3	0	4	5	1	3	4	2	0	3[b]	3[c]	4	3	3	5	5[d]	2	3
Pintail duck	0	0	0	1[e]	0	0	0	0	0	0	0	0	3[e]	0	0	3[e]	0	0	0	2[e]	3
Common teal	0	0	0	0	0	0	0	1	0	0	0	0	0	0	0	0	0	0	0	0	0
Eurasian golden plover	0	3	1	3	1	0	3[f]	1	0	1	1	1	1	1	2	2	0	0	1	1	5
White-rumped sandpiper	0	0	0	0	0	0	1	0	0	0	1	0	0	0	0	0	0	0	0	0	0
Pectoral sandpiper	0	0	0	1	0	0	0	2	0	0	0	1	1	0	1	1	0	0	0	0	0
Purple sandpiper	0	0	0	0	0	0	0	1[g]	0	0	0	0	0	0	0	0	0	1	0	0	0
Red phalarope	0	0	0	4-5[f]	0	0	4[f]	0	1	0	2[f]	11[f]	0	2[f]	0	2[f]	0	3[f]	0	3[f]	4
Common snipe	0	0	0	0	0	0	0	0	0	0	0	0	1	0	0	0	0	1	0	0	0
Whimbrel	0	0	0	0	0	1	1	0	0	2	1	0	1	2	0	0	0	1	0	0	0
Eurasian curlew	0	0	1	0	0	0	0	0	0	0	0	0	0	0	0	0	0	0	0	0	0
Redshank	0	0	0	0	0	0	0	0	0	0	0	0	0	1	0	0	0	0	0	0	0
Lesser yellowlegs	0	0	0	0	0	0	0	0	0	0	0	0	0	0	0	0	1[h]	0	0	0	0
Pomarine skua	0	0	0	0	0	0	2	0	0	0	0	0	0	0	0	0	0	5	0	0	0
Arctic skua	0	0	11	6	0	2	7	4	3	2	0	1	0	0	0	0	0	0	1	2[f]	3
Great skua	0	0	0	4	0	0	0	1	0	0	0	0	0	0	0	0	0	0	0	0	0
Black-headed gull	0	0	0	0	0	0	0	0	0	0	0	0	0	0	0	0	0	0	0	1	1
Lesser black-backed gull	0	0	0	0	0	0	1	0	1	2	1	4	0	0	0	0	1	2	0	0	0
Iceland gull	0	0	0	0	0	0	0	0	0	0	0	2	0	0	0	0	0	3	0	0	0
Great black-backed gull	0	0	0	0	0	1	3	0	0	0	0	0	0	0	0	0	0	0	0	1	1
Black-legged kittiwake	0	0	0	0	0	0	0	0	14	0	0	0	0	0	0	0	0	0	1	0	0
Arctic tern	≈200	2	1	2	0	14	0	0	32	0	0	0	0	57	0	0	0	0	7	5	3
Snowy owl	0	0	2	1	1	1-2	≥4[e]	0	0	0	0	0	1[b]	0	0	0	0	0	0	1	1
Meadow pipit	0	0	0	1	0	0	0	0	0	0	1[e]	1[e]	0	0	0	0	0	0	0	0	0
White wagtail	0	1	0	0	0	0	0	0	0	0	0	0	1	0	0	0	0	0	0	0	0
Bohemian waxwing	0	0	0	0	0	0	0	0	0	0	0	0	0	0	0	0	0	2[g,i]	0	0	0
Lapland longspur	0	0	0	0	1-2	0	1	0	0	0	1	0	0	0	0	2[f]	3[f]	2	1	1	4

[a]Two outside census area, [b]See Hansen et al. 2010, [c]Some observations could be double counts, but we estimate numbers between 1 and 3 individuals, [d]Some observations could be double counts, but we estimate numbers between 5 and 7 individuals, [e]Northernmost records in East Greenland (cf. Bortmann 1994), [f]At least one territory, possible territory or breeding found, [g]Juveniles, [h]4th record in Greenland, first in N.E. Greenland, [i]5th observation in Greenland

The first common eiders *Somateria mollissima* observation was on 11 July (day 191); a pair. No eider ducklings were recorded in 2014. Common eiders were seen in flocks of up to 23 individuals from late July into August.

The first king eiders *Somateria spectabilis* observed were two pairs on 11 June (day 162). No ducklings were seen in 2014. Long-tailed ducks *Clangula hyemalis* were seen from 7 June (day 156), after which time pairs were seen almost daily until late August. Two nests were found (unknown fates), but no ducklings were recorded. In 2014, the first gyrfalcon was seen on 24 June (day 175). Two more records from the summer were from 30 June and 15 August (day 181 and 227, respectively).

A northern wheatear, *Oenanthe oenanthe,* was first observed on 6 May, and

again on 24 May. An adult was seen again three times in July and mid-August. The last observations, on 10 and 11 August (day 222 and 223) were of one, later two immature birds, flying around the research station.

As in recent years, two common raven *Corvus corax* pairs occupied each their territories, with home ranges well beyond the BioBasis census area. Nesting is believed to take place outside the study area. The first observation of a juvenile bird was made on 27 June (day 178). Ravens are present in the study area throughout the season.

Visitors and vagrants

In table 4.20, we present data on avian visitors and vagrants. Four observations of a total of eight Canada geese, all believed to be the larger subspecies *interior*: on 18 June (day 169) two, on 24 June (day 175) four; on 28 June (day 179) two and on 4 July (day 185) two individuals.

Pintail ducks *Anas acuta* were observed near the research station on several occasions. On 30 May a pair was seen bathing in a pond near the research station. The male was seen again on 6 and 7 June. This is the 4th season with pintail ducks at Zackenberg, and the northernmost observations in East Greenland (cf. Boertmann 1994).

Three observations were made of what is considered one individual Eurasian golden plover *Pluvialis apricaria* on 15, 17 and 19 June (day 166, 168 and 170, respectively) in areas around the research station.

A pair of Arctic skua *Stercorarius parasiticus* was recorded on 17 July (day 198) during the census, and maintained a territory there for at least a few days. Observations of single individuals were made regularly throughout early and mid-July. The last observation was definitely of another bird, as it was a dark phase Arctic skua, rarely seen at Zackenberg; 21 July (day 202).

On 8 June (day 159), during stormy weather, a black-headed gull *Larus ridibundus* was observed at the research station. This is the first observation of this species at Zackenberg since the beginning of the monitoring programme.

A greater black-backed gull *Larus marinus* was observed on 19 July (day 200) by the coast, flying eastwards. This is the 3rd season this species has been encountered at Zackenberg since the start of BioBasis in 1995.

Arctic terns *Sterna paradisaea* were observed three times at Zackenberg, twice two birds (on 22 June and 9 July (day 173 and 190, respectively)), and once a single bird (on 8 June (day 159)).

A single snowy owl was seen at the foothills of Aucellabjerg on 24 June (day 175). Since 2001, this is only the second snowy owl observation in the valley.

Sandøen

BioBasis only made one short visit to Sandøen after the main part of the breeding season in 2014. It was too late to make any counts of breeding pairs.

Daneborg

At Daneborg, the common eider colony between the sledge dog pens had below average numbers of nests: 1550 nests (Sirius Patrol, pers. comm.; 2002-2012 average nest numbers: 2357). The colony is the largest in Greenland (Meltofte 1978).

4.4 Mammals

The mammal monitoring programme was conducted by Lars Holst Hansen, Jannik Hansen, Palle Smedegaard Nielsen, Jakob Humaidan, and Niels Martin Schmidt. The station personnel and visiting researchers did supplemental observations during the entire field season.

The collared lemming *Dicrostonyx groenlandicus* census area was surveyed for winter nests during July and August. When weather permitted, arctic hares *Lepus arcticus* in the designated monitoring area on the south-east and east facing slopes of the mountain Zackenberg were censused during the period 21 July – 19 August. The total numbers of musk oxen, including sex and age classification of as many individuals as possible, were censused weekly within the 47 km^2 census area from July to October. The 16 known arctic fox *Vulpes lagopus* dens (no. 1-10 and 12-17) within the central part of the Zackenberg valley were checked approximately once a week for occupancy and breeding. The 29 fixed sampling sites for predator scats and casts were checked in late August. Observations of other mammals than collared lemming, arctic fox, musk ox and arctic hare are presented in the section 'Other observations' below. As in previous years, BioBasis collected arctic fox scats for the analysis of parasitic load.

Collared lemming *Dicrostonyx groenlandicus*

In 2014, a total of 59 collared lemming nests from the previous winter were recorded within the 1.06 km² census area (table 4.21). No nests were found to have been depredated by stoat during the 2014 season (figure 4.3). No lemmings were observed in the field by the bird observer.

Table 4.21 Annual numbers of collared lemming winter nests recorded within the 1.06 km² census area in the Zackenberg valley 1996-2014 together with the numbers of animals encountered by one person with comparable effort each year within the 15.8 km² bird census area during June-July.

Year	New winter nests	Old winter nests	Animals seen
1996	84	154	0
1997	202	60	1
1998	428	67	43
1999	205	36	9
2000	107	38	1
2001	208	13	11
2002	169	20	4
2003	51	19	1
2004	238	15	23
2005	98	83	1
2006	161	40	3
2007	251	21	1
2008	80	20	4
2009	55	9	0
2010	27	23	0
2011	27	3	0
2012	212	20	6
2013	101	14	0
2014	59	51	0

Musk ox *Ovibos moschatus*

Based on the weekly field censuses, table 4.22 lists the sex and age composition over the seasons during July and August. The season had unusually few young individuals. The mean number of animals pr. count was a rather low 38.6. Figure 4.4 illustrates the temporal development in the proportions of the different sex and age classes during the 2014 season. The figure illustrates clearly the low proportion of younger individuals.

A record high number of 50 fresh musk ox carcasses was found during the 2014 season (table 4.23). This extremely high number of carcasses is likely related to ice on the ground in the fall of 2013 and the relatively large amount of snow during the winter.

Table 4.22 Sex and age composition of musk oxen based on weekly counts within the 47 km² census area in the Zackenberg valley from July – August 1996-2014.

Year	M4+		F4+		M3		F3		M2		F2		1M+1F		Calf		Unsp. adult		No. of weekly counts
	Total	%	Total	%	Total	%	Total	%	Total	%	Total	%	Total	%	Total	%	Total	%	
1996	98	14	184	27	7	1	31	5	54	8	17	3	146	22	124	18	15	2	9
1997	–	–	–	–	–	–	–	–	–	–	–	–	–	–	–	–	–	–	–
1998	97	29	97	29	22	7	19	6	30	9	27	8	14	4	22	7	1	0	8
1999	144	38	106	28	21	6	21	6	9	2	12	3	5	1	30	8	32	8	8
2000	109	30	118	32	11	3	15	4	2	1	7	2	31	8	73	20	3	1	8
2001	127	30	120	29	8	2	19	5	26	6	19	5	43	10	55	13	4	1	7
2002	114	20	205	36	20	3	24	4	38	7	43	8	51	9	77	13	0	0	8
2003	123	23	208	39	24	5	23	4	16	3	19	4	44	8	72	14	0	0	8
2004	122	22	98	18	13	2	28	5	5	1	8	1	32	6	124	23	119	22	7
2005	212	23	260	28	11	1	46	5	43	5	21	2	116	13	200	22	6	1	9
2006	205	29	123	17	29	4	55	8	62	9	34	5	102	14	94	13	0	0	7
2007	391	25	341	22	73	5	152	10	80	5	83	5	202	13	246	16	8	1	9
2008	267	34	189	24	38	5	57	7	44	6	58	7	58	7	63	8	18	2	8
2009	269	42	176	28	32	5	38	6	32	5	23	4	30	5	18	3	21	3	8
2010	246	49	101	20	40	8	26	5	29	6	21	4	8	2	18	4	15	3	9
2011	267	46	181	31	24	4	16	3	6	1	12	2	11	2	53	9	8	1	8
2012	235	56	106	25	16	4	17	4	16	4	9	2	8	2	10	2	1	0	9
2013	264	35	243	32	8	1	21	3	13	2	6	1	26	3	172	23	8	1	8
2014	219	63	111	32	2	1	4	1	2	1	4	1	0	0	1	0	4	1	9

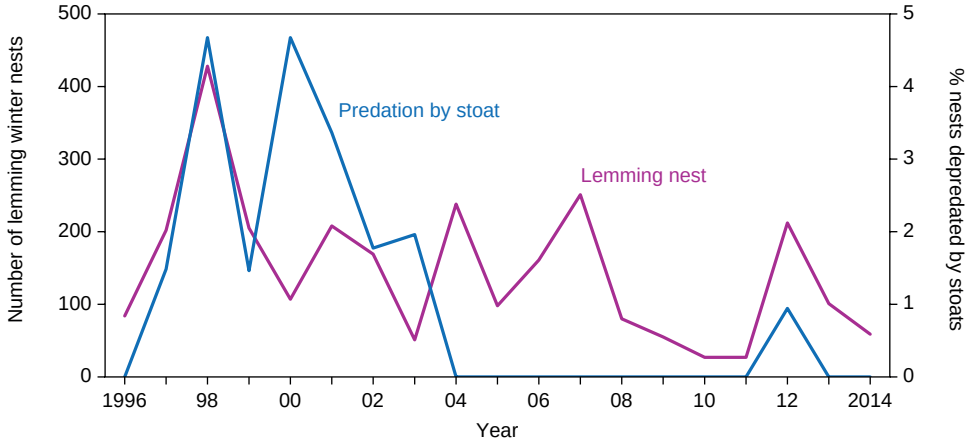

Figure 4.3 Number of collared lemming winter nests registered within the 1.06 km² designated lemming census area (red line), along with the percentage of winter nests taken over by stoats (blue line) 1996-2014.

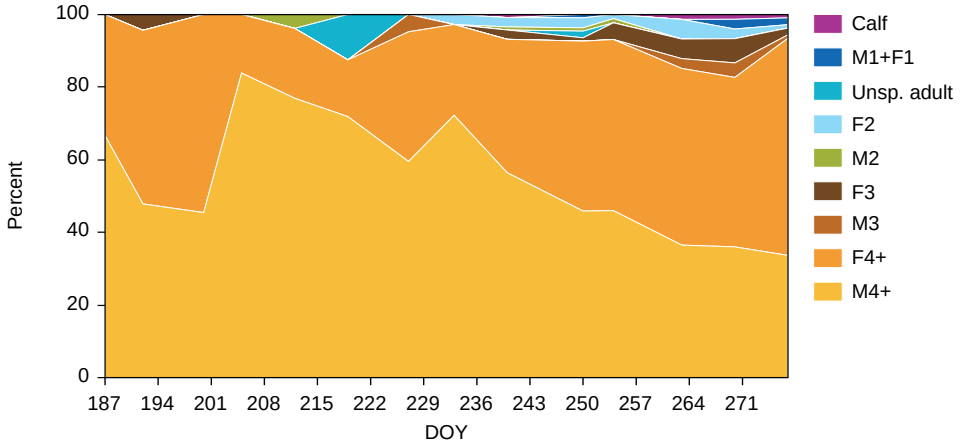

Figure 4.4 Sex and age composition of musk oxen registered during the weekly field censuses within the census area during the 2014 season (for the counts from day 249 onwards, only a part of the area was censused due to the length of daylight).

Table 4.23 Fresh musk oxen carcasses found during the field seasons 1995-2014. F=female, M=male.

Year	Total carcasses	4+ yrs F / M	3 yrs F / M	2 yrs F / M	1 yr	Calf
1995	2	0 / 1				1
1996	13	7 / 1	0 / 1	0 / 2	2	
1997	5	0 / 2		1 / 0	1	1
1998	2	0 / 2				
1999	1	0 / 1				
2000	8	0 / 6	1 / 0			1
2001	4	0 / 4				
2002	5	1 / 2	1 / 0			1
2003	3	0 / 2				1
2004	2	1 / 1				
2005	6	2 / 3				1
2006	5	0 / 2			1	2
2007	12	3 / 4	1 / 0		1	3
2008	10	3 / 1	2 / 0			4
2009	16	5 / 3				8
2010	6	2 / 1	0 / 1			2
2011	5	2 / 3				
2012	27	1 / 8	0 / 3		3	12
2013	1	1 / 0				
2014	50	5 / 8			2	35

Table 4.24 Numbers of known fox breeding den complexes checked, number of active breeding den complexes and total number of pups recorded at their maternal den complex within and outside the central part of the Zackenberg valley 1995-2014. Photos from automatic cameras showed additional three and nine pups in 2008 and 2012 respectively. W=white phase and D=dark phase.

Year	No. of known den complexes checked inside/outside	No. of active breeding den complexes inside/outside	Total no. of pups recorded at their maternal den complex
1995	2 / 0	0 / 0	0
1996	4 / 0	2 / 0	5W + 3D
1997	4 / 0	0 / 0	0
1998	4 / 0	1 / 0	5W
1999	6 / 0	0 / 0	0
2000	6 / 0	3 / 0	8W
2001	8 / 2	3 / 1	16W + 1D
2002	9 / 2	0 / 0	0
2003	9 / 1	3 / 0	19W
2004	9 / 2	4 / 1	18W
2005	9 / 2	0 / 0	0
2006	9 / 2	2 / 1	16W
2007	9 / 2	3 / 1	23W
2008	9 / 2	4 / 1	20W
2009	9 / 2	3 / 0	10W
2010	10 / 2	3 / 0	16W
2011	10 / 2	3 / 0	8W
2012	10 / 2	5 / 0	23W + 2D
2013	10 / 2	3 / 0	10W + 2D
2014	10 / 2	3 / 0	6W + 0D

Table 4.25 Numbers of Arctic hares within the designated census area per observation day counted during July and August 2014.

Year	Counts	Average	SD	Range
2001	22	1.2	1.3	0-5
2002	16	0.4	0.6	0-2
2003	20	2.4	1.8	0-6
2004	23	0.9	1.1	0-3
2005	48	5.5	5.1	0-26
2006	39	5.9	3.7	1-19
2007	18	4.8	3.0	0-11
2008	17	2.5	2.3	0-7
2009	16	4.8	2.8	1-12
2010	18	3.1	1.9	0-7
2011	14	2.7	1.7	1-7
2012	14	4.3	2.2	2-9
2013	16	3.9	2.3	0-8
2014	9	5.8	4	0-11

Arctic fox *Vulpes lagopus*

In 2014, breeding was verified in three fox den complexes. Despite the record high number of musk ox carcasses, a relatively low number of six Arctic fox pups were observed at their maternal den complexes (table 4.24).

Arctic hare *Lepus arcticus*

In 2014, nine counts with good visibility were carried out during July and August with a mean of 5.8 Arctic hares per census (table 4.25).

Other observations

Polar bear *Ursus maritimus* was observed in the central research area during 2014 on three occasions. An adult bear was observed briefly on 26 June east of the research station at a distance of approximately 400 m. The bear slowly approached with stops where it stood on its hind legs. It was rather foggy and the observer quickly went away from the bear and back to the station where all fieldworkers were alarmed over the radio. The bear was not seen again. The second bear was observed late in the evening on 6 August as it was approaching the research station from Sydkærene. As it got close to the buildings, it was successfully scared away by the use of a flare gun with a cracker shell. It was then observed heading in a north westerly direction crossing the river and inspecting a musk ox carcass before disappearing over the hills. Lastly, one young adult male bear was observed near the research station on 25 September where it was discovered and surprised at close range (approx. 30 m) while it was eating from a musk ox carcass. It got scared and ran towards the river delta. As it slowed down, the observer yelled and the bear speeded up again away from the observer. It disappeared in the direction of the old trapping station. A few days later it was found that it had destroyed one of the windows of the boat shed at the trapping station.

In 2014, no Arctic wolves *Canis lupus* were seen in the Zackenberg area.

No stoats *Mustela erminea* nor tracks of them were observed in 2014, and no new lemming winter nests found in the census area were found depredated by stoats. During the standardised collection of scats and casts, no stoat scat was found (table 4.27).

Table 4.26 Wildlife specimens collected for tissue samples in 2014 and all seasons collectively.

Species	2014	1997-2014
Arctic char	0	11
Arctic fox	1	16
Arctic hare	3	19
Collared lemming	0	10
Common raven	0	2
Dunlin	0	5
Glaucous gull	0	1
Gyr falcon	0	1
Musk oxen	51	153
Northern wheatear	0	1
Rock ptarmigan	0	3
Ruddy turnstone	0	1
Seal (sp.)	0	1
Three-spined stickleback	0	6
Fourhorn sculpin	0	5
Snow bunting	0	2
Lapland bunting	0	1
Barnacle goose	0	2

Table 4.27 Numbers of casts and scats from predators collected from 29 permanent sites in the Zackenberg valley. The samples represent the period from mid/late August the previous year to mid/late August in the year denoted.

Year	Fox scats	Stoat scats	Skua casts	Owl casts
1997	10	1	44	0
1998	46	3	69	9
1999	22	6	31	3
2000	31	0	33	2
2001	38	3	39	2
2002	67	16	32	6
2003	20	1	16	0
2004	16	3	27	0
2005	24	0	7	6
2006	29	0	15	4
2007	54	4	13	3
2008	30	1	16	0
2009	22	2	11	1
2010	22	1	3	0
2011	28	7	15	1
2012	23	1	21	1
2013	6	0	10	1
2014	16	0	3	0

Since there was an Arctic Science Partnership project going to Sandøen regularly throughout the 2014 season, BioBasis did not do any formal monitoring of the number of Walrus there. On 19 September four walrus were observed on the island in two groups of two.

Collection of wildlife samples

Tissue samples from dead vertebrate species encountered in the field were collected (table 4.26). Also, scats and casts were collected at 29 permanently marked sites in the valley (table 4.27).

4.5 Lakes

Sommerfuglesø and Langemandssø, situated in Morænebakkerne, became ice-covered during the first part of September 2013 and were covered by snow during October. According to the surveillance cameras the snow remained on the lakes throughout the winter and spring, but eventually started to melt in late May at Langemandssø and some weeks later on Sommerfuglesø. The ice cover on both lakes lasted long with ice still remaining during the first weeks of July in 2014. The lakes froze over again at the beginning of September leaving a fairly short ice-free period of less than 2 months.

Table 4.28 Physico-chemical variables and chlorophyll a concentrations in Sommerfuglesø (SS) and Langemandssø (LS) during June-October 2014.

Lake	SS	SS	SS	SS	LS	LS	LS	LS
DOY	191	213	234	272	191	213	234	272
Ice cover (%)	10	0	0	100	25	0	0	100
Temperature (°C)	3.0	9.8	9.3	1.4	2.0	10.3	9.4	0.9
pH	6.4	6.7	6.6	6.5	6.5	6.7	6.8	6.7
Conductivity (µS cm^{-1})	9	12	26	35	25	13	23	30
Chlorophyll *a* (µg l^{-1})	0.05	0.34	0.94	0.28	0.26	0.62	0.74	0.87
Total nitrogen (µg l^{-1})	90	160	440	110	140	140	150	220
Total phosphorous (µg l^{-1})	8	2	8	2	8	8	8	8

Thus, in 2014 the sampling took place from 10 July to 29 September and included just four sampling dates. In addition, daily pictures were taken by two surveillance cameras situated between the lakes. The pictures are used to follow the changes in the snow cover and to help identify the exact duration of the ice coverage period.

The 2014 ice-free season was characterized by the later ice break up dates and a cold summer (see elsewhere in this report). Consequently, the average water temperatures in July and August

Table 4.29 Average physico-chemical variables in Sommerfuglesø (SS) in 1999-2014 (July-August) as well as single values from mid-August 1997 and 1998. ND = no data.

Lake	SS	SS	SS	SS	SS	SS	SS	SS	SS	SS	SS	SS	SS	SS	SS	SS	SS	SS
Year	1997	1998	1999	2000	2001	2002	2003	2004	2005	2006	2007	2008	2009	2010	2011	2012	2013	2014
Date of 50% ice cover		192	199	177	183	184	175	176	169	186	166	181	179	165	176	179	166	186
Temperature (°C)	6.3	6.5	6.1	10.1	8.4	8.3	11	8.7	9.8	10.1	10	10.6	9.5	10.4	10.8	7.2	11.3	7.4
pH	6.5	7.4	6.7	5.8	6.6	6	6.5	6.3	6	6.2	6.6	5.9	6.7	6.7	6.6	6.7	6.8	6.6
Conductivity (µS cm^{-1})	15	13	10	18	18	8	12	15	22	11	10	16	22	18	22	23	36	16
Chlorophyll *a* (µg l^{-1})	0.84	0.24	0.41	0.76	0.67	1.27	1.84	1.62	1.59	0.65	1.49	0.57	0.89	1.26	0.50	0.59	0.46	0.44
Total nitrogen (µg l^{-1})	ND	130	210	510	350	338	277	267	263	293	323	238	298	248	220	193	397	200
Total phosphorous (µg l^{-1})	4	9	11	10	19	11	11	7	9	8	10	6	7	5	8	6	7	5

Table 4.30 Average physico-chemical variables in Langemandssø (LS) in 1999-2014 (July-August) as well as single values from mid-August 1997 and 1998. ND = no data.

Lake	LS	LS	LS	LS	LS	LS	LS	LS	LS	LS	LS	LS	LS	LS	LS	LS	LS	LS
Year	1997	1998	1999	2000	2001	2002	2003	2004	2005	2006	2007	2008	2009	2010	2011	2012	2013	2014
Date of 50% ice cover	ND	204	202	182	189	187	183	178	173	191	167	182	172	174	178	184	166	188
Temperature (°C)	6.8	6.4	4	9.5	8.4	8.1	11.1	9.1	10.5	9.8	10.6	8.8	9.1	9.2	11.4	6.7	9.6	7.2
pH	6.5	7	6.3	5.5	6.4	5.5	6.1	6.1	6	6.3	6	5.7	6.5	6.6	6.7	6.6	6.6	6.7
Conductivity (µS cm^{-1})	8	9	7	9	8	6	6	8	14	5	7	7.8	18	15	31	20	26	20
Chlorophyll *a* (µg l^{-1})	1.04	0.32	0.38	0.9	1.46	2.72	3.14	0.98	1.62	0.56	1.54	0.92	1.06	1.20	0.60	0.95	0.30	0.54
Total nitrogen (µg l^{-1})	ND	80	120	290	340	387	237	230	247	203	268	138	172	208	227	230	257	143
Total phosphorous (µg l^{-1})	8	7	7	11	20	13	10	11	11	6	8	6	9	10	4	7	8	8

were around 7 °C in both lakes (table 4.29 and 4.30). The mean temperatures for the entire sampling period (July to October) were 7.4 and 6.0 °C in Sommerfuglesø and Langemandssø, respectively. When compared to previous years, it appears that 2014 is among the coldest years since the lake monitoring program started in 1997 (see tables 4.29 and 4.30).

The basic water chemistry included measurement of total nitrogen and total phosphorus, conductivity and pH (table 4.28). The data showed that conductivity was 16-20 µg S/cm, pH slightly acid (6.6-6.7), total nitrogen less than 200 µg/l and phosphorus less than 8 µg/l. The average summer values July-August were within recordings from previous years (see tables 4.29 and 4.30) but in the low end.

It follows that the average phytoplankton biomass (chlorophyll *a* concentration) was low with 0.44 and 0.54 µg/l in Sommerfuglesø and Langemandssø, respectively (see tables 4.29 and 4.30). The phytoplankton communities were dominated by dinophytes and chrysophytes (table 4.31) during most of the season in both lakes. Dinophyceae appeared during the late summer and the remaining biomass included chlorophytes, chrysophytes and diatoms. Some of the most typical genera were *Gymnodium*, *Peridinium*, *Uroglena*, *Mallomonas* and *Ochromonas*. The results are comparable to findings from previous years (tables 4.32 and 4.33).

The zooplankton community in Sommerfuglesø included cladocerans (*Daphnia pulex*), copepods (*Cyclops abyssorum*) and rotifers (*Polyarthra dolicopthera*). The average abundance for the summer period was 15 individuals l^{-1} with the largest contribution from the rotifers (table 4.34). Langemandssø had a much larger average zooplankton density of 211 individuals per litre because of an unusual high abundance of rotifers. The zooplankton species composition as well as densities in the summer period (July-August) were within the range found for previous years (tables 4.35 and 4.36). The differences in species composition between the two lakes are controlled by the population of

Table 4.31 Biovolume (mm³ l⁻¹) of phytoplankton groups in Sommerfuglesø and Langemandssø during June-October 2014.

Lake	SS	SS	SS	SS	LS	LS	LS	LS
DOY	**191**	**213**	**234**	**272**	**191**	**213**	**234**	**272**
Nostocophyceae	0.003	0.000	0.000	0.000	0.000	0.000	0.000	0.000
Dinophyceae	0.002	0.090	1.069	0.000	0.016	0.077	0.373	0.005
Chrysophyceae	0.004	0.121	0.8231½	0.039	0.030	0.689	0.7966	0.239
Diatomophyceae	0.007	0.005	0.001	0.000	0.002	0.017	0.007	0.015
Chlorophyceae	0.000	0.000	0.000	0.0082	0.003	0.018	0.048	1.117
Others	0.000	0.005	0.000	0.000	0.000	0.002	0.000	0.000
Total	**0.017**	**0.221**	**1.071**	**0.039**	**0.051**	**0.803**	**0.428**	**1.377**

Table 4.32 Average biovolume (mm³ l⁻¹) of phytoplankton groups in Sommerfuglesø during summer (July and August) from 1997 to 2014 (note that some years are missing).

Lake	SS	SS	SS	SS	SS	SS	SS	SS	SS	SS	SS	SS	SS	SS	SS
Year	**1998**	**1999**	**2001**	**2002**	**2003**	**2005**	**2006**	**2007**	**2008**	**2009**	**2010**	**2011**	**2012**	**2013**	**2014**
Nostocophyceae	0	0.005	0	0	0	0	0	0	0	0	0	0	0.002	0	0.001
Dinophyceae	0.034	0.044	0.015	0.006	0.027	0.185	0.068	0.113	0.184	0.053	0.248	0.590	0.242	0.628	0.290
Chrysophyceae	0.022	0.096	0.358	0.066	0.237	0.554	0.145	0.386	0.092	0.261	0.303	0.089	0.034	0.486	0.062
Diatomophyceae	0.002	0	0.001	0	0	0	0.007	0	0	0.003	0.005	0.001	0.003	0.006	0.003
Chlorophyceae	0.005	0.002	0	0	0.002	0.009	0.004	0.001	0	0	0	0.001	0	0.003	0.000
Others	0	0	0.004	0	0	0	0	0	0	0.002	0	0	0	0	0.002
Total	**0.063**	**0.147**	**0.377**	**0.073**	**0.266**	**0.749**	**0.223**	**0.499**	**0.276**	**0.319**	**0.555**	**0.680**	**0.280**	**1.123**	**0.359**

Table 4.33 Average biovolume (mm³ l⁻¹) of phytoplankton groups in Langemandssø during summer (July and August) from 1997 to 2014 (note that some years are missing).

Lake	LS	LS	LS	LS	LS	LS	LS	LS	LS	LS	LS	LS	LS	LS	LS	LS
Year	**1997**	**1998**	**1999**	**2001**	**2002**	**2003**	**2005**	**2006**	**2007**	**2008**	**2009**	**2010**	**2011**	**2012**	**2013**	**2014**
Nostocophyceae	0	0	0	0	0	0	0	0	0	0	0	0	0	0	0.001	0.000
Dinophyceae	0.291	0.185	0.305	0.04	0.156	0.123	0.03	0.068	0.05	0.222	0.095	0.118	0.094	0.78	0.120	0.155
Chrysophyceae	0.066	0.187	0.048	0.592	0.377	0.358	0.296	0.318	0.192	0.262	0.424	0.48	0.184	0.155	0.228	0.360
Diatomophyceae	0.002	0	0	0.002	0	0	0	0.009	0	0	0	0	0.002	0.003	0.002	0.009
Chlorophyceae	0.016	0	0.002	0.002	0	0.003	0.019	0.008	0.017	0.004	0.013	0.099	0.038	0.036	0.030	0.023
Others	0	0	0	0	0	0	0	0	0	0	0	0		0	0.000	0.001
Total	**0.375**	**0.372**	**0.354**	**0.637**	**0.533**	**0.484**	**0.345**	**0.404**	**0.259**	**0.487**	**0.532**	**0.697**	**0.316**	**0.271**	**0.381**	**0.547**

Table 4.34 Density (no l⁻¹) of zooplankton in Sommerfuglesø (SS) and Langemandssø (LS) during June-October 2014.

Lake	SS	SS	SS	SS	LS	LS	LS	LS
DOY	**191**	**213**	**234**	**272**	**191**	**213**	**234**	**272**
Cladocera		0.0	2.4	0.8	0.0	0.0	0.0	0.0
Copepods	0.1	2.8	1.1	1.9	2.0	44.9	47.5	19.5
Rotifers	7.0	39.3	2.3	0.2	82.9	438.9	15.7	5.0
Others	0.0	0.0	0.0	0.0	0.0	0.0	0.0	0.0
Total	**7.1**	**42.1**	**5.9**	**2.9**	**84.9**	**483.7**	**63.2**	**24.5**

Table 4.35 Average density (no l^{-1}) of zooplankton species in Sommerfuglesø during summer (July and August) from 1997 to 2014.

Lake	SS	SS	SS	SS	SS	SS	SS	SS	SS	SS	SS	SS	SS	SS	SS	SS	SS	SS
Year	**1997**	**1998**	**1999**	**2000**	**2001**	**2002**	**2003**	**2004**	**2005**	**2006**	**2007**	**2008**	**2009**	**2010**	**2011**	**2012**	**2013**	**2014**
Cladocera																		
Daphnia pulex	0.3	10.5	0.3	6.7	8.2	6.8	7.7	0.7	6.4	7.07	3.8	6.33	2.87	7.8	3.4	4	5.33	0.73
Macrothrix hirsuiticornis	0.1	0	0	0	0	0	0	0	0.07	0	0	0	0	0	0	0	0.002	0.02
Chydorus sphaericus	0.05	0	0	0	0.06	0	0	0	0.13	0	0	0	0	0.1	0	0.3	0	0.00
Copepoda																		
Cyclops abyssorum alpinus (adult+copepodites)	0.8	0.5	0.5	0.3	0.5	0.2	0.9	0.3	0.07	0.27	2	1.27	0.47	2	1.5	1	1.29	2.56
Nauplii	5.7	1.3	6.5	1.1	1.4	2.3	0.3	0.3	0.2	1.67	0.13	1.93	0.07	3.7	6.9	1.7	1.32	1.07
Rotifera																		
Polyarthra dolicopthera	171	90	185	97	74	11	0.5	1.87	7.67	42.2	108	49.8	150.18	45	12.3	5.8	36.51	15.36
Keratella quadrata group	4.5	3	17	0	0	0.4	0.1	0	0	0.33	0	0	0	0	0	0.2	0	0.07
Conochilus sp.	0	0	0	0	0	0	0	0	0	0	0	0	0	0	0	0	0	0.07
Euchlanis sp.	0	0	0	0	0	0	0	0	0.33	0.07	0	0	1.78	0	0	0	0	0.00

Table 4.36 Average density (no l^{-1}) of zooplankton species in Langemandssø from during summer (July and August) 1997 to 2014.

Lake	LS	LS	LS	LS	LS	LS	LS	LS	LS	LS	LS	LS	LS	LS	LS	LS	LS	LS
Year	**1997**	**1998**	**1999**	**2000**	**2001**	**2002**	**2003**	**2004**	**2005**	**2006**	**2007**	**2008**	**2009**	**2010**	**2011**	**2012**	**2013**	**2014**
Cladocera																		
Daphnia pulex	0	0	0	0	0	0	0.1	0	0	0	0	0	0	0	0	0.1	0	0
Macrothrix hirsuiticornis	0	0	0.2	0	0	0	0	0	0	0	0	0	0	0	0	0	0	0
Chydorus sphaericus	0	0.1	0	0.5	0.1	0.07	0	0	0.13	0.07	0.07	0	0	0	0.1	0.2	0.002	0
Copepoda																		
Cyclops abyssorum alpinus (adult+copepodites)	3.3	2.9	4.1	22	13.4	6.8	8.6	4.9	5.8	11.74	8.93	2.27	14.11	15	13.6	14.1	21.13	12.56
Nauplii	5.2	3.8	6.4	3.1	4.5	4.5	4.2	0	2.2	5.13	1.07	3.07	2.27	5.3	5.4	13	2.51	18.91
Rotifera																		
Polyarthra dolicopthera	316	330	274	168	248	22	78	71	99	181.33	40	185.3	32.67	46.3	9.9	92.1	15.29	171.67
Keratella quadrata group	4.5	28	34	0	0	0.3	0	1.3	0	41.33	0	2.6	0	1.3	0	3.3	0.002	7.47
Conochilus sp.	0	0	0	0	0	0	0	0	0	0	0	0	0	0	0	0	0	0
Euchlanis sp.	0	0	0	0	0	0	0	0	0	0	0	0	0	0	0	0	0	0

dwarf-sized Arctic char in Langemandssø and no fish in Sommerfuglesø. Copepods and rotifers dominate in Langemandssø as they can escape fish predation by their swimming pattern (copepods) and small size (rotifers). Cladocerans and especially *Daphnia pulex* thrive in Sommerfuglesø and can out-compete other zooplankton spices because they feed efficiently and can consume a large food spectrum. However, despite no fish there was a low abundance of cladocerans in Sommerfuglesø in 2014 compared to previous years (table 4.35). It is most likely an effect of low average temperatures and limitation in food availability (low chlorophyll concentration).

No attempts were made to sample the fish population in Langemandssø but the presence of fish is obvious from the zooplankton species composition with lack of cladocerans and high abundance of rotifers.

5 Zackenberg Basic

The MarineBasis programme

Mikael K. Sejr, Thomas Juul-Pedersen, Egon Frandsen, Ivali Lennart, Kunuk Lennart, Tage Dalsgaard, Eva Friis Møller, Sophia E.B. Nielsen, Ane Middelboe, Maria Lund Paulsen, Antonio Delgado Huertas, Elena Mesa Cano, Kristine Arendt, Mathias Middelboe, Stiig Markager and Aud Larsen

This chapter presents data from the 12th year of the MarineBasis programme. The programme conducts long-term monitoring of physical, chemical and biological parameters of the coastal marine ecosystem at Zackenberg. The intention is to be able to identify and quantify changes in key physical and chemical properties of Young Sound and the potential biological consequences for the marine ecosystem. The programme is usually conducted during a three-week field campaign in late July-early August combined with continuous measurements by moored instruments during the rest of the year. Summer measurements are primarily conducted in the outer part of Young Sound but supplemented with data from Tyrolerfjord and the Greenland Sea. The sampling strategy during summer is to describe the spatial variation in hydrographic parameters by sampling a number of stations once (figure 5.1) and also to determine the day-to-day variation at a single station. The programme includes hydrographic measurements (salinity, temperature, pressure, dissolved oxygen, fluorescence, light profiles and turbidity) combined with determination of nutrient concentrations (NOx, PO_4^{3-}, SiO_4) and surface pCO_2. The species composition of phyto- and zooplankton is determined at a single station. On the seafloor, the sediment-water exchange of nutrients, dissolved inorganic carbon, DIC and oxygen is quantified. Also the annual growth rate of the kelp *Saccharina latissima* is estimated. To supplement data collected in summer, a mooring is established in the outer part of Young Sound where continuous measurements of temperature and salinity are conducted at two depths and the vertical flux of sinking particles is estimated throughout the year using a sediment trap.

In 2014, the monitoring programme was supplemented by an extensive

Figure 5.1 Map of the sampling area. The dots represent the hydrographic sampling stations from the innermost Tyrolerfjord on the left to the East Greenland Shelf on the right.

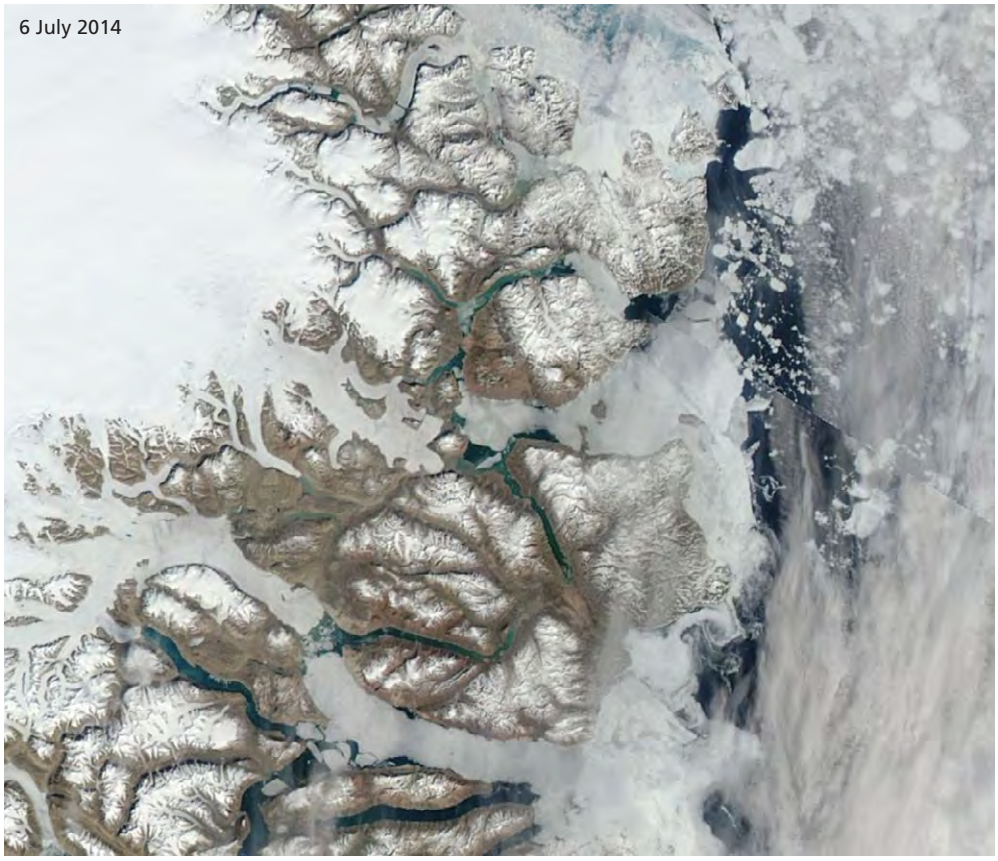

Figure 5.2 Examples of images used to monitor ice conditions in 2013-2014 in Young Sound. Top lef photo shows satellite image of the area. Courtesy Danish Meteorological Institute (http://ocean.dmi.dk/arctic/satimg.uk.php).

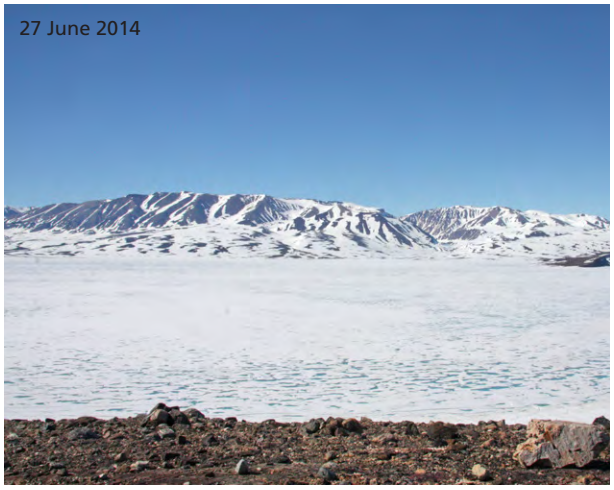

research project funded by the Danish Ministry of the Environment, The Carlsberg Foundation, the Greenland Institute of Natural Resources and the Arctic Centre at Aarhus University. The aim was two-fold: 1) to enable sampling of key monitoring parameters throughout the ice-free season to resolve seasonal variation outside the normal field period and 2) complement the existing monitoring programme with focused research projects aiming to increase the understanding of how the marine carbon cycling is linked to climatic drivers. This resulted in four field campaigns, from 8 July – 22 July, 22 July – 12 August, 2 September – 23 September and 23 September – 7 October.

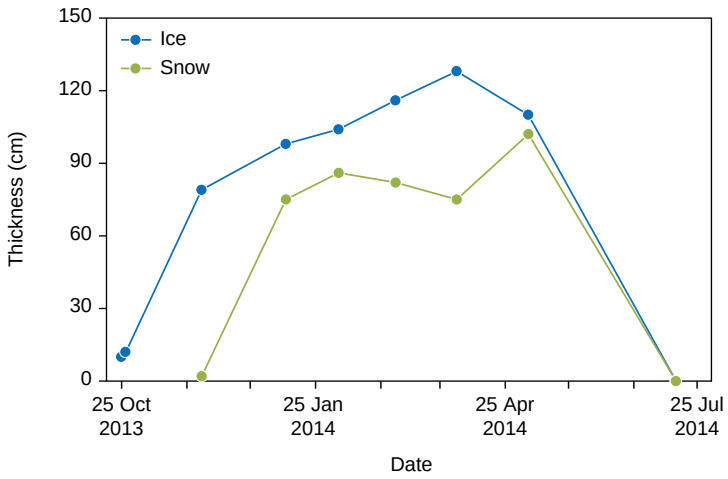

Figure 5.3 Seasonal changes in thickness of sea ice and snow cover. Data kindly provided by members of the Sirius Patrol at Daneborg.

5.1 Sea ice

The extent and duration of the seasonal ice cover in Young Sound is an important driver of ecosystem processes. The duration of the ice-free period in summer is increasing slightly but with a distinct increase in the year-to-year variability. This variability is primarily related to the date of fast ice formation in autumn whereas the date for ice break up in early summer remains relatively stable. In 2014, the summer break up of sea ice occurred on 15 July (figure 5.2). It can also been seen, as observed in previous year, that the sea ice melts sooner in the inner fjord where open water was visible in satellite images around 6 July. Fast ice was formed in Young Sound around 10 October, resulting in an ice-free period of 91 days. This contributes to the long-term trend of increasing duration of the open water season in Young Sound, which since 1950 has increased by 0.4 days per year. Seasonal data on snow and ice cover provided by the Sirius Patrol showed that maximum snow cover reached 102 cm (figure 5.3). The higher than average snow depth (table 5.1) acted as insulation and likely contributed to the relatively thin ice cover of 128 cm.

5.2 Water column

Seasonal data from hydrographic mooring

The hydrographic mooring is used to monitor the seasonal changes in temperature and salinity and to estimate the annual flux of inorganic particles and organic carbon to the seafloor. The mooring was deployed on 8 August 2013 and retrieved again on 11 August 2014. Three CTDs positioned at 22, 30 and 64 m depth recorded temperature and salinity. Variation in temperature displayed the typical seasonal variation (figure 5.4) where warm surface water is gradually mixed with deeper lying cold water during late summer and autumn. Compared to the data from 2012 to 2013, several differences were observed: 1) in the summer of 2012, temperature at 29 m did not exceed 1.0 but exceeded 2.0 in 2013. 2) From 2012-2013 salinity at 61 m showed a steady decrease from 32.05 to 31.85 and throughout the period there was a distinct difference between salinity at 29 and 61 m. In 2013-2014, salinity at 64 continued to decrease until a minimum of about 31.5 in mid-December, then a distinct increase was observed, to a maximum of

Table 5.1 Summary of sea ice and snow conditions in Young Sund.

	2003	2004	2005	2006	2007	2008	2009	2010	2011	2012	2013	2014
Ice thickness (cm)	120	150	125	132	180	176	155	148	144	148	175	128
Snow thickness (cm)	20	32	85	95	30	138	45	45	20	77	29	102
Days with open water	128	116	98	75	76	132	90	99	101	87	105	91

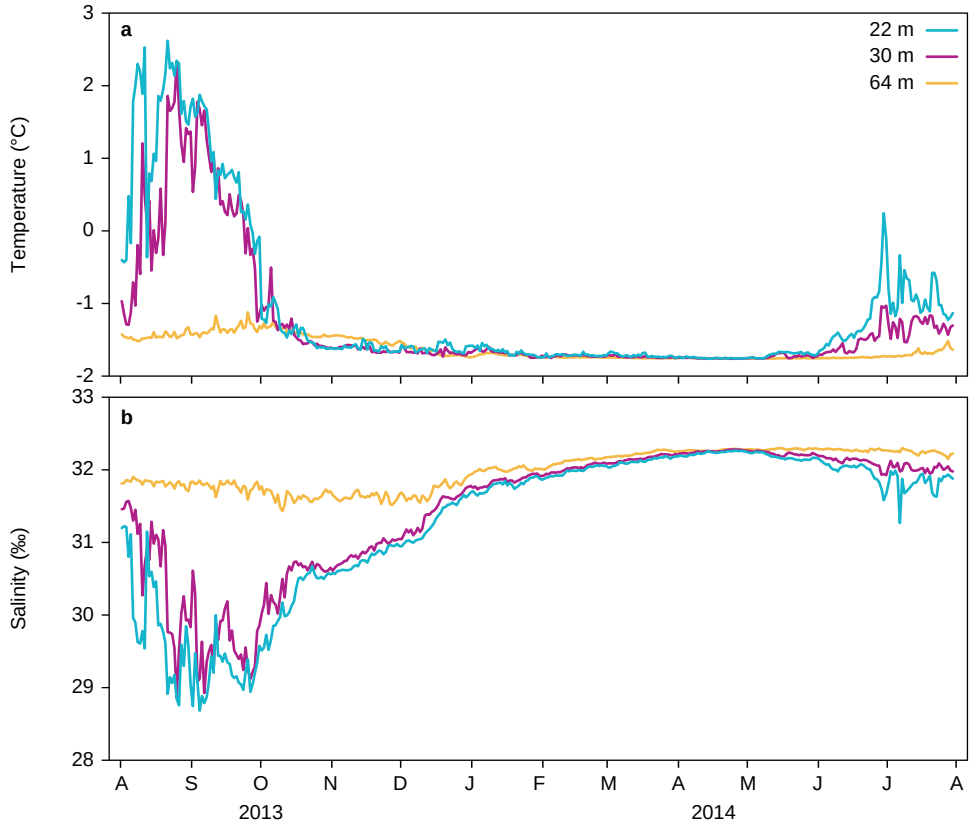

Figure 5.4 Time series of temperature and salinity at three depths in outer Young Sound.

32.3 in mid-May. In mid-May 2014, the difference in salinity between the three samplings depths was <0.05 indicating a homogenous water column compared to 2012-2013 where the difference in salinity between 29 and 61 m exceeded 0.3. Finally, a distinct drop in salinity was observed already in May 2014 at 22 and 30 m which was absent at 29 m in 2013.

Seasonal distribution of hydrological parameters

The spatial variation in hydrological conditions is quantified by measuring vertical profiles with a CTD along the Tyrolerfjord-Young Sound fjord (figure 5.5). The first transect was measured on 25-26 July. This was approximately two weeks before the usual monitoring work. The overall pattern was largely similar to previous observations. A distinct freshwater lens had formed based on sea ice melt and runoff from land. The fluorescence indicated a peak in chlorophyll *a* situated across the sill. The next transect was sampled on 6 August (figure 5.6), with minimal changes compared to 25-26 July. In the top two meters, temperatures had increased slightly and salinity was lower. Next sampling was on 17-18 September (figure 5.7). The top 25 m now showed significant cooling and much of the freshwater previously isolated in the upper 5-6 m had now been mixed down to 50 m. Peak fluorescence was now found in Tyrolerfjord associated with areas with stratification. Interestingly, highest turbidity was now observed in the Greenland Sea. The final transect was measured on 2 and 5 October (figure 5.8). Compared to September, additional cooling of the surface water has taken place. As in September, highest turbidity is found in the outer fjord possibly related to suspension of sediments along the coast during several days with high winds. The upper 50 m of the water column was almost homogenous but with slightly warmer temperatures in Tyrolerfjord.

The seasonal trends as seen clearly at the main station where the thin warm and low saline freshwater lens is present early in the summer but cools and is mixed down during September (figure 5.9). The increase in turbidity in October peaks at 30-40 m indicating that the seafloor could be the source of suspended sediment in contrast to surface freshwater as seen in July and August.

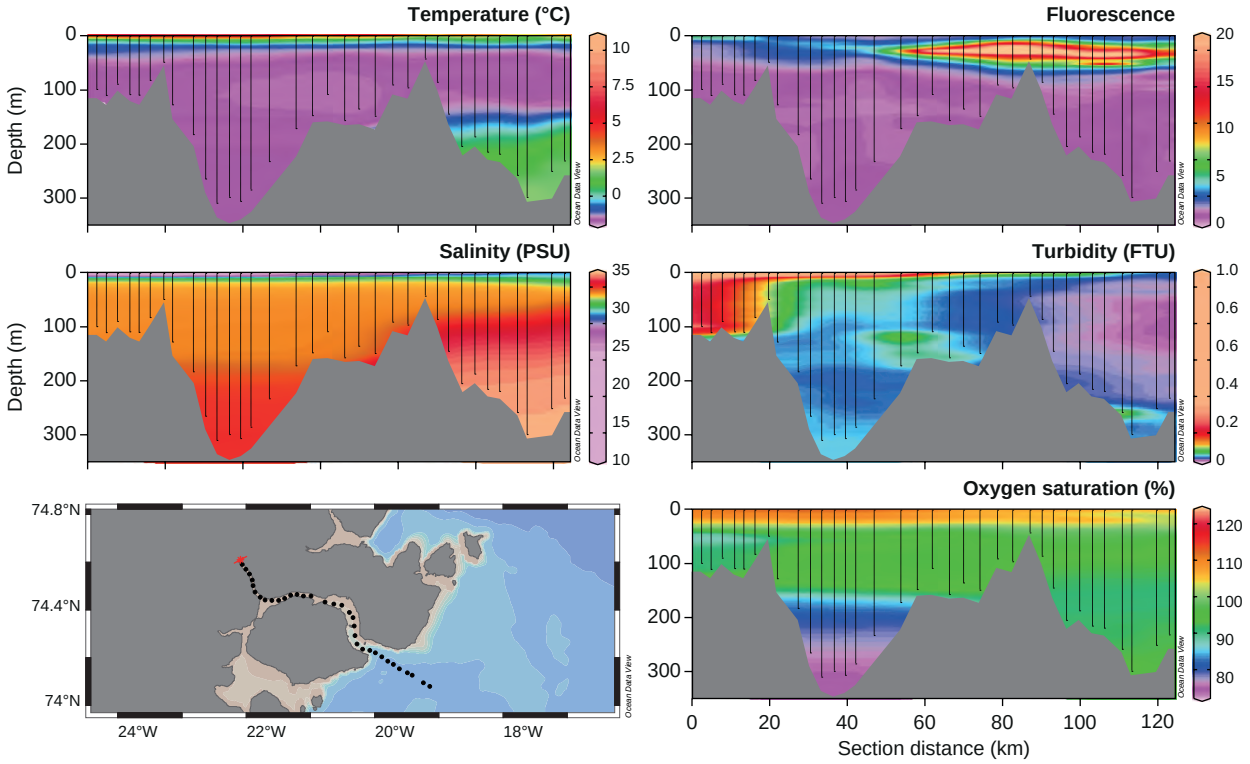

Figure 5.5 Spatial variation in temperature, salinity, fluorescence, turbidity and oxygen saturation measured along a transect from Tyrolerfjord into the Greenland Sea on 25-26 July.

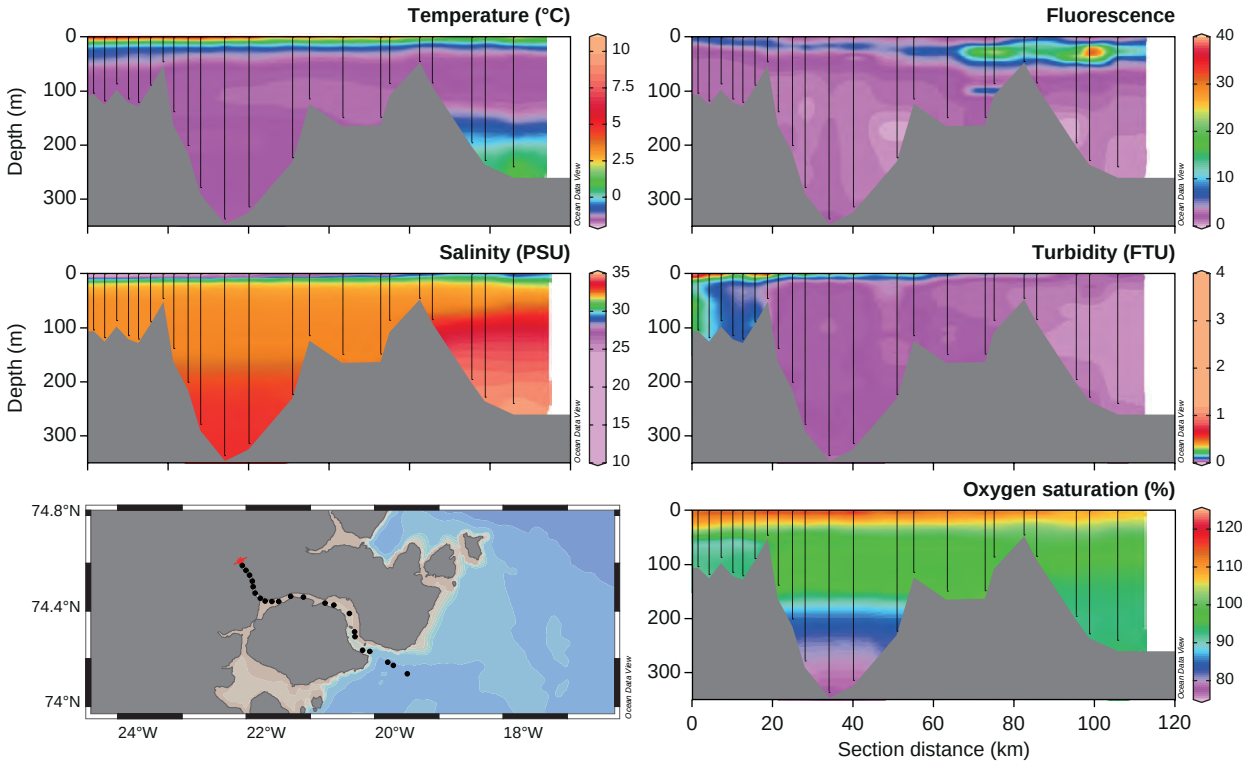

Figure 5.6 Spatial variation in temperature, salinity, fluorescence, turbidity and oxygen saturation measured along a transect from Tyrolerfjord into the Greenland Sea on 6 August.

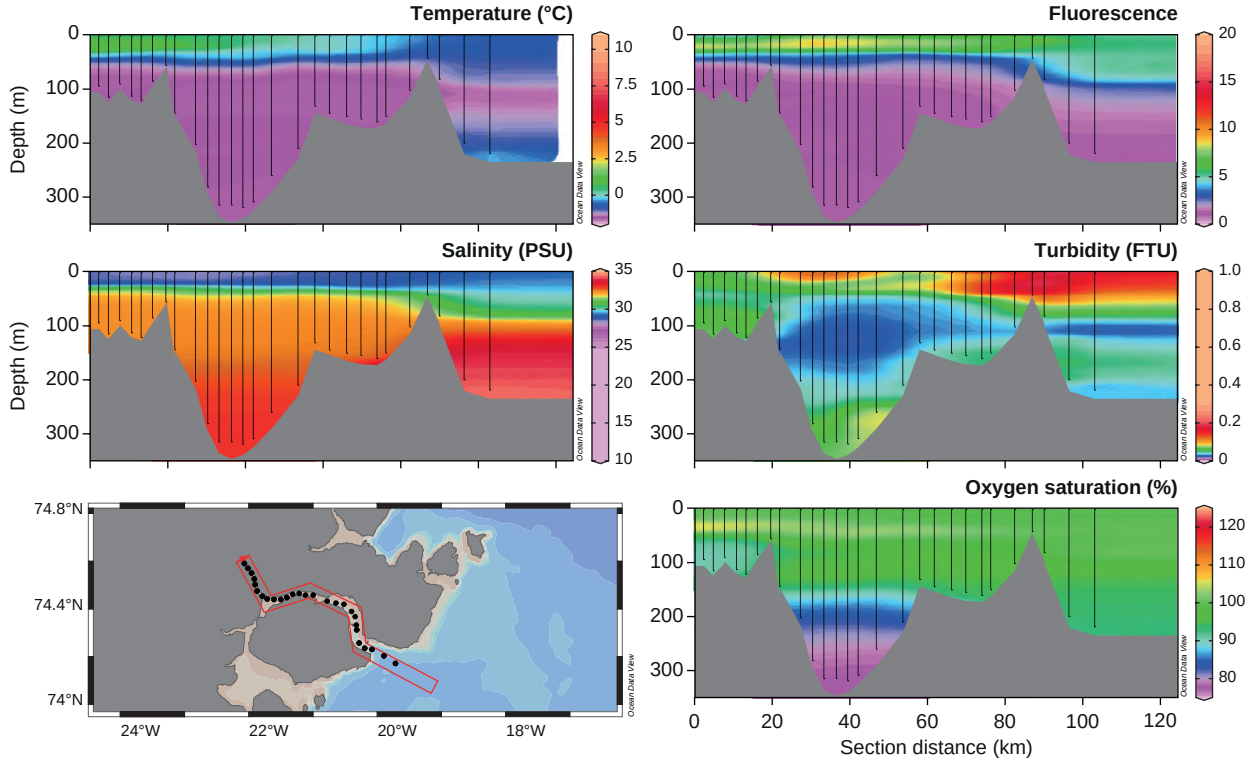

Figure 5.7 Spatial variation in temperature, salinity, fluorescence, turbidity and oxygen saturation measured along a transect from Tyrolerfjord into the Greenland Sea on 17-18 September.

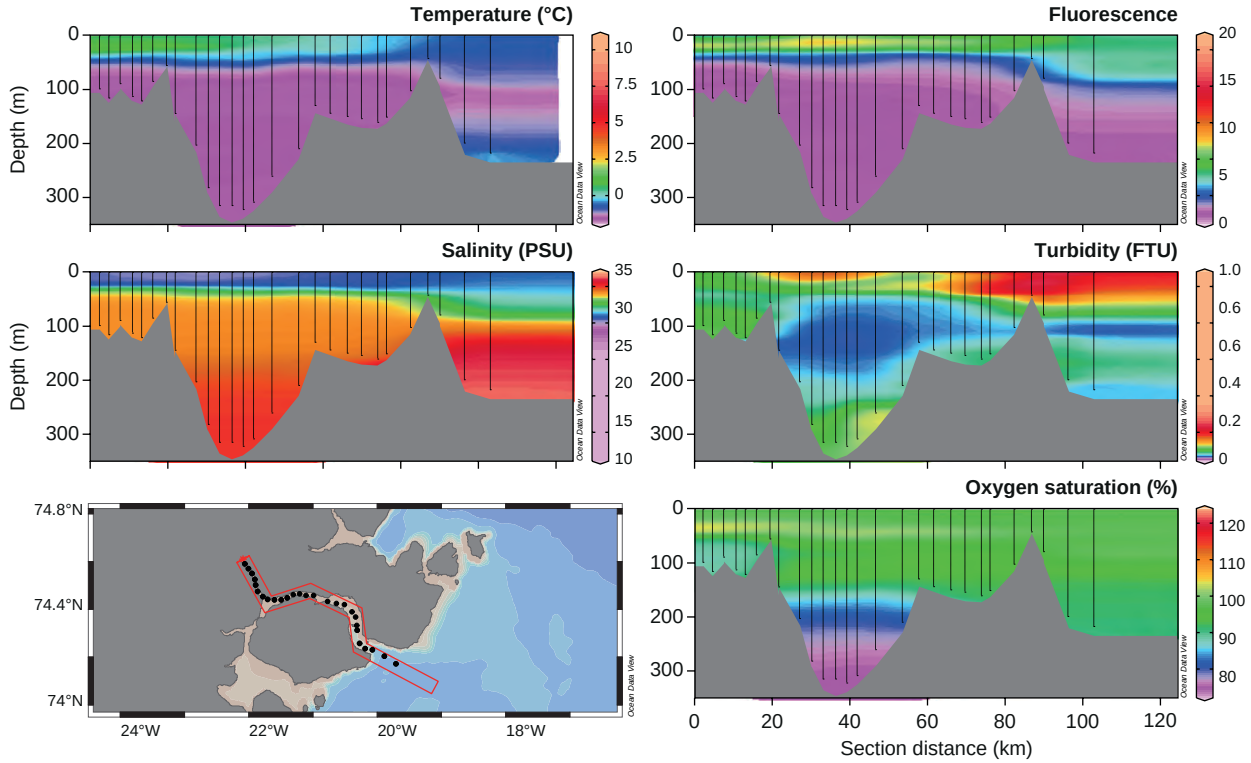

Figure 5.8 Spatial variation in temperature, salinity, fluorescence, turbidity and oxygen saturation measured along a transect from Tyrolerfjord into the Greenland Sea 2 October and 5 October.

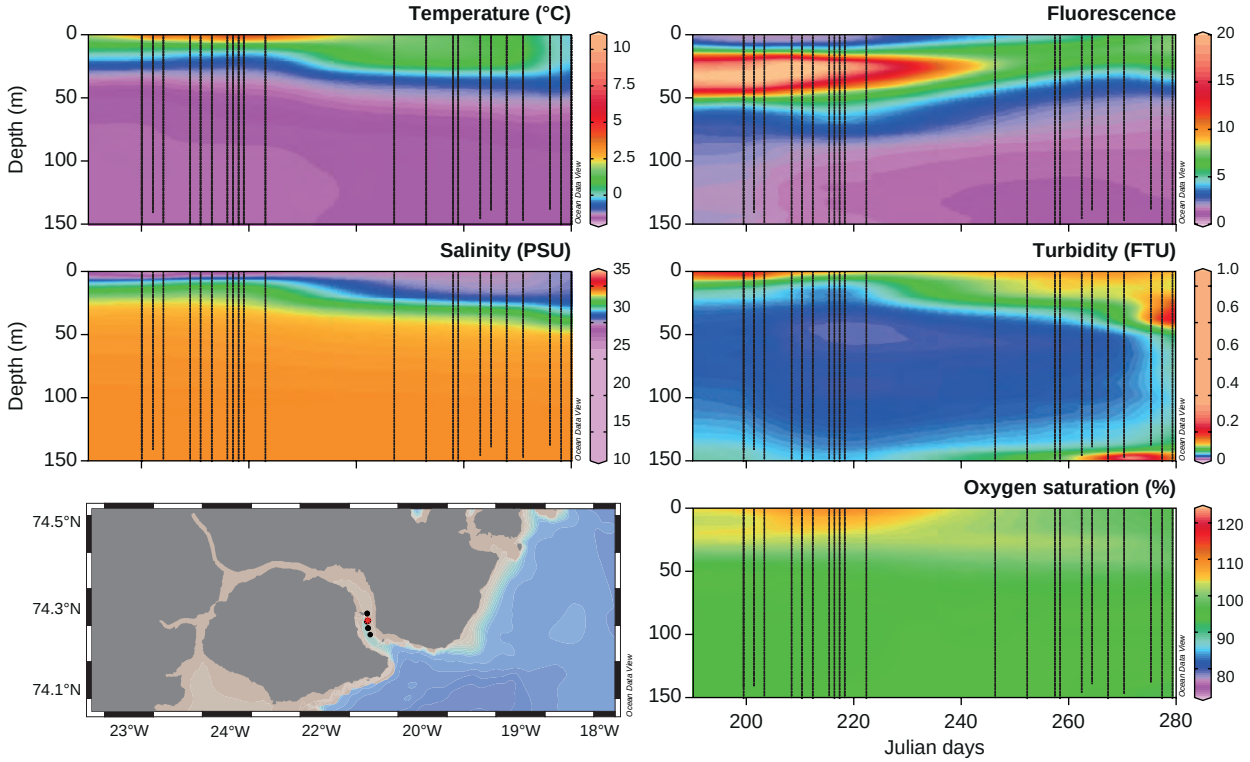

Figure 5.9 Seasonal variation in temperature, salinity, fluorescence, turbidity and oxygen saturation measured at the main sampling station in Young Sound (red dot).

Chlorophyll *a*

The spatio-temporal variation in the integrated chlorophyll *a* concentration is shown in figure 5.10. In general, low total concentration was found in the inner fjord (station 1). At station 3 and 4 there was also a tendency towards a reduction in September and October. The relative contribution from large phytoplankton cells (>10 µm) showed a similar trend: lower in the inner fjord and decreasing towards the end of the season.

Light attenuation

Light availability is an important factor influencing chlorophyll biomass and especially its distribution in the fjord. Using data from the main station, it is apparent that the photic zone (depth of 1 % of surface radiation) ranged between 20 and 35 m, with no significant trend during the season (figure 5.11). It can be seen that the light attenuation coefficient (K_d) is influenced be the average turbidity in the upper 20 m. The turbidity decreased during July and August, but increased again in September and October and shows larger variability. In general, the turbidity is correlated to salinity showing that freshwater from land is a source of turbidity. However, in autumn storms

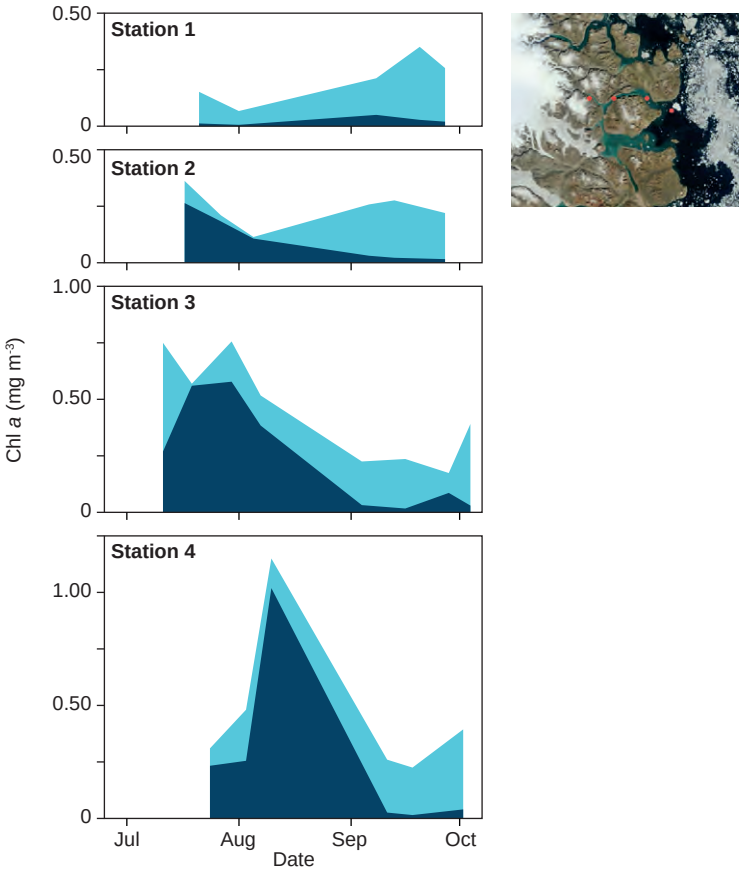

Figure 5.10 Mean chlorophyll a concentrations in the upper 100 m at four sampling stations in Young Sound (stations are numbered from west to east). Light blue shows total chlorophyll a concentration whereas dark blue shows contribution from cells > 10 µm.

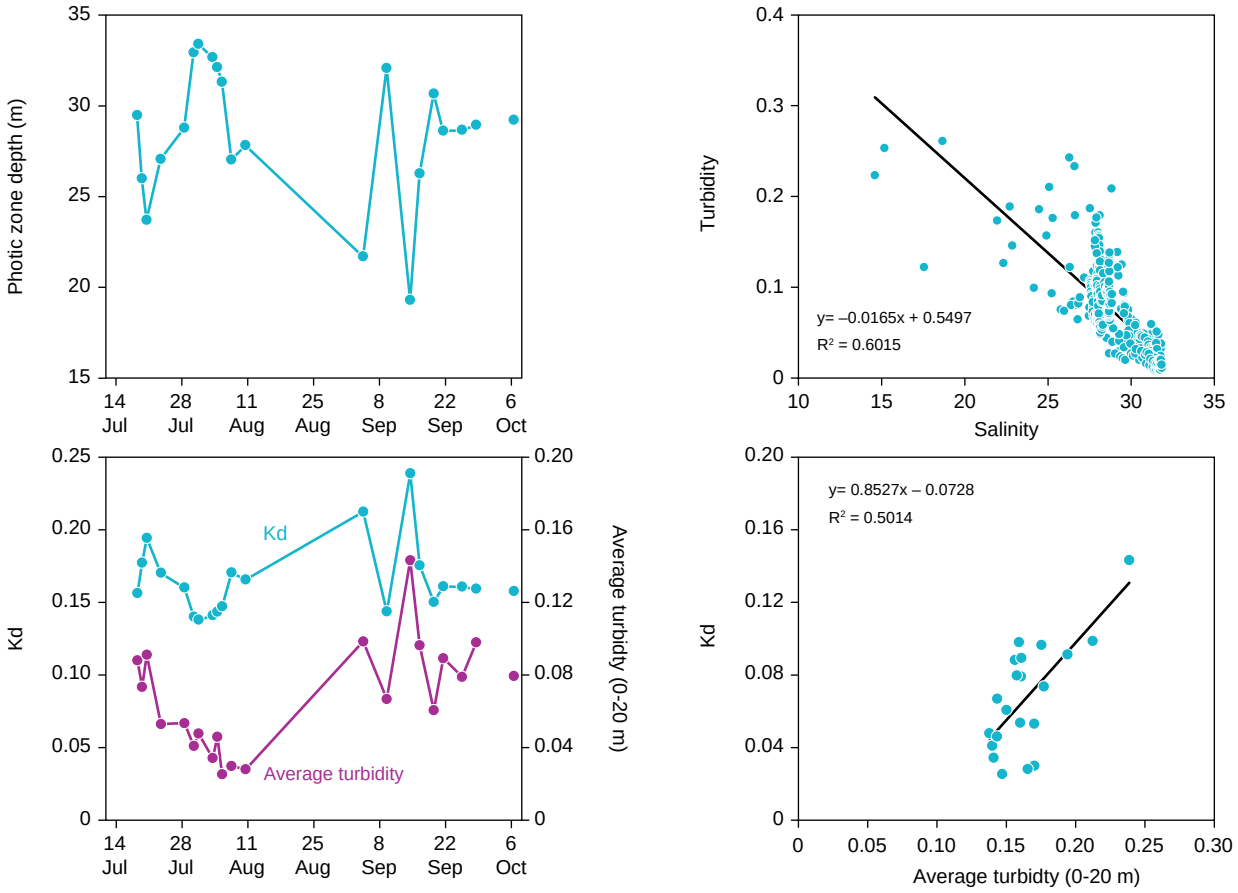

Figure 5.11 Top left: Seasonal variation in photic zone depth at the main station in Young Sound (1 % of radiation measured at 1 m). Bottom left: Seasonal variation in the light attenuation coefficient (Kd, m-1) and average turbidity. Top right:Correlation between salinity and turbidity. Bottom right: Correlation between average turbidity and the light attnuation coefficient.

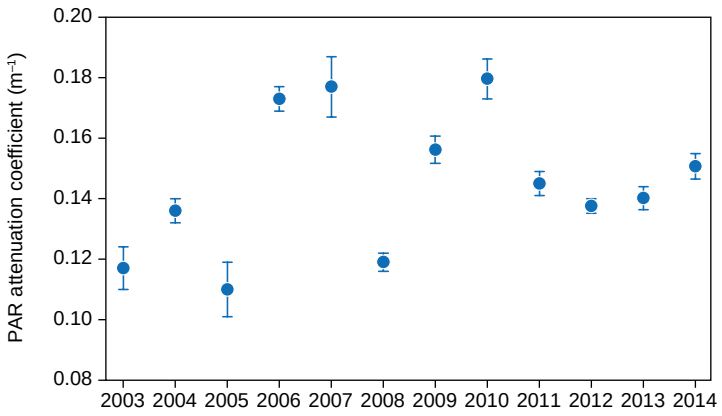

Figure 5.12 Average PAR attenuation coefficients at the main sampling station in Young Sound from 2003-2014.

and waves caused suspension of bottom sediments along the shore which is likely the cause for the high turbidity found in the outer fjord in figures 5.7 and 5.8 where large shallow areas around the Sandøen were affected by 3-4 m high ocean swells breaking.

When comparing the attenuation coefficient from the usual monitoring period at the main station with previous years, it can be seen that 2014 was close to the average for the period (figure 5.12).

Nutrients

Nitrite, nitrate, phosphate and silicate were measured on the same occasions and at the same stations as the chlorophyll concentrations. Here we focus on the seasonal variation at the main station in the outer fjord. Nitrite + nitrate showed a distinct deficit in the upper 40 m at the first sampling on 11 July (figure 5.13). This indicates that significant primary production has already occurred, both in the inner fjord and outside the fjord. Ice-free areas outside Young Sound occurred through June and July. Also the presence of meltwater on top of the sea ice increased the irradiance passing through the ice into the water column and primary production in the water below the sea ice most likely occurred throughout the month of June. A gradual increase in the concentration in the photic zone was observed in late September and early October. Phosphate (figure 5.14) is generally less depleted in the surface water compared to nitrate, and except for the very low surface value measured on 11

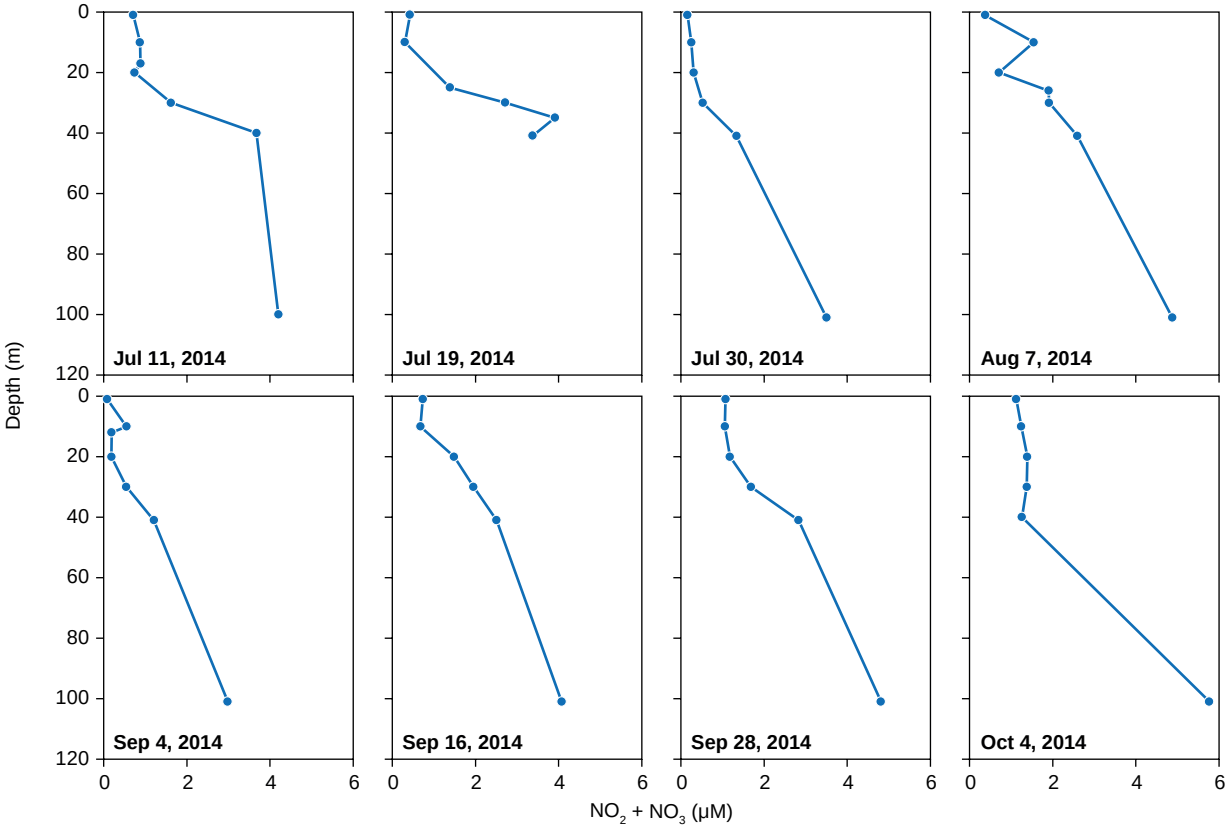

Figure 5.13 Vertical profiles of the concentration of nitrite + nitrate at the main sampling station in Young Sound.

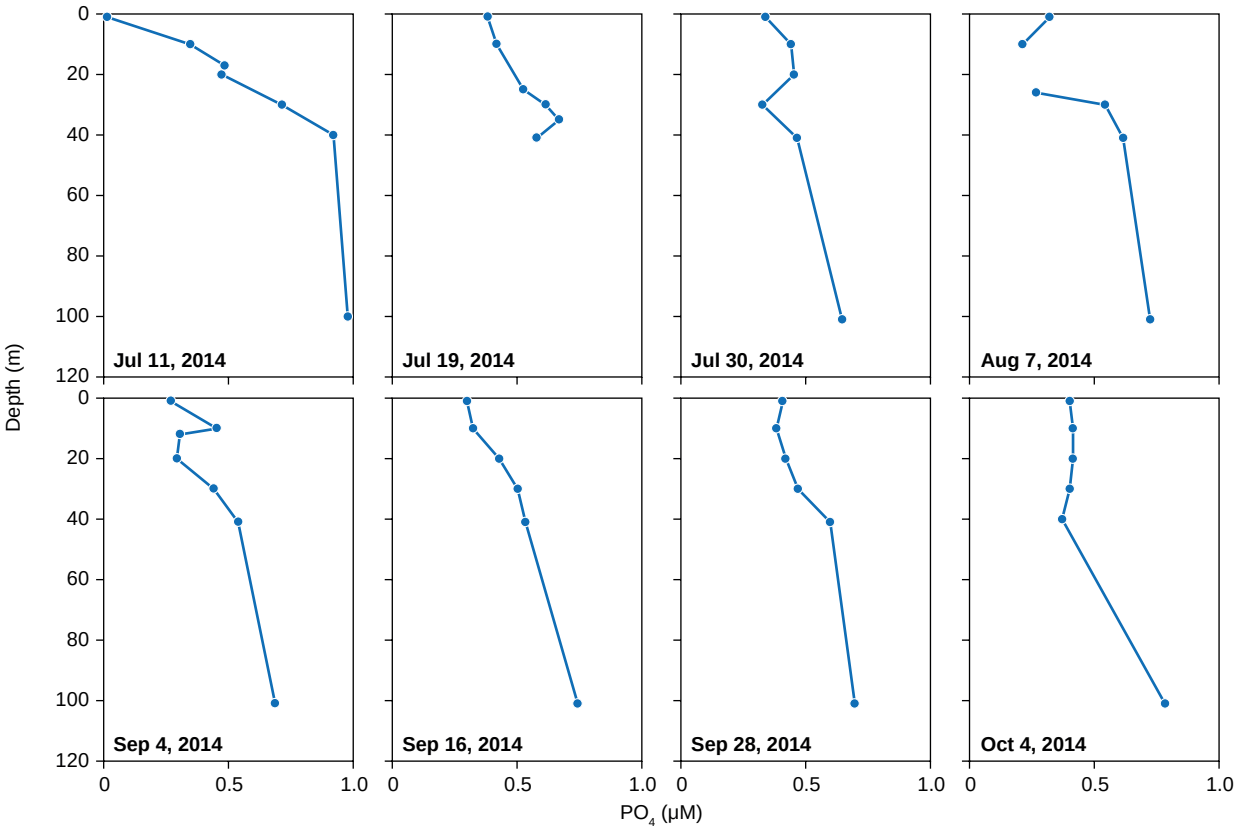

Figure 5.14 Vertical profiles of the concentration of phosphate at the main sampling station in Young Sound.

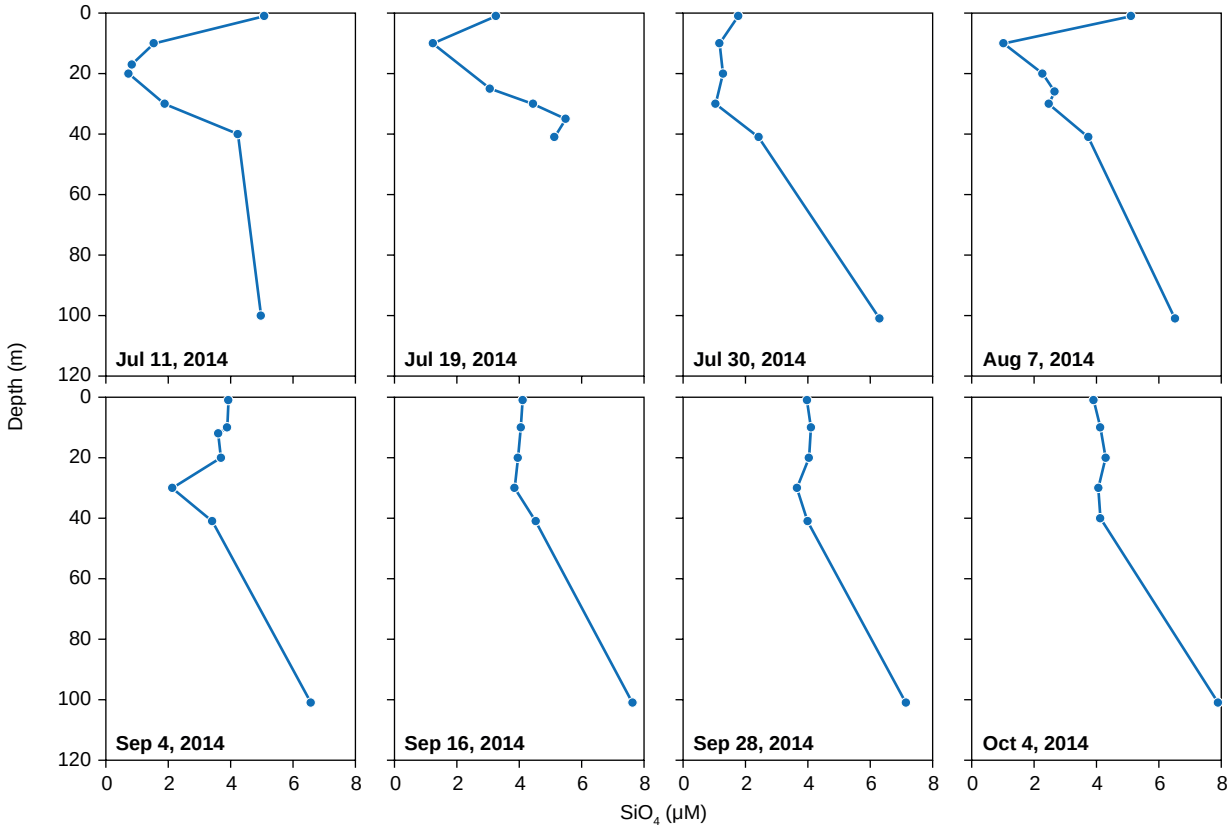

Figure 5.15 Vertical profiles of the concentration of silicate at the main sampling station in Young Sound.

July, which is likely a result of meltwater from the sea ice, the seasonal dynamics were limited. Like for nitrate, silicate showed strong depletion in the surface water except that meltwater from land was relatively high in silicate resulting in high surface values (figure 5.15).

Plankton

Phytoplankton species distribution at the main station changed during the sampling period. In July, it was completely dominated by diatoms of the species *Chaetoceros*, *Thalassiosira* and *Fragilariopsis*. In August, September and October the contribution from diatoms to the total abundance decreased to 50 % or less. This is also part of the explanation for the dominance of the chlorophyll *a* fraction that is smaller than 10 µm (figure 5.16). The composition of the zooplankton community at station 1 to 4 is shown in figure 5.17. The genus *Oithona* was the numerically most abundant, whereas the large *Calanus* species clearly dominated in terms of biomass (data not shown). There are no large spatial differences between the four stations reflecting that advection is minimizing the differences. But as for the chlorophyll *a* size distribution, there was a tendency towards dominance of small species in the inner fjord and late in the season.

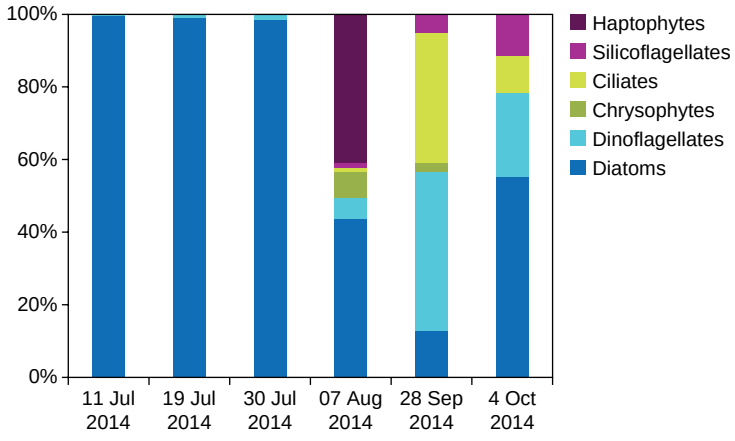

Figure 5.16 Variation in the phytoplankton composition at the main sampling station in Young Sound.

Surface pCO_2

To estimate the potential for ocean uptake of atmospheric CO_2, the partial pressure of CO_2 (pCO_2) is measured in surface waters. The difference between pCO_2 in air and water (ΔpCO_2) determines the direction

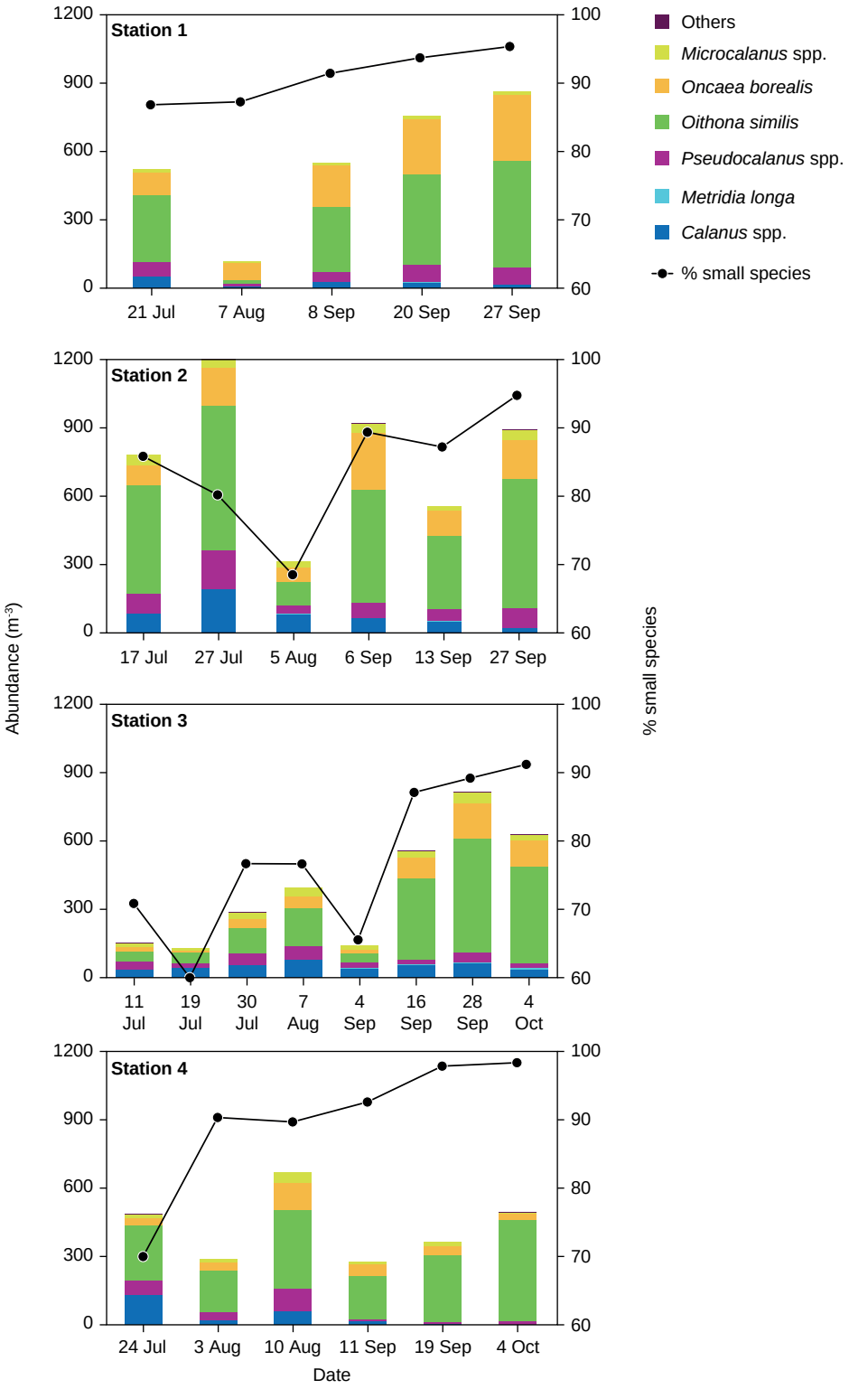

Figure 5.17 Seasonal and spatial variation in the composition of major zooplankton groups in Young Sound.

of the flux, with negative values corresponding to ocean uptake of CO_2. In 2014, measurements were conducted four times in the fjord system, compared to the usual measurements in early August (figure 5.18). The pCO_2 of the surface water was on all occasions below the atmospheric content indicating ocean uptake of CO_2 throughout the ice-free season. A distinct change is visible in the Tyrolerfjord from July/August to September/October: The pCO_2 becomes less negative late in season and the spatial variation is much lower. This corresponds to the increase in surface salinity from early to late season due to mixing and decreasing run-off from land. In the Greenland Sea more negative ΔpCO_2 values are seen in September and

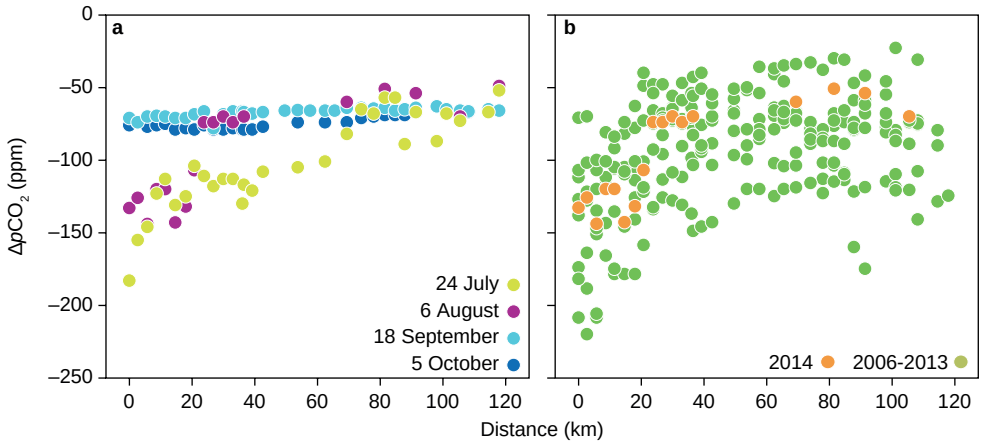

Figure 5.18 Left panel shows the difference between the partial pressure of CO_2 in the atmosphere and the ocean surface in Young Sound. Negative values indicate ocean uptake of CO_2. Data shows surface values starting in the inner Tyrolerfjord and ending in the Greenland Sea at different dates during the ice-free season. Right panel shows ΔpCO_2 in the same area in August from 2006 to 2014.

August, which is likely due to decreasing surface temperatures. When comparing data from August with previous years, data from 2014 are near average for the period 2006-2013.

In addition to these measurements, measurements of dissolved inorganic carbon and total alkalinity were conducted along with pCO_2 at different depths in the fjord to resolve depth variation. Measurement of the partial pressure of methane was also conducted. The preliminary analysis of these data indicates low concentrations in the water column, but with a tendency toward efflux of methane from the fjord.

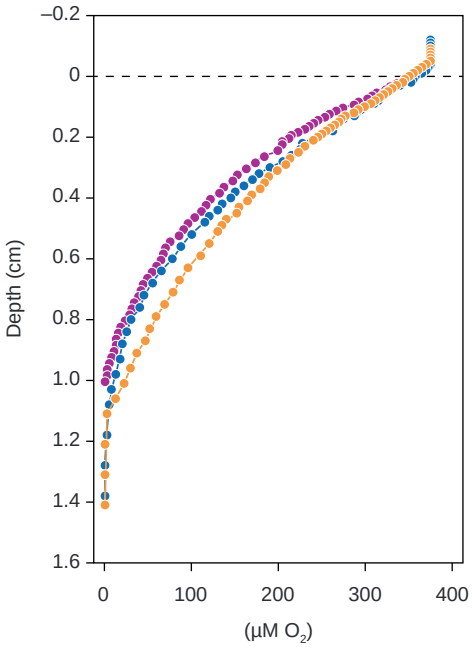

Figure 5.19 Vertical profiles of oxygen concentration in the sediment in Young Sound.

5.3 Sediment

Sediment-water exchange rates of oxygen and nutrients, oxygen conditions

Organic material transported to the seafloor may be degraded by oxidation within the upper oxic zone and by sulphate reduction below. Only a fraction of the organic material reaching the sediment is buried. Sediment cores were collected at a permanent sampling station (water depth approximately 60 m) and used for measuring exchange rate of solutes across the sediment-water interface. After recovery, the sediment cores were incubated at *in situ* temperatures during the experiments in the laboratory. The total oxygen uptake (TOU) into the sediment (4.250 mmol m^{-2} d^{-1}) was well within the range of values recorded since 2003 (ranging from 2.834 – 6.624 mmol m^{-2} d^{-1}). The average oxygen penetration depth, i.e. depth of the oxic zone, was 1.19 cm (figure 5.19), which is comparable to most previous years. The dissolved oxygen uptake (DOU) and sediment-water exchange rates of dissolved inorganic carbon (DIC) and nutrients were not recorded in 2014, but remain part of the monitoring programme.

Annual growth of *Saccharina latissima*

Large specimens of the brown algae *Saccharina latissima* are sampled in early August every year. In this species annual production of new leaves can be identified and the length, biomass and production in terms of carbon can be estimated (figure 5.20).

In 2014, the length of the new leave was 123 cm which is near the average of the sampling period. Light availability is most likely the primary driver of annual growth in this species. Ice conditions are thus an important factor determining growth. Because the species is perennial, the length of the leaf most likely reflects light conditions from unfolding to collection (potentially several years).

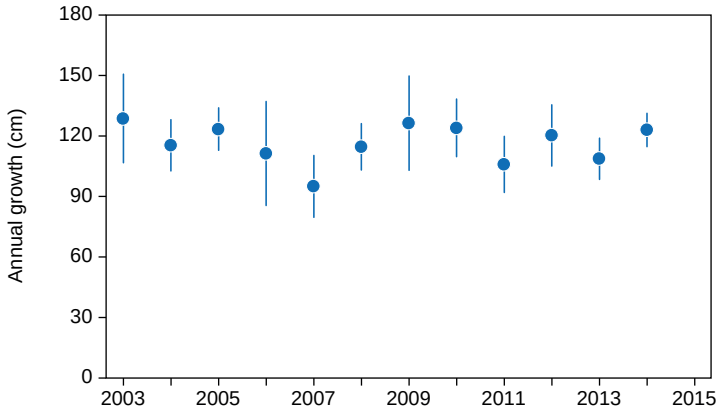

Figure 5.20 Average leaf growth (±SE) of the macroalgae Saccharina latissima *at 10 m depth in Young Sound.*

6 Research projects

6.1 Spatial impact of outburst floods on the A.P. Olsen Ice Cap dynamics

Geo Boffi, Daniel Binder, Andreas Wieser and Wolfgang Schöner

The southeast outlet glacier of the A.P. Olsen Ice Cap (74°38'N, 21°26'W) temporarily blocks drainage of a side valley and causes annual Glacial Lake Outburst Floods (GLOFs) that are recorded in the river Zackenberg. Measurements using Ground Penetration Radar (GPR) in 2008 carried out by the Central Institute for Meteorology and Geodynamics (ZAMG), showed prominent englacial reflections situated on the southeast outlet below the side valley where the dammed lake is built up.

These two reasons motivated to develop a monitoring strategy at the southeast outlet glacier of the A.P. Olsen Ice Cap. Since the GLOFs are occurring more or less annually, this site is appropriate for process-orientated GLOF studies. Firstly a monitoring network with single-frequency GPS measurement systems (ublox EVK-6T GPS receiver and AeroAntenna AT575-142 GPS antenna), as well as passive seismic equipment (Reftek 130S-01), was installed in spring 2012.

In late summer 2012, the monitoring stations were visited, in order to collect data and check the device's conditions.

Afterwards, a second field trip was carried out on spring 2013, in order to collect the data and install a pressure sensor on the lake bottom. Most GPS stations were in stable conditions and delivered measurement data for the first time over spring, summer and fall. However, we observed that the power supply provided by just the wind turbine was not sufficient for a full operation of the station, which means that we had a data gap during the polar night when no sun was available. The first results were very encouraging as it was possible to process high rate GPS measurement around the GLOF (figure 6.1). First analysis of the 2012 GPS dataset indicated an increased horizontal flow immediately before and during the GLOF. Sugiyama *et al.* (2007) reported similar dynamic consequences during the outburst of Gornerlake, Switzerland. In order to yield better time resolution of the

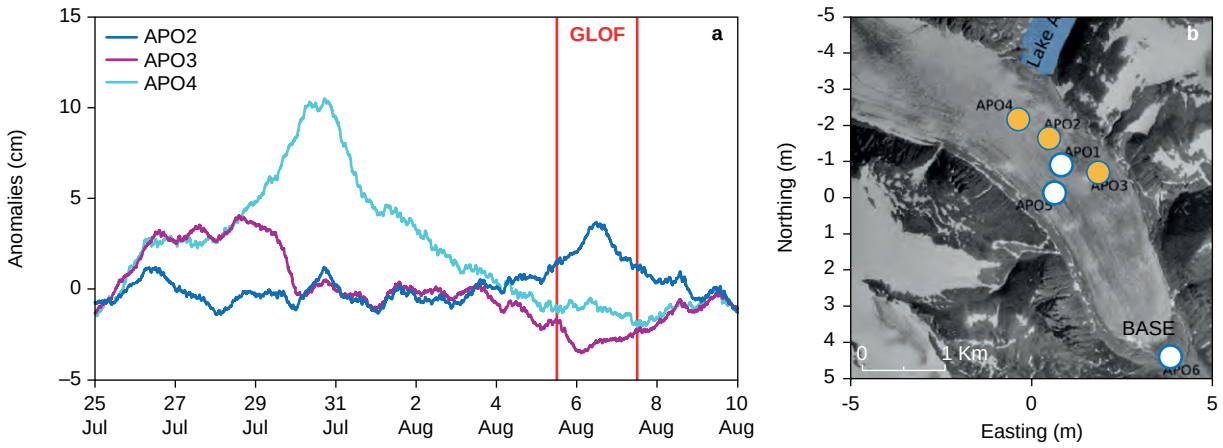

Figure 6.1 GPS data of stations APO 2-4 of initiation and outburst phase (6 August) of the GLOF in 2012. Data of stations APO1 and APO5 were not available. In order to separate the local motion anomalies caused by the lake outburst from the long-term ablation process, a linear trend is subtracted from the height variation. It is observable that this part of the glacier already began to lift up seven days before the outburst. Significant uplifts are observed at station 4, the nearest one to the ice dam, which is the first one to be influenced and it reaches a peak of 10 cm. Station 2 is less influenced in the height, compared to station 4, and also later on, when the lake is already draining.

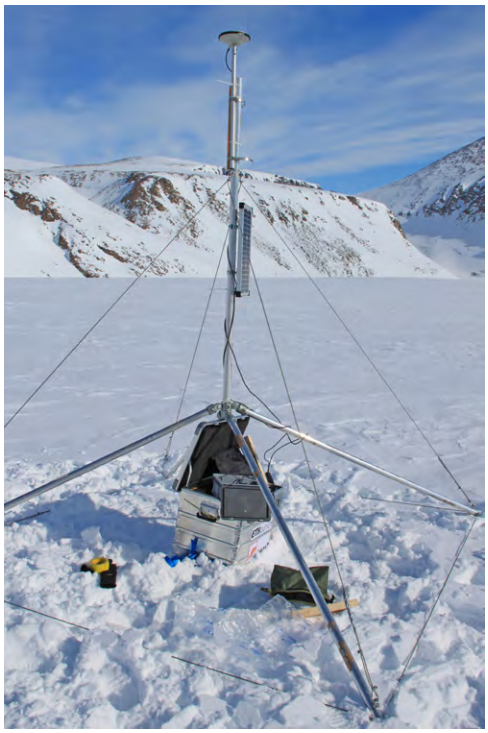

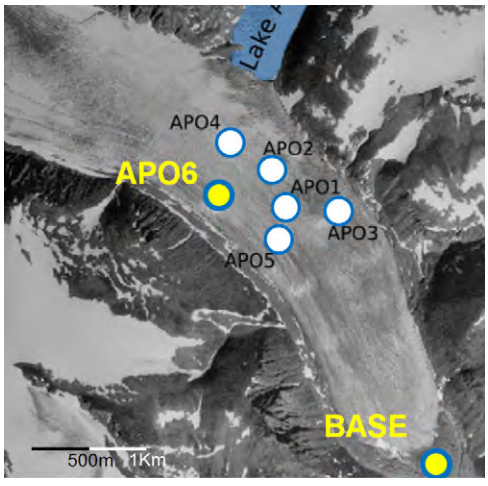

Figure 6.2 a) The new measurement station (APO6) located on the southeast outlet of the A.P. Olsen glacier. b) Monitoring Network on the A.P. Olsen Ice Cap. APO1 to APO6 provide continuous GPS measurements. BASE in the glacier forefield is the reference station.

surface dynamics and stress field changes, we used kinematic processing of all GPS data (0.1 Hz) in a Kalman Filter. The scientific GPS postprocessing software (Matlab based) currently uses a coordinate random walk model to represent site motions.

Due to bad meteorological conditions, no field trip has been carried out during the summer. An additional field trip was accomplished in spring 2014 to install an additional GPS measurement station at the southeast outlet A.P. Olsen glacier, in order to obtain a better spatial resolution of the dynamic response of the glacier to the GLOF. Furthermore, data recorded by the measurement stations, as well as by the pressure sensor, have been collected. The new measurement station (Novatel OEM6 GPS receiver with Novatel GPS-701-GG GPS Antenna) shall improve the reliability and avoid data gap during the important phase of the glacier motion (figure 6.3). Also the base station has been equipped with a more robust and reliable set up (Trimble 5700 GPS receiver with Trimble Zephyr GPS Antenna), because it is a crucial point to estimate differential positioning of the stations on the glacier. We equipped the new station with GPS sensors which have similar characteristics to the temporary version, which means low power consumption and a measurement rate of 10 seconds. The sensors are fixed to the same mechanical structure used for the first monitoring stations (figure 6.2). Unfortunately the other GPS stations (APO1, 2, 3, 4 and 5) got damaged during the winter and therefore did not save the collected data during the summer 2013. Without information about the health status of the stations and the limited logistic possibility on site, it was not possible to fix the problem.

The outburst of summer 2013 was recorded by the pressure sensor located on the lake bottom (figure 6.4). Unfortunately the sensor stopped measuring at the beginning of August 2014 and it did not record the outburst of summer 2014 because it was out of memory.

A field trip in August 2014 collected the first data of the new station APO6 (figure 6.4). We can observe that, although the station is not located close to the ice dammed lake, the dynamic of the glacier is still influenced in the horizontal component by the lake outburst.

Travel costs were funded by INTERACT Transnational Access.

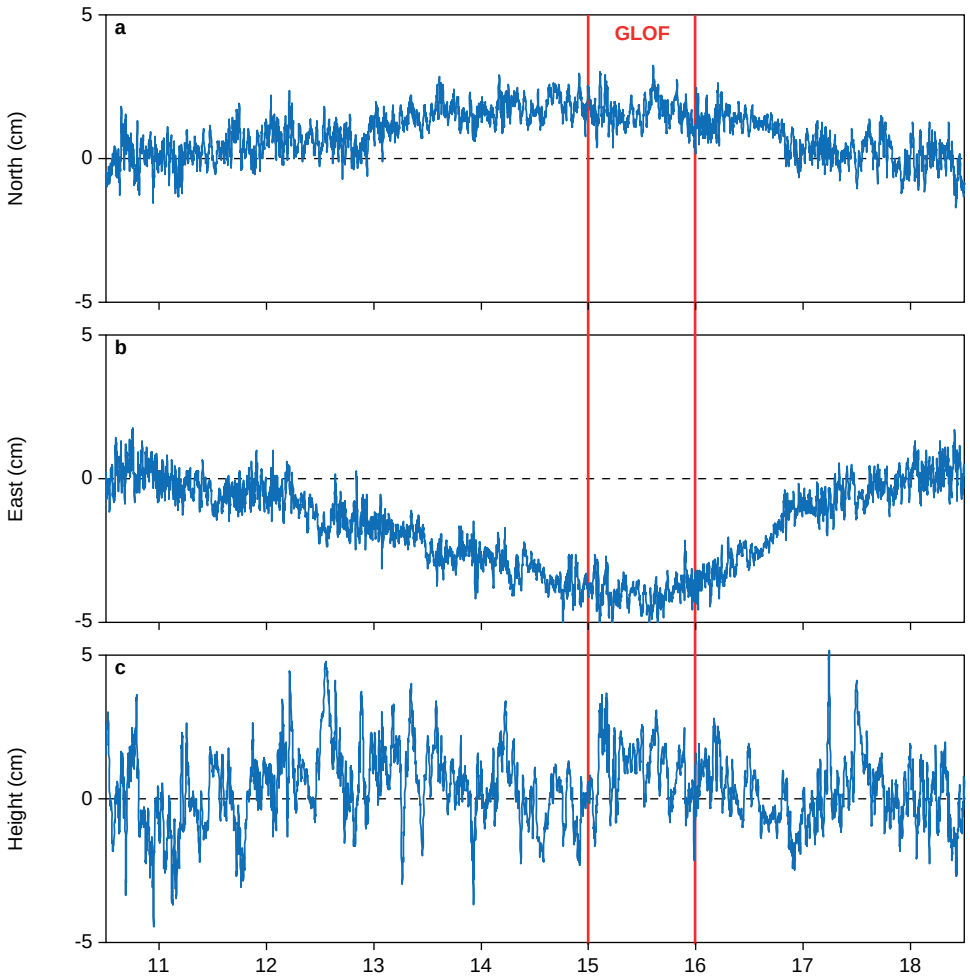

Figure 6.3 Horizontal and vertical displacement anomaly of station 6 during the outburst of summer 2014 (15 – 16 August).

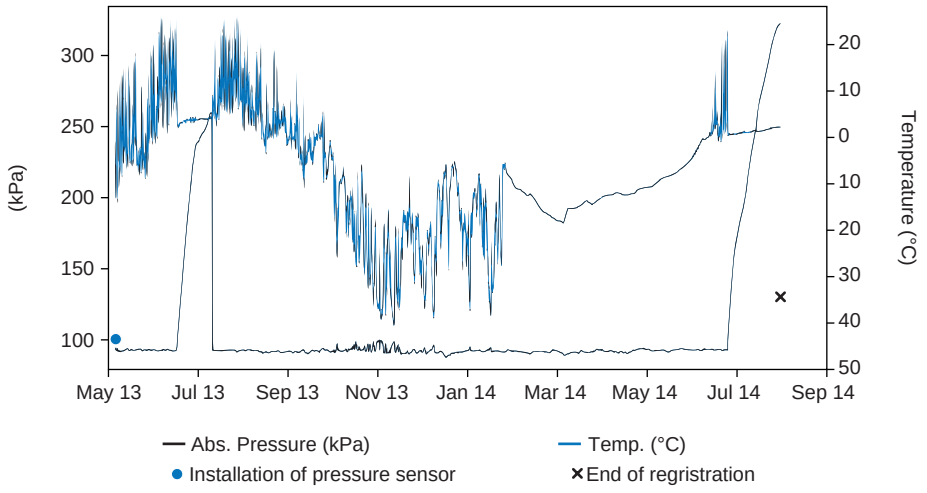

Figure 6.4 The water pressure increases over the summer months, which agree with a growing water level at the glacial lake, and suddenly decrease during the GLOF, meaning a rapid empting of the lake takes place at the beginning of August 2013.

6.2 Regional snow survey in Norteast Greenland

Stine Højlund Pedersen and Glen E. Liston

The aim of snow fieldwork was to gain knowledge of the regional snow distributions and to document an expected gradient in winter precipitation and the wind speed across the region extending from the inland parts of Tyrolerfjord near the Greenland Ice Sheet margin, through the Zackenberg valley to the east coast of Wollaston Forland (figure 6.5). The collected snow data will furthermore be used in validation of modelled snow distributions and coupled to biological components in the arctic ecosystems such

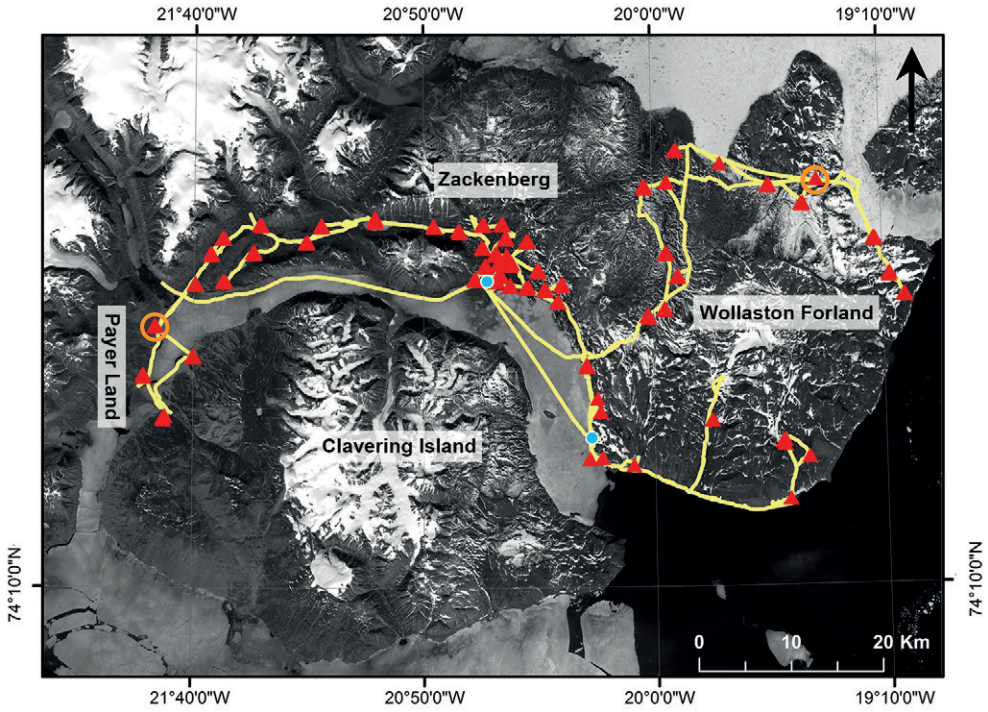

Figure 6.5 Map showing snow mobile route (yellow lines), snow sampling sites (red triangles), Zackenberg Research Station and Daneborg (blue circles), and two snow sampling sites (orange circles) where photos in Figure 6.6 were taken. Based on Landsat 7 image from 12 July 2001.

as the spatial distribution of vegetation greenness (NDVI) and musk oxen movement patterns within the region.

We had 21 field days with multi-day excursions covering 1100 km on snow mobiles within the region (figure 6.5). In order to document the differences in winter precipitation, we measured snow depth at 57 sites each including approximately 100 snow depth observations in triangle transects to cover the snow depth variability along, perpendicular, and diagonal to the dominant wind direction. To document a gradient in wind speed across the region, we analysed 45 snow pits to record the stratigraphy, snow density, grain type, grain size, and hardness. During the 1-month fieldwork, we observed a gradient in both snow depth and density from coast and inland. We observed snow depths above 2 m at all sites in north-northeast Wollaston Forland (figure 6.6 left), approximately 1 m snow depth within the Zackenberg valley, and inland at Payer Land the snow thickness was less than 10 cm (figure 6.6 right). Furthermore, the density and hardness of the snow decreased from the coast and inland.

Figure 6.6 Left: Snow pit dug near Flaskebugt, north-eastern Wollaston Forland (74°33'26.7"N, 19°24'20.2"W). Right: Snow-depth transect at PayerLand (74°25'18.2"N, 21°48'27.0"W), Photos: Glen E. Liston.

6.3 Microbial communities in Arctic environments – The effects of thawing permafrost soils on biogeochemical processes driving the terrestrial carbon cycle

Oliver Müller and Maria Lund Paulsen

The conducted fieldwork in the Zackenberg area (figure 6.7) aims to complete a comparative project including Svalbard and Greenland, studying microbial communities in Arctic environments and the effects of thawing permafrost soils on biogeochemical processes (e.g. methane production, nitrogen fixation, etc.) driving the terrestrial carbon cycle.

With thawing permafrost, the rate of decomposition of formerly stored organic carbon increases and more greenhouse gases are released into the atmosphere. We aim to indicate the potential and changes of dominant microbial groups and metabolic key processes due to accelerated thaw. A specific focus lies on the degradation potential of organic matter in distinctive different layers of the permafrost soil.

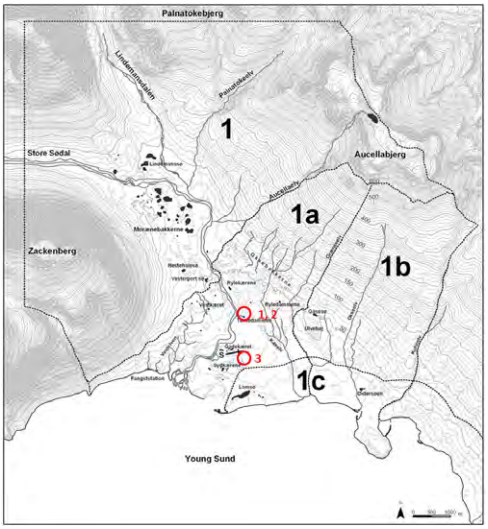

Figure 6.7 Map of the Zackenberg area showing the two sample sites where a total of three permafrost cores were drilled.

Soil cores have been obtained from a characteristic low-centred ice-wedge polygon site in the Zackenberg valley in NE Greenland during Arctic summer.

We intend to extract DNA and RNA from subsamples from the active and permafrost layer as well as the transition zone between (table 6.1). The extracted DNA will be used as template in 16S

Table 6.1 Sample identification key.

Sample ID	Depth interval from surface (cm)	Length	Comments	Location
1-01	0 - 6*		Vegetation + roots 0-10 cm	
1-02	10 - 16*		Active layer	
1-03	20 - 26*		Active layer	74.47708 N 20.55297 W
1-04	41 - 47*		Frozen table starts at 65 cm	
1-05	65 - 85	20 cm		
1-06	84 -101	17 cm		
1-07	101-120	19 cm		
2-01	0 - 6*		Vegetation + roots 0-10 cm	
2-02	10 - 16*		Active layer	
2-03	36 - 42*		Active layer	74.47722 N 20.55266 W
2-04	64 - 70*		Frozen table starts at 70 cm	
2-05	70 - 105	35 cm		
2-06	105 - 120	15 cm		
3-01	0 - 6*		Vegetation + roots 0-10 cm	
3-02	10 - 16*		Active layer	
3-03	20 - 26*		Active layer	74.46956 N 20.55194 W
3-04	41 - 47*		Frozen table starts at 72 cm	
3-05	72 - 88	16 cm		
3-06	88 - 130	42 cm		

*Separate soil samples

rRNA amplification sequencing to obtain a description of the microbial community along the core. Additionally, metatranscriptomic analyses will be performed to indicate the key functional processes in the distinctive layers. To identify both the changes in community structure and gene abundance differences due to thaw, the same permafrost samples will be used in incubation experiments. Gas fluxes of CO_2; CH_4 and N_2O are going to be monitored over the course of hours up to several days while incubating under temperatures occurring during the thawing season and DNA/RNA extracted after the incubation is terminated.

These analyses are currently being carried out and the results are planned to be published in a PhD thesis and as a peer reviewed paper.

6.4 Controls on glacial landform preservation in Northeast Greenland

Kathryn Adamson and Timothy Lane

Ice caps and valley glaciers provide sensitive indicators of environmental change. Recent research highlights the role of local topography in moderating glacier behaviour in response to climate change. However, few studies have tested in detail the influence of valley geometry on the formation and preservation of the glacial geomorphological record. Establishing these relationships is important for the accurate reconstruction of past glacier behaviour.

During the 2014 field season, we examined the Holocene glacial geomorphological record of outlet valleys draining ice caps close to Zackenberg. We completed detailed geomorphological mapping and sediment sampling of glacial and glaciofluvial deposits. Our analyses were used to examine spatial variations in landform characteristics, and to test the role of topography on landform development and preservation. This forms part of a wider project that explores the glacial geomorphological record of Greenlandic ice caps.

Our observations indicate that glacial geomorphology varies between neighbouring valleys. In some valleys clear moraine ridges are preserved (figure 6.8). In others, large areas of hummocky terrain, ice moulded bedrock, or ice marginal alluvial fans are present (figure 6.9). This is likely to reflect complex interactions between outlet glacier behaviour, meltwater and sediment supply, valley aspect and

Figure 6.8 Clear moraine ridge and proglacial alluvial fan preserved in an outlet valley draining into Slettedalen, northwest of Zackenberg. Photo: Kathryn Adamson

Figure 6.9 Hummocky moraine in Slettedalen. Photo: Kathryn Adamson.

geometry (e.g. long profile, width, gradient). These results mirror the evidence found in our recent research on Disko Island, West Greenland, and indicate that no single land system model can be applied to all valleys.

6.5 ASP Young Sound Campaign 2014 – Carbon balance

Magnus Lund, Torben R. Christensen, Line V. Hansen, Marcin Jackowicz-Korczynski, Mikhail Mastepanov, Maria R. Mylius, Lau G. Petersen, Norbert Pirk, Laura H. Rasmussen, Kirstine Skov, Lena Ström and Mikkel P. Tamstorf

The land-atmosphere exchange of carbon dioxide (CO_2) and methane (CH_4) in the Zackenberg valley as well as the carbon (C) transport in the river Zackenberg have been monitored by the GeoBasis program during multiple years. In order to advance our current understanding on the dynamics behind these processes and how they are inter-connected, we carried out a measurement campaign during 2014 sponsored by the Arctic Science Partnership (ASP). This campaign was divided into three sub-projects:

1. Snow pack fluxes of CO_2 and CH_4 and within snow pack $\delta^{13}CH_4$ concentrations
2. Distributed sampling of water table depth, runoff and soil water chemistry in a fen (*Rylekærene*)
3. Eddy covariance CO_2, CH_4 and energy flux measurements in the Zackenberg river delta

During spring 2014, experimental plots were laid out close to GeoBasis' autochamber site in the fen *Rylekærene*. Fluxes of CO_2 and CH_4 between snow surface and atmosphere were measured using a closed chamber connected to an LGR GGA analyser (Los Gatos Inc., USA). Furthermore, we measured gradients of CH_4 concentration and $\delta^{13}CH_4$ within the snow pack using a probe connected to a LGR MCIA analyser (Los Gatos Inc., USA). Similar measurements were carried out in Zackenberg in 2012, as well as in Adventdalen on Svalbard in 2015. The objectives of this study were to 1) quantify the snow-atmosphere fluxes, 2) assess the spatial and temporal variation in relation to environmental characteristics, and 3) study the dynamics behind the emissions. Data from Zackenberg and Adventdalen are currently being analysed by PhD student Norbert Pirk at Lund University.

The hydrology and associated lateral C and nutrient fluxes in the fen *Rylekærene* are poorly understood. During summer 2014, we installed a distributed network of 16 Odyssey Capacitance Water Level loggers (Dataflow Systems Limited, New Zealand) in the fen, as well as a v-notch in an outlet from the fen into the river Zackenberg (figure 6.10). Soil water was collected throughout the summer and analysed for dissolved organic carbon (DOC), nitrate (NO_3^-), ammonium (NH_4^+) and organic acids. The data can be used to model the hydrological patterns of the fen, the spatial variation in soil water chemistry, as well as inputs and outputs of waterborne C. Thus, we will be able to quantify lateral fluxes of C; and in combination with GeoBasis' land-atmosphere

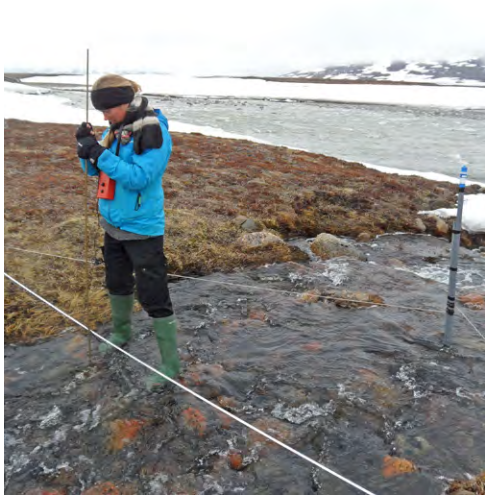

Figure 6.10 Measurements of a stream profile by Kirstine Skov, June 2014. Photo: Laura H. Rasmussen.

Figure 6.11. Torben R. Christensen and Marcin Jackowicz-Korczynski next to the newly installed eddy covariance system in the river Zackenberg delta, August 2014. Photo: Lau G. Petersen.

exchange measurements of CO_2 and CH_4, the full C budget of the fen can be established.

Direct measurements of the exchanges of CO_2, CH_4 and energy between Arctic coastal areas and the atmosphere are scarce. During August-September 2014, we set up a mobile eddy covariance system north-west of the river Zackenberg delta (figure 6.11). The system consisted of a 3D sonic anemometer (Gill-HS, Gill Instruments Ltd., UK), an enclosed path CO_2 and H_2O gas analyser (LI-7200, LiCor Inc., USA) and an open path CH_4 analyser (LI-7700, LiCor Inc., USA). We were fortunate to have the flux measurements running during a glacial lake outburst flood (GLOF) on 16 August, resulting in a dramatic increase in river discharge affecting the flux rates. The acquired data, which are currently being analysed, may provide an important link related to the C transport between terrestrial and marine ecosystems.

6.6 The effect of plant-soil-herbivore interactions on greenhouse gas dynamics in the Arctic

Lena Ström, Julie M. Falk, Torben R. Christensen and Niels Martin Schmidt

The effect of herbivory on ecosystems involves an intricate web of processes and feedback mechanisms between these. Processes that are very likely to be affected by grazing include e.g. carbon sequestration, greenhouse gas flux, vegetation composition, structure and diversity, and soil physical parameters (soil moisture and temperature, decomposition rates and nutrient availability) (Sjögersten 2008; Tanentzap 2012). Consequently, a detailed understanding of the various processes mentioned above is needed, especially if generalizations are to be made as to how the C-sink strength function of arctic ecosystems may change as a consequence of climate change.

During 2014 Julie Maria Falk defended her PhD. thesis "Plant-soil-herbivore interactions in a high arctic wetland – Feedbacks to the carbon cycle" and the results from the project was published or accepted for publication in per-reviewed scientific journals (Falk *et al.* 2014; Falk *et al.* 2015; Ström *et al.* 2015). The results, thus far, show that exclusion of herbivory (Falk *et al.* 2015) and other manipulations (Falk *et al.* 2015; Ström *et al.* 2015) to the ecosystem has resulted in effects on vegetation development and suppressed growth of the sedge *Eriophorum scheuchzeri*, with direct feedbacks to the fluxes of CO_2 and CH_4 in the Rylekærene fen area (figure 6.12) (Ström *et al.* 2015). The results from the project clearly show that the drivers of the greenhouse gas balance are the vegetation composition, with a high density of *Eriophorum* leading to high fluxes of CO_2 and CH_4 (figure 6.12), due to the positive effect this species has on productivity (net ecosystem and gross primary produc-

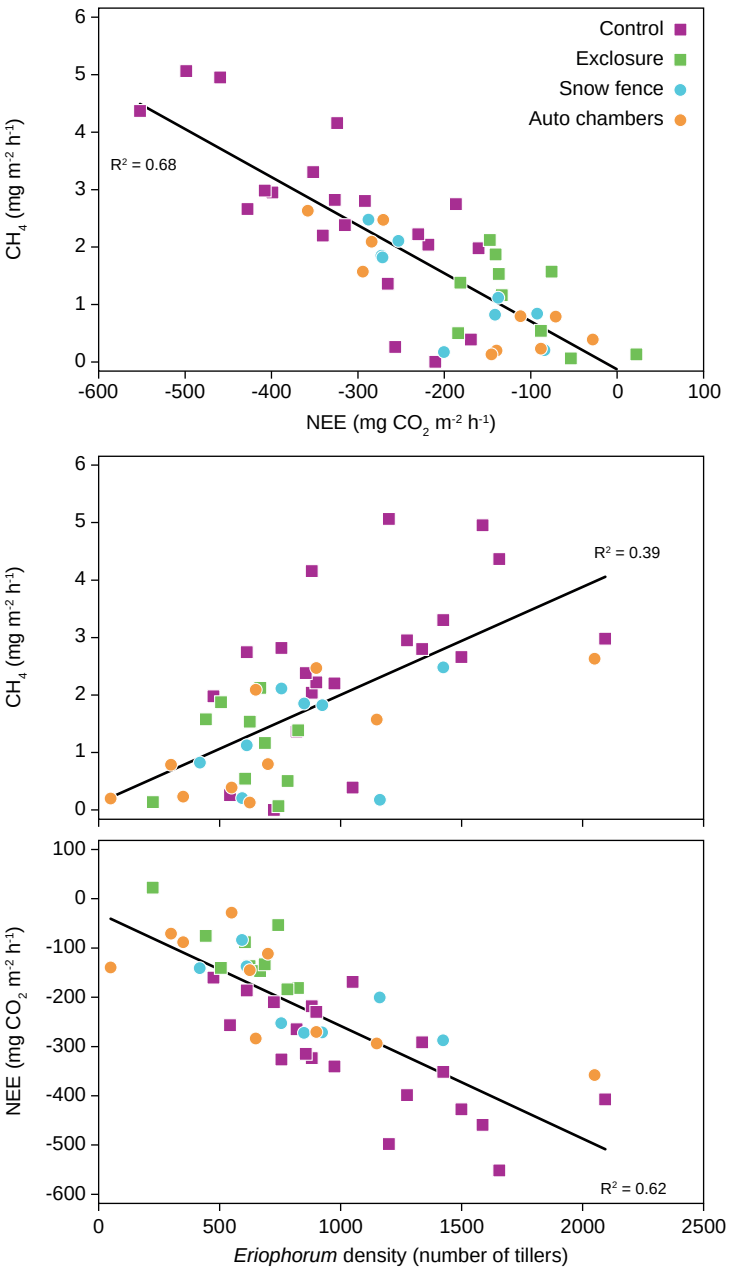

Figure 6.12 The mean July relationship between CH_4 flux and Net Ecosystem Exchange of CO_2 (NEE), the CH_4 flux and Eriophorum density and NEE and Eriophorum density measured in control and treated plots in a high arctic wetland, correlation lines ($p < 0.05$) are based on all data points ($n = 49$). *Muskoxen exclosure (10 × 10 m), snow control (fence in main wind direction) and auto chamber (permanently installed plexiglas frame) plots.*

tivity) and pore-water concentration of acetate, an important substrate for CH_4 production.

In 2014, we continued the measurements of greenhouse gas fluxes and environmental variables in the Rylekærene fen area and the effect of grazing exclusion on the ecosystem carbon balance. These data are currently under evaluation. In conclusion, the results from the project indicate that future environmental changes in wet arctic ecosystems that affect the vegetation composition and productivity will have large impact on their carbon balance and CH_4 flux, irrespective of whether these changes are driven directly by climate or indirectly through effects on species composition or grazing pressure.

6.7 ZackSAR II – Retrieval of environmental parameters in Arctic tundra landscapes from remote sensing data

Jennifer Sobiech-Wolf and Tobias Ullmann

The project aims to evaluate radar remote sensing data for Arctic tundra landscapes. Remote sensing is a good possibility to monitor vast uninhabited regions cost efficiently and near real time. Radar remote sensing is especially useful, as it operates independent from sunlight and is almost unaffected by clouds. However, good evaluation of the data is necessary as the interpretation of radar images is not intuitive. Zackenberg is an ideal place for validation of remote sensing data from tundra landscapes, as different tundra types are easily reachable. In addition, the ongoing monitoring of the weather conditions, the state of the vegetation and soil moisture give valuable information for the evaluation of the remotely sensed data.

To evaluate radar images, precise information about the vegetation cover, the near surface soil moisture and the surface roughness are necessary as these parameters all influence the radar signal. In summer and fall 2013, comprehensive mapping of the vegetation (more than 2000 GPS tagged photographs were taken) and soil moisture (more than 6000 measurements) was carried out. In addition, 60 biomass samples were taken at 20 different locations. The 2014 fieldwork took place in the first half of July and was follow-up work of the measurements taken in 2013. As the soil moisture conditions in 2013 were very dry, follow-up work was necessary to gather data under wetter conditions. In 2014, we found very wet conditions. Again more than 6000 soil moisture measurements were conducted (figure 6.13). Mainly, the locations of 2013 were revisited. In addition, the same locations were visited twice, before and

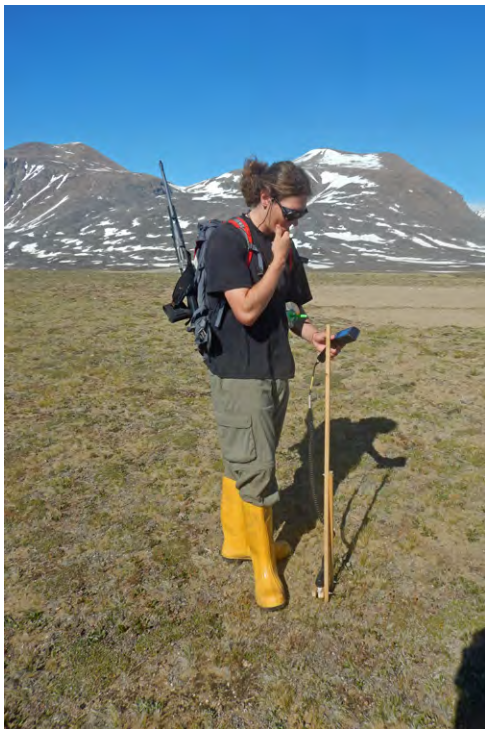

Figure 6.13 Soil moisture measurements. Photo: Alfred Wegener Institute, Germany 2014

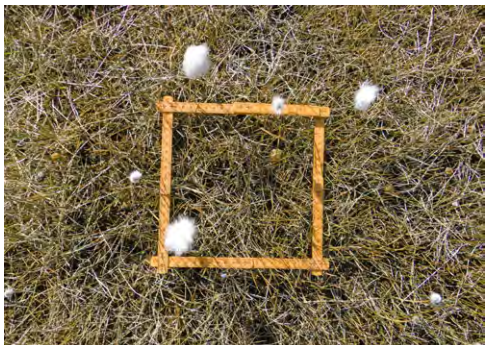

Figure 6.14 Two photographs show the location for biomass sampling at 74°27'41,8" N, 20°34'7,5" W at different dates a) 27.7.2013 b) 2.7.2014. The site was dry in 2013 and flooded in 2014. Photo: a) Alfred Wegener Institute, Germany 2013. b) Alfred Wegener Institute, Germany 2014.

after rainfall events, which allows monitoring if significant differences occurred in the soil moisture values of the first 12 cm of the soil column before and after rainfall events, or if the water was mainly trapped in the vegetation cover. All sites where biomass was harvested in 2013 were revisited in 2014 to take additional samples under the wetter conditions. However, only 10 of the 20 locations were dry enough for sampling, the other 10 locations were flooded. One example is shown in figure 6.14. To get a better idea of the surface roughness, photographs were taken for 3D modelling of different surfaces.

As the snow was not melted all over the valley at the beginning of July, the size and position of several snowfields were mapped in addition. This allows analysis of the accuracy of snow field size estimates based on time series of remote sensed radar images.

Ongoing analyses concentrate on relationships between the radar signal and the moisture patterns as well as the identification of moisture changes from time series of radar images. In a second step, the effect of the biomass water content, the vegetation structure and the surface roughness will be considered.

6.8 Climate effects in terrestrial arctic ecosystems in Young Sound, NE Greenland

Jacob Nabe-Nielsen, Oskar Liset Pryds Hansen, Minna Mathiasson, Lærke Stewart, Toke Thomas Høye, Cæcilie Gervin and Katrine Raundrup

The composition of arctic plant and arthropod communities is strongly linked to abiotic environmental factors (Karlsen and Elvebakk 2003; Drees and Daniëls 2009). Altitude and distance to the ocean can have particularly large impact on the communities through their influence on temperatures and precipitation patterns (Böcher 1979). The exact relationship between these key environmental variables and community compositions is, however, poorly understood in Greenland due to the scarcity of large-scale studies based on randomly selected plots. The objective of the current project was to investigate how the plant and arthropod community compositions changed along altitudinal and continentality gradients in Young Sound, Northeast Greenland. A secondary objective was to establish a large number of permanent plots in order to study the long-term impact of climate change on the plant communities.

Figure 6.15. The vegetation cover was low in most plots in Blæsedalen. Photo: Jacob Nabe-Nielsen.

A total of 180 permanent plots were established at two localities: An oceanic site by Blæsedalen (figure 6.15), at the eastern end of Young Sound, and Zackenberg, approx. 20 km further west. On each site the plots were placed in three groups of 6 plots at selected altitudes. The distance between the plots was fixed, and they were therefore randomly distributed with respect to environmental variables. In Zackenberg, plots were established up to 500 m a.s.l, in Blæsedalen only up to 300 m a.s.l (figure 6.16). For each plot the presence of plant species was recorded within a 2-m circle and pin-point analyses were conducted to determine the plant cover. Arthropods were sampled using yellow pitfall traps and malaise traps and collected along moisture and altitude gradients across vegetation types in Zackenberg and Blæsedalen.

The composition of the plant communities was strongly related to both altitude and degree of continentality. The way the most abundant plant species were distributed with respect to altitude in the two sites roughly fell in three categories: (1) The three most abundant species (*Salix arctica*, *Polygonum viviparum* and *Dryas* sp.) occurred in most plots at all altitudes on both sites (see *Salix arctica* figure 6.16). (2) Some species (e.g. *Luzula confusa*, *Stellaria longipes*, *Potentilla hyparctica* and *Alopecurus alpinus*) occurred in a far larger

Figure 6.16. Occurrence of selected species along altitudinal gradients in two study areas along Young Sound. A species can at most occur in 18 plots on a particular altitude. All plots were located at 20–300 m a.s.l. in Blæsedalen, up to 500 m a.s.l. at Zackenberg.

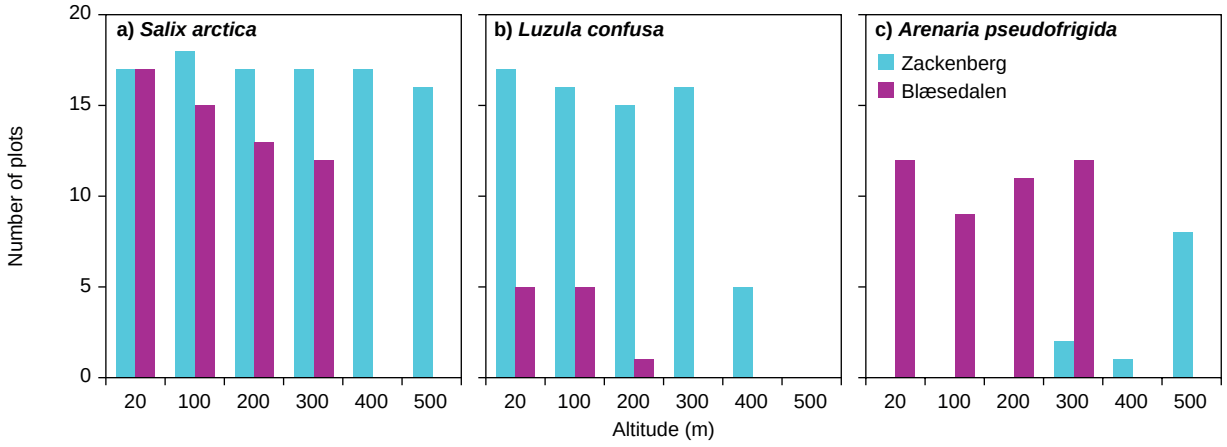

proportion of the plots in Zackenberg than in Blæsedalen (see *Luzula confusa* figure 6.16). (3) Some species (*Arenaria pseudofrigida*, *Festuca hyperborea* and *Poa glauca*) occurred at low altitudes in Blæsedalen, but mostly at higher altitudes in Zackenberg (see *Arenaria pseudofrigida* figure 6.16). For arthropods only butterflies from Zackenberg have been identified. All four butterfly species known to Zackenberg were found. The most common butterfly species (*Boloria chariclea*) was found in all habitat types, but abundantly at lower altitudes. *Colias hecla* and *Plebejus glandon* appeared to be more habitat specific (figure 6.17).

The occurrence of three different distribution patterns for the plants suggests that some species possess functional traits that allow them to become dominant in more protected areas, but to have lower survival in exposed oceanic areas (cat. 2). The plants that are found at low altitudes in Blæsedalen, but mostly at higher altitudes in Zackenberg (cat. 3) are likely to be poor competitors that survive better in more open plant communities (e.g. Blæsedalen; figure 6.15). The lower frequency of *B. chariclea* at higher elevations could be due to a later flight season at higher elevations. Identification of additional arthropod species groups and analyses of the association of plant and arthropod communities with particular climatic conditions or other abiotic factors are still on-going. A third site may be established in a more continental part of Young Sound in 2015.

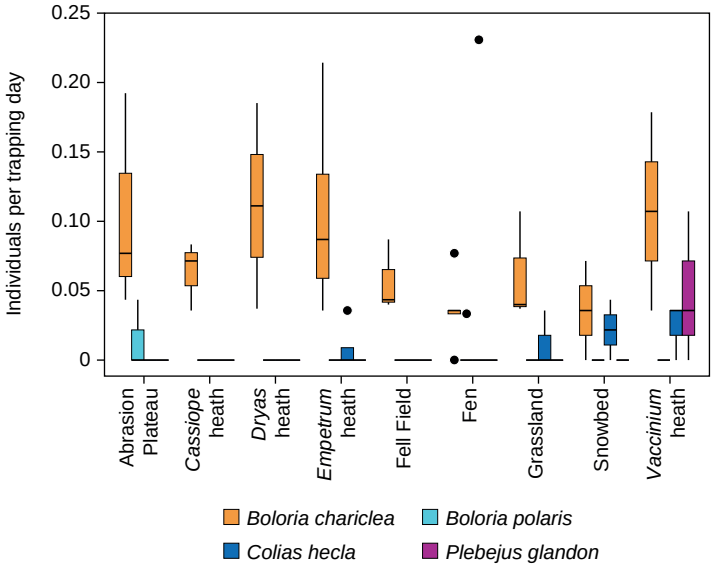

Figure 6.17 Butterflies trapped per day for each vegetation type in Zackenberg.

6.9 Multi-scale influences of elevation on arthropods in Zackenberg

Camille Ameline, Clémence Demay, Cyril Courtial, Philippe Vernon and Julien Pétillon

The International Network for Terrestrial Research and Monitoring in the Arctic (INTERACT) is currently funding the SPACEWOLF project (Spatial gradients in physiological adaptation and life history variation in Arctic wolf spiders). This project aims at (i) increasing the knowledge of ground-active arthropods (mainly spiders) ecology and (ii) investigating the effects of elevation and latitude on the fitness of wolf spiders (Lycosidae). To fulfil this goal, arthropods were collected in Iceland and in the Faroe Islands in 2012, in Kobbefjord in 2013 (Pétillon *et al.* 2014) and in Zackenberg from 5 to 12 August 2014. During this last sampling mission, 24 pitfall traps were set along with temperature loggers at 70 and 200 m a.s.l. on a north-facing slope (Zackenberg) and on a south-facing slope (Aucella), collecting a total of 416 arthropods. A few spiders (Aranea) were also collected on sight. All arthropods were identified to order or family level while a portion of the spiders were identified to species level.

On the south-facing slope, there were 281 individuals found in the six traps at 70 m and 52 individuals at 200 m while on the north-facing slope, there were 50 individuals found in the six traps at 70 m and 33 individuals at 200 m. Thus, on the south-facing slope, the abundance of arthropods at low elevation was more than five times the abundance at high elevation although on the north-facing slope, the difference does not appear significant. On the south-facing slope, the mean number of taxa per trap was 7.2 ± 0.3 at 70 m and 4.2 ± 0.9 at 200 m while on the north-facing slope, it was 3.2 ± 0.4 at 70 m and 3.3 ± 0.5 at 200 m. Thus, it appears that the diversity of arthropods is higher at low elevation than at high elevation on the south-facing slope while there is once again no significant difference on the north-facing slope.

We assessed the relative abundance of arthropods' taxa in figure 6.18. We can observe that there were Lepidoptera, Hymenoptera (Apocrita, Parasitica and

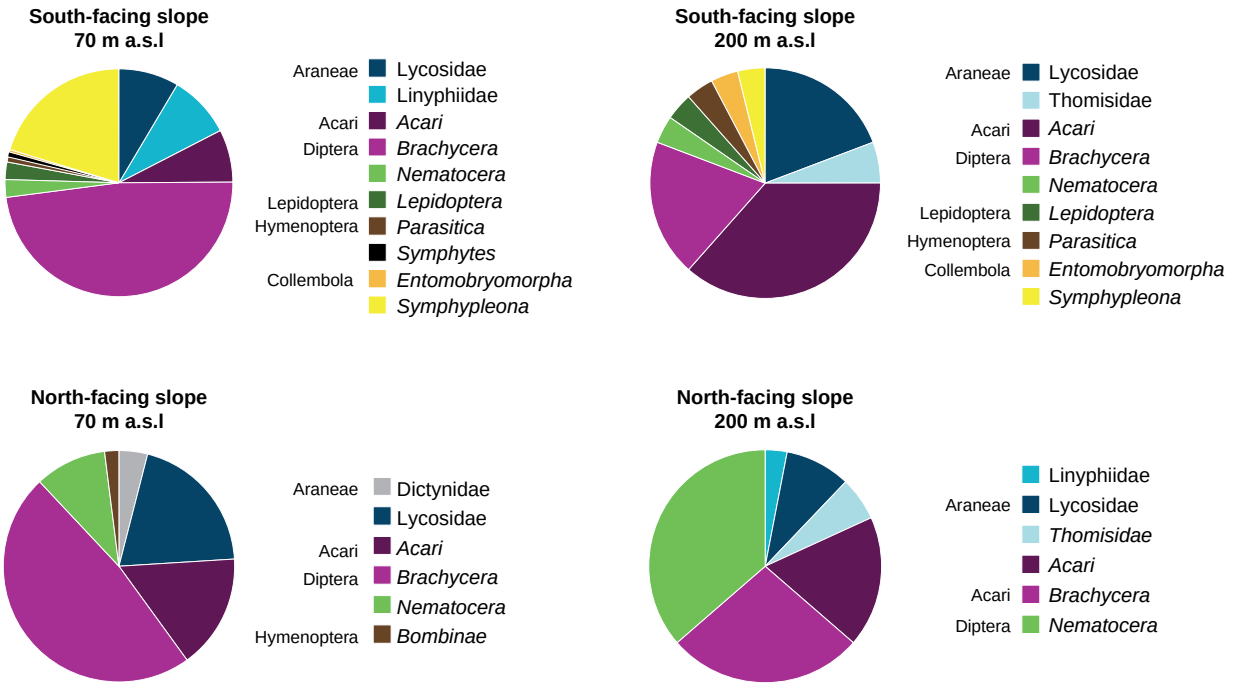

Figure 6.18 Arthropods' relative abundance in Zackenberg during August 2014.

Symphytes) and Collembola (Arthopleona, Entomobryomorpha and Symplypleona) on the south-facing slope while there was only one Hymenoptera (Bombinae) on the north-facing slope. We expected that there would be no Collembola on the north-facing slope because the ground was very rocky and there was little soil in the traps. If we exclude this last order, we can see that the three main orders at each site were Diptera, Araneae and Acari. Within the Araneae order, Lycosidae were found everywhere; Thomisidae were found on both slopes but only at 200 m; Dictynidae were found only on the north-facing slope at 70 m and Linyphiidae were found surprisingly on the south-facing slope at 70 m and on the north-facing slope at 200 m, which are very different habitats.

We identified six species of spiders. *Emblyna borealis*, *Collinsia thulensis*, *Pardosa glacialis* and *Xysticus deichmanni* were found on sight and in traps whereas *Meioneta nigripes* and *Hilaira vexatrix* were found on sight.

Given its abundance, *Pardosa glacialis* was collected on sight as 30 female individuals with egg sacs every 50 meters along an elevational gradient (0, 50, 100, 150 and 200 m a.s.l.) on the south-facing slope. Its mean body size (prosoma width) was of 2.60±0.15 mm and did not show any variation along the elevational gradient (Linear Least Squares Regression, F = 1.546, 149 df, R^2 = 0.003627, p = 0.2157) (figure 6.20a).

In the laboratory, the egg sacs were open, the eggs counted and measured. We could observe that a large part of the eggs were hatched. In figure 6.19 we can see that the proportion of hatched eggs decreases when elevation increases, which shows that there is a slight delay in hatching at higher elevations. We removed data from 200 m because on sight catching at this elevation was not done at the same time as the other ones. We did not use the mean volume of the eggs given the small number of

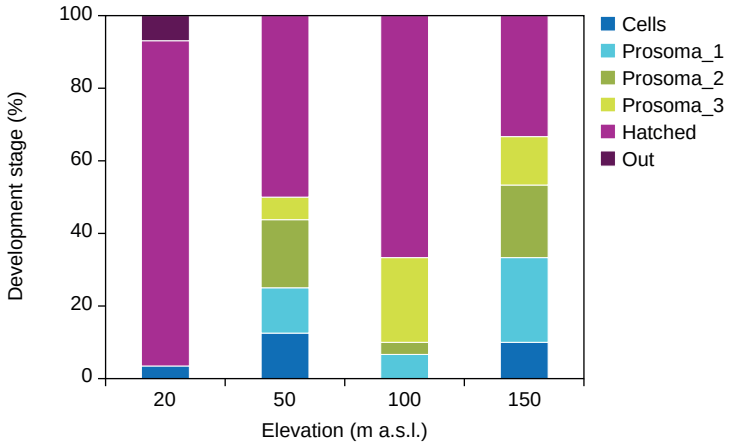

Figure 6.19 Development stage of Pardosa galcialis' *cocoon eggs in Zackenberg during August 2014. Thirty females with egg sacs were collected at each elevation. The different stages correspond to the development phase of more than half of the clutch in the cocoon. Cells: only cells are visible; prosoma_1: small legs are developed; prosoma_2: the prosoma is developed; prosoma_3: the prosoma is hatched; hatched: the pulli is hatched within the cocoon; out: the pulli is out of the cocoon.*

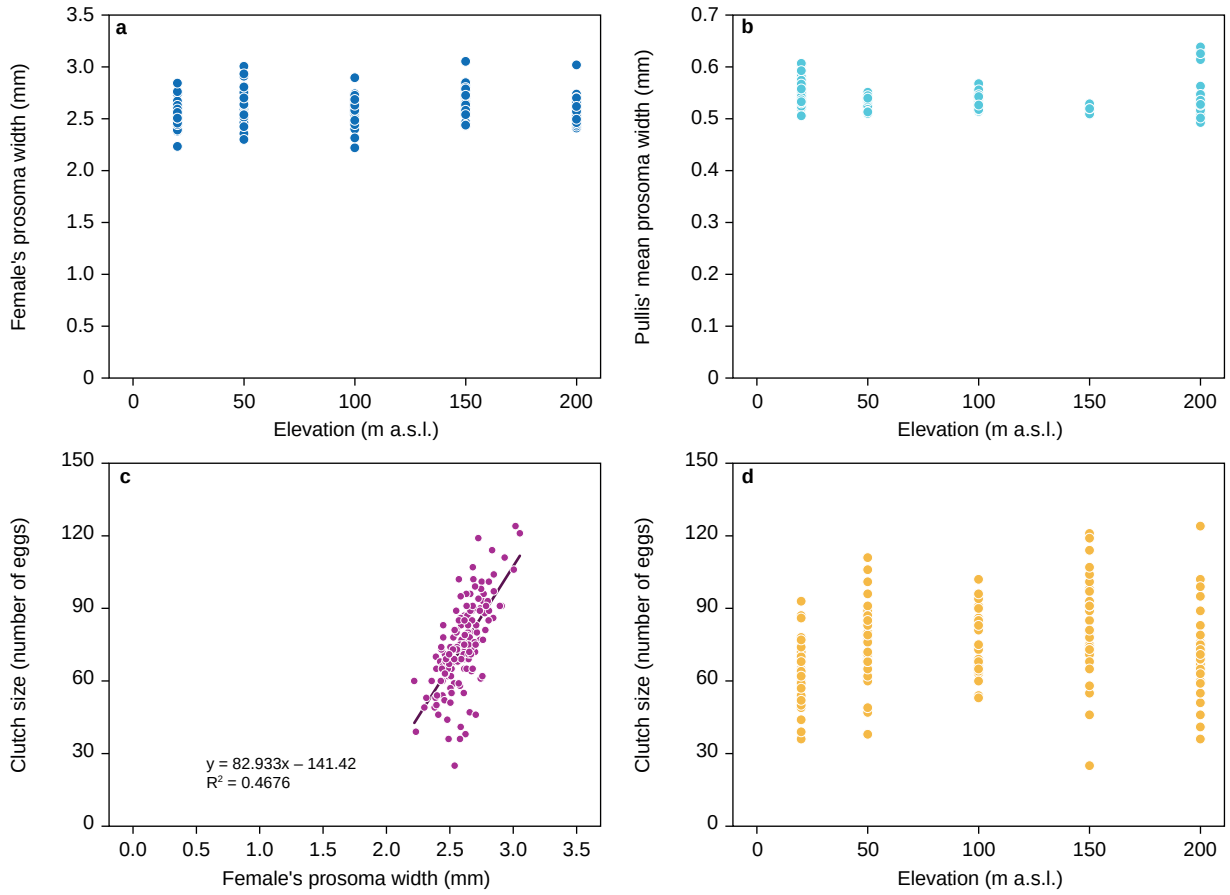

Figure 6.20 Fitness and reproductive traits of P. glacialis *in Zackenberg during August 2014. a. Size of the female along the elevational gradient. b. Mean size of the pullis along the elevational gradient. c. Clutch size in function of the size of the female. d. Clutch size along the elevational gradient.*

unhatched eggs. Instead we used the mean size of the pullis (prosoma width) which did not depend on the size of the female nor on elevation (ANCOVA, $F = 0.5364$, 97 df, $R^2 = -0.0141$, $p = 0.6584$) (figure 6.20b). Clutch size was for its part positively affected by the size of the female but not by elevation (ANCOVA, $F = 132.7$, 149 df, $R^2 = 0.4676$, $p < 2.2.10^{-16}$) (figures 6.20c and 6.20d). We suppose that the lack of reaction of the species when confronted to harder environmental conditions can be due to its enhanced ability to adapt to arctic conditions.

We would like to thank Oskar Hansen from Aarhus University, Department of Bioscience, Arctic Research Centre (ARC), for his help during the collecting session in Zackenberg.

6.10 Dissecting the interaction web of Zackenberg: targeting the pollinators of Dryas

Mikko Tiusanen, Helena Wirta, Bess Hardwick and Tomas Roslin

In 2014, we continued our long-term work on dissecting the interaction web of Zackenberg by multiple methods (cf. Várkonyi and Roslin 2013; Roslin *et al.* 2013; Visakorpi *et al.* 2014; Wirta *et al.* 2014, 2015). As a new initiative for this year, we applied our previously developed DNA-barcodes (see Wirta *et al.* 2013) to identify the relationship between pollinator diversity and a simple measure of ecological functioning: the seed set of an abundant plant, Avens in the genus *Dryas* (Rosaceae).

For pollination, it has been assumed that Avens relies on insects (Kevan 1972) – a hypothesis explicitly tested and supported by Visakorpi *et al.* (2014). Consequently, variation in the structure of the

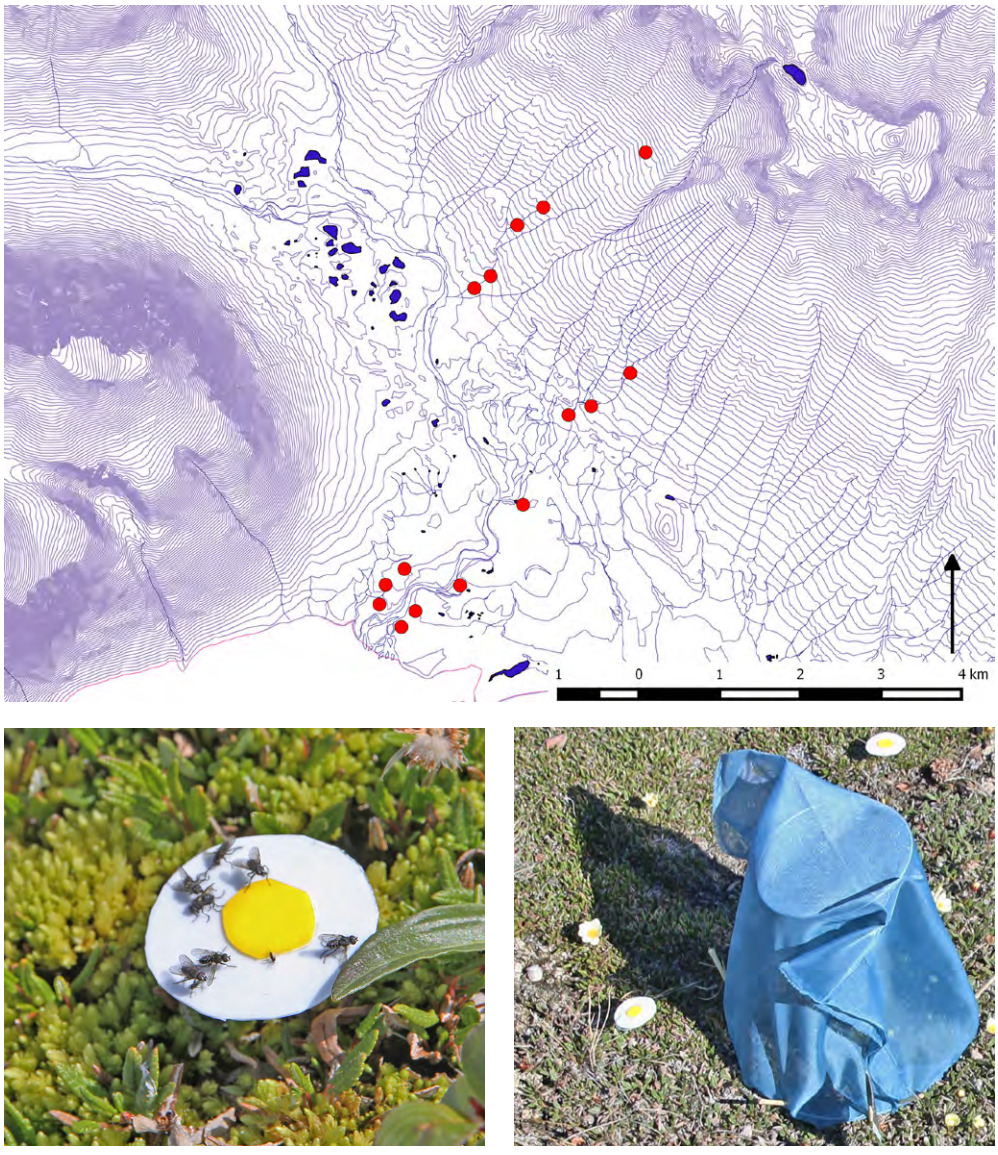

Figure 6.21 Experimental setup used to study the pollination biology of Avens, showing A) the distribution of sampling sites (red circles) across the Zackenberg valley and B) the trap flowers used to sample local pollinator communities. At each site, we deployed 100 such flowers across 15 sampling plots of 1 m² each. To record background seed production of Avens, we used C) cages of cloth to exclude all pollinators from a reference set of flowers in each plot. Photos: Mikko Tiusanen.

pollinator community has been hypothesized to reflect directly into variation in rates of Avens seed set (Kevan 1972). *A priori*, we may contrast several predictions of the patterns to be found. Based on general relations between biodiversity and ecosystem functioning (Cardinale *et al.* 2002; Cardinale *et al.* 2012), we may expect a decrease in species richness to result in impaired function (i.e. lower pollination rates). Such a relationship should result from both complementarity effects (where increased numbers of species use up available resources more completely, or mutually benefit from one another; Fridley 2001; Loreau *et al.* 2001; Loreau *et al.* 2002) and from straightforward sampling effects (where increased species richness leads to a higher probability of including particular functionally dominant species; Loreau and Hector 2001). As an alternative hypothesis, we may predict stronger effects of species identity than of plain species numbers: Previous work (Elberling and Olesen 1999; Schmidt *et al.* in prep.) suggest that the flies (superfamily Muscoidea) as the dominant group in the North may be more efficient pollinators than the midges (family Chironomidae) dominating the insect communities at lower latitudes. In this case, we predict higher pollination rates with a higher proportion of muscids in the local pollinator community.

To critically examine the association between pollinator community structure and the seed set of Avens, we used trap flowers developed in 2013 (see Visakorpi *et al.* 2014) to sample the local pollinator community across 15 sites varying in elevation, aspect and other physical features (figure 6.21). Overall, our sampling yielded a massive material of 8397 pollinators, of which many represent taxonomically challenging taxa. For species identification, we therefore relied on DNA-based techniques. Each individual was sequenced for the CO1 barcoding region, and its species identity determined by comparison to our previously established reference library (Wirta *et al.* 2013).

The material compiled in 2014 will now allow for a unique test of *a priori* predictions (Tiusanen *et al.* in prep.). Associations between pollinator community composition and *Dryas* seed set observed at the scale of the Zackenberg valley will also be compared to Pan-Arctic patterns observed in a large-scale collaboration among Arctic research stations, the Global Dryas Project (Anonymous 2014). Ultimately, by examining present-day associations between pollinator community structure and *Dryas* seed set, then combining them with projections of shifts in community composition with future climate change, we hope to predict impending changes in arctic pollination services.

6.11 Serial-sectioning applied to tundra shrubs for dendrochronological analyses in the high and low Arctic locations

Agata Buchwal and Grzegorz Rachlewicz

Tundra ecosystems and their important component, i.e. arctic shrubs, respond to climate change rapidly. Since shrubs can become old (more than 100 years old) and its annual ring growth registers valuable environmental information, dendrochronological studies on tundra shrubs are becoming more important in polar studies, gaining more attention especially in the last two decades. However, all studies conducted in the Arctic till now have indicated many problems in developing reliable chronologies, caused by discontinuous development of growth rings. Our findings from tundra shrubs studies from Central Spitsbergen show that there is high intra- and inter-plant variability in the annual growth pattern of shrubs (Buchwal *et al.* 2013). This is a common feature of Arctic shrubs, living on the edge of growth conditions of woody plants and this pattern has to be investigated much more in detail in order to understand growth strategies of tundra shrubs and their response to climate change.

The main goal of our study is to obtain the highest confidence in the annual date assignment of shrub growth rings in order to present reliable chronologies of tundra shrubs growing in both high and low Arctic locations. The goal will be achieved by dendrochronological and wood-anatomical studies on Arctic shrubs sampled in western (Disko Island, Kobbefjord) and eastern Greenland (Zackenberg). The analyses will be conducted on various species, mainly *Betula nana*, which is a shrub species represented in all three study sites and gives a great opportunity to study this species under various environmental and climatic settings. We are especially interested in how annual radial growth allocation of a dwarf birch vary between different geographical location between western (Hollesen *et al.* 2015) and eastern Greenland. Applying the method of detailed serial-sectioning, we will be able to trace intra-plant growth allocation pattern and obtain a high-resolution proxy, which can be correlated with the existing data (i.e. climate records) and finally form the base for dendroclimatological and dendroecological studies.

For this purpose in late July/early August 2014 we have sampled whole tundra shrubs in order to establish growth-rings chronology for shrubs in Zackenberg Valley. In total we sampled 30 individuals of *Betula nana* – whole shrubs (above- and below-ground plant parts) across the Zackenberg valley, i.e. in two major microsites were *Betula nana* individuals were spotted. Additionally we took 45 *Salix arctica* from the snow bed microsite and 16 *Dryas octopetala*, both as testing species for wood anatomical analyses. Additionally, in order to asses properties of plant habitats we took 20 soil and sediment (surface) samples from nine locations, representing all major plants' collecting sites.

First microscopic analyses revealed high growth rings irregularity repre-

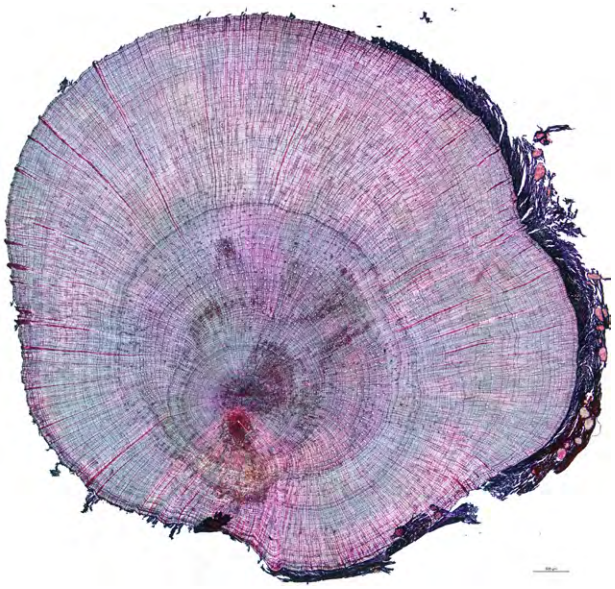

Figure 6.22 Cross-section of a stem of a around 106 years old dwarf birch (Betula nana) from Zackenberg valley. Diameter of a stem equals approximately 1 cm.

sented by frequent occurrence of missing and partially missing rings in *Betula nana* which confirmed the need of serial sectioning application and intra-plant cross-dating. Preliminary assessment of woody plant age revealed that some birch shrubs from Zackenberg valley are older than 100 years (figure 6.22).

Final stage of arctic shrubs radial growth investigation will focuse on a correlation of shrub chronologies and anatomical parameters with accessible climatic data from the ZERO station. Moreover, a correlation between the shrub chronologies from eastern and western Greenland will be performed, in order to determine climate induced species-specific growth responses of arctic shrubs.

6.12 Drone and dendroecological investigations of tundra change

Signe Normand, Sigrid Schøler Nielsen and Urs Albert Treier

Understanding the drivers of differential responses of different shrub individuals and shrub species to climate change across time and space is challenging. The aim of our fieldwork at Zackenberg and Blæsedalen (east of Daneborg) in July and August 2014 was twofold: (i) Using dendroecological analyses to understand the drives of wood anatomical variation as well as local recruitment and growth pulses of *Salix arctica*, and (ii) map the local distribution and diversity patterns of different shrub species across the landscape by the use of aerial imagery from drones (figure 6.23 and 6.24). Below we outline the background and collected data for each of these two endeavours.

Recruitment and growth are driving shrub expansion beyond current distribution limits in response to climate change. However, there is little knowledge on how shrub recruitment and growth vary across space and time, as well as between species. One reason for this is that previous dendroecological analyses have only investigated temporal changes based on few individuals from few species at few given locations. In a recent study, we applied a new approach showing that with a larger sample of individuals and species, signals of climate-driven recruit-

Figure 6.23 High-resolution visible and near-infrared images of vegetation in the Zackenberg valley. The white square and insert measure 80 x 80 cm.

ment pulses over time can be detected (Büntgen *et al.* 2015). Specifically, almost 900 individual plants from 10 shrub species were collected at Scoresbysund in 2012. Building on this approach, we developed for the fieldwork at Zackenberg and Blæsedalen in 2014 a stratified-random sampling strategy and collected many individuals of one species randomly across an altitudinal gradient. This sampling strategy allows us to detect and quantify growth and recruitment pulses across environmental gradients.

The dendroecological samples will also provide insight into another important question related to climate change: To which degree are shrub species able to modify wood anatomical features (e.g., vessel size and vessel grouping) and adapt to increasingly warm and dry conditions?

During our field campaign in 2014, we collected 490 *Salix arctica* plants in 30 plot groups distributed along altitudinal clines at 20, 100, 200, 300, 400, and 500 m a.s.l. In the Zackenberg Valley, we collected 295 plants from 18 plot groups and in Blæsedalen we collected 195 plants from 12 plot groups. The dendroecological analyses of these samples are currently being conducted.

Site-based surveys, e.g. plot-based vegetation surveys of species cover, diversity or dendroecological sampling, provide detailed, but spatially non-continuous information, which is suboptimal for understanding shrub dynamics at the landscape scale. Different shrub species have a different spectral signal and with high-resolution imagery taken from a drone, it is possible to map their distribution at the landscape scale. Furthermore, growth and recruitment pulses change the age-structure of the shrub communities. Thus, linked with the dendroecological investigations the high-resolution imagery might provide insight into potential landscape scale changes in shrub dynamics. Last, the distribution of ecosystem dominants, here shrub species, might be an important determinant of the local variation in species richness. This hypothesis will be tested by investigating the degree to which indices derived from the high-resolution imagery can explain local-scale variation in plot-based measurements of species richness.

During the fieldwork at Zackenberg and Blæsedalen in 2014, we used a quadcopter (MikroKopter, HiSystems GmbH,

Figure 6.24 Sigrid S. Nielsen collecting Salix arctica *in Blæsedalen, Urs A. Treier flying the quadrocopter at a Dryas dominated site in the Zackenberg valley, and Signe Normand preparing the drone flight plans at Blæsedalen.*

Germany) equipped with a SLR digital camera (Canon EOS 550D, Canon Inc., Japan) to collected imagery of 13 areas of approx. 5000 m² (100 x 50 m) at 0.5-1 cm pixel resolution. Each area covered 2-6 permanent vegetation plots at 20, 100, 200, 300 m a.s.l. From each area, we collected approx. 700 visible and near-infrared images (modified Canon EOS 550D camera only allowing wavelengths above 830 nm). Processing of these images is currently underway.

6.13 Mapping of the Zackenberg valley

Niels Martin Schmidt and Erik Lysdal

In August 2014, a project to map the central parts of the monitoring areas at Zackenberg was initiated. The Danish consulting company, COWI, was in charge of the actual mapping of the 75 km² area. Using a fixed-wing eBee drone, the project aimed at producing accurate, high-resolution data that would enable the development of 1) a precise digital terrain model (DTM) covering all 75 km², 2) a near-infrared (NIR), 10 cm GSD orthophoto and 3) a colour (RGB), 10 cm GSD orthophoto covering the same 75 km².

The project succeeded in collecting almost all data as planned, though a number of technical problems resulted in an extension of the project beyond the planned two weeks. A total of approximately 10.000 NIR images, of which about 90 % were suitable for processing, were taken. Approximately 7.500 RGB images were taken, of which 7.000 were suitable for processing. The difference in number of NIR and RGB images was mainly caused by snow fall events late in the season. Consequently, the DTM covers all 75 km², whereas RGB orthophoto only covers 50 km² (figure 6.25 and 6.26).

In addition to mapping the area using the drone, a total of 72 geo-referenced ground control points and 40 additional check points were to georeference the products.

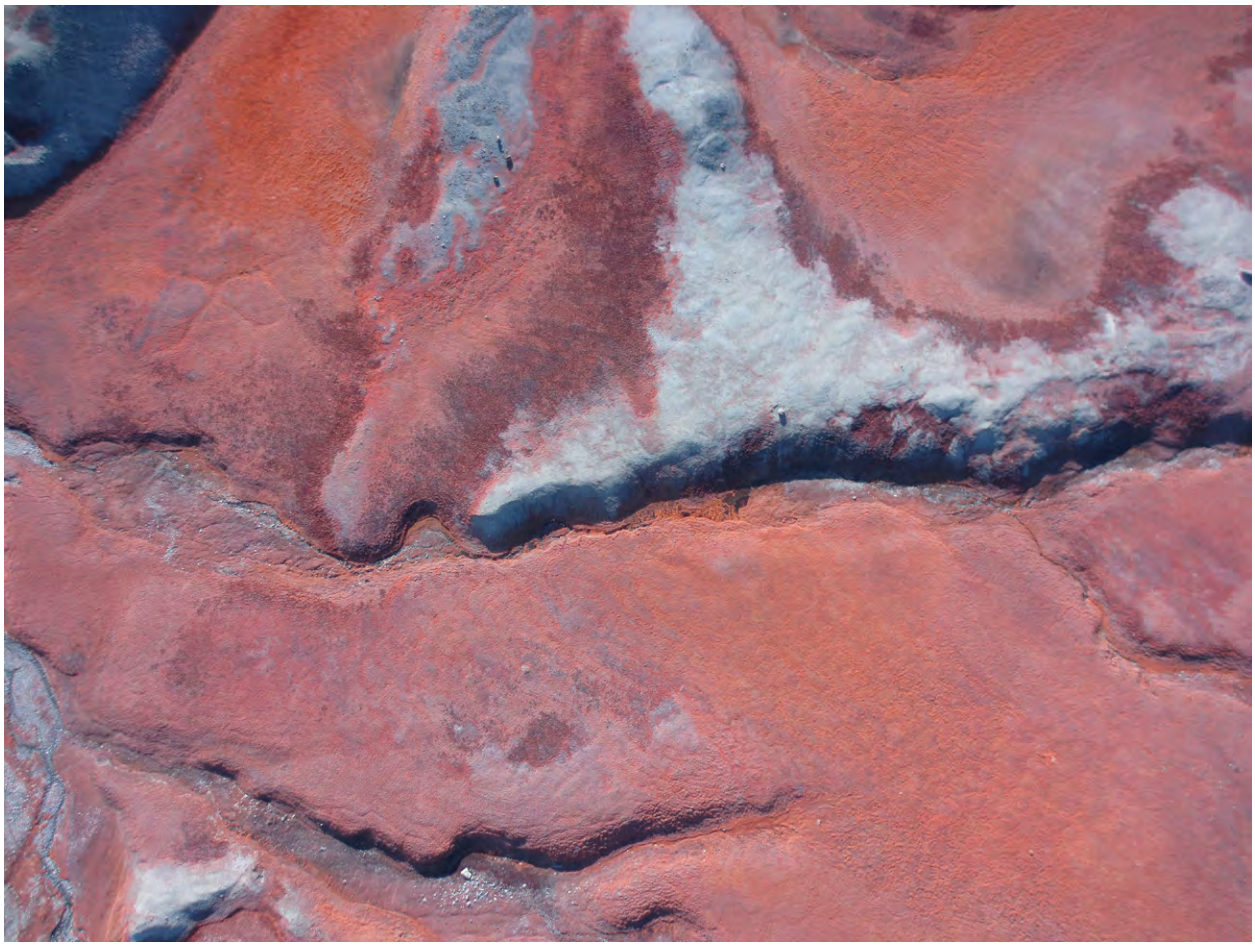

Figure 6.25 A section of the 10 cm/pixel near-infrared (NIR) orthophoto, showing the various vegetation types and three muskoxen (dark spots in blue area) on the slopes of Aucella.

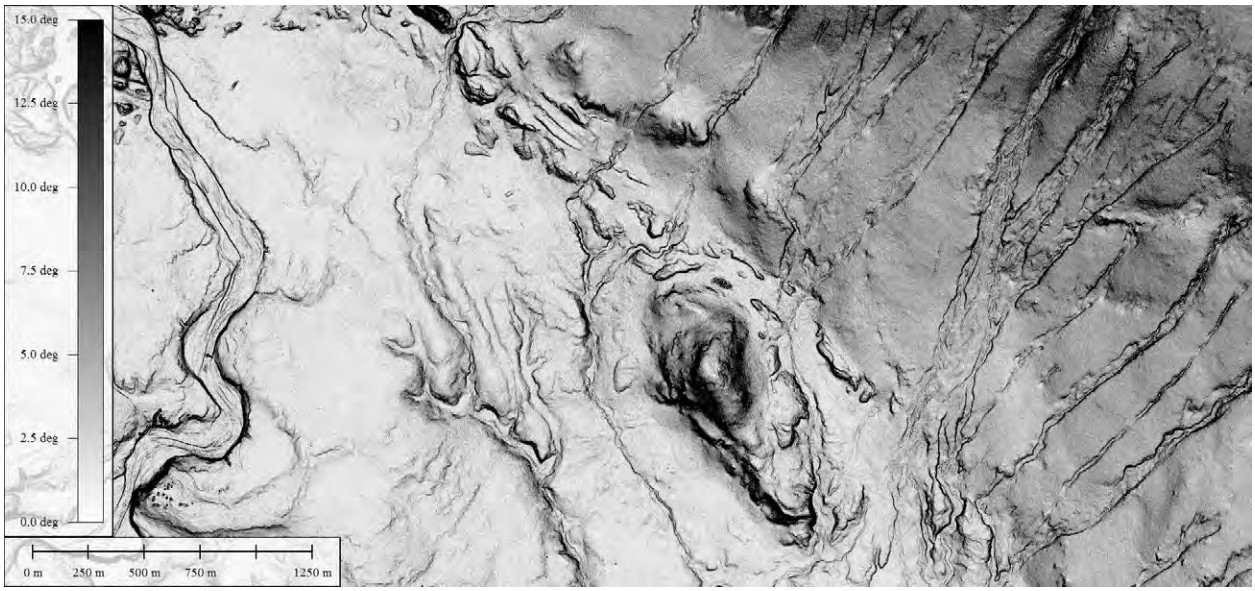

Figure 6.26 A slope/shade version of the high-resolution digital terrain model (DTM). The Zackenberg research station is just visible in the south-western corner.

Based on the data collected during the intense field campaign, the planned products have now all been finalized, and will be made available to scientists and others with an interest in the Zackenberg area through the GEM web site. In particular, an updated high-resolution DTM for the Zackenberg area has been long awaited, and will form the basis for a large number of research and monitoring activities in the area.

6.14 The migration of a sanderling between Northeast Greenland and Guinnea-Bissau tracked with a light-level geolocator

Jeroen Reneerkens, Tom Versluijs, Jesse Conklin, Moray Souter, Olivier Gilg, Jerome Moreau and Ron Porter

Most Greenlandic birds are migratory. Tracking individual birds for a full annual cycle may indicate essential stop-over sites (Gilg *et al.* 2013), determine ecological factors influencing bird migration (Both 2010; Tøttrup *et al.* 2012) or help to get accurate estimates of arrival date in the breeding area (e.g. Doll *et al.* 2015). As part of a study on sanderlings *Calidris alba* in Zackenberg to identify factors that may limit their population growth (e.g. Reneerkens *et al.* 2009; Ntiamoa-Baidu *et al.* 2014), ten male sanderlings were deployed with geolocators in 2013 (figure 6.27). We used 0.65 g geolocators, which log light level over time. Those data are used to estimate latitude (deducted from day length at given dates) and longitude (deducted from the moment of highest sun elevation per day; Bridge *et al.* 2011). Here, we report of the details of the first track of a sanderling from the Zackenberg Valley.

After deployment on 19 June 2013, the sanderling continued incubation for

Figure 6.27 Sanderling with geolocator attached to a plastic ring. The track of this particular bird is depicted in this contribution.

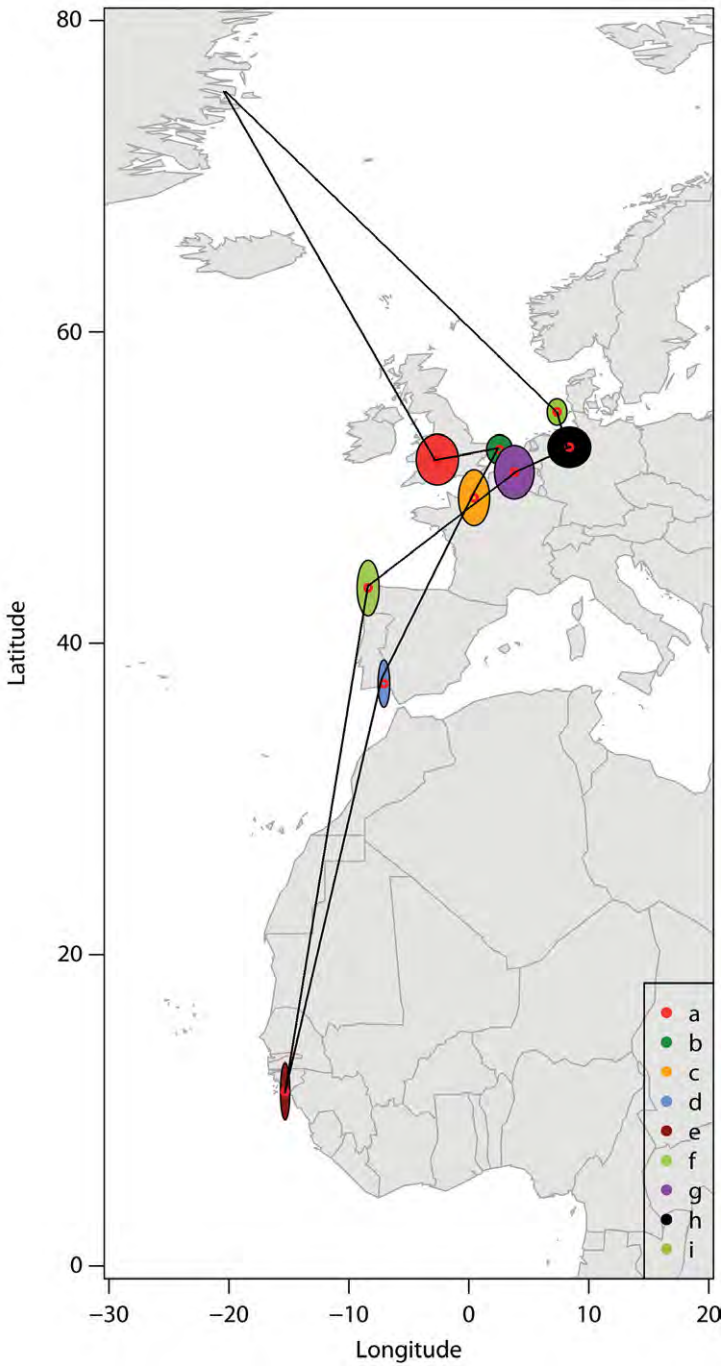

Figure 6.28 Year-round geolocations of a male sanderling deployed with a light-level geolocator in Zackenberg. Each coloured area indicates the average (red dot) and standard error (ellipse) of locations where the bird was located for at least three days in a row. See text for the periods during which the bird occurred in the given areas. The black line connects areas which were successively visited.

another 20 days and its chicks hatched on 9 July. It arrived in SW England, probably in the Severn estuary close to Bristol on 28 July (red ellipse in figure 6.28). The geolocator data suggest three distinct stopover sites, but with short flights of less than a day in between in NW Europe (England, and France; red, dark green and orange ellipses in figure 6.28) It left Normandy, France, on 18 August and flew southwards to an area close to Huelva in Spain (blue ellipse in Spain in figure 6.28) for a stay of 15 days between 26 August and 9 September. Taking these stopovers into account, the bird spent 53 days on migration after it left Zackenberg. Its winter destination in the Bijagós archipelago, Guinea-Bissau (southern dark purple ellipse in figure 6.28) was reached on 19 September. The wet/dry data suggest that the bird also stopped shortly on 11 September, but the location could not be determined with the light level data due to the equinox. The bird spent almost seven months in Guinea-Bissau until departure for spring migration on 10 May 2014. During northward migration it made several short stops along the northwest coast of Europe. The first stop was in northwest Spain along the coast close to Vigo (light green ellipse in figure 6.28) between 12 and 18 May. It then stayed along the coast of Belgium and Germany for four days each (purple and black ellipses, respectively, figure 6.28) until it reached the German or Danish Wadden Sea on 29 May (light green ellipse). It also stayed here for four days until it departed for a non-stop flight to Greenland. The geolocator recorded permanent light conditions on 4 June 2014, which is most likely the date of arrival in Zackenberg. With 26 days, northward migration was twice as short as southward migration. The bird was first seen in Zackenberg, paired with a female, on 13 June. The pair started incubation on 23 June, which is late relative to the arrival date. Due to cold and foggy weather in June 2014, snow melted slowly. This caused sanderlings to breed late and lay incomplete clutches. The average in 2013 was 3.2 eggs per clutch, compared to 3.7-3.9 in 2007-2013, suggesting that arthropod prey in the pre-breeding period limited females to lay complete clutches (c.f. Meltofte *et al.* 2006).

The track shows that a tropical wintering sanderling used multiple European staging sites during both southward and northward migration for a few days only. Furthermore, this individual spent twice as much time on southbound migration than on northward migration. The long time between arrival in the breeding area and clutch completion suggests that Arctic conditions may limit the onset of reproduction at least as much as conditions during northward migration. Future studies will indicate whether arrival time in Greenland depends on migration distance.

6.15 NUFABAR – Nutrient fluxes and biotic communities in Arctic rivers with different water source contributions

Catherine Docherty, Tenna Riis, Simon Leth, Alexander Milner and David Hannah

Arctic river ecosystems are influenced significantly by cryospheric and hydrological processes. Strong links are evident between atmospheric forcing, snow packs, glacier mass balance, stream flow, physicochemical habitat and biotic communities.

An understanding of the influence of altered snowmelt, glacier, permafrost and groundwater contributions to Arctic river flow and their effect on biotic communities is essential in the context of increased climate variability. Changes in water source contributions (deglaciation, reduced snowpack extent, greater rainfall/snowfall) and habitat conditions will be a major driver of shifts in the biodiversity of Arctic stream benthic communities with potential loss of beta diversity.

The principal aim of this highly interdisciplinary project is to evaluate the links in the process cascade between water source contributions, physicochemical habitat and stream biodiversity, and thus, develop tools to assess the vulnerability of Arctic river ecosystems to climate change.

Fieldwork was conducted in five streams near the Zackenberg field station for three weeks in July 2014. Streams were selected based on data collected during fieldwork in 2013. The field program included: (1) the collection of water samples to elucidate stream water source, and analysis of major ions, (2) the temporary installation of gauging stations to monitor stream physicochemical properties including water temperature, turbidity, dissolved oxygen and conductivity, (3) short-term nutrient releases and nutrient diffusing substrate experiments to quantify nutrient uptake and determine nutrient limitation in streams of different water sources and (4) sampling of benthic invertebrate communities.

Hypotheses to be tested were: (1) maximum alpha diversity will occur in streams with 40- 60 % meltwater contributions; (2) beta diversity will decrease with reduced inputs of meltwater and (3) the highest uptake of nutrients will occur in groundwater fed systems, (4) nutrient limitation of primary producers will be highest in streams most influenced by glacial run-off.

Our results indicate that winter water temperature of groundwater streams was less variable with higher temperatures than meltwater streams. All macroinvertebrate samples have now been identified. Chironomidae was the dominant taxon in all streams except one, where Oligochaeta were. Higher Chironomidae biodiversity and abundance were found in groundwater sourced streams compared to meltwater. Temporal differences in Chironomidae community structure were found within the same streams when comparing 2013 to the 2014 data potentially due to contrasting weather conditions between the two years (figure 6.29).

Most streams had no significant uptake of the added nutrients. This is most likely due to little biotic demand. In the groundwater stream (EZ-1), we found an uptake of both NH_4^+ and PO_4^{3-}, but no uptake of NO_3^- or NH_4^+ + acetate. In the meltwater stream (WZ-3) the uptake length of NH_4^+

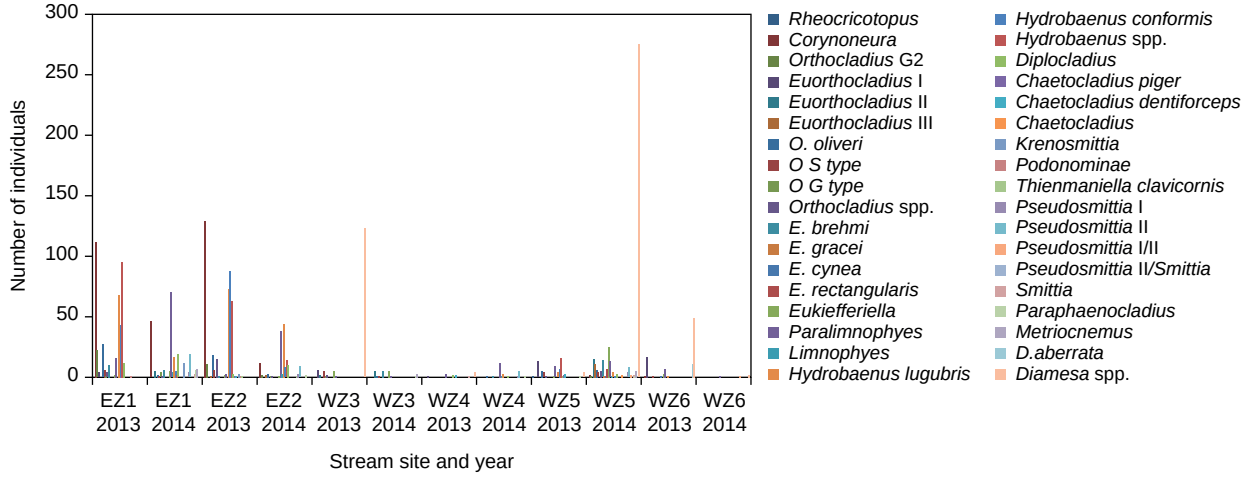

Figure 6.29 Shows chironomidae community structure in 2013 and 2014. EZ1 and EZ2 – the first four columns – are the predominantly groundwater sourced streams. The rest are predominantly meltwater sourced.

was approximately reduced by half, indicating heterotrophic uptake as the primary mechanism for the NH_4^+ uptake in this stream.

Nutrient diffusion substrate (NDS) was used to investigate nutrient limitation among algae in the biofilm. Results indicate that the two meltwater influenced streams sampled (WZ1 and WZ4) are limited by nitrogen and phosphorus, whereas in the groundwater influenced stream (EZ-2), primary producers in the biofilm were only limited by nitrogen.

6.16 Studies of arctic lakes and streams

Kirsten S. Christoffersen

There are plenty of small lakes and ponds as well as numerous streams in the Zackenberg Valley. These biotopes are in close connection with surrounding terrestrial environment and are important habitats for e.g. birds (figure 6.30). Freshwater ecosystems are integrated elements in the landscape and respond to geochemistry processes- lakes and ponds are often referred to as sentinels for disturbances such as climate change. A number of lakes and ponds have been surveyed with intervals of 1-5 years. Furthermore, two lakes (Sommerfuglesø and Langemandssø) have been sampled 4-6 times for water chemistry and plankton during the ice-free period (July/August) as part of the BioBasis-programme (see chapter 4).

A research project "Ecology of Arctic lakes", funded by University of Copenhagen, has been running for some years to provide data of the day-to-day dynamics in these two lakes. Both lakes are equipped with data loggers that continuously record temperature, light and oxygen on a daily basis year round (figure 6.31). Such data series from the high Arctic are needed in order to better understand the dynamics that set the living conditions for plankton, invertebrates and fish.

Figure 6.31 Various data loggers and other sampling devises that are placed at the lake bottom for up to 12 months. Photo: Kirsten S. Christoffersen.

Data from most of the sensors deployed one year ago in Langemandssø and Sommerfuglesø respectively were successfully retrieved at the beginning of September 2014. It appeared that annual patterns in temperature and light followed the trends seen in previous years. This included a rapid cooling of the water column to 1-2 °C during September when the ice cover was established and a slight increase from October due to the heat capacity in the sediment. Meanwhile the light was disappearing and by the end of October no light can be recorded. The temperatures in the water column remained low during the entire winter and started to increase in May-June while the lake was still ice covered but snow had melted and light was becoming more powerful.

For the 2013-14 season it has also been possible to get information about the oxygen concentration in both lakes. Unfortunately the sensor in Langemandssø lost power during December, but the data that were present showed surprisingly high

Figure 6.30 Many birds use lakes and ponds for feeding, breeding and protection from enemies. Photo: Kirsten S. Christoffersen.

Table 6.2 Basic conditions of four streams sampled in the beginning of September 2014.

Locality	Main water source	Position	Altitude (m a.s.l.)	Temp. (°C)	Conductivity (µSi cm^{-1}, 20°C)	pH	Width (mean m)	Depth (mean m)	Current (mean m s^{-1})	Macropyte/ Moss
Aucella elv	Glacier	74°29'38"N; 20°34'33"W	64	0.1	869	7.3	1.88	0.06	0.2	none
Vestelven	Mixed; lake, snow	74°28'09"N; 20°36'58"W	20	1.7	93	na	3.32	0.17	na	none
Kærelven	Mixed; glacier, snow	74°28'30"N; 20°31'41"W	33	0.3	286	6.83	2.24	0.09	0.29	none

oxygen concentrations (14-15 mg l^{-1}) from September to December. This lake holds a population of Arctic char and good oxygen conditions are vital for the fish. On the contrary, the more shallow lake Sommerfuglesø went from well-oxygenated waters (12-14 mg l^{-1}) in September to no detectable oxygen from the beginning of November 2013. This condition lasted until the heavy snow layer melted and ice-cover broke up at end of June 2014. Within a week, the entire water column had regained high oxygen concentrations. Obviously this lake is not suited for a permanent fish population.

All data loggers were cleaned, repaired and recharged before deployed in the lakes before the freeze over. A new sampling period of one year is expected to bring series of temperature, light and oxygen which combined with daily photographs from surveillance cameras of the ice and snow cover on the lakes will allow further analyses of the patterns seen until now.

The lake project was extended with a pilot study of basic conditions in several streams that are close to the areas with lakes and ponds. The rationale for this is to provide insight into the connections between still and running waters as well as to obtain a general knowledge about streams in the area. At present no streams are monitored in the Zackenberg Valley but it appears obvious to include such ecosystems in the future as streams are likely to reflect the melting of glaciers and thawing of the permafrost. The activities in 2014 included four streams (table 6.2) that at the time of sampling (September) are fairly shallow and with low velocities. Apart from basic physical and chemical measurements, biological samples were taken. This included benthic invertebrates by Surber sampling as well as phytobenthos (chlorophyll). The samples are currently being analysed.

6.17 Young Sound fjord physical oceanography: under-ice dynamics and coastal polynya interaction

Igor Dmitrenko, Sergei Kirillov, Wieter Boone, Vlad Petrusevich, Søren Rysgaard and David Babb

An oceanographic field campaign was carried out from 30 April to 8 June 2014 to assess the influence of ice-related processes for the hydrography of Young Sound. Several along-fjord transects were executed to determine the vertical structure of temperature, salinity and dissolved oxygen (figure 6.32). These data, supplemented with measurements from three ice-tethered moorings, that were deployed in October 2013 and samples of the water column, allowed us to characterize the fjord water dynamics, brine production in the polynya in front of the Young Sound, ice growth rate, carbon dynamics and ice-ocean heat flux during winter. A detailed description of the fieldwork can be found in Dmitrenko *et al.* (2015).

The description of a two-layer circulation pattern was one of the major results obtained from our analysis of the velocity current profilers which we deployed at several locations along the fjord. A local vertical circulation cell is characterized by outflow at the surface and inflow at the intermediate depths. Though this pattern was stable throughout the entire winter, the winds favourable for polynya formation in the Young Sound mouth strongly enhanced the circulation cell from December to March. Thermodynamic ice formation under cold air temperatures combined with continuous removal of ice by northerly winds resulted in a very efficient polynya driven ventilation of the fjord: the salty and oxygen enriched water from the polynya were transported

Figure 6.32 Sampling of vertical CTD profile. Photo: Søren Rysgaard.

into the subsurface layer of the inner fjord (Dmitrenko *et al.* 2015). The average outflow velocity over the surface layer was ~2-4 cm/s which is two times greater than the average inflow velocity in the subsurface (40-80 m) layer of ~1-2 cm/s (figure 6.33). Characterization of the polynyas induced circulation cells is important for our understanding of role of sea ice formation in the carbonate system.

More research was done on the impact of ocean heat on the ice growth rate. The large amount of solar heat accumulated in the water column impacts the ice growth rate and results in sufficient ablation of seasonal landfast ice. The heat content in the outer and inner fjord attained by the end of October 213 and 407 MJ m^{-2}, respectively. A majority of this heat was lost during winter, with a reduction of 193

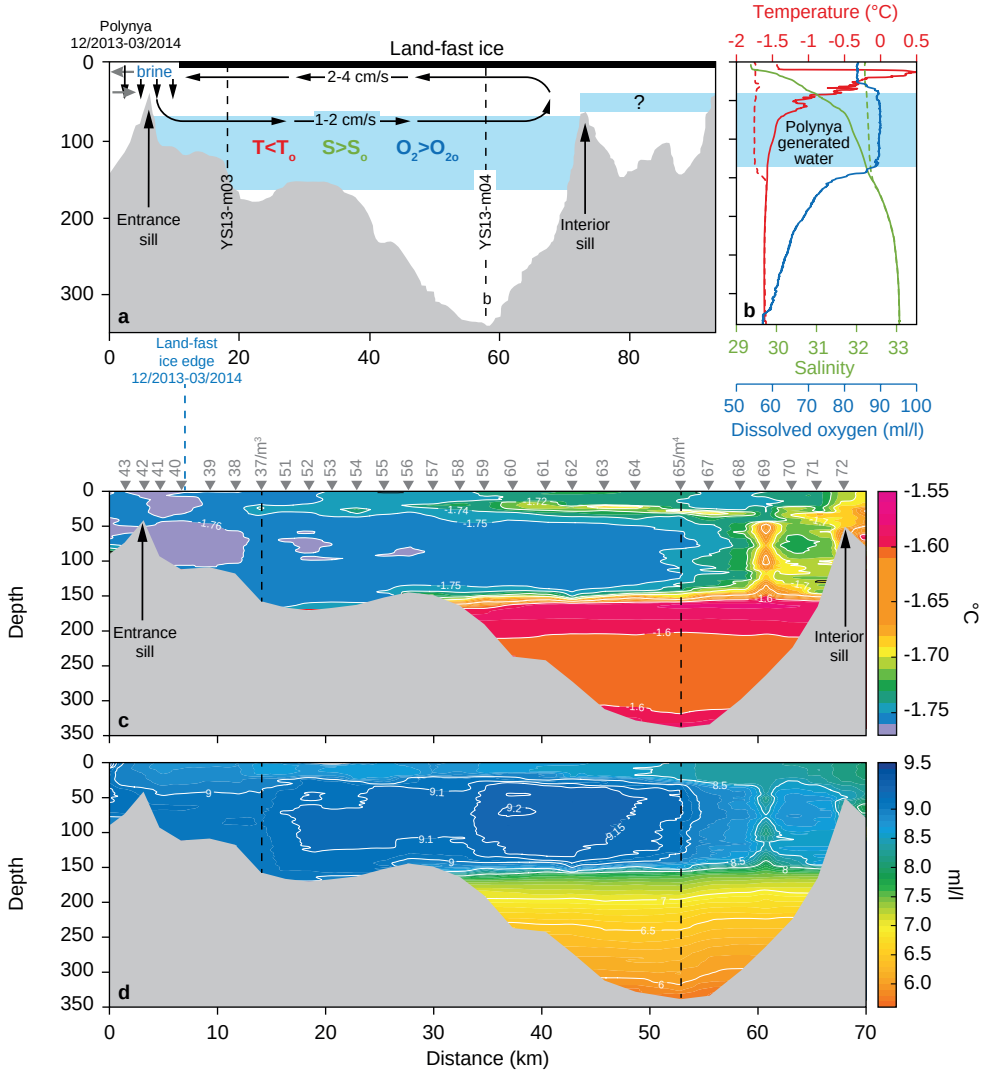

Figure 6.33 a) Schematic depiction of polynya impact on the Young Sound circulation. b) Vertical distribution of temperature (red, °C), salinity (green) and Dissolved Oxygen (blue, ml l-1) on 26 October 2013 (solid lines) and 5 May 2014 (dashed lines) at mooring YS13-m04. (c-d) The along-fjord transect of temperature and Dissolved Oxygen (adopted from Dmitrenko et al. 2015).

and 354 MJ m^{-2} between October and May (figure 6.34). The highest impact of this heat loss on ice growth is evident from late October to February-March when differences between the water temperatures and freezing point were up to 0.7 °C. Our results showed that the ocean heat flux strongly affects the seasonal ice thickness and causes 39 and 26 cm of sea ice ablation in the outer and inner fjord (Kirillov *et al.* 2015).

We gratefully acknowledge the support by the Canada Excellence Research Chairs (CERC) and the Canada Research Chairs (CRC) programmes. This work is a contribution to the joint Arctic Science Partnership collaboration.

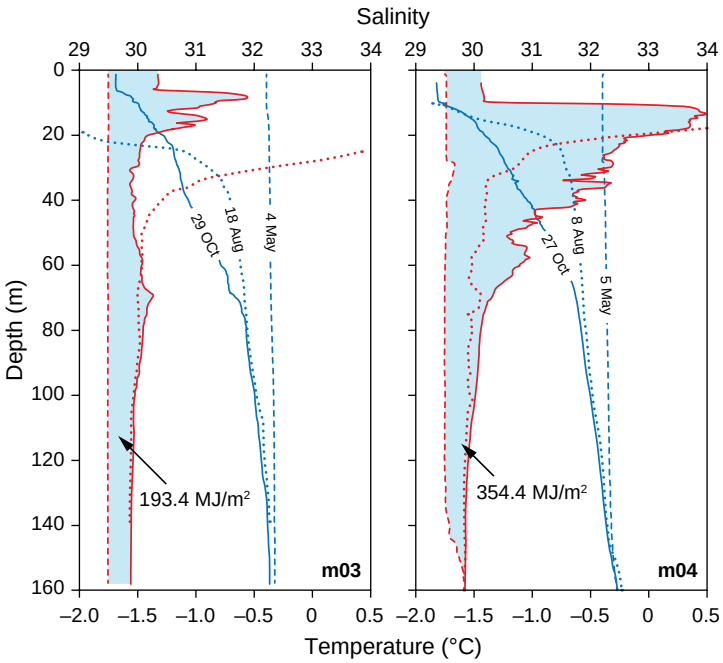

Figure 6.34 Vertical distribution of temperature (°C, red) and salinity (blue) in August 2013 (dotted lines), October 2013 (solid lines) and May 2014 (dashed lines) in the outer (left) and inner (right) Young Sound. Shaded areas indicate the changes of temperature from October to May (from Kirillov et al. 2015).

6.18 Melt ponds on Arctic sea ice as 'pumps' for the delivery of Current Use Pesticide (CUP) to the Arctic Ocean – a Young Sound case study

Monika Pućko, Alexis Burt, Gary Stern, Liisa Jantunen, David Barber and Søren Rysgaard

In the past, sea ice has been thought of as a physical barrier to the airborne delivery of organic contaminants (OCs) to the Arctic Ocean and a complete deterrent to the gas flux between seawater and air (Hargrave *et al.* 1997). However, based on α-HCH studies as a process tracer (Pućko *et al.* 2012), Current Use Pesticide (CUP) concentrations and calculated fluxes at the ocean-sea-ice-air (OSA) interface in the Beaufort Sea in the summer (Pućko et al. 2015), we have postulated that first-year sea ice (FYI) likely plays a profound role as a facilitator of the delivery of OCs to Arctic food webs through loading into melt ponds and their subsequent drainage. The efficacy of the process depends greatly on the ice type present, specifically FYI *versus* multi-year ice (MYI). While MYI presents a weak brine engine (low content of salts in the brine fraction) with transient, relatively fresh melt ponds that refreeze in winter, FYI forms widespread melt ponds containing greater quantities of brine, and the water in these ponds enters the surface ocean as the ice rots through during summer.

The process of atmospheric loading of contaminants to surface meltwater and their subsequent drainage to the Arctic Ocean can be described as a 'pump' that transfers contaminants from the atmosphere to an ice-covered ocean via pond meltwater (figure 6.35). To determine the significance of this contaminant input route to the Arctic Ocean, we calculated the total quantity of various CUPs that would be delivered to the surface seawater of the Beaufort Sea in 2008 via melt pond leakage into the ocean compared to the standing stock of CUPs held in the mixed layer of the Beaufort Sea. The total amount of CUPs discharged to the Beaufort Sea with surface meltwater drainage was calculated to be 6 kg for dacthal, 16 kg for chlorpyrifos, 6 kg for endosulfan I, and 54 kg for chlorothalonil. The hypothetical contaminant 'pump' could, therefore, deliver approximately 2 % of dacthal, 4 % of chlorpyrifos, 10 % of endosulfan I, and 4 % of chlorothalonil annually relative to the standing stock in the polar mixed layer (40 m). More importantly, however, we observed that concentrations of some CUPs in melt ponds were up to 20 times higher compared to those recorded at the ice-seawater interface giving rise to increased biological exposure during the Arctic I.C.E. field campaign (Resolute Bay, NU, Canada 2012; Pućko *et al.* 2015, in

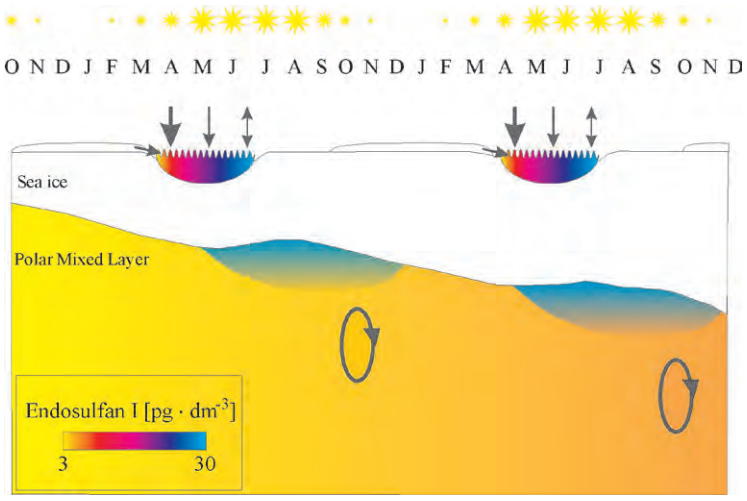

Figure 6.35 Hypothetical contaminant pump functioning schematic using endosulfan I as an example; colours denote endosulfan I concentrations in melt ponds and seawater (from Pućko et al. 2015).

preparation). Presence of ice cover with melt ponds was also proven to increase the flux of some CUPs (e.g. dacthal) from the atmosphere to the ocean by almost two times compared to the open-water scenario over the duration of pond-covered ice presence in the Resolute Passage, Canadian Archipelago (Pućko *et al.*, in preparation). The work done in 2014 at Young Sound compliments and builds on our past knowledge of contaminant behaviour in sea ice environments from projects done in the Beaufort Sea (2008/09) and in Resolute Bay (2012).

In our study period (22 May – 2 July 2014), we monitored air, snow pack, surface meltwater, and seawater at the ice-ocean interface and 5 m for concentrations of CUPs (e.g. dacthal, trifluralin, chlorpyrifos, PCNB, chlorothalonil) and legacy OCPs (e.g. HCHs, chlordanes, endosulfan, dieldrin). Samples were taken every three days, along with snow, surface meltwater, seawater and ice physical variables such as temperature, salinity and oxygen isotopic composition ($\delta^{18}O$).

The transition from perennial to annual ice in the Arctic is changing the role of sea ice in contaminant pathways; we propose that for some chemicals this has meant a shift from inhibiting the transport of atmospheric contaminants into the ocean surface to facilitating such transport. With an increasing percent coverage of the Arctic by FYI relative to old ice, a hypothetical contaminant pump will be turned on over vast areas of the Arctic Ocean with as of yet poorly understood consequences. Almost certainly, this sort of climate change will complicate the interpretation of contaminant trends measured in marine biota. Transition towards a FYI-dominated summer Arctic may, therefore, result in an over 40 % increase of efficacy of the melt pond hypothetical contaminant 'pump' due to complete melting of ice each year, and a greater volume of meltwater due to higher air temperatures and increased precipitation. In such a scenario, however, the importance of atmospheric deposition of OCs to the surface meltwater will depend on the length of time meltwater will have to accumulate contaminants from the atmosphere before complete thawing takes place, again, a climate change parameter of significance.

6.19 Case Study: Seasonal transition of geophysical parameters of ice types present in Young Sound, NE Greenland

David Babb, Satwant Kaur, Geoffrey Gunn and Kerri Warner

In early May 2014 as part of the collaborative Arctic Science Partnership (ASP), some researchers from the University of Manitoba travelled to the research house in Daneborg, Greenland to participate in a late spring/early summer field campaign. This project was part of a collaborative research campaign between the Arctic Research Centre (ARC), Greenland Institute of Natural Resources (GINR) the Centre for Earth Observation Science (CEOS) and others studying marine biology, marine chemistry, sea ice geophysics and atmospheric exchanges.

The objective of this research was to gain a better understanding of the geophysical and thermodynamic processes at the ocean-sea ice-atmosphere (OSA) interface as the snow melt, melt pond evolution and sea ice breakup periods occurred. The Daneborg Research Station was ideally situated to study sea ice and monitor the thermodynamic and geophysical response throughout the transition from cold winter ice to breakup. The project focused on analysing the geophysical properties of snow and sea ice, coincident meteorological and remote sensing data; ultimately leading to increased knowledge of how remote sens-

ing signatures respond to various features in young ice types during the seasonal transition from winter into summer.

During this project, we monitored the progression of the geophysical and thermodynamic processes occurring at the ocean-sea ice-atmosphere (OSA) interface as the snowmelt began, as melt ponds evolved and just prior to the sea ice breakup occurred. We chose two sites in the fjord (figure 6.36): one towards the mouth, Hans, representing younger sea ice (as a result of a polynya) and the second further inside the fjord, Gael, representing thicker first year ice (FYI). Not only did we collect data for analysing how the surface albedo changed during the melt progression (every 5 m in a 100 m transect at both Hans and Gael), but we also measured the geophysical properties of snow with density and temperature profiles at both sites, sea ice with temperature and salinity profiles at both sites (figure 6.37) and combined this with coincident meteorological data measured from the met site (figure 6.38) including temperature, wind speed, direction, humidity, pressure and albedo. Unfortunately due to warm temperatures and no access to a cold lab (set to –18 °C), we were unable to do any microstructure measurements of sea ice. The collection of the physical properties of the snow and ice are important for scientists studying the biology of the ice and surface water, the contaminants, the $C0_2$ flux occurring between the OSA interface, as well as scientists studying signatures from various remote sensing platforms to gain a better understanding of how the signatures respond to melt.

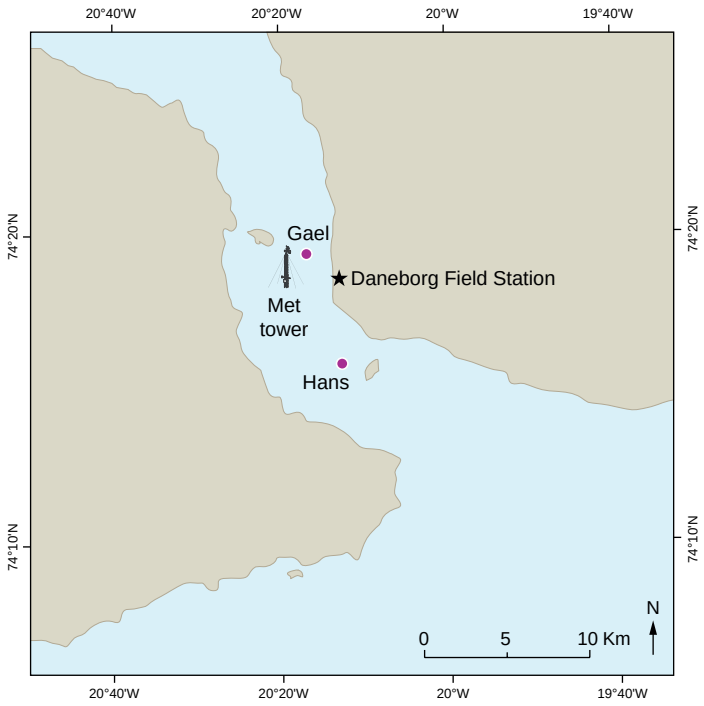

Figure 6.36 Map displaying two study sites (Hans and Gael), the meteorological tower site and the Daneborg Research Station. Photo: Geoffrey Gunn.

Figure 6.37 Ice team physically sampling sea ice (Nix Geilfus: ARC, Alexis Burt and Kerri Warner: CEOS). Photo: Bruno Delille.

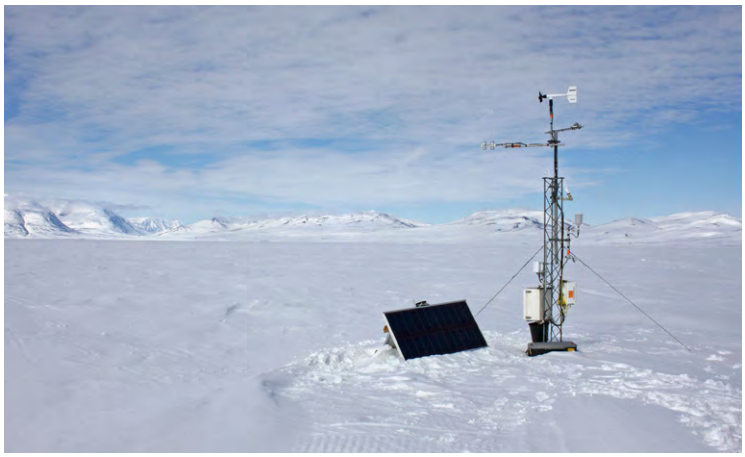

Figure 6.38 Meteorological station in Young Sound (measuring temperature, wind speed, direction, humidity, pressure and albedo).

6.20 Greenhouse gases dynamics on landfast sea ice in Daneborg, NE Greenland

Geilfus Nicolas-Xavier, Ryan Galley, Odile Crabeck, Kerri Warner, Bruno Delille, Marie Kotovich and Søren Rysgaard

Methane (CH_4) and its oxidation product (carbon dioxide, CO_2) are both greenhouse gases with atmospheric concentrations of 1.9 and 397 ppm, respectively. The CH_4 global warming potential is 28 times higher than that of CO_2 over a 100-year time frame, and both atmospheric concentrations are increasing. While the Arctic Ocean represents an important sink for

atmospheric CO_2, with current estimates of net air-sea CO_2 fluxes from –66 to –199 Tg C yr^{-1} (Bates and Mathis 2009; Takahashi *et al.* 2009), the Arctic Ocean also represents a source of CH_4 with current estimates of up to 8 Tg C yr^{-1} (Parmentier *et al.* 2013). However, for long sea ice has been perceived as an impermeable layer impeding the air-sea gas exchanges (Tison *et al.* 2002). Therefore, the role of sea ice is still poorly understood (e.g. Parmentier *et al.* 2013).

Recent studies suggest that sea ice plays an active role in the air-sea exchanges of CO_2 through its control of the partial pressure of CO_2 (pCO_2) of surface water by the sea ice pump (Rysgaard *et al.* 2011; Delille *et al.* 2014). This sea ice pump exports atmospheric CO_2 to the deeper water through processes that are inherent to the formation and melting of the sea ice cover, as well as chemical mechanisms within the sea ice. Sea ice has also been suggested to act as a transient layer for CH_4 release from the sub-sea permafrost, therefore controlling the exchange of CH_4 between the atmosphere and the ocean.

Our understanding of CO_2/CH_4 dynamics during the sea ice melt season and the importance to the annual exchange of CO_2/CH_4 across the atmosphere-sea ice-ocean interfaces is incomplete. As the ice warms up and becomes permeable, abrupt changes occur for both CO_2 and CH_4. Sea ice concentration of CH_4 decrease due to oxidation within the sea ice itself and/or the release of CH_4 bubble into the atmosphere (Zhou *et al.* 2014; Crabeck *et al.* 2014). The internal ice melt promotes the brine dilution and a decrease of the brine pCO_2, which can be further enhanced by the increase in TA associated with the ikaite dissolution (Geilfus *et al.* 2012; 2014a,b). These favourable conditions will turn the ice into a sink for atmospheric CO_2 (Nomura *et al.* 2010; Geilfus *et al.* 2012; Nomura *et al.* 2013; Geilfus *et al.* 2014a,b). However, the net impact of the sea ice melt on the oceanic uptake of atmospheric CO_2 or CH_4 release remains largely uncharacterized, despite the fact that they are a major and increasing surface feature of Arctic sea ice during spring and summer (Rösel and Kaleschke 2012).

In Daneborg, NE Greenland, a nine-week field project was conducted from mid-May to early July 2014 to study CO_2 and CH_4 dynamics on landfast ice inside the fjord. An international team of 7 scientists worked toward the main objective focusing their efforts on the following sub-projects:

- Sea ice and snow geophysics and thermodynamics during the spring/summer melt
- CO_2/CH_4 dynamics in landfast sea ice during the spring/summer melt
- Evolution of the melt ponds' formation and its impact on the CO_2/CH_4 dynamics
- CO_2 fluxes across the ice-atmosphere interface

The main objective was to examine how melting snow and sea ice and the associated formation of melt ponds affect CO_2/CH_4 dynamics therein and the air-ice CO_2 exchanges. The evolution of the carbonate system and CH_4 was examined using measurements of total alkalinity, total dissolved inorganic carbon and CH_4 concentrations on melted bulk sea ice, brine and melt ponds in association with CO_2 flux measurements over sea ice and melt ponds. Percolation of meltwater from melt ponds was tracked using the isotopic ratios $\delta^{18}O$ within bulk sea ice and brine.

Acknowledgements: We acknowledge the Canada Excellence Research Chairs (CERC) Programme, Natural Sciences and Engineering Research Council (NSERC) of Canada, ArcticNet and the Arctic Science Partnership (ASP).

6.21 Importance of benthic primary production and carbon turn over as assessed by *in situ* eddy-correlation measurements

Kasper Hancke, Karl Attard, Mikael K. Sejr and Ronnie N. Glud

Shallow water sediments can host significant potential for primary production, but are also highly enriched in deposited organic material (Glud 2008). Therefore, benthic production and mineralization of organic material are important for the biogeochemical and biological functioning of coastal ecosystems (Middelburg and Soetaert 2004). The changing Artic climate is predicted to decrease sea ice cover and increase terrestrial run-off with consequences for light availability and deposition of organic material that both

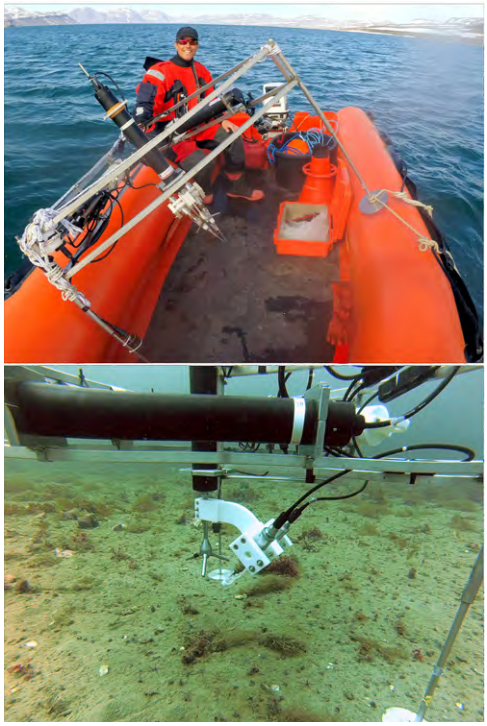

Figure 6.39 Deployment of an "Underwater Eddy correlation" (EC) lander from a Zodiak rubber boat in Young Sound outside the Daneborg Research House (a), and the EC lander at the seafloor at 20 m water depth (b), where it measures oxygen exchange rate across the seafloor-water interface. Photos: Karl Attard and Kasper Hancke.

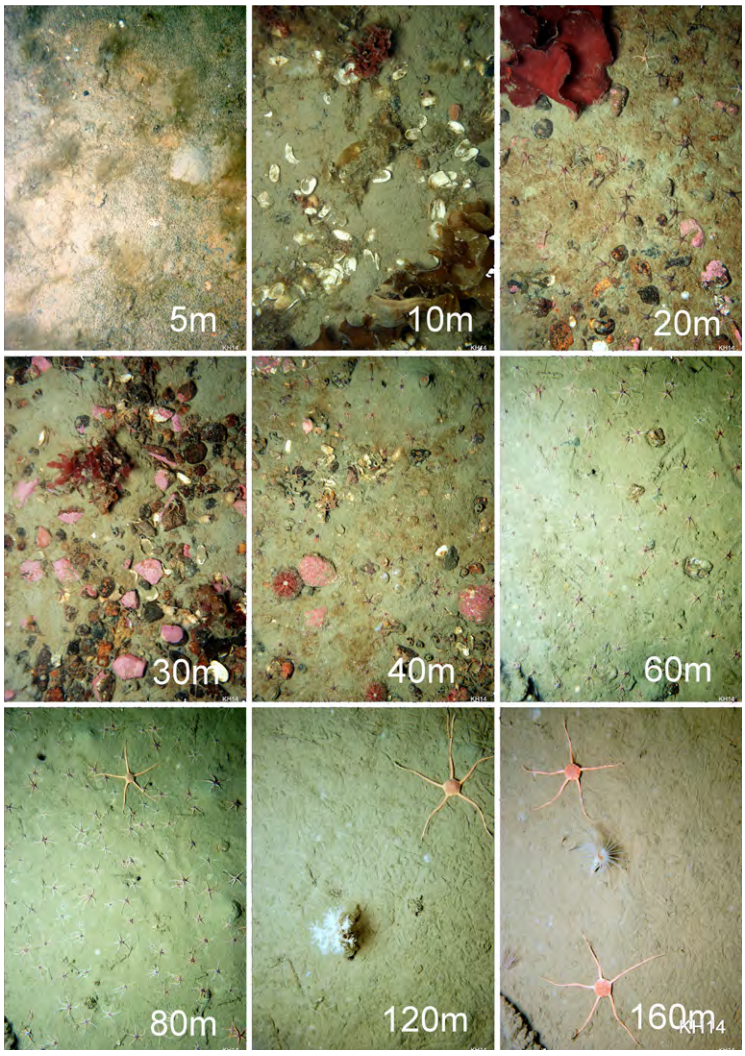

*Figure 6.40 A mosaic of high-resolution images of the seafloor in Young Sound at water depths from 5 to 160 m. Abundance of macrofauna and coverage of microalgae were derived from the images. Bivalves (*Hiatella arctica *and* Mya truncate*) and brittle stars (*Ophiocten *spp. and* Ophiopleura *spp.) were dominating the fauna, while diatoms and coralline algae were the dominating microalgae. Photos: Kasper Hancke and Mikael K. Sejr.*

sustain the activity of the costal benthic communities.

In the present project we aimed to 1) quantify the net O_2 production and consumption at the seafloor as a function of light and water depth, 2) estimate the faunal and fauna-stimulated contribution to the seafloor O_2 consumption, and 3) provide input parameters for an ecosystem model constraining the seafloor carbon turnover in Young Sound.

During a three-week campaign in July/August, O_2 fluxes across the seafloor-water interface were measured by applying the novel non-invasive aquatic 'Eddy covariance' (EC) technique (figure 6.39). Instrument deployments lasted from 24 to 48 hours and the EC technique provided continues *in situ* data on the production and consumption rates of O_2 at the seafloor under prevailing light conditions. The deployments were focused along a transect outside the Daneborg field station and covered water depths from 5 to 160 meters. Additional, bottom water O_2 concentration, current velocity, temperature, salinity, chlorophyll fluorescence and light availability were sampled at the depth transect. Sediment characteristics, chlorophyll concentration and presence of benthic fauna were described from recovered sediment cores and *in situ* high-resolution images (figure 6.40).

We found, that seafloor microalgae sustained a net O_2 production to depths of ~30 m during the day, and that sufficient light was present to drive gross photosynthesis at depths of > 40 m. These preliminary results support that seafloor microalgae are important for the carbon turnover in the coastal region of the high Arctic and that seafloor net primary production contributes to the system net productivity at water depths of > 30 m (Glud *et al.* 2009; Attard *et al.* 2014). At depth > 60 m we were

*Figure 6.41 Close-up studies of the Arctic fox (*Vulpes lagopus*), and its interactions with human researchers. Photo: Kasper Hancke.*

not able to detect any photosynthesis, and the O_2 uptake decreased gradually with increasing water depth. Combining EC measurements with laboratory-determined O_2 microprofiles and digital images of the fauna abundance, we wish to explore the importance of fauna for the benthic O_2 consumption rate and thereby the net turnover of organic material in the sediment of Young Sound. These data are still under evaluation.

This project was conducted at Zackenberg (figure 6.41) and is a contribution to the Arctic Science Partnership (ASP), asp-net.org., and funded through the Arctic Research Centre, Aarhus University(Denmark), the Nordic Center for Earth Evolution/Danish National Research Foundation (Nord-CEE, DNRF#53), and the Commission for Scientific Research in Greenland (GCRC#6507).

6.22 The role of copepods in the pelagic carbon turn-over: impacts of increasing freshwater discharge, Northeast Greenland

Ane Middelboe, Eva Friis Møller, Kristine Arendt and Mikael K. Sejr

Copepods are key organisms in Arctic pelagic food chains responsible for the transfer of carbon from primary producers to higher trophic levels and their fast sinking faecal pellets contribute to transport of particulate organic carbon (POC) from the euphotic zone to benthic communities. To understand the carbon turnover and how environmental changes will affect the pelagic food chains, it is essential to understand how grazing, production, and temporal and spatial distribution of copepods are controlled.

Figure 6.43 Collection of zooplankton data. Photo: Mikael K. Sejr.

In this study, we quantified species composition, biomass, and grazing pressure of the copepod community in Young Sound. This was done during the ice-free summer from July to October at four sites under increasing influence of meltwater from the Greenland ice sheet (figure 6.43). Based on the seasonal and spatial variation within Young Sound and through comparison to other Greenland sites, we attempted to evaluate the potential impacts of meltwater on the role of the copepod community.

Our study suggests that low productivity in Young Sound is related to the amount of freshwater and how it is supplied. Freshwater enters the fjord as surface runoff, which limits light availability and nutrient replenishment (figure 6.42a) resulting in dominance by small phytoplankton cells (figure 6.42b). The copepods are not able to graze on these small cells, resulting in low grazing rates (figure 6.42d) and therefore decreasing the amount of carbon transferred from the primary producers to higher trophic levels in the food webs (figure 6.42e) at increasing freshwater discharge.

6.23 Controls of microorganisms during the ice-free season in Young Sound, NE Greenland

Maria Lund Paulsen, Aud Larsen, Colin Stedmon and Mikael K. Sejr

The microbial food web comprises a variety of single-celled organisms, and is often divided into the functional groups of heterotrophic bacteria, virus, heterotrophic nanoflagellates, microzooplankton (ciliates and dinoflagellates) and phototrophic pico (0.2-2 µm)-, nano (2-20 µm)- and micro (20-200 µm)-sized phytoplankton (figure 6.44). These components are responsible for the major part of carbon cycling in the marine system and regulate nutrient flow by uptake and re-mineralization. In order to get a better understanding of the pelagic system in Young Sound, it is essential to monitor the microbial part of the food web.

In this study we enumerated the microbial components by flow cytometry, at four sites throughout the fjord (inner fjord under increasing influence of meltwater)

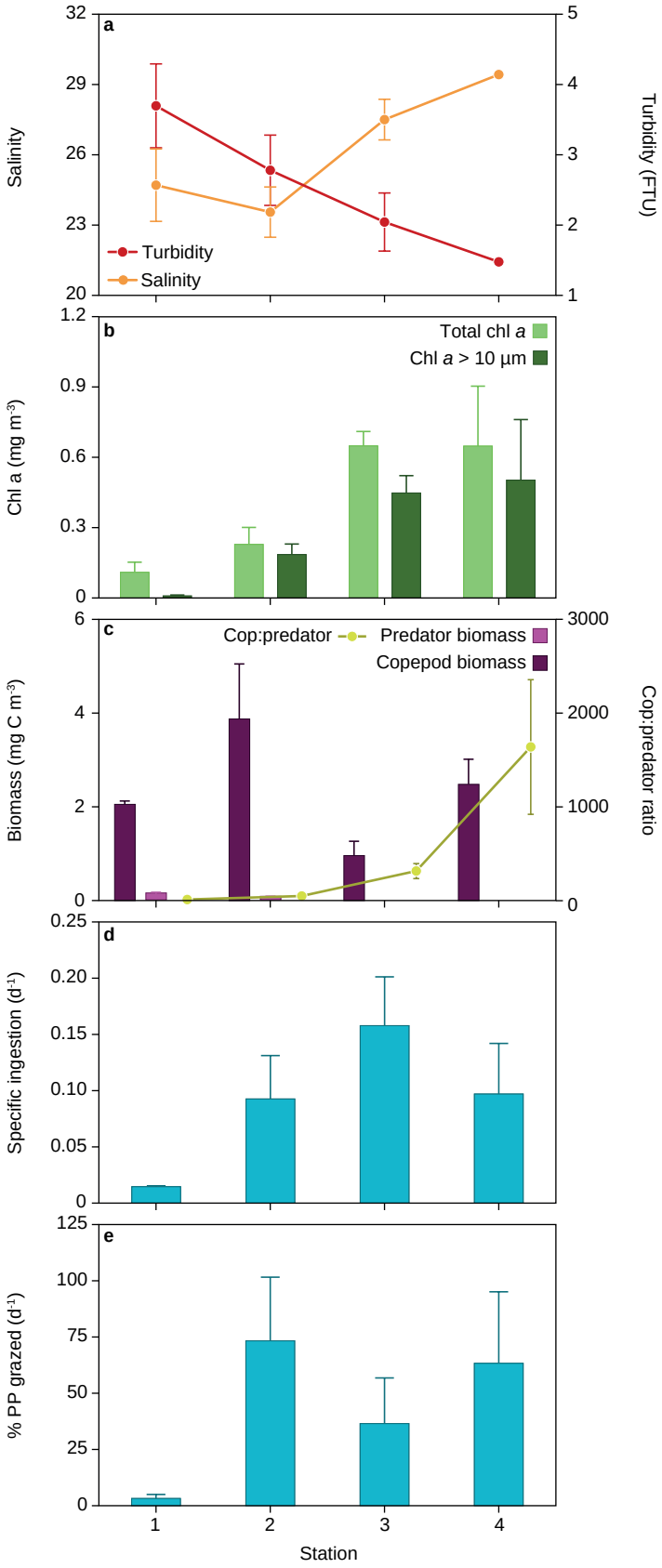

Figure 6.42 Spatial variations in Young Sound. Bars represent pooled values for July and August. Error bars indicate mean ± SE (n = 2-5). (a) Salinity and turbidity, (b) chlorophyll a concentrations, (c) copepod biomass, predator biomass, and copepod:predator ratio, (d) specific ingestion rates, and (e) copepod grazing impact on daily primary production.

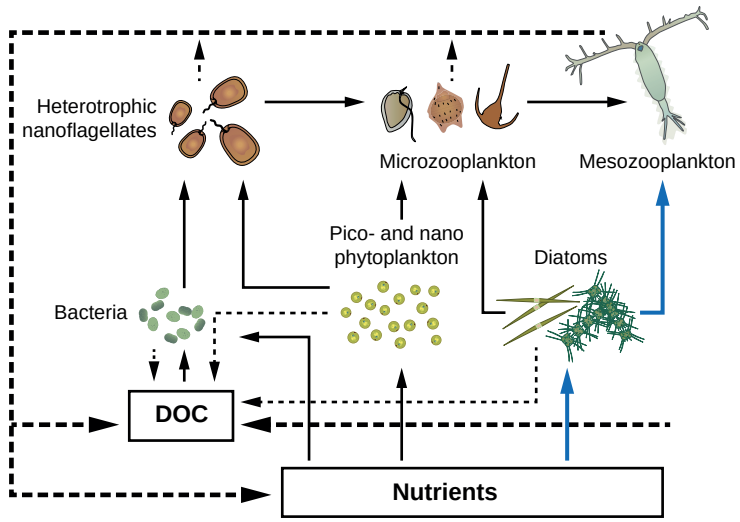

Figure 6.44 The dominant pathways of carbon in the pelagic food web. Blue arrows illustrate "the classical food web", while black arrows indicate the microbial food web. The dashed arrows indicate the reminralisation of nutrients and production of dissolved organic matter (DOM).

during the ice-free summer from July to October. Seven depths at each site were sampled once per week (only microzooplankton and micro-phytoplankton were monitored less intensively; only sampled at surface and Chl *a* max). We found that the bacterial abundance was positively linked to the surface phytoplankton production and not to the meltwater nor to the inflow from outside the fjord. Pico-phytoplankton abundances were highest (up to 10,000 cells ml^{-1}) in the inner fjord and thus positively linked to meltwater runoff and increased during the period. Nano- and micro-phytoplankton on the other hand decreased in abundance during the period and were found in highest abundances at the outer part of the fjord.

To investigate the interactions between microorganisms (figure 6.44) we conducted large-scale incubation experiments three times during the period and estimated growth and grazing rates of the various microorganisms by size-fractionation (< 0.8 µm, < 3 µm, < 10 µm and < 90 µm) (see figure 6.45 for further explanation). In the two latter experiments we added the copepod *Calanus hyperboreus* and the pelagic snail *Limacina helicina* in order to explore effects imposed by such grazers. We further observed how the different size fractions altered chemical components such as nutrients and character of dissolved organic matter (DOM), and smaller experiments were conducted more frequently (from all sites) to examine the viral lyses and net-growth of bacteria.

The bacterial degradation of DOM comprises the major carbon turnover in the ocean, and the quantity of this turnover depends largely on the character and concentration of DOM. In order to better understand the bottom-up control of bacteria, we measured concentration of carbon bound in DOM, the C:N ratio, the light absorption and fluorescence signal of DOM at the various sites. It is thus possible to link the different DOM characteristics to different sources (i.e. from meltwater, costal inflow or *in situ* marine production) to the bacterial activity.

Figure 6.45 Open incubation tank with a surface water flow though system and days at approx. 30 % surface irradiation. Sampled water was size-fractionated into < 0.8 µm (water containing only bacteria and virus), < 3 µm (bacteria, virus and picophytoplankton), < 10 µm (all pico- and small nano-sized organisms) and < 90 µm (pico-, nano- and most micro-sized organisms). Each treatment was incubated in triplicate 5 l containers for 5-10 days at approx. 30 % irradiation and sampled daily.

6.24 Primary production in Young Sound, NE Greenland

Tage Dalsgaard, Thomas Juul-Pedersen, Antonio Delgado Huertas, Elena Mesa Cano, Stiig Markager and Mikael K. Sejr

The aim was to estimate the magnitude of the primary production (PP) in Young Sound throughout the open water season and to elucidate its controlling factors. Primary production may be estimated as gross (GPP) or net (NPP), the former being the instantaneous conversion of CO_2 into biomass and the latter being what is left after respiration has consumed some of the C fixed by GPP. There are several methods available for quantifying PP and each of these may give either GPP, NPP or something in between depending on the environmental conditions and how the methods are applied. We applied four methods in parallel in order to get the best possible estimate of PP and to investigate how these methods perform in a very low-productive Arctic environment. These methods were all applied on four sampling stations and two depths selected to represent the different parts of the fjord.

We applied the ^{14}C-method in which ^{14}C-labeled bicarbonate was added to short-term incubations (4 h) of water from the stations and the incorporation of ^{14}C into biomass was followed. This was expected to give an estimate of PP close to GPP. Gross PP was also estimated through the ^{18}O-H_2O technique in which ^{18}O-labeled water was added to the incubations and the production of ^{18}O-labeled O_2 was quantified. It is assumed that the ratio O_2 production to CO_2 uptake, the photosynthetic quotient, is approximately 1.

In another approach we measured changes in O_2 concentration in glass bottles incubated *in situ* in either natural light or darkness for one or two full diurnal cycles (figure 6.46 and 6.47). Changes in O_2 concentrations will be an estimate of NPP in bottles incubated in light, an estimate of respiration in bottles incubated in darkness, and the difference between the two will be an estimate of GPP. Finally, PP was estimated through *in situ* incubations under natural light to which ^{13}C-labeled bicarbonate was added. These bottles were also incubated for one or two full diurnal cycles and the incorporation of ^{13}C into biomass was measured and assumed to be an estimate of NPP.

These methods for estimating PP rely on quite a number of chemical and mass spectrometric analyses and data handling, some of which are still pending.

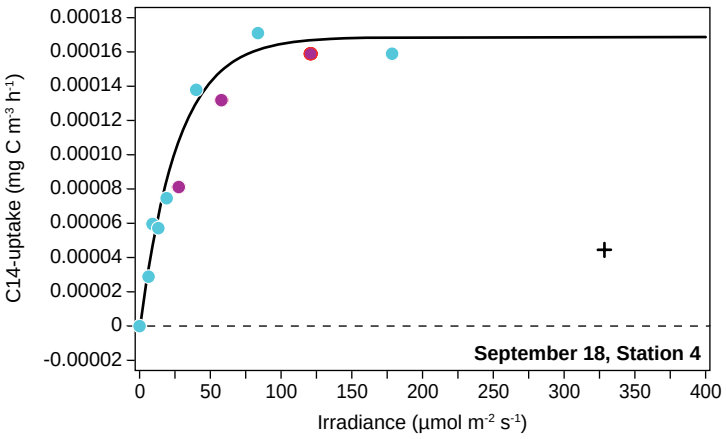

Figure 6.46 Preliminary data showing carbon incorporation at different light intensities in the laboratory.

Figure 6.47 Measurements of photosynthetic activity in the Daneborg "open air" laboratory. Photo: © Jean GAUMY/Magnum Photos

6.25 Bioavailability and microbial decomposition of organic matter in Young Sound, NE Greenland

Sophia Elisabeth Bardram Nielsen, Maria Lund Paulsen, Eva Friis Møller, Colin Stedmon, Aud Larsen, Mikael K. Sejr and Mathias Middelboe

Effects of climate change are believed to be particularly strong in Arctic fjords, where decreased ice coverage, increased freshwater runoff and increased stabilization of the water column are expected to cause changes in marine carbon and nutrient cycling, with potentially large implications for ecosystem metabolism and trophic interactions. Pelagic bacteria contribute significantly to ecosystem metabolism in these fjords and it is therefore essential to quantify microbial carbon consumption and the factors controlling microbial activity in order to understand their role in the turnover of the allochthonous and autochthonous organic matter in the Fjord at changing environmental conditions.

Measurements of bacterial biomass, net production and respiration allowed a quantification of total carbon turnover and bacterial growth efficiency, and thus to establish the bacterial contribution to ecosystem metabolism in the Fjord. During a seasonal study from July to October, the variations in bioavailability and bacterial turnover of the organic material in the pelagic zone were quantified across a spatial gradient in Young Sound from glacial outflow and stations in the inner part of the fjord with strong influence of fresh water and turbidity, to stations in the outer part more influenced by autochthonous production, and to oceanic stations influenced by the East Greenland current. In the figure 6.48, depth profiles of bacterial production (mg C m^{-3} d^{-1}) are shown for the Standard Station from July to October. The horizontal bars indicate the relative distribution (%) of bacterial production between the free-living and particle associated fractions in two selected depths (1 m and deep chlorophyll max). Our data show large spatial and temporal variations in bacterial activities and in relative contributions of bacteria to ecosystem metabolism in the fjord.

6.26 SCLERARCTIC: Using bivalves of the genus *Astarte* spp. as bioarchives of the impacts of climate change on Arctic food webs

Silvia de Cesare, Jean Gaumy, Mikael K. Sejr and Frédéric Olivier

As a consequence of global warming, the alteration of sea-ice dynamics in the marine Arctic ecosystem is expected to affect microalgal blooms, particularly the dynamics of sea-ice algae. The potential consequences of such changes on the mac-

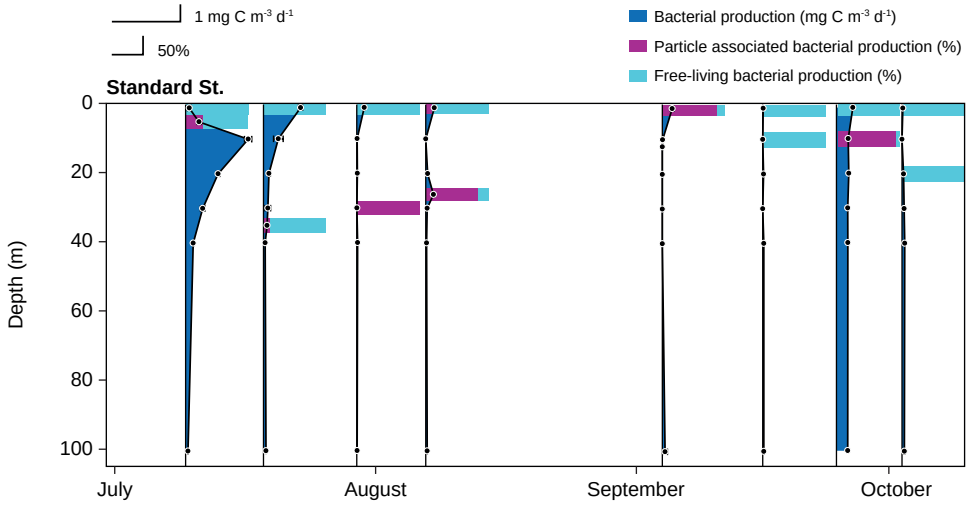

Figure 6.48 The figure shows the bacterial production (mg C m^{-3} d^{-1}) from 0-100 meters' depth (vertical scatterline) over the season (July to October) at the Standard Station at Young Sound. Horizontal bars indicate the relative distribution (%) of the bacterial production between particle associated (purple) and free-living fractions (light blue) in 1 meter and deep chlorophyll max.

Figure 6.49 Cross-section of the hinge tooth of Astarte borealis *sampled in Kongsfjorden (Svalbard) in May 2013.*

rozoobenthic community, especially on the filter-feeding bivalves, are still largely unknown.

Within this context, the overall goal of the 'SCLERARCTIC' project is to use the *Astarte* spp. bivalves as bioarchives of environmental changes under the influence of the climate change on a large scale in contrasting trophic environments. This project involved a calibration/validation phase in Young Sound and one acquisition phase from the Beaufort Sea to the Greenland Sea (4 sites). The final objective was to estimate the effects of climate change on the primary production's export towards the benthos in North American/Greenland Arctic.

The analyses of the bivalves' shells, including the patterns of internal growth lines (sclerochronology) and involving geochemical methods of carbonates' analyses (sclerogeochemistry), can provide robust datasets about past environmental changes (temperature, salinity) and some biotic dynamics (primary production). The species of the *Astarte* genus are largely distributed in the Arctic and their lifespan can exceed one century allowing a best focus on the last 50-year period. In complement, trophic analyses of their soft tissues (fatty acid trophic markers FATM, stable isotopes…) give new insights into the assimilated diet of those organisms.

During fieldwork in August 2014, several specimens of *A. borealis* and *A. elliptica* were collected near the Daneborg Main Station (74°18N, 20°14W average depth 23 m) and next to the Zackenberg delta (74°24N, 20°19W, average depth 20 m). Actually we have prioritized the analyses of bivalves belonging to the *A. borealis*, because this complex is well adapted for sclerochronological studies, with clear patterns of shell's growth lines and increments (figure 6.49). The growth dynamics of 50 individuals from the Daneborg station will be estimated soon, and some shells will be used to study the dynamics of $\delta^{18}O$ stable isotopic ratios (related to both temperature and salinity) and of some trace elements(Ba/Ca, Sr/Ca…) as it has been already demonstrated to be related to the PP dynamics. The study of young individuals will allow a calibration of our proxies, as they can be compared to environmental parameters monitored by the MarineBasis programme since 2005.

We have also analysed two tissues (digestive gland and adductor muscle) of the specimens from the Daneborg populations and their potential feeding sources (POM, sea-ice algae, macroalgae, surficial sediments). FATM, bulk isotopes ($\delta^{13}C$ and $\delta^{15}N$) and compound-specific stable carbon isotope on individual fatty acids methods will be used.

In addition, we collected some fossils of the *A. borealis* complex near Zackenberg station; they should come from a period corresponding to the middle of the Holo-

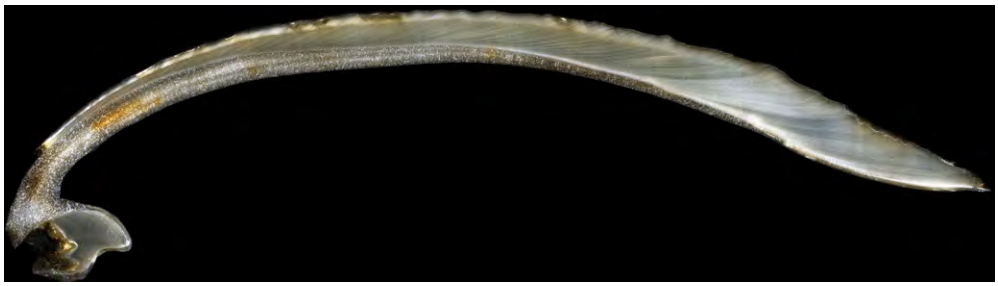

Figure 6.50 Cross-section of the shell of one fossil of Astarte borealis *(4000 to 8000 BC) collected near the river Zackenberg delta in August 2014.*

Figure 6.51 Sorting Astarte borealis from dredge samples in the Yung Sund (high Arctic fjord of NE Greenland).

*Figure 6.52 Discussion between Danish and French scientists about fossil bivalves of the Young Sound (*Astarte borealis *and* Mya truncata*).*

cene (4000-8000 BC, M.K. Sejr pers. com). We are confident about future paleoenvironmental studies on these fossils as shell's growth line patterns are easily detectable (figure 6.50).

Our team included a professional photographer member of Magnum Photos agency, Jean Gaumy. In the frame of the project he was supposed to photograph the survey (figures 6.51 and 6.52) and was also invited to develop his own personal project on the arctic landscape. His photographs should be part of an exhibition and a possible collective book in 2017.

6.27 Zackenberg Research Station

Peter Bondo Christensen

In the summer of 2014 I followed closely the research work of scientists in Zackenberg and Daneborg. My observations formed the basis for a number of articles published in Danish and Greenlandic media and at the websites of the Arctic Science Partnership and Arctic Research Centre, and these will now be included in a series of articles marking the 20th anniversary of the Zackenberg research station. Additionally, an interview for the Danish Broadcasting Corporation was carried out with Deputy Scientific Leader and BioBasis Field Biologist Lars Holst Hansen – directly from Zackenberg.

At Zackenberg, the scientists worked with everything from small insects to roaring musk oxen. A Finnish team studied the insects pollinating the small dryas plants through their short flowering season. Scientists from Aarhus University were fortunate enough to recapture migrating skuas fitted the previous year with small data loggers around one leg, and the data gathered revealed that the birds perform a formidable journey from Northeast Greenland to South Africa and back. Other and significantly larger transmitters were fitted around the necks of 14 different musk oxen, permitting the scientists, through daily contact with satellites, to follow the movements of the different groups of musk oxen and thereby record where they stayed and what they ate. At Daneborg, 12 scientists from Belgium, Greenland, Canada, Denmark and Finland turned the new research station into a lively place. Their main area of focus was directed at carbon cycling in the sea ice that had started to melt in early July. An impressive set of data was gathered from

Figure 6.53 A number of articles published in Danish and Greenlandic media and at the websites of the Arctic Science Partnership and Arctic Research Centre.

when the ice was formed at the beginning of the previous autumn until it disappeared again in July – a unique dataset which is not available in any other parts of the world. The scientists were busy around the clock but also fulfilled their kitchen duties where the teams took turns to prepare the food during an entire day. On the last night in the camp, Carl Isaksen and Ivali Lennert from the Greenland Institute of Natural Resources, responsible for logistics, performed a little stunt. With small knives they split a large, flat stone in two, which they used as pizza stones on which grilled specialties were prepared to give the many foreign guests a "taste of Greenland" in the midnight sun with the sea ice as a scenic background.

Photo: Lars Holst Hansen.

7 Disturbances in the study area

Jannik Hansen

This account covers the period from 2 April to 28 October 2014. For details about the opening and operations of the station, see chapter 8.

7.1 Surface activities in the study area

May – August: The number of 'person days' (one person in the field one day) spent within the main research area, Zone 1 (table 7.1) was 1202, which is high. The 'low impact area', Zone 1b, was visited in numbers similar to previous seasons. The 'goose protection area', Zone 1c, was visited on few occasions during the closed period, 20 June-10 August. Only one accidental entry of people meant a higher number than usual for July. Unfortunately, data for use of the research areas were unavailable for May. This season, the use of the all-terrain vehicle (ATV) was mainly along the designated roads to the climate station and the beach at the delta of the river Zackenberg. Only twice in June and twice in July and five times during September were ATVs in use off the designated road system. However, the use of the ATV at and near the station has become higher since 2007, and is remaining at a high level. During the early and late part of the season, snowmobiles were used for transportation of equipment and personnel.

Table 7.1 'Person-days' and trips in the terrain with an All-Terrain Vehicle (ATV) allocated to the research zones in the Zackenberg study area June –August 2014. 1c, the "Goose Protection Area" is closed for human traffic from 20 June to 10 August (DOY: 171-222). Trips on roads to the climate station and the delta of the river Zackenberg are not included.

Research zone	Jun	Jul	Aug	Sep	Total
All of 1 (incl. 1a)	245	607	267	83	1202
1b	2	30	9	5	46
1c (20 Jun-10 Aug)	1	15	N/A	N/A	16
1 Part of zone 1*	26	138	36	10	210
2	0	18	16	0	34
ATV-trips	2	2	0	5	9

*The area west of river Aucella

7.2 Aircraft activities in the study area

For details on number of visits by fixed wing aircrafts and helicopters see chapter 8. During the 2014 season, the arrival of aircrafts did not make waterfowl fly up from the lakes, ponds and fens nearby. Possibly, geese get accustomed to regular disturbance (cf. Madsen and Boertmann 2008).

7.3 Discharges

Water closets in the residential house were in use from April onwards, while the separate toilet building opened early June. From here, all toilet waste was grinded in an electrical mill and led into the river. Likewise, solid, biodegradable kitchen waste was run through a grinder mill and into the river. The mill was in use until the end of the season. The total amount of untreated wastewater (from kitchen, showers, sinks and laundry machine) equalled approximately 1461 'person-days' during May-August, which is high compared to previous years. The gradual phase-out of perfumed and non-biodegradable detergent, soap, dishwashing liquid, etc. is well under way. More environmentally friendly products are now in use. Combustible waste (paper, cardboard, wood, etc.) was burned at the station. For management of other waste, please see chapter 8.

7.4 Manipulative research projects

The coordinates and extent of all manipulation sites mentioned below are registered with BioBasis Zackenberg. For the tenth consecutive season, shade, snowmelt and temperature were manipulated at two sites, each with 25 plots (see Jensen 2012).

Five enclosures were set up in 2010 to study the effect of musk oxen grazing on vegetation and related ecological effects (see Jensen *et al.* 2014).

A project looking at the "effect of inorganic and organic nutrient content on stream ecosystem function" made low concentration nutrient additions to selected streams, with an effect for 1-3 hours. The exact streams and amounts added are registered with BioBasis Zackenberg (see section 6.15).

7.5 Removal of organisms and other samples

The 'Interactions 2011-2014' project collected one dunlin chick that was found dead in the nest cup, after the clutch had successfully hatched two days prior. This project also collected the following: Ten blood samples of 20 µl from nine adults and one juvenile, as well as nine samples of 10 µl from chicks of dunlin (at Zackenberg, this project is run by BioBasis).

During the 2014 season, 20151 land arthropods were collected as part of the BioBasis programme (see chapter 4).

Twenty blood samples of 80 µl were collected from adults and 19 of 10 µl from chicks of sanderlings for a parentage and breeding strategy project. In addition, this project collected nine eggs that had failed to hatch (see section 6.14).

Tissue samples were collected from a number of animal species for the BioBasis DNA bank (see table 4.26, chapter 4).

For the "High Arctic Food Web" project, an estimated 32268 arthropods were caught in seven malaise traps. Additionally, 8397 were caught on artificial flowers and 370 were caught by netting (see section 6.10).

A project named "Climate effects in terrestrial arctic ecosystems" collected arthropods in malaise traps and arthropods in pitfall traps. Additionally, similar collections were done at Blæsedalen, approx. 40 km outside the monitoring area (see section 6.8).

For the "Spacewolf" project, 30 Arctic wolf spiders (*Pardosa glacialis*) were collected from each of five different sites at different altitudes. Also, 90 aphids on *Dryas* flowers were collected at one altitude. Arthropods on north facing and south facing slopes were collected at 4 sites, from 6 traps at each site (see section 6.9).

Whole shrubs of each species (*Betula nana*, *Dryas octopetala* and *Salix arctica*) were collected by a dendrochronological study of high and low arctic plants. *Betula nana*: from two site, 25 and five plants, respectively. *Dryas octopetala*: from three sites, four, nine and three plants, respectively. And finally, *Salix arctica*: from one site, 45 whole plants (see section 6.11).

In the second year of the SAR study, 3 × 12 samples of 20 × 20 cm vegetation samples were harvested, in order to monitor moisture content (see section 6.7).

For a master's project, 10 soil samples, containing the upper 10 cm of the soil, were taken. A total of 5 kg soil was sampled.

Microbial communities in Arctic environments were studied at three sites, at which 3 soil samples were taken at each. Each soil sample was approximately 50 cm^2, taken at 0 cm, 20 cm and 40 cm in the active layer and permafrost cores (20 cm^2) were taken down to 120 cm (see section 6.3).

Nine to eighteen whole *Salix arctica* were dug up at 18 sites at Zackenberg and sampled. Additionally, more sites at another locality, Blæsedalen, were sampled (see section 6.12).

8 Logistics

Henrik Spanggård Munch

8.1 Use of the station

In 2014, the field season at Zackenberg was open from 2 April to 24 October, in total 206 days. During the period, 79 researchers/guests visited Zackenberg Research Station and 50 visited the research house in Daneborg. They were serviced by eight logisticians employed by the Department of Bioscience at Aarhus University.

The total number of bed nights during 2014 was 3018, with 1464 and 1167 bed nights for visiting researchers at Zackenberg Research Station and Daneborg respectively, and 387 bed nights for logisticians.

During the season, the station was visited by researchers from 19 countries: Austria, Belgium, Canada, Denmark, Finland, France, Greece, Greenland, India, Italy, Netherland, Norway, Poland, Russia, Spain, Sweden, Switzerland, UK and USA.

8.2 Transportation

During the field season, fixed winged aircrafts (De Havilland DHC-6 Twin Otter) landed 49 times at Zackenberg.

8.3 Maintenance

During 2014, no larger maintenance work was carried out at Zackenberg Research Station. The maintenance condition of the station is very good. Besides the normal painting of the houses, we do not expect larger maintenance costs during the year to come.

8.4 Handling of garbage

Non-burnable waste was removed from Zackenberg Research Station by aircraft to Daneborg on the empty return flights during the fuel lifts from Daneborg to Zackenberg and from there the waste was sent by ship to Denmark. Non-burnable waste was also removed from the research house at Daneborg and send by ship to Denmark. Approximately 33 m^3 of waste were removed from the station and from the research house.

8.5 Acquisitions

No new equipment was purchased in 2014.

9 Personnel and visitors

Compiled by Charlotte Hviid

Agata Buchwal, Institute of Geoecology and Geoinformation of Adam Mickiewicz University in Poznan, Polen
Alexis Burt, University of Manitoba, Winnipeg, Canada
Alexsander Milner, School of Geography, Earth and Environmental Sciences, University of Birmingham, United Kingdom
Anders Michelsen, Terrestrial Ecology, University of Copenhagen, Denmark
Anders Rasmussen, Department of Bioscience, Aarhus University, Denmark
Ane Middelboe, Department of Bioscience, Aarhus University, Denmark
Antionio Delgardo Huertas, Spanish National Research Council, Madrid, Spain
Aud Larsen, UniResearch, Bergen, Norway
Bjarne Jensen, Department of Environmental Science, Aarhus University, Denmark
Brigitte Sabard, Groupe de Recherche en Ecologie Arctique (GREA), Francheville, France
Bruno Delille, Unité d'océanographie Chimique, Université de Liège, Belgium
Carl Isaksen, Greenland Institute of Natural Resources, Greenland
Cathrine Docherty, School of Geography, Earth and Environmental Sciences, University of Birmingham, United Kingdom
Charalampos Charalampidis, Geological Survey of Denmark and Greenland, Denmark
Daniel Binder, Zentralanstalt für Meteorologie und Geodynamik, Austria
David Barber, University of Manitoba, Winnipeg, Canada
Dean Childs, IRIS PASSCAL Instrument Center, Socorro, USA
Dina Laursen, Department of Bioscience, Aarhus University, Denmark
Egon Frandsen, Department of Bioscience, Aarhus University, Denmark
Elena Mesa Cano, Instituto Andaluz de Ciencias de la Tierra, Spain
Eric Buchel, Groupe de Recherche en Ecologie Arctique (GREA), Francheville, France
Erik Lysdal, COWI, International Land Adminstration and Technical Land Surveying, Denmark
Eva Friis Møller, Department of Bioscience, Aarhus University, Denmark
Frederic Olivier, Département Milieux et Peuplements aquatiques, Muséum national d'Histoire naturelle, Paris, France
Genti Toyokuni, Tohoku University, Japan
Geo Boffi, Swiss Federal Institute of Technology, Zurich (ETHZ), Switzerland
Geofrey Gunn, University of Manitoba, Winnipeg, Canada
Glen Eddy Liston, Cooperative Institute for Research in the Atmosphere (CERA), Colorado State University, Fort Collins, USA
Grzegorz Rachlewicz, Institute of Geoecology and Geoinformation of Adam Mickiewicz University in Poznan, Polen
Heidi Sørensen, Greenland Institute of Natural Resources, Greenland
Helle Hildebandt, Department of Bioscience, Aarhus University, Denmark
Henning Ting, Pensioneret
Henrik Spanggård Munch, Department of Bioscience, Aarhus University, Denmark
Igor Dmitrenko, University of Manitoba, Winnipeg, Canada
Ivali Lennert, Greenland Institute of Natural Resources, Greenland
Jacob Nabe-Nielsen, Department of Bioscience, Aarhus University, Denmark
Jakob Abermann, Asiaq, Greenland Survey, Greenland
Janni Fries Linnebjerg, Department of Bioscience, Aarhus University, Denmark
Jannik Hansen, Department of Bioscience, Aarhus University, Denmark

Jean Gaumy, Département Milieux et Peuplements aquatiques, Muséum national d'Histoire naturelle, Paris, France
Jean-Pierre Wiest, Groupe de Recherche en Ecologie Arctique (GREA), Francheville, France
Jeroen H. Reneerkens, Centre for Ecological and Evolutionary Studies Animal Ecology Group, Groningen, The Netherlands
Jonas Andersen, Department of Bioscience, Aarhus University, Denmark
Jonathan N. K. Petersen, Asiaq, Greenland Survey, Greenland
Julien Petillon, University of Rennes, France
Jørgen Skafte, Department of Bioscience, Aarhus University, Denmark
Jørn Ladegaard, Department of Bioscience, Aarhus University, Denmark
Jörn Thiede, Alfred Wegener Institute, Germany
Karl Attard, NordCEE, Institute of Biology, University of Southern, Denmark
Kasper Hancke, University of Southern Denmark, Odense, Denmark
Kathryn Adamson, Queen Mary, University of London, United Kingdom
Katrine Randrup, Department of Bioscience, Aarhus University, Denmark
Kenny P. Madsen, Department of Bioscience, Aarhus University, Denmark
Kerrie Warner, University of Manitoba, Winnipeg, Canada
Kim Holmén, Norwegian Polar Institute, Norway
Kirsten S. Christoffersen, Freshwater Biological Laboratory, University of Copenhagen, Denmark
Kirstine Skov, Department of Bioscience, Aarhus University, Denmark
Kristine E. Arendt, Greenland Institute of Natural Resources, Greenland
Kunuk Lennert, Greenland Institute of Natural Resources, Greenland
Lars Holst Hansen, Department of Bioscience, Aarhus University, Denmark
Lau Gede petersen, Department of Bioscience, Aarhus University, Denmark
Laura Helene Rasmussen, Department of Bioscience, Aarhus University, Denmark
Laura Reinert, Department of Physical Geography and Ecosystem Science, Lund University, Sweden
Lena Ström, Department of Physical Geography and Ecosystem Sciences, Lund University, Sweden
Line Vinter Hansen, Department of Bioscience, Aarhus University, Denmark
Lise-Lotte Sørensen, Department of Bioscience, Aarhus University, Denmark
Lærke Stewart, Department of Bioscience, Aarhus University, Denmark
Magnus Lund, Department of Bioscience, Aarhus University, Denmark
Maria Lund Paulsen, Bergen University, Norway
Maria Rask Pedersen, Department of Geosciences and Natural Resource Management, University of Copenhagen, Denmark
Marie Kotovitch, Unité d'océanographie Chimique, Université de Liège, Belgium
Mathias Middelboe, Marine Biological Section, University of Copenhagen, Denmark
Michele Citterio, Geological Survey of Denmark and Greenland, Denmark
Michelle Schollert, Department of Biology, University of Copenhagen, Denmark
Mickael Sage, Groupe de Recherche en Ecologie Arctique (GREA), Francheville, France
Mikael K. Sejr, Department of Bioscience, Aarhus University, Denmark
Mikhael Mastepanov, Department of Physical Geography and Ecosystem Science, Lund University, Sweden
Mikkel P. Tamstorf, Department of Bioscience, Aarhus University, Denmark
Mikko Tiusanen, Department of Bio- and Environmental Sciences, University of Helsinki, Finland
Moray Mcakay Souter, Centre for Ecological and Evolutionary Studies Animal Ecology Group, Groningen, The Netherlands
Niels Hartmann, Alfred Wegener Institute, Germany
Niels Martin Schmidt, Department of Bioscience, Aarhus University, Denmark
Niels Tornsberg, Rambøll, Denmark
Niocolas-Xavier Geilfus, Department of Bioscience, Aarhus University, Denmark
Odilie Crabeck, University of Manitoba, Winnipeg, Canada
Olivier Gilg, Université de bourgogne, Biogéosciences, Equipe Ecologie-Evolution, Dijon, France
Oskar Liset Pryds Hansen, Department of Bioscience, Aarhus University, Denmark
Palle Smedegard Nielsen, Department of Bioscience, Aarhus University, Denmark

Peter Bondo Christensen, Department of Bioscience, Aarhus University, Denmark
Rasmus Egede, Asiaq, Greenland Survey, Greenland
Ronnie N. Glud, Department of Bioscience, Aarhus University, Denmark
Roy Eric Collins, University of Alaska, Fairbanks, Alaska, USA
Ryan Galley, University of Manitoba, Winnipeg, Canada
Satwant Kaur, University of Manitoba, Winnipeg, Canada
Sergey Kirillov, University of Manitoba, Winnipeg, Canada
Stine Højlund Petersen, Department of Bioscience, Aarhus University, Denmark
Signe Normand, Department of Bioscience, Aarhus University, Denmark
Sigrid Schøler nielsen, Department of Bioscience, Aarhus University, Denmark
Siiri Wickström, University of Helsinki, Finland
Silvia DE Cesare, Département Milieux et Peuplements aquatiques, Muséum national d'Histoire naturelle, Paris, France
Simon Rosenhøj Leth, Department of Bioscience, Aarhus University, Denmark
Sophia E B Nielsen, Marine Biological Section, University of Copenhagen, Denmark
Steve Alban, James Hutton Institute, Aberdeen, Scotland, UK.
Stiig Markager, Department of Bioscience, Aarhus University, Denmark
Søren Rysgaard, Faculty of Environment, Earth and Resources University of Manitoba, Canada
Tage Dalsgaard, Department of Bioscience, Aarhus University, Denmark
Tenna Riis, Department of Bioscience, Aarhus University, Denmark
Thomas Juul-Pedersen, Greenland Institute of Natural Resources, Greenland
Tim Papakyriakou, University of Manitoba, Winnipeg, Canada
Timothy Lane, Laboratoire de Geographie Physique, Environnements Quaternaires et Actuels – UMR 8591, Meudon, France
Tobias Ullman, Institut für Geographie und Geologie, Lehrstuhl für Physische Geographie, Wuerzburg, Germany
Tom S. L. Versluijs, Centre for Ecological and Evolutionary Studies Animal Ecology Group, Groningen, The Netherlands
Tomas Roslin, Department of Agricultural Sciences, University of Helsinki, Finland
Torben R. Christensen, Department of Bioscience, Aarhus University, Denmark
Urs Albert Treier, Department of Bioscience, Aarhus University, Denmark
Vadim Heuacker, Groupe de Recherche en Ecologie Arctique (GREA), Francheville, France
Vald Petrushevich, University of Manitoba, Winnipeg, Canada
Vladimir Gilg, Groupe de Recherche en Ecologie Arctique (GREA), Francheville, France
Wieter Boone, University of Manitoba, Winnipeg, Canada

10 Publications

Compiled by Lillian Magelund Jensen

Scientific publications

Barber, D.G., Ehn, J.K., Pućko, M., Rysgaard, S., Deming, J. W., Bowman, J.S., Papakyriakou, T., Galley, R.J. & Søgaard, D.H. 2014. Frost flowers on young Arctic sea ice: The climatic, chemical, and microbial significance of an emerging ice type. *Journal of Geophysical Research: Atmospheres, 119*(20), 11-593.

Barraquand, F., Høye, T.T., Henden, J.A., Yoccoz, N.G., Gilg, O., Schmidt, N.M., Sittler, B. & Ims, R.A. 2014. Demographic responses of a site-faithful and territorial predator to its fluctuating prey: long-tailed skuas and arctic lemmings. *Journal of animal ecology, 83*(2), 375-387.

Bendtsen, J., Mortensen, J., & Rysgaard, S. 2014. Seasonal surface layer dynamics and sensitivity to runoff in a high Arctic fjord (Young Sound/Tyrolerfjord, 74° N). *Journal of Geophysical Research: Oceans*, *119*(9), 6461-6478.

Bonnet, P., Gonzalez, J., & Granados, J.A.A. 2014. Distributed Architecture for Sharing Ecological Data Sets with Access and Usage Control Guarantees. Proceedings of the 7th International Congress on Environmental Modelling and Software. Ames, D.P., Quinn, N.W.T. & Rizzoli, A.E. (eds.). 7 p.

Boulanger-Lapointe, N., Lévesque, E., Boudreau, S., Henry, G.H., & Schmidt, N.M. 2014. Population structure and dynamics of Arctic willow (Salix arctica) in the High Arctic. *Journal of Biogeography*, *41*(10), 1967-1978.

Dmitrenko, I.A., Kirillov, S.A., Rysgaard, S., Barber, D.G., Babb, D., Toudal Pedersen, L., Koldunov, N.V., Boone, W., Crabeck, O., and Mortensen, J. 2015. Polynya impacts on water properties in a Northeast Greenland Fiord. Estuarine, Coastal and Shelf Science, doi: 10.1016/j.ecss.2014.11.027.

Falk, J.M., Schmidt, N.M., & Ström, L. 2014. Effects of simulated increased grazing on carbon allocation patterns in a high arctic mire. *Biogeochemistry*, *119*(1-3), 229-244.

Falk, J.M., Schmidt, N.M., Christensen, T.R. and Ström, L. 2015. Large herbivore grazing affects the vegetation structure and greenhouse gas balance in a high arctic mire. Environmental Research Letters 10: 045001.

Gittel, A., Bárta, J., Kohoutová, I., Schnecker, J., Wild, B., Čapek, P., Kaiser, C., Torsvik, V.L., Richter, A., Schleper, C. & Urich, T. 2014. Site-and horizon-specific patterns of microbial community structure and enzyme activities in permafrost-affected soils of Greenland. *Frontiers in microbiology, 5*.

Grau, O., Ninot, J.M., Pérez-Haase, A., & Callaghan, T.V. 2014. Plant co-existence patterns and High-Arctic vegetation composition in three common plant communities in north-east Greenland. *Polar Research*, *33*.

Hansen, J., Ek, M., Roslin, T., Moreau, J., Teixeira, M., Gilg, O. and Schmidt N.M. 2015. First observation of a four-egg clutch of Long-tailed Jaeger *Stercorarius longicaudus*. Wilson Journal of Ornithology, in press.

Hansen, J., Hansen, L.H., Mortensen, L.O., Kyhn, L.A., Schmidt, N.M., & Reneerkens, J. 2014. Bird Monitoring at Zackenberg, Northeast Greenland, 20111, 2. *Bird Populations*, *13*, 17-27.

Hassel, K., Zechmeister, H., & Prestø, T. 2014. Mosses (Bryophyta) and liverworts (Marchantiophyta) of the Zackenberg valley, northeast Greenland.

Høye, T.T., Eskildsen, A., Hansen, R.R., Bowden, J.J., Schmidt, N.M., & Kissling, W.D. 2014. Phenology of high-arctic butterflies and their floral resources: Species-specific responses to climate change. *Current Zoology*, *60*(2), 243-251.

Jørgensen, C.J., Johansen, K.M.L., Westergaard-Nielsen, A., & Elberling, B. 2015. Net regional methane sink in High Arctic soils of northeast Greenland. *Nature Geoscience*, *8*(1), 20-23.

Kirillov, S., Dmitrenko, I., Babb, D., Rysgaard, S., Barber, D. 2015. The effect of ocean heat flux on seasonal ice growth in Young Sound (Northeast Greenland), submitted to Journal of Geophysical Research, Volume 120, Issue 7: 4803–4824.

Krogh, P.H., Peter, G., Wirta, H.K., Roslin, T., Gavor, Z., Elin, J., Schmidt, N.M., Petersen, H., Raundrup, K., Nymand, J. & Aastrup, P. 2014: Soil microarthropods collected in Kobbefjord and Zackenberg. In: Jensen, L.M. & Christensen, T.R. (Eds.). 2014. Nuuk Ecological Research Operations: 7th Annual Report 2013. Aarhus University, DCE – Danish Centre for Environment and Energy, pp. 70-73.

Leavitt, S.D., Esslinger, T.L., Hansen, E.S., Divakar, P.K., Crespo, A., Loomis, B.F., & Lumbsch, H.T. 2014. DNA barcoding of brown Parmeliae (Parmeliaceae) species: a molecular approach for accurate specimen identification, emphasizing species in Greenland. *Organisms Diversity & Evolution*, *14*(1), 11-20.

Legagneux, P., Gauthier, G., Lecomte, N., Schmidt, N.M., Reid, D., Cadieux, M.C., Berteaux, D., Bêtu, J., Krebs, C.J., Ims, R.A., Yoccoz, N.G., Morrison, R.I.G., Leroux, S.J. & Gravel, D. 2014. Arctic ecosystem structure and functioning shaped by climate and herbivore body size. *Nature Climate Change, 4*(5), 379-383.

Lund, M., Hansen, B.U., Pedersen, S.H., Stiegler, C., & Tamstorf, M.P. 2014. Characteristics of summer-time energy exchange in a high Arctic tundra heath 2000-2010. *Tellus B, 66*.

Lund, M., Hansen, B.U., Pedersen, S.H., Stiegler, C. and Tamstorf, M.P. 2014. Characteristics of summer-time energy exchange in a high Arctic tundra heath 2000-2010. Tellus 66B: 21631.

Mastepanov, M., Christensen, T.R., Lund, M., & Pirk, N. 2014. A Modern Automatic Chamber Technique as a Powerful Tool for CH_4 and CO_2 Flux Monitoring. In *AGU Fall Meeting Abstracts* (Vol. 1, p. 0061).

Mbufong, H.N., Lund, M., Aurela, M., Christensen, T.R., Eugster, W., Friborg, T., Hansen, B.U., Humphreys, E.R., Jackowicz-Korczynski, M., Kutzbach, L., Lafleur, P.M., Oechel, W.C., Parmentier, F.J.W., Rasse, D.P., Rocha, A.V., Sachs, T., van der Molen, M.K. & Tamstorf, M.P. 2014. Assessing the spatial variability in peak season CO_2 exchange characteristics across the Arctic tundra using a light response curve parameterization. *Biogeosciences*, *11*(17), 4897-4912.

Mortensen, L.O., Jeppesen, E., Schmidt, N.M., Christoffersen, K.S., Tamstorf, M.P., & Forchhammer, M.C. 2014. Temporal trends and variability in a high-arctic ecosystem in Greenland: multidimensional analyses of limnic and terrestrial ecosystems. *Polar biology*, *37*(8), 1073-1082.

Pedersen, S.H., Liston, G.E., Tamstorf, M.P., Westergaard-Nielsen, A. and Schmidt, N.M. 2015. Quantifying Episodic Snowmelt Events in Arctic Ecosystems. Ecosystems, doi: 10.1007/s10021-015-9867-8.

Petrescu, A.M.P., Lohila, A., Tuovinen, J-P., Baldocchi, D.D., Desai, A.R., Roulet, N.T., Vesala, T., Dolman, A.J., Oechel, W.C., Marcolla, B., Friborg, T., Rinne, J., Matthes, J.H., Merbold, L., Meijide, A., Kiely, G., Sottocornola, M., Sachs, T., Zona, D., Varlagin, A., Lai, D.Y., Veenendaal, E., Parmentier, F-J.W., Skiba, U., Lund, M., Hensen, A., van Huissteden, J., Flanagan, L.B., Shurpali, N.J., Grünwald, T., Humphreys, E.R., Jackowicz-Korczyński, M., Aurela, M.A., Laurila, T., Grüning, C., Corradi, C.A.R., Schrier-Uij, A.P., Christensen, T.R., Tamstorf, M.P., Mastepanov, M., Martikainen, P.J., Verma, S.B., Bernhofer, C. & Cescatti, A. 2015. The uncertain climate footprint of wetlands under human pressure. PNAS, doi: 10.1073/pnas.1416267112.

Petrusevich, V., Dmitrenko, I., Ehn, J., Kirillov, S., Rysgaard, S., & Barber, D. 2014. Mechanisms of zooplankton diel vertical migration in Young Sound Fjord during the polar night. Conference paper.

Reneerkens, J., van Veelen, P., van der Velde, M., Luttikhuizen, P., & Piersma, T. 2014. Within-population variation in mating system and parental care patterns in the Sanderling (*Calidris alba*) in northeast Greenland. *The Auk*, *131*(2), 235-247.

Roslin, T. & Wirta, H. 2015. Arkstiksen ravintoverkot uusiksi. Luonon Tutkija 118: 144-150.

Roslin, T., O'Hara, J.E., Várkonyi, G., & Wirta, H.K. 2014. Studying tachinids at the top of the world. Tachinid times, 27, pp 4-10.

Schollert, M., Burchard, S., Faubert, P., Michelsen, A., & Rinnan, R. 2014. Biogenic volatile organic compound emissions in four vegetation types in high arctic Greenland. *Polar biology*, *37*(2), 237-249.

Søndergaard, J., Tamstorf, M.P., Elberling, B., Larsen, M.M., Mylius, M.R., Lund, M., Abermann, J. and Riget, F.F. 2015. Mercury exports from a High-Arctic river basin in Northeast Greenland (74°N) largely controlled by glacial lake outburst floods. Science of the Total Environment 514: 83-91.

Ström, L., Falk, J.M., Skov, K., Jackowicz-Korczynski, M., Mastepanov, M., Lund, M., Christensen, T.R. and Schmidt, N.M. 2015. Controls of spatial and temporal variability in CH_4 flux in a high arctic fen over three years. Biogeochemistry: in press.

Tiusanen, M. 2014. Zackenberg. Symbiontti 3:11-16.

Visakorpi, K., Ek, M., Várkonyi, G., Wirta, H.K., Hardwick, B., Hambäck, P. & Roslin, T. 2014 Dissecting the interaction web of Zackenberg: targeting pollinators. In: Jensen, L.M., Christensen, T.R. & Schmidt, N.M. (Eds.). 2014. Zackenberg Ecological Research Operations, 19th Annual Report, 2013. Aarhus University, DCE – Danish Centre for Environment and Energy. pp. 99-101.

Visakorpi, K., Wirta, H.K., Ek, M., Schmidt, N.M & Roslin, T. No detectable trophic cascade in a high-arctic arthropod food web. Basic and Applied Ecology, in revision (and thus no final acceptance as yet!).

Westermann, S., Elberling, B., Højlund Pedersen, S., Stendel, M., Hansen, B.U., & Liston, G.E. 2014. Future permafrost conditions along environmental gradients in Zackenberg, Greenland. *The Cryosphere Discussions*, *8*(4), 3907-3948.

Westermann, S., Elberling, B., Pedersen, S.H., Stendel, M., Hansen, B.U. and Liston, G.E. 2015. Future permafrost conditions along environmental gradients in Zackenberg, Greenland Cryosphere 9: 719-735.

Wirta, H.K., Hebert, P.D., Kaartinen, R., Prosser, S.W., Várkonyi, G., & Roslin, T. 2014. Complementary molecular information changes our perception of food web structure. *Proceedings of the National Academy of Sciences*, *111*(5), 1885-1890.

Wirta, H.K., Weingartner, E., Hambäck, P.A. and Roslin, T. 2015. Extensive niche overlap among the dominant arthropod predators of the High Arctic. Basic and Applied Ecology 16: 86–98.

Reports and books

Falk, J.M. 2014. *Plant-soil-herbivore interactions in a high Arctic wetland-Feedbacks to the carbon cycle* (Doctoral dissertation, Lund University).

Lindstein, A. 2015. Land-atmosphere exchange of carbon dioxide in a high Arctic fen: importance of wintertime fluxes. Master Thesis, Lund University, Department of Physical Geography and Ecosystems Science. 60 pp.

General information

Bondo Christensen, P. Gas- og vandmester i verdens største nationalpark. Sermitsiaq 32, 2014.

Presentations

Boffi, G., Wieser, A., Binder, D., Schöner, W. 2014. GNSS-based monitoring of kinematic glacier surface deformation at the A.P. Olsen Ice Cap 12th Swiss Geoscience Meeting, Fribourg 21-22 November 2014.

Chauvaud L., Richard J., Thébault J., Clavier J., Jolivet A., David-beausire C., Amice E., Olivier F., Meziane T., Tremblay R., Archambault P., Winkler G., Gaillard B., Martel A., Ambrose W., Rysgaard S., Blicher M., Carroll M., Strand O, Strohmeier T., Gaumy J. & Paumelle S. 2014. 'Pan-Arctic bivalves as polar bioarchives (B.B. Polar)'. Bivarc Workshop «Bivalves in Artic», 18-19 February 2014, Tromsø, Norway.

Christensen, T.R., Mastepanov, M., Lund, M., Tamstorf, M.P., Parmentier, F J.W., Rysgård, S., & Lilienthal, A.J. 2014. Reducing Uncertainty in Methane Emission Estimates from Permafrost Environments. In *AGU Fall Meeting Abstracts* (Vol. 1, p. 01).

Christensen, T.R., Mastepanov, M., Lund, M., Tamstorf, M.P., Parmentier, F-J., Rysgård, S. and Lilienthal, A. 2014. Reducing Uncertainty in Methane Emission Estimates from Permafrost Environments. Invited presentation at AGUS Fall Meeting 2014, San Fransisco, USA, 15-19 December 2014.

De Cesare S. & Olivier F. 2014. Le couplage pélagos-benthos en Arctique : approche «multiproxy» sur les bivalves

filtreurs. Scientific days of the UMR 7208 BOREA, 30 June 2014, Caen, France.

Dmitrenko I. *et al.* 2014. Polynya Ventilates High-Arctic Fjord in Northeast Greenland. Arctic Change, Ottawa, Canada, 8-12 December.

Docherty, Catherine 2015. Presentation at RGS – IBG Postgraduate Midterm Conference in March 2015 in Sheffield UK.

Falk, J.M., Schmidt, N.M., Christensen, T.R., Forchhammer, M.C., Jackowicz-Korczynski, M., & Ström, L. 2014. Three years exclusion of large herbivores in a high arctic mire in NE Greenland resulted in changed vegetation density and greenhouse gas emission and uptake. In *EGU General Assembly Conference Abstracts* (Vol. 16, p. 3728).

Gaillard B., Meziane T., Tremblay R., Archambault P., Blicher M., Rysgaard S., Chauvaud L. & Olivier F. 2014. Determining the diet of bivalve *Astarte* spp. in a subarctic fjord. Physiomar 2014, 3-9 November 2014, La Serena, Chili.

Hassel, K., Prestø, T., & Schmidt, N.M. 2009. Bryophyte diversity in high and low arctic Greenland. In *CAFF Biodiversity Conference*.

Wirta, H. 2015. A High-Arctic food web – a tightly bound arthropod community to face fast warming. Xth European Congress of Entomology, York 4.8.2015.

Hynek, B., Binder, D., Boffi, G., Schöner, W., & Verhoeven, G. 2014. Application of terrestrial'structure-from-motion'photogrammetry on a medium-size Arctic valley glacier: potential, accuracy and limitations. In *EGU General Assembly Conference Abstracts* (Vol. 16, p. 1783).

Jacobsen, C.S., Nielsen, M.S., Priemé, A., Holben, W.E., Stibal, M., Morales, S., Bælum, J., Elberling, B., Kuhry, P., & Hugelius, G. 2014. Greenlandic Microbiomes and Greenhouse Gas Emissions. In *AGU Fall Meeting Abstracts* (Vol. 1, p. 0135).

Jung, J.Y., Michelsen, A., Schmidt, N.M., & Lee, Y.K. 2014. Changes in Soil Organic Carbon in Response to Climate Manipulation under Cassiope Tetragona in Zackenberg, Greenland. In *20th World Congress of soil science* (pp. 443-443).

Kirillov S. *et al.* 2014. The Effect of Ocean Heat Flux on Seasonal Ice Growth in Young Sound Fjord (North-East Greenland). Arctic Change 2014, Ottawa, Canada, 8-12 December.

Mastepanov, M., & Christensen, T. 2014. Application of a methane carbon isotope analyzer for the investigation of delta13C of methane emission measured by the automatic chamber method in an Arctic Tundra. In *EGU General Assembly Conference Abstracts* (Vol. 16, p. 6341).

Mosbacher, J.B., Nielsen, P.S., Rasmussen, C., Roslin, T., Høye, T.T., & Schmidt, N.M. 2014. Temporal dynamics of a plant-pollinator network in a warming Arctic. In *CAFF Biodiversity Conference*.

Nielsen, S.S. 2015. Dendroecology in the Arctic. Presentation. OIKOS-DK Meeting 06.03.2015, Aarhus, Denmark.

Normand, S. 2014. Arktisk tundra i forandring – droneøkologi forbinder stor og lille skala. Presentation. Tjenestemændsmøde, Department of Bioscience, 01.10.14, Denmark.

Normand, S. and Treier, U.A. 2014. Tundra change at the dawn of drone ecology. Presentation. Drone Workshop 22.10.14, Kalø, Denmark.

Normand, S. and Treier, U.A. 2014. Tundra change at the dawn of drone ecology. Presentation. Ecoinformatics and Biodiversity Seminar 09.12.14, Aarhus, Denmark.

Normand, S. 2015 Tundra change at the dawn of drone ecology. Invited Talk. University of Innsbruck, March 2015, Austria.

Olivier F., Archambault P., Blicher M., Chauvaud L., Gaillard B., Martel A., Meziane T., Rysgaard S., Thébault J., Tremblay R. & Winkler G. 2012. 'SCLERACTIC project: the use of *Astarte* spp. bivalves as archives of climate changes' impacts on Arctic benthic ecosystems'. Les journées de l'Arctique, 14-16 November 2012, IUEM Plouzané, France.

Olivier F., Gaillard B., de Cesare S., Richard J., Tremblay R., Thébault J., Chauvaud L., Archambault P., Bélanger S., Blicher M., Gosselin M., Rysgaard S., Martel A. & Winkler G. 2014. Coupling multi-trophic markers and sclera-chronology/-chemistry methods on Arctic bivalves to assess climate changes effects on the pelagic-benthic coupling. 2014 Ocean Sciences Meeting, 22-28 February 2014, Honolulu, USA.

Palmtag, J., Ramage, J., Hugelius, G., Lashchinskiy, N., Richter, A., & Kuhry, P. 2014. Landscape-level soil profile inventories of soil organic matter with emphasis on cryoturbation in three regions of continuous permafrost (Zackenberg, Greenland; Taymyr Peninsula, Siberia; and Eastern Siberia). In *EGU General Assembly Conference Abstracts* (Vol. 16, p. 661).

Petrusevich V. *et al.* 2014. Mechanisms of Zooplankton Diel Vertical Migration in Young Sound Fjord during the Polar Night. Arctic Change 2014, Ottawa, Canada, 8-12 December.

Reneerkens, J. 2014. Ecological constraints of reproduction during the optimal period for chick growth and survival in an Arctic migratory bird – International Wader Study Group Conference, Haapsalu, Estonia 28 September 2014.

Reneerkens, J. 2015. High early predation of Sanderling clutches may prevent adaptive advancement of breeding phenology – CanMove, University of Lund, Sweden 21 April 2015.

Roslin, T. 2014. Project ARCDYN: Exposing Arctic ecosystem change. Seminar on Arctic Know-how as Strength (Academy of Finland and Tekes). Helsinki, Finland. Poster.

Roslin, T. 2014. Arktiksen ravintoverkot uusiksi. [Revising our view on artic foodwebs] Suomen Biologian Seura Vanamo, November 29 2014, Helsinki, Finland.

Roslin, T. 2014. Arthropods as the glue of Arctic food webs. Conservation of Arctic Flora and Fauna (CAFF) working group of the Arctic Council, December 2–4 2014, Trondheim, Norway.

Roslin, T. 2015. Ravintoverkkojen ymmärtäminen DNA -viivakoodien avulla. [Exposing food web structure by DNA barcodes] FinBOL Seminar on Barcoding Finnish Biota: 15 000 Finnish species barcoded. April 18–19 2015, Helsinki, Finland.

Schmidt, N.M., Humaidan, J., Pedersen, S.H., Gilg, O., & Sittler, B. 2014. Collapsing lemming cycles in Greenland-demographic consequences for lemming predators and its linkages to snow. In *CAFF Biodiversity Conference*.

Stiegler, C., Lindroth, A., Lund, M., Pirk, N., Christensen, T.R., Mastepanov, M. and Parmentier F.-J. 2015. A comparative approach to assess variation in surface energy fluxes in northern high-latitude ecosystems. Presentation at EGU General Assembly 2015, Vienna, Austria, 12-17 April 2015.

Strom, L., Falk, J.M., Skov, K., Jackowicz-Korczynski, M., Mastepanov, M., Christensen, T. R.,Lund, M. & Schmidt, N.M. 2014. Controls of Spatial and Temporal Variability in CH_4 Flux in a High Arctic Fen over Three Years. In *AGU Fall Meeting Abstracts* (Vol. 1, p. 0257).

Treier, U.A. 2014. Drone Ecology in Greenland – Impressions from Fieldwork. Presentation. Remote Sensing Group Seminar, WSL. 01.12.14, Birmensdorf, Switzerland.

Posters

Chauvaud, L., Richard, J., Thébault, J., Clavier, J., Jolivet, A., David-Beausire, C., Amice, E., Olivier, F., Meziane, T., Tremblay, R., Archambault, P., Winkler, G., Gaillard, B., Martel, A., Ambrose, W., Rysgaard, S., Blicher, M., Carrol, M., Strand, O. & Strohmeir, T. 2013. "Sclérochronologie des mollusques polaires pour l'observation des variations environnementales". Chantier Arctique Français, 'Arctique: les grands enjeux scientifiques', 3-5 June 2013, Collège de France, Paris, France.

Chauvaud, L., Richard, J., Thébault, J., Clavier, J., Jolivet, A., David-Beausire, C., Amice, E., Olivier, F., Meziane, T., Tremblay, R., Archambault, P., Winkler, G., Gaillard, B., Martel, A., Ambrose, W., Rysgaard, S., Blicher, M., Carrol, M., Strand, O., Strohmeir, T., Gaumy, J. & Paumelle S. 2013. 'Bivalves Pan-Arctiques comme bioarchives polaires. Projet scientifique BB Polar'. Chantier Arctique Français, 'Arctique: les grands enjeux scientifiques', 3-5 June 2013, Collège de France, Paris, France.

Gaillard, B., Meziane, T., Tremblay, R., Archambault, P., Blicher, M.E., Rysgaard, S., Chauvaud, L. & Olivier, F. 2014. Characterization of the diet of Astarte elliptica (Brown, 1827) and potential use a bioarchive of primary production in a subarctic fjord. Arctic Change 2014 symposium, 8-12 December 2014, Ottawa, Canada.

Gaillard, B., Meziane, T., Tremblay, R., Archambault, P., Blicher, M.E., Rysgaard, S., Chauvaud, L. & Olivier, F. 2014. Caractérisation du régime alimentaire d'*Astarte elliptica* dans un fjord subarctique. AGA 2014 Québec-Océan,

17-19 November 2014, Rivière-du-Loup, Canada.

Lund, M., Christensen, T.R., Elberling, B., Hansen, B.U., Sigsgaard, C. and Tamstorf, M.P. 2014. Flux Monitoring Stations In Greenland. Poster presentation at the 1st ICOS Science Conference, Brussels, Belgium, 23-25 September 2014.

Mastepanov, M. and Christensen, T.R. 2015. A Modern Automatic Chamber Technique as a Powerful Tool for CH_4 and CO_2 Flux Monitoring. Poster presentation at EGU General Assembly, Vienna, Austria, 28 April-2 May 2015.

Mastepanov, M., Christensen, T.R., Lund, M. and Pirk, N. 2014. A Modern Automatic Chamber Technique as a Powerful Tool for CH_4 and CO_2 Flux Monitoring. Poster presentation at AGU Fall Meeting 2014, San Fransisco, USA 15-19 December 2014.

Mbufong, H., Lund, M., Christensen, T.R., Jackowicz-Korczynski, M., Parmentier, F.J.W., Dolman, H., van der Molen, M.M. and Tamstorf, M.P. 2014. Changing trends in carbon dioxide exchange components in three Arctic tundra sites. Poster presentation at EGU General Assembly, Vienna, Austria, 28 April-2 May 2015.

Normand, S., Treier, U.A., Boesch, R., Psomas, A., Zimmermann, N.E. and Ginzler, C. 2015. Assessing vegetation dynamics at the dawn of drone ecology. Poster session internal projects, WSL. 30.3.15, Birmensdorf, Switzerland.

Pedersen, S.H., Schmidt, N.M., Liston, G.E., Tamstorf, M.P. & Westergaard-Nielsen, A. 2014. Quantifying episodic snowmelt events in Arctic ecosystems. Poster presentation at Arctic Change 2014, Ottawa, Canada, 8-12 December 2014.

Ström, L., Falk, J.M., Skov, K., Jackowicz-Korczynski, M., Mastepanov, M., Lund, M., Christensen, T.R. and Schmidt, N.M. 2014. Controls of Spatial and Temporal Variability in CH_4 Flux in a High Arctic Fen over Three Years. Poster presentation at AGU Fall Meeting 2014, San Fransisco, USA 15-19 December 2014.

11 References

Compiled by Lillian Magelund Jensen

Ahlstrøm, A.P., van As, D., Citterio, M., Andersen, S.B., Maghami Nick, F., Gravesen, P., Edelvang, K., Fausto, R.S., Kristensen, S.S., Christensen, E.L., Merryman Boncori, J.P., Dall, J., Forsberg, R., Steenseng, L., Hanson, S. and Petersen, D. 2009. PROMICE 2007-2008: Status report for the first two years of the Programme for Monitoring of the Greenland Ice Sheet. GEUS Report 2009/77.

Anonymous. 2014. Fake flowers fool Arctic insects. Science 345: 494.

Attard, K., Glud, R.N., McGinnis, D., Rysgaard, S. 2014. Seasonal rates of benthic primary production in a Greenlandic fjord measured by aquatic eddy correlation. Limnology & Oceanography 59: 1555-1569.

Bates, N.R. and Mathis, J.T. 2009. The Arctic Ocean marine carbon cycle: evaluation of air-sea CO_2 exchanges, ocean acidification impacts and potential feedbacks. Biogeosciences 6(11): 2433-2459.

Böcher T.W. 1979. Birch woodlands and tree growth in southern Greenland. Holarct. Ecol. 2: 218–221.

Böcher, J. 2009. Fund af den grønlandske mariehøne (Coccinella transversoguttata Falderman, 1835) i Zackenbergdalen, Nordøstgrønland. Entomologiske Meddelelser 77: 115-116.

Boertmann, D. 1994. An annotated checklist of the birds of Greenland. Meddelelser om Grønland. Bioscience 38. 63 pp.

Both, C. 2010. Flexibility of timing of avian migration to climate change masked by environmental constraints en route. Current Biology 20: 243-248.

Bridge, E.S., Thorup, K., Bowlin, M.S., Chilson, P.B., Diehl, R.H., Fléron, R.W., Hartl, P., Kays, R., Kelly, J.F., Robinson, W.D., Wikelski, M. 2011. Technology on the move: recent and forthcoming innovations for tracking migratory birds. Bioscience 61: 689-698.

Buchwal, A., Rachlewicz, G., Fonti, P., Cherubini, P. and Gärtner, G. 2013. Temperture modulates intra-plant growth of *Salix polaris* from a high Arctic site (Svalbard). Polar Biology 36(9): 1305-1318.

Büntgen, U., Hellmann, L., Tegel, W., Normand, S., Myers-Smith. 2015. – In Kirdyanov, A. Nievergelt, D, & Schweingruber, F.H. 2015. Temperature-induced recruitment pulses of Arctic dwarf shrub communities. Journal of Ecology 103: pp. 489-501.

Cardinale, B.J., Palmer, M.A. and Collins, S.L. 2002. Species diversity enhances ecosystem functioning through interspecific facilitation. Nature 415: 426-429.

Cardinale, B.J., Duffy, J.E., Gonzalez, A., Hooper, D.U., Perrings, C., Venail, P. Narwani, A., Mace, G.M., Tilman, D., Wardle, D.A., Kinzig, A.P., Daily, G.C., Loreau, M., Grace, J.B., Larigauderie, A., Srivastava, D.S. and Naeem, S. 2012. Biodiversity loss and its impact on humanity. Nature 486: 59-67.

Citterio, M., van As, D., Ahlstrøm, A.P., Andersen, M.L., Andersen, S.B., Box, J.E., Charalampidis C., Colgan, W.T., Faust, R.S., Nielsen, S. and Veicherts, M. 2015 Automatic Weather Stations for Basic and Applied Glaciological Research. Geological Survey of Denmark and Greenland Bulletin 33 (2015): 69–72.

Crabeck, O., Delille, B., Thomas, D.N., Geilfus, N.X., Rysgaard S. and Tison, J.L. 2014. CO_2 and CH_4 in sea ice from subarctic fjord. Biogeosciences Discuss. 11: 4047-4083.

Delille, B. *et al.* 2014. Southern Ocean CO_2 sink: The contribution of the sea ice. Journal of Geophysical Research: Oceans 119(9): 6340-6355.

Dmitrenko, I.A., Kirillov, S.A., Rysgaard, S., Barber, D.G., Babb, D., Toudal Pedersen, L., Koldunov, N.V., Boone, W., Crabeck, O., and Mortensen, J. 2015.

Polynya impacts on water properties in a Northeast Greenland Fiord. Estuarine, Coastal and Shelf Science, doi: 10.1016/j.ecss.2014.11.027.

Doll, A.C., Lanctot, R.B., Stricker, C.A., Yezerinac, S.M., Wunder, M.B. 2015. Improved arrival date estimates of Arctic-breeding Dunlin (*Calidris alpina arcticola*). The Auk: Ornithological Advances 132: 408-421.

Drees B. and Daniëls F.J.A. 2009. Mountain vegetation of south-facing slopes in continental West Greenland. Phytocoenologia 39: 1-25.

Elberling, H. and Olesen, J.M. 1999. The structure of a high latitude plant-flower visitor system: the dominance of flies. Ecography 22: 314-323.

Falk, J.M., Schmidt, N.M. and Ström, L. 2014. Effects of simulated increased grazing on carbon allocation patterns in a high arctic mire. Biogeochemistry 119: 229-244.

Falk, J.M., Schmidt, N.M., Christensen, T.R. and Ström, L. 2015. Large herbivore grazing affects the vegetation structure and greenhouse gas balance in a high arctic mire. Environmental Research Letters 10, doi:10.1088/1748-9326/10/4/045001.

Fridley, J.D. 2001. The influence of species diversity on ecosystem productivity: how, where, and why? Oikos 93: 514-526.

Geilfus, N.X., Carnat, G., Papakyriakou, T., Tison, J.L., Else, B., Thomas, H., Shadwick, E. and Delille, B. 2012. Dynamics of pCO_2 and related air-ice CO_2 fluxes in the Arctic coastal zone (Amundsen Gulf, Beaufort Sea). Journal of Geophysical Research-Oceans 117 (C00G10).

Geilfus, N.X., Galley, R.J., Crabeck, O., Papakyriakou, T., Landy, J.C., Tison, J.L. and Rysgaard, S. 2014a. Inorganic carbon dynamics of melt-pond-covered first-year sea ice in the Canadian Arctic. Biogeosciences 12: 2047-2061.

Geilfus, N.X., Tison, J.L., Ackley, S.F., Rysgaard, S., Miller, L.A. and Delille, B. 2014b. Impact of snow cover on CO_2 dynamics in Antarctic pack ice. The Cryosphere 8: 2395-2407.

Gilg, O., Moe, B., Hanssen, S.A. Schmidt, N.M., Sittler, B., Hansen, J., Reneerkens, J., Sabard, B., Chastel, O., Moreau, J., Phillips, R.A., Oudman, T., Biersma, E.M., Fenstad, A., Lang, J., Bollache, L. 2013. Trans-equatorial migration routes, staging sites and wintering areas of a high-arctic avian predator: the long-tailed skua (*Stercorarius longicaudus*). PLoS ONE 8: e64614.

Glud, R.N. 2008. Oxygen dynamics of marine sediments. Marine Biology Research 4(4): 243-289.

Glud, R.N., Woelfel, J., Karsten, U., Kuhl, M. and Rysgaard, S. 2009. Benthic microalgal production in the Arctic: Applied methods and status of the current database. Botanica Marina 52: 559-571.

Hansen, J., Schmidt, N.M., Hansen, L.H., and Reneerkens, J. 2009. Bird monitoring at Zackenberg, Northeast Greenland, 2008 – with comparison to 1995-2007. Bird Populations 10: 68-78.

Hargrave, B.T., Barrie, L.A., Bidleman, T.F., and Welch, H.E. 1997. Seasonality of exchange of organochlorines between Arctic air and seawater. Environ. Sci. Technol. 31: 3258-3266.

Hollesen, J., Buchwal, A., Rachlewicz, G., Hansen, B.U., Overgaard, M., Stecher, O. and Elberling, B. 2015. Winter warming as an important co-driver for *Betula nana* growth in Western Greenland during the past century. Global Change Biology 21: 2410-2423.

Jensen, L.M. (ed.) 2012. Zackenberg Ecological Research Operations, 17th Annual Report, 2011. Aarhus University, DCE – Danish Centre for Environment and Energy. 120 pp.

Jensen, L.M. and Rasch, M. (eds.) 2009. Ecological Research Operations, 14th Annual Report, 2008. National Environmental Research Operations, Aarhus University, Denmark.

Jensen, L.M., Rasch, M. and Schmidt, N.M. (eds.) 2013. Zackenberg Ecological Research Operations, 18th Annual Report, 2012. National Environmental Research Institute, Aarhus University, Denmark, 122 pp.

Jensen, L.M., Christensen, T.R. and Schmidt, N.M. (ed.) 2014. Zackenberg Ecological Research Operations 19th Annual Report, 2013. Aarhus University, DCE – Danish Centre for Environment and Energy. 130 pp.

Johnson, D.H. 1979. Estimating nest success: The Mayfield method and an alternative. Auk 96: 651-661.

Karlsen S.R. and Elvebakk A. 2003. A method using indicator plants to map local climatic variation in the Kangerlussuaq/Scoresby Sund area, East Greenland. J. Biogeogr. 30: 1469-1491.

Kevan, P.G. 1972. Insect pollination of high arctic flowers. Journal of Ecology 60: 831-847.

Kirillov, S., Dmitrenko, I., Babb, D., Rysgaard, S., Barber, D. 2015. The effect of ocean heat flux on seasonal ice growth in Young Sound (Northeast Greenland), submitted to Journal of Geophysical Research, Volume 120, Issue 7: 4803–4824

Klitgaard, A.B., Rasch, M. and Caning, K. (eds.) 2007. Zackenberg Ecological Research Operations, 12th Annual Report, 2006. Copenhagen, Danish Polar Center, Ministry of Science, Technology and Innovation.

Klitgaard, A.B., Rasch, M. and Caning, K. (eds.) 2008. Zackenberg Ecological Research Operations, 13th Annual Report, 2007. Copenhagen, Danish Polar Center, Ministry of Science, Technology and Innovation.

Larsen, M., Petersen, D. and Thorsøe, K. 2011. Discharges in ice affected periods in Zackenbergelven. Asiaq Report 2011-16. B15-02-005.

Liang, S. 2001. Narrowband to broadband conversions of land surface albedo I: Algorithms. Remote Sensing of Environment 76(2): 213–238.

Lisovski, S., Hewson, C.M., Klaassen, R.H.G., Korner-Nievergelt, F., Kristensen, M.W., Hahn, S. 2012 Geolocation by light: Accuracy and precision affected by environmental factors. Methods in Ecology and Evolution 3: 603-612.

Loreau, M. and Hector, A. 2001. Partitioning selection and complementarity in biodiversity experiments. Nature 412: 72-76.

Loreau, M., Naeem, S., Inchausti, P., Bengtsson, J., Grime, J.P., Hector, A., Hooper, D.U., Huston, M.A., Raffaelli, D., Schmid, B., Tilman, D. and Wardle, D.A. 2001. Biodiversity and ecosystem functioning: Current knowledge and future challenges. Science 294: 804-808.

Loreau, M., Naeem, S. and Inchausti, P. 2002. Biodiversity and ecosystem functioning: synthesis and perspectives. Oxford University Press, Oxford. 294 pp.

Lüers, J., Westermann, S., Piel, K. and Boike, J. 2014. Annual CO_2 budget and seasonal CO_2 exchange signals at a high Arctic permafrost site on Spitsbergen, Svalbard archipelago. Biogeosciences 11: 6308-6322.

Machguth, H., Rastner, P., Bolch, T., Mölg, N., Sandberg Sørensen, L., Aðalgeirsdottir G., van Angelen J.H., van den Broeke M.R. and Fettweis X. 2013. The Future Sea-level Rise Contribution of Greenland's Glaciers and Ice Caps. Environmental Research Letters 8(2): 1-13.

Madsen, J and Boertmann, D. 2008. Animal behavioral adaptation to changing landscapes: spring-staging geese habituate to wind farms. Landscape Ecology 23: 1007-1011.

Mastepanov, M., Sigsgaard, C., Dlugokencky, E.J., Houweling, S., Ström L., Tamstorf, M.P. and Christensen, T.R. 2008. Large tundra methane burst during onset of freezing. Nature 456: 628-631.

Meltofte, H. 1978. A breeding association between Eiders and tethered huskies in North-east Greenland. Wildfowl 29: 45-54.

Meltofte, H. and Thing, H. (eds.) 1996. Zackenberg Ecological Research Operations, 1th Annual Report, 1995. Danish Polar Center, Ministry of Research & Technology.

Meltofte, H., Høye, T.T., Schmidt, N.M., Forchhammer, M.C. 2006. Differences in food abundance cause inter-annual variation in the breeding phenology of High Arctic waders. Polar Biology 30: 601-606.

Meltofte, H., Høye, T.T., Schmidt, N.M., Forchhammer, M.C. 2006. Differences in food abundance cause inter-annual variation in the breeding phenology of High Arctic waders. Polar Biology 30: 601-606.

Middelburg J.J. and Soetaert, K. 2004. *The role of sediments in shelf ecosystem dynamics*. In: Robinson A, Brink KH (ed) The Sea, vol 13. Harvard Univ Press, Cambridge, pp 353–374.

Nomura, D., Eicken, H., Gradinger, R. and Shirasawa, K. 2010. Rapid physically driven inversion of the air-sea ice CO_2 flux in the seasonal landfast ice off Barrow, Alaska after onset surface melt. Continental Shelf Research 30(19): 1998-2004.

Nomura, D., Granskog, M.A., Assmy, P., Simizu, D. and Hashida, G. 2013. Arctic and Antarctic sea ice acts as a sink for atmospheric CO_2 during periods of snowmelt and surface flooding. Journal of Geophysical Research: Oceans 118: 6511-6524.

Ntiamoa-Baidu, Y., Nuoh, A.A., Reneerkens, J. and Piersma, T. 2014. Population increases in non-breeding Sanderlings in Ghana indicate site preference. Ardea 102: 131-137.

Parmentier, F.-J.W., Christensen, T.R., Sørensen, L.L., Rysgaard, S., McGuire, A.D., Miller, P.A. and Walker, D.A. 2013. The impact of lower sea-ice extent on Arctic greenhouse-gas exchange. Nature Climate Change 3: 195-202.

Pedersen S.B. and J. Hinkler 2000. The Spatiotemporal Snow Cover Distribution in Zackenbergdalen, Northeast Greenland mapped using different remote sensing techniques. MSc thesis, University of Copenhagen, Denmark. 118 pp.

Pétillon, J., Courtial, C. and Vernon, P. 2014. Population and assemblage-based study of Arctic spiders (Araneae): first results from Kobbefjord, pp 75-77 in Jensen, L.M. and Christensen, T.R. (eds.) 2014. Nuuk Ecological Research Operations, 7th Annual Report, 2013. DCE – Danish Centre for Environment and Energy, Aarhus University, Denmark. 94 pp.

Pućko, M., Stern, G.A., Barber, D.G., Macdonald, R.W., Warner, K.-A. and Fuchs, C. 2012. Mechanisms and implications of -HCH enrichment in melt pond water on Arctic sea ice. Environ. Sci. Technol. 46: 11862-11869.

Pućko, M., Stern, G.A., Macdonald, R.W., Jantunen, L.M.M., Bidleman, T.F., Wong, F., Barber, D.G. and Rysgaard, S. 2015. The delivery of organic contaminants to the Arctic food web: why sea ice matters. Sci. Total Environ. 506-507: 444-452.

Pućko, M., Stern, G.A., Burt, A., Jantunen, L.M.M., Bidleman, T.F., Macdonald, R.W., Barber, D.G., Geilfus, N.-X., Landy, J., Papakyriakou, T. and Rysgaard, S. 2015 (in preparation). Current Use Pesticide (CUP) and legacy Organochlorine Pesticide (OCP) dynamics at the ocean-sea-ice-atmosphere (OSA) interface in the Resolute Passage, Canadian High Arctic during winter-summer transition. For Environ. Sci. Technol.

Rasch, M., Elberling, B., Jakobsen, B.H. and Hasholt, B. 2000. High-resolution measurements of water discharge, sediment, and solute transport in the river Zackenbergelven, Northeast Greenland. Arctic, Antarctic and Alpine Research 32(3): 336-345.

Rasch, M. and Caning, K. (eds.) 2003. Zackenberg Ecological Research Operations, 8th Annual Report, 2002. Copenhagen, Danish Polar Center, Ministry of Science, Technology and Innovation.

Rasch, M. and Caning, K. (eds.) 2004. Zackenberg Ecological Research Operations, 9th Annual Report, 2003. Copenhagen, Danish Polar Center, Ministry of Science, Technology and Innovation.

Reneerkens, J., Benhoussa, A., Boland, H., Collier, M., Grond, K., Günther, K., Hallgrimsson, G.T., Hansen, J., Meissner, W., de Meulenaer, B., Ntiamoa-Baidu, Y., Piersma, T., Poot, M., van Roomen, M., Summers, R.W., Tomkovich, P.S., Underhill, L.G. 2009. Sanderlings using African-Eurasian flyways: a review of current knowledge. Wader Study Group Bulletin 116: 2-20.

Rösel, A., and Kaleschke, L. 2012. Exceptional melt pond occurrence in the years 2007 and 2011 on the Arctic sea ice revealed from MODIS satellite data. Journal of Geophysical Research-Oceans 117: C05018.

Roslin, T., Wirta, H., Hopkins, T., Hardwick, B. and Várkonyi, G. 2013. Indirect interactions in the High Arctic. PLoS ONE 8(6): e67367, doi:10.1371/journal.pone.0067367.

Rysgaard, S., Bendtsen, J., Delille, B., Dieckmann, G.S., Glud, R.N., Kennedy, H., Mortensen, J., Papadimitriou, S., Thomas, D.N. and Tison, J.L. 2011. Sea ice contribution to the air-sea CO_2 exchange in the Arctic and Southern Oceans. Tellus, Series B, Chemical and Physical Meteorology 63(5): 823-830.

Sjögersten, S., Van Der Wal, R. and Woodin, S.J. 2008. Habitat type determines herbivory controls over CO_2 fluxes in a warmer arctic. Ecology 89: 2103-2116, doi:10.1890/07-1601.1.

Schmidt, N.M. Hansen, L.H., Hansen, J., Berg, T.B., Meltofte, H. 2014. BioBasis Manual. Conceptual design and sampling procedures of the biological monitoring programme within Zackenberg Basic. 17th edition. Zackenberg Ecological Research Operations. Department of Bioscience, Aarhus University, 2014. 104 pp.

Stocker, T.F., D. Qin, G.-K. Plattner, M. Tignor, S.K. Allen, J. Boschung, A.

Nauels, Y. Xia, V. Bex and P.M. Midgley (eds.) 2013. IPCC Climate Change 2013. The Physical Science Basis. Contribution of Working Group I to the Fifth Assessment Report of the Intergovernmental Panel on Climate Change. Cambridge University Press, Cambridge, United Kingdom and New York, NY, USA, 1535 pp.

Ström, L., Falk, J.M., Skov, K., Jackowicz-Korczynski, M., Mastepanov, M., Christensen, T.R., Lund, M. and Schmidt, N.M. 2015. Controls of spatial and temporal variability in CH_4 flux in a high arctic fen over three years. Biogeochemistry (in press).

Sugiyama, S., Bauder, A., Weiss, P. and Funk., M. 2007. Reversal of ice motion during the outburst of a glacier-dammed lake on Gornergletscher, Switzerland. J. Glaciol. 53(181): 172–180.

Sørensen E.V., Bjerager, M. and Citterio, M (submitted). Digital models based on images from hand-held cameras – on land, on ice, from the sea. Submitted to Geological Survey of Denmark and Greenland Bulletin.

Takahashi, T., *et al.* 2009. Climatological mean and decadal change in surface ocean pCO_2, and net sea-air CO_2 flux over the global oceans. Deep-Sea Research, Part II, Topical Studies in Oceanography 56(8-10): 554-577.

Tanentzap, A.J. and Coomes, D.A. 2012. Carbon storage in terrestrial ecosystems: Do browsing and grazing herbivores matter? Biological Reviews 87: 72-94, doi:10.1111/j.1469-185X.2011.00185.x.

Tison, J.L., Haas, C., Gowing, M.M., Sleewaegen, S. and Bernard, A. 2002. Tank study of physico-chemical controls on gas content and composition during growth of young sea ice. Journal of Glaciology. 48(161): 177-191.

Tøttrup A.P., Klaassen R.H.G., Kristensen M.W., Strandberg, R., Vardanis, Y., Lindström, Å., Rahbek, C., Alerstam, T. and Thorup, K. 2012. Drought in Africa caused delayed arrival of European songbirds. Science 338 (6112): 1307.

Várkonyi, G. and Roslin, T. 2013. Freezing cold yet diverse: dissecting a high-Arctic parasitoid community associated with Lepidoptera hosts. Canadian Entomologist 145: 193-218.

Visakorpi, K., Ek, M., Várkonyi, G., Wirta, H.K., Hardwick, B., Hambäck, P. & Roslin, T. 2014. Dissecting the interaction web of Zackenberg: targeting pollinators. In: Jensen, L.M., Christensen, T.R. & Schmidt, N.M. (Eds.). 2014. Zackenberg Ecological Research Operations, 19th Annual Report, 2013. Aarhus University, DCE – Danish Centre for Environment and Energy. pp. 99-101.

Wirta, H., Várkonyi, G., Hardwick, B., Kaartinen, R. and Roslin, T. 2013. DNA barcodes for the terrestrial species of Zackenberg. In: Jensen, L.M., Rasch, M. and Schmidt, N.M. (ed.) 2013. Zackenberg Ecological Research Operations, 18th Annual Report, 2012. Aarhus University, DCE – Danish Centre for Environment and Energy. p. 96.

Wirta, H.K., Hebert, P.D.N., Kaartinen, R. Prosser, S.W., Várkonyi, G. and Roslin, T. 2014. Complementary molecular information changes our perception of food web structure. PNAS 111: 1885-1890.

Wirta, H.K., Weingartner, E., Hambäck, P.A. and Roslin, T. 2015. Extensive niche overlap among the dominant arthropod predators of the High Arctic. Basic and Applied Ecology 16: 86-98.

Zatwarnicki, T. and Mathis, W.N. 2015. Ephydridae (Shore flies). In. Böcher *et al.* (eds): The Greenland Entomofauna. Brill.

Zhou, J.Y., Tison, J.L., Carnat, G., Geilfus, N.X. and Delille, B. 2014. Physical controls on the storage of methane in landfast sea ice. The Cryosphere 8(3): 1019-1029.

12 Appendix

Day of Year

Regular years	Jan	Feb	Mar	Apr	May	Jun	Jul	Aug	Sep	Oct	Nov	Dec
1	1	32	60	91	121	152	182	213	244	274	305	335
2	2	33	61	92	122	153	183	214	245	275	306	336
3	3	34	62	93	123	154	184	215	246	276	307	337
4	4	35	63	94	124	155	185	216	247	277	308	338
5	5	36	64	95	125	156	186	217	248	278	309	339
6	6	37	65	96	126	157	187	218	249	279	310	340
7	7	38	66	97	127	158	188	219	250	280	311	341
8	8	39	67	98	128	159	189	220	251	281	312	342
9	9	40	68	99	129	160	190	221	252	282	313	343
10	10	41	69	100	130	161	191	222	253	283	314	344
11	11	42	70	101	131	162	192	223	254	284	315	345
12	12	43	71	102	132	163	193	224	255	285	316	346
13	13	44	72	103	133	164	194	225	256	286	317	347
14	14	45	73	104	134	165	195	226	257	287	318	348
15	15	46	74	105	135	166	196	227	258	288	319	349
16	16	47	75	106	136	167	197	228	259	289	320	350
17	17	48	76	107	137	168	198	229	260	290	321	351
18	18	49	77	108	138	169	199	230	261	291	322	352
19	19	50	78	109	139	170	200	231	262	292	323	353
20	20	51	79	110	140	171	201	232	263	293	324	354
21	21	52	80	111	141	172	202	233	264	294	325	355
22	22	53	81	112	142	173	203	234	265	295	326	356
23	23	54	82	113	143	174	204	235	266	296	327	357
24	24	55	83	114	144	175	205	236	267	297	328	358
25	25	56	84	115	145	176	206	237	268	298	329	359
26	26	57	85	116	146	177	207	238	269	299	330	360
27	27	58	86	117	147	178	208	239	270	300	331	361
28	28	59	87	118	148	179	209	240	271	301	332	362
29	29		88	119	149	180	210	241	272	302	333	363
30	30		89	120	150	181	211	242	273	303	334	364
31	31		90		151		212	243		304		365

Day of Year

Leap years	Jan	Feb	Mar	Apr	May	Jun	Jul	Aug	Sep	Oct	Nov	Dec
1	1	32	61	92	122	153	183	214	245	275	306	336
2	2	33	62	93	123	154	184	215	246	276	307	337
3	3	34	63	94	124	155	185	216	247	277	308	338
4	4	35	64	95	125	156	186	217	248	278	309	339
5	5	36	65	96	126	157	187	218	249	279	310	340
6	6	37	66	97	127	158	188	219	250	280	311	341
7	7	38	67	98	128	159	189	220	251	281	312	342
8	8	39	68	99	129	160	190	221	252	282	313	343
9	9	40	69	100	130	161	191	222	253	283	314	344
10	10	41	70	101	131	162	192	223	254	284	315	345
11	11	42	71	102	132	163	193	224	255	285	316	346
12	12	43	72	103	133	164	194	225	256	286	317	347
13	13	44	73	104	134	165	195	226	257	287	318	348
14	14	45	74	105	135	166	196	227	258	288	319	349
15	15	46	75	106	136	167	197	228	259	289	320	350
16	16	47	76	107	137	168	198	229	260	290	321	351
17	17	48	77	108	138	169	199	230	261	291	322	352
18	18	49	78	109	139	170	200	231	262	292	323	353
19	19	50	79	110	140	171	201	232	263	293	324	354
20	20	51	80	111	141	172	202	233	264	294	325	355
21	21	52	81	112	142	173	203	234	265	295	326	356
22	22	53	82	113	143	174	204	235	266	296	327	357
23	23	54	83	114	144	175	205	236	267	297	328	358
24	24	55	84	115	145	176	206	237	268	298	329	359
25	25	56	85	116	146	177	207	238	269	299	330	360
26	26	57	86	117	147	178	208	239	270	300	331	361
27	27	58	87	118	148	179	209	240	271	301	332	362
28	28	59	88	119	149	180	210	241	272	302	333	363
29	29	60	89	120	150	181	211	242	273	303	334	364
30	30		90	121	151	182	212	243	274	304	335	365
31	31		91		152		213	244		305		366

Greenland Ecosystem Monitoring

Greenland Ecosystem Monitoring (GEM) is an integrated monitoring and long-term research programme on ecosystem dynamics and climate change effects and feedbacks in Greenland.

ClimateBasis Programme

The GEM ClimateBasis Programme studies climate and hydrology providing fundamental background data for the other GEM programmes.

GeoBasis Programme

The GEM GeoBasis Programme studies abiotic characteristics of the terrestrial environment and their potential feedbacks in a changing climate.

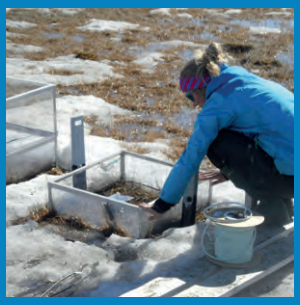

BioBasis Programme

The GEM BioBasis Programme studies key species and processes across plant and animal populations and their interactions within terrestrial and limnic ecosystems.

MarineBasis Programme

The GEM MarineBasis Programme studies key physical, chemical and biological parameters in marine environments.

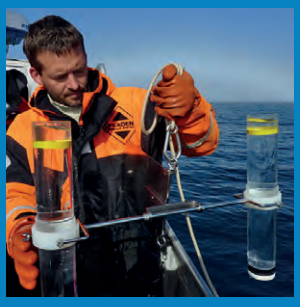

GlacioBasis Programme

The GEM GlacioBasis Programme studies ice dynamics, mass balance and surface energy balance in glaciated environments.

AARHUS UNIVERSITY

ASIAQ

GEUS

Grønlands Naturinstitut
Pinngortitaleriffik • Greenland Institute of Natural Resources

DTU Technical University of Denmark

UNIVERSITY OF COPENHAGEN